Digital film dosimetry in radiotherapy and the development of analytical applications software

Yang Wang
University of Wollongong

DIGITAL FILM DOSIMETRY IN RADIOTHERAPY

and the

DEVELOPMENT OF ANALYTICAL APPLICATIONS SOFTWARE

A thesis submitted in fulfillment of the requirements

for the award of the degree

DOCTOR OF PHILOSOPHY

from the

UNIVERSITY OF WOLLONGONG

By

Yang Wang (BSc, Post GDip)

ENGINEERING PHYSICS

2005

CERTIFICATION

I, Yang Wang, declare that this thesis, submitted impartial fulfilment of the requirements for the award of Doctor of Philosophy, in the Department of Biological Sciences, University of Wollongong, is wholly my own work unless otherwise referenced or acknowledged. The document has not been submitted for qualifications at any other academic institution.

Yang Wang

31 October 2005

Preface

The clinical imperative

Film dosimetry started being used for radiotherapy quality assurance checks in the 1950s and 1960s. From the 1990s film dosimetry has become an important tool for the dose distribution checks in 3-D conformal radiotherapy and intensity modulated radiotherapy treatment (IMRT). However, film dosimetry results have in the past suffered from large uncertainties. The low accuracy relates to a variety of causes including the film response to radiation beams, dosimetry, and film development and measurement procedures.
The use of film for dosimetry requires the establishment of procedures which minimize the uncertainties in each stage from exposure through development to measurement and analysis.

Digital technique for image optical density calibration

Low cost computer desktop scanners are becoming possibly used for reliable clinical film dosimetry. Desktop transparency scanners, when properly calibrated, provide a reliable and accurate means to measure of film transparency digitally. Both scanner and film response can be linearised to improve the dosimetry analysis results. A software package has been developed to undertake the complex signal analysis and image mapping techniques required for accurate film dosimetry.

Clinical performance of film dosimetry result improvement

The film scanner dynamic range, linearity, gain variations and light source variability must be calibrated before the scanner can be used for dosimetry, the film dosimetry. Perturbations resulting from film processing or image processing are dealt with separately from those arising in digitising.

The film response depends on film type, radiation beam type and energy dependence, phantom buildup, angle of entry and radiation field size. These factors are directly compensated in the film analysis software.

Film dosimetry reliability and accuracy are improved by using this film dosimetry software package.

Acknowledgement

I would like to thank my supervisor Professor William Zealey for the support he has provided over the past few years. His supervision and leadership helped me tremendously.
I give my greatest thanks to Dr Peter Cross, co-supervisor of this project, for his encouragement and support in the experimental work, phantom design and chapter writing. Our discussions will remain long in my memory.

My thanks, also, to the University of Wollongong and St. Vincent's Hospital Sydney, for allowing me the great opportunity to undertake this research and to complete my thesis study.

I also give special thanks to William Paterson, the Director, Chief Physicist of Radiation Oncology, Victoria. He was very supportive of my work during the two years I worked in the Ballarat-Austin Radiation Oncology Centre. I also thank the staff from both Geelong Andrew Love Cancer Centre, Victoria and Austin Radiation Oncology Centre, Ballarat for their friendship and cooperation in supporting all the study cases for the project.

And I finally thank my wife Shuyuan for supporting my study with loving patience, and to my son Sean for lot of interesting discussions on software development techniques.

Table of Contents

Abstract

This study is focused on the analysis, evaluation and calibration of low cost computer desktop scanners for possible use in film dosimetry. The study also includes the development a software package to use the digital output of such scanners for image processing. This software has matured commercially into a suite of programs named **R**adiation **O**ncology **D**osimetry **M**anagement **S**ystem (**RODOMS**) for use in radiotherapy quality assurance protocols. The input to the software is a bitmap image created by the scanner. The scan signal greyscale value (GSV) is converted into an optical density value (OD) and a calibration is made to the equivalent radiation doses (DOSE). The software functions include:

- Scanner signal calibration – using a standard step wedge film to set and calibrate the dynamic range and scan signal linearity
- OD vs DOSE response curve calibration – using film strips to read the optical density for different dose exposures to establish the OD-DOSE conversion curve.
- Background level uncertainty control – analysis and subtraction of the base + fog value from the film base material and the film over response to radiation scatter.
- Processing noise smoothing – polynomial and mean smoothing, alternately used to reduce the noise caused by film artifacts.
- Beam quality dependence correction – using individual OD-DOSE calibration curves to correct the exposure for a combined beam modality field film dosimetry quality assurance.
- Clinical film dosimetry analysis – graphic user interface (GUI) designed program for radiation field quality assurance in advanced comparison of 3-D and IMRT dose distribution analysis. This includes the IMRT field with the planning computer curve overlaid for a comparative analysis.

Dosimetry phantoms have been designed and used in the testing and evaluation of RODOMS. The software is currently in clinical use in several radiotherapy centers in Australia and Asian countries. The clinical results give

on average a ±3% uncertainty level in most of the clinical cases compared with the ionization or TLD measurement results of up to ±5%. By using this software in a variety of clinical situations it is shown in this study that the traditional uncertainty levels in film dosimetry have been significantly reduced.

Chapter 1 Introduction

This study is focused on radiation film dosimetry and analysis. The study aims to establish a practical, effective, easy-to-operate, reproducible and reliable film dosimetry method. Most of this study focuses on using an ordinary desktop scanner to aid hospital physicists in routine dosimetry and treatment planning check in radiotherapy quality assurance.

Radiotherapy quality assurance (QA) is a package of programs and protocols used to calibrate, verify and guarantee that the dose and positional accuracy is delivered as planned.

The QA task in radiotherapy includes absolute dose calibration and dose distribution. As an important part of radiotherapy QA, film dosimetry has been used to check the radiation dose for over 50 years. In current radiation therapy, especially 3D treatment and Intensity Modulation Radiation Therapy (IMRT), external radiation beam dose distribution quality assurance (QA) is increasingly carried out using film.

QA places a heavy routine workload on hospital physicists, especially if the department has two or three accelerators plus simulator, after-loading device, and a low energy x-ray system. Monthly QA could require the physicist to check more than 20 different energy set-ups. The use of film simplifies the QA process and removes some of the difficulties associated with using ionisation chambers.

Water scanners give very high accuracy, high reproducibility, and reliability. However, as they are large and expensive it is not possible to use them for the routine QA.

In comparison, film techniques are simpler to undertake, requiring the physicist to spend less time on the treatment machine and hence minimum beam exposure. It allows routine QA tasks to be performed more frequently. Film dosimetry techniques however, have been limited by the noise in the densitometry readings, reliability of film response to the radiation beam, and artefacts created by the film processing.

The absolute value of measured film density can have inaccuracies of $\pm$5%. For this reason, the film dosimetry used in radiotherapy QA is commonly restricted to providing qualitative information or relative dosimetry only.

Film densitometers have been used widely over the past two decades. In these the film is illuminated by a stabilised light source and the transmitted intensity measured by a detector. The analogue signal is converted into a digital number and recorded at each position in a scan. This technique has been commonly used in radiotherapy clinical film dosimetry since 1980 (WelHofer and RFA Scanditronics densitometers). These scanning densitometers have limitations in spatial resolution, scan step size and scanning speed. The positional resolution is limited by the diameter of the detector and the light source spot and may be larger than l.0 mm diameter. The scanning time is not much reduced compared to the water scan technique. Results can be influenced by stray light from the ambient room lighting. The above reasons have made the film dosimetry using conventional film scanning densitometers unsatisfactory and not recommended for routine QA work.

In recent years, rapid development of personal computer technology has brought a revolution in many areas. Fast computers, low cost, and high- resolution computer scanners now allow the 2D analysis of film transparencies, with high accuracy.

These timely developments have allowed us to carry out a detailed evaluation of film densitometry for routine QA. A commercially available desktop scanner is used to create a bitmap image from QA films, which is then calibrated pixel-by-pixel, to monitor the dose distribution consistency.

The advantages of using a desktop scanner are:

1. Economical and low cost.
2. Saving of time compared with other techniques.
3. Accurate position determination ±0.15mm.
4. Fast scanning speed allowing optimisation of settings.
5. Digital data allowing complex calculations to be performed.

However, to obtain acceptable reproducibility and reliability using an ordinary desktop scanner for film densitometry several problems have to be solved. These include:

1. Non-linear response correction.
2. Pixel noise correction.
3. Non-uniform illumination of film due to the scanner light source (flat field correction).

4. Calibration of greyscale value to equivalent dose.
5. Energy sensitivity of film calibration.
6. Solid phantom and water scatter factor correction.

Other issues studied in this project include a comparison of the modelling effectiveness for different signal depths from 8bit, 12bit, 14bit and 16bit model scanners, and how the spectrum of electrons influences the film response.

A film analysis software package has been developed suitable for hospital use to perform the above processes. The software includes the following functions:

1. Scanner signal linearity optimisation
2. Scanner calibration: conversion of grayscale value to dose
3. Bitmap image display and modification
4. Pixel value tracking and conversion to equivalent dose with/without full background value subtraction
5. Equivalent dose distribution - isodose tracking and plotting
6. Profile / percentage depth dose curve processing and analysis.
7. Multiple scanned film analysis result combination procedure
8. 3D dose distribution image display.
9. Analysis report output.

Summary of the layout of this thesis

Chapters 1 to 4 discuss the history of the use of film, film processing, the use of film in medical images, and film dosimetry used in radiotherapy QA. Chapter 5 reviews existing film digitising technology and chapter 6 summarises the technology of desktop scanner development and introduces the idea that desktop scanners are suitable for analysing QA film. Chapters 7 to 9 develop techniques and software for film QA leading to the full implementation in Chapter 10. Chapters 11 to 12 discuss experimental studies leading to corrections to the raw scan data. Chapter 13 onwards present extensions to the protocol developed for radiotherapy using a linear accelerator and other applications in which film has been applied to QA. These include dosimetry of

- IMRT dynamic radiation fields
- Multiple beam radiation fields

- Brachytherapy

Published conference proceedings and papers are included for completeness in an Appendix

1. An evaluation of a document scanner for film dosimetry applications
Wang. Y & Cross. P, Aust Phys Sci Med, vol 22 n1, p18-22, 1999

2. An investigation into the source of low energy scattered radiation of significance in film dosimetry
Wang.Y, Zealey.W, Cross.P, APESM, vol. 25, September 2002.

Presentations: -

1999 Film dosimetry used in small beam dynamic radiation field dose distribution check
International Medical Image Conference, Hong Kong, 1999,

2000 Solid wedge phantom used in Electron and Photon beam routine checks.
Australian EPSM-2000 Conference (Engineering Physics and Science in Medicine), Newcastle, NSW, Australia, Nov 2000

2001 An investigation of unexpected background value correction in film dosimetry, Australian EPSM-2000 Conference (Engineering Physics and Science in Medicine), Newcastle, NSW, Australia, Nov 2000

Pre-exposure dose correction for the film dosimetry used in multiple beam field junction dose checks, Melbourne, ICRO 2001 (International Congress of Radiation Oncology)

Computerized film dosimetry applied for HDR brachytherapy unit.
EPSM-2001, Australian & New Zealand wide college conference. Perth Nov 2001.

2003 Equivalent Square size estimation and correction technique used in 3D treatment planning MU check, CMS 2003 (Computerised Medical System) users meeting, Sydney, NSW, May 2003

Field segmentation film dosimetry check – Error and discrepancy study, WC2003, (World Congress of Medical Physics), Sydney, August 2003

2004 Virtual film technique in 3D and step-shot IMRT planning check, Australian EPSM-2004 Conference (Engineering Physics and Science in Medicine), Geelong, VIC, Australia, Nov 2004

Review of BEQS Calculation in 3D Conformal Planning MU check EPSM-2004 Conference (Engineering Physics and Science in Medicine), Geelong, VIC, Australia, Nov 2004

Chapter 2. The History of Film and Film Dosimetry

2.1 Review of the Photographic Process

Joseph Nicephone Niepce produced the first permanent photograph in 1826 (Harmant and Marillier 1967). The first x-ray image was recorded 1895 taken Frau Roentgen's hand after X-ray were discovered by W. C. Roentgen, followed very quickly by Hall-Edwards, (and others) x-ray picture in early 1896." (CF Richard Mould, A Century of X-rays and Radioactivity in Medicine, IOPP Bristol). The earliest x-ray films used glass as a base material, but current films all use a plastic/mylor base to support the radiation sensitive emulsion. Radiographic film has comparatively low quantum efficiency in response to X-rays compared to visible light. Therefore in normal radiography the film is used with a fluorescent screen. The double emulsion film is sandwiched between two fluorescent screens to increase the imaging efficiency and reduce the patient irradiation dose. In this kind of imaging the film responds to visible light. In QA, the film is used without fluorescent screens and responds directly to X-rays. The historical reviewed that follows the deals mainly with film response to visible light.

Background of photographic film and photography

Photographic film used in radiography consists of a thin plastic base with an emulsion coat on one or both sides. The emulsion is composed of micro-particles or grains suspended in a gelatine support. These grains are usually light-sensitive silver halide crystals. When the silver halide crystal is exposed to the light, the silver halide produces development centres of silver, which we call the latent (or hidden) image. If the film is not immediately developed these development centres can fade due to thermal processes.

When the film is chemically developed (reduction process) each grain containing development centres will be converted to form metallic silver through the whole emulsion depth. The unexposed silver grains are later removed by chemical fixing. In the final image, different transparencies in the film results from different densities of fixed metal silver in the film.

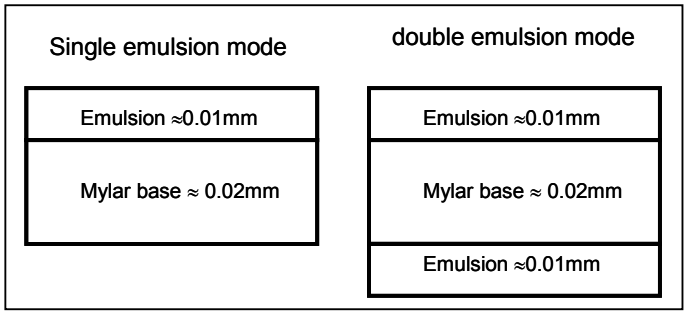

Figure 2.1 Radiographic Film Structure

Most single emulsion films include an annihilation backing on the underside of the base to prevent halo effects or flare around bright objects when light reflects from rear surface of the mylar so passing through the emulsion a second time. An extra protective coat is also used to cover the halide to minimise the abrasion when the film is handled or processed.

The basic photographic emulsion is sensitive to high energy photons in the violet and blue end of the visible spectrum. By adding different types of sensitising dyes to the emulsion, film can be made to react to the entire visible spectrum or to limited portions of it. This response to different wavelengths of light is called colour sensitivity. Film that is sensitive to light over the entire visible spectrum is called panchromatic and is the type used for most general photography.

Different dyes added to make the film sensitive to different wavelengths (spectral response) also change the speed of film. The film speed is classified by ASA (American Standard Association determined film speed or the exposure index (EI) of a film, e.g. a slow film ASA 100 vs a faster film ASA 800.)

When two films containing different concentrations of silver halide in the emulsion are exposed to the same light intensity, different film transmissions will result. Control of the silver halide concentration in the film emulsion during manufacture is used to provide different film contrast and speed.

2.2 History of photography

Four researchers are important in the development of the photographic plate. Joseph Nicephore Niepce (1827) and William Henry Talbot in England (1833) (Schoaf, 2000), Louis J. M. Daguerre [1839], and Hippolyte Bayard (1839),
Each based their work on two well-known fundamental principals:

- The Camera Obscura

  This optical device was commonly used by some artists and scientists to accurately reproduce complex scenes. Light passing through a small aperture in a wall of a darkened room produces an inverted image on the opposite wall rather like a large pinhole camera. Placing a lens in the hole made the image brighter and sharper. The final result was a portable box used by artists as sketching aid.

- Chemical Photosensitivity

  The second technique was a chemical effect first noted by Johann Heinrich Schulze [1727] (Gernsheim, 1955). He discovered that some chemicals, especially silver halides, darkened on exposure to light. Thomas Wedgwood in about 1800 made the first attempt use light sensitive chemicals to record the image of the camera obscura.
  An alternative process using a light sensitised metal surface was developed by Daguerre in 1839.

The word “photography” was coined from the Greek words for light and writing, by Sir John Herschel in (1839). Herschel fixed the transient images formed using silver halides with sodium hyposulphite (a fixative still used today). His choice of fixative was based on his discovery twenty years previously that sodium hyposulphite could dissolve silver salts.

Talbot published the first print on a chemically sensitised paper, exposed to light though the negative in 1840. From 1851 glass replaced Talbot’s paper negative and photography was much as we know it today.

2.3 The Characteristic Curve (figure 2.2)

Initial work by Sir William Abney in the late 1800s *(1800*), *Herschel*, (1*800*) followed by Ferdinand Hurter and Vero Driffield in 1890 led to procedures for characterising film response. Instead of visual comparison of the blackening of a film against a standard film template, a variety of photometers and film densitometers had been developed which measured film transmission ($T = I_{transitted}/I_{incident}$) and later photographic density ($D = \log_{10}(1/T)$).

Hurter and Driffield plotted photographic density against the logarithm of exposure, producing what became known as a 'HD' or 'characteristic' curve. (1890) Hurter and Driffield showed that the film transmission was related to the mass of metallic silver by:

$$\log_{10}\left(\frac{1}{T}\right) \quad \propto \text{ Mass of metallic silver}$$

This is known as the optical density D which is defined as the mass of metallic silver per unit area, so:

$$D = \log_{10}\left(\frac{1}{T}\right) = -\log_{10}(T)$$

Response curves can be obtained using simple, reproducible techniques requiring measurements of a small number of density steps.

The characteristic curves all possess similar properties (figure 2.2).

- Fog level - the section at low exposure where the film density does not change with exposure
- Linear response - the section at higher exposures which is linear
- Saturation - a flattened response at the highest exposures

The response curve can be represented by five numerical characteristics

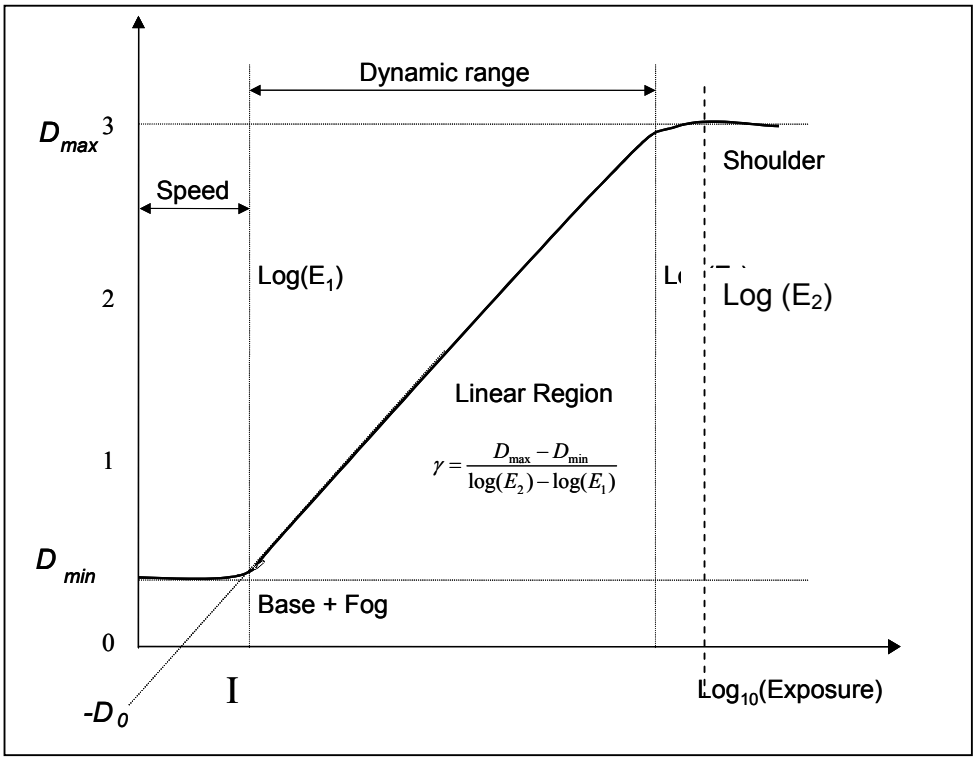

Figure 2.2 The HD Characteristic Curve, presented by Hurter and Driffield 1890

1. Fog or threshold density (D_{min}): The optical density in the region where there is no change of D with log(E) for low exposures (figure 2.3b). This constant *'Fog Level'* is due to chemical fogging during development, thermal effects and the the transmission of the film base (typically $D_{min} \approx 0.2 - 0.3$)
   The minimum useful exposure is determined from the point where the response begins to vary with exposure.
2. Dynamic range or latitude: The range of exposures, E_1 to E_2, between which optical density varies linearly with exposure i.e. $D \propto \log_{10}(E)$

3. Contrast or Film Gamma: The slope of the linear part of the response curve (figure 2.3c)

$$\gamma = \frac{D_2 - D_1}{\log(E_2) - \log(E_1)}$$

4. Speed: The exposure needed to raise the optical density from the base + fog value up to a density of 1.0 above the middle of the range of contrast (commonly 0.5 – 2.0 optical density, Hans,2001) is used to present the film speed (figure 2.3a). And subsequently radiographic film speed is defined as the reciprocal of the absorbed air dose which gives rise to a density of one above threshold (Heggie et.al., 2001)

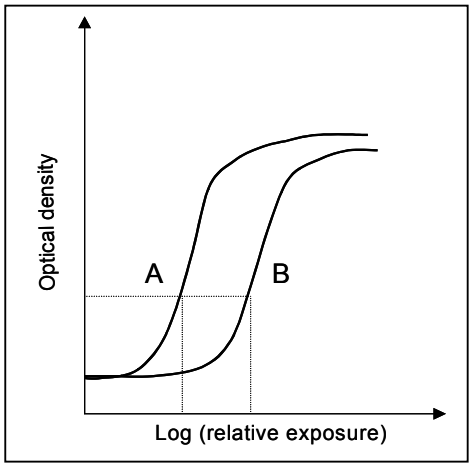

Figure 2.3a curve A and B showing emulsions with different speed

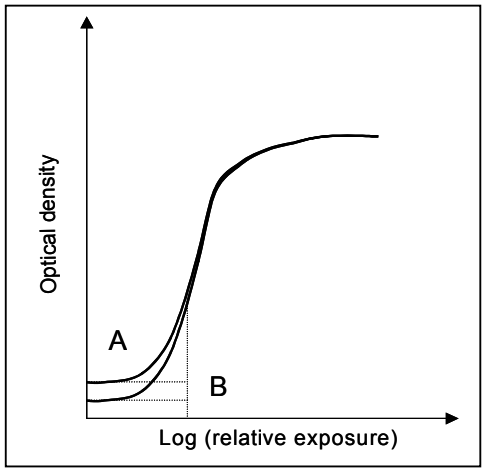

Figure 2.3b curve A and B showing emulsions with different base + fog

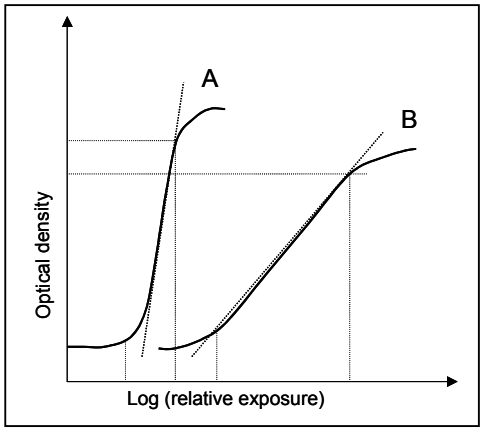

Figure 2.3c curve A and B with different contrast value

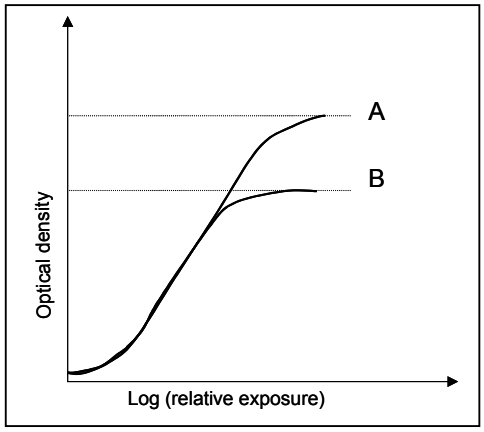

Figure 2.3d curve A and B with different d_{max} value

5. Maximum exposure E_{max}: Saturation density is the exposure (all grains developed into silver) beyond which optical density no longer varies linearly with exposure (figure 2.3d). Typically $D_{max} \approx 3.0 – 4.0$ (0.01% transmittance)

The **base + fog** level represents the optical density reading for the film background noise level after the film has been developed. The background can be affected by the film development temperature, storage conditions, packing, and background radiation.

The **dynamic range** of a film is to some extent linked to **contrast**. A film with large γ has a high contrast useful for x-ray imaging of a narrow range of tissue densities i.e. small dynamic range. On other hand, a wider dynamic range, more useful in the film dosimetry, can be achieved using a film with smaller γ.

The **sensitivity** of film response to the exposure is represented by the **speed** which is the logarithm exposure measured under the integration part with base + fog level. The faster speed film would need less radiation to achieve the exposure to obtain required optical density.

The HD Characteristic Curve provided the basis of all photographic film calibration and continues to be used today for the quantitative measure of film response. It's use has extended beyond photography to provide a tool for the physical testing of X-ray film and film sensitivity to the radiation beams.

2.4 History of Film Dosimetry

Work on the sensitivity of photographic plates, film and papers to visible light was well under way by the late 19^{th} century. The concepts of transmission and optical density and their relationship to exposure continue to be used today to define the characteristics of photographic emulsions.

Thus, when Roentgen (1896) discovered X-rays, glass plates, flexible films, and sensitised papers developed for photography were already available. Rontgen discovered that X-rays were transmitted through optically opaque materials to produce an image on photographic film.

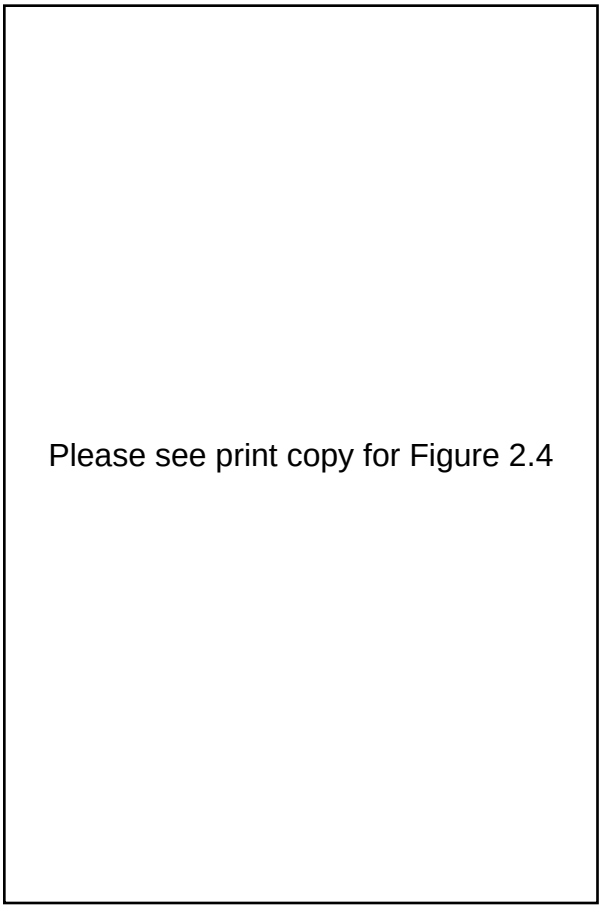

Figure 2.4. First X-ray film, the hand of Mrs. Wilhelm Roentgen: the first X-ray image, 1895 In *Otto Glasser, Wilhelm Conrad Rontgen and the early history of the Roentgen rays. London, 1933. National Library of Medicine.*

He demonstrated his discovery with a radiograph of his wife's hand. (Figure 2.4) Some important points he made in his later publication became the basis of film dosimetry:

- ***Density is a major factor affecting the transparency of materials.***
- ***Increasing thickness reduces transparency.***
- ***Fluorescence is produced in many materials by the radiation.***
- ***Photographic plates respond to exposure by the radiation.***

Soon after Roentgen's discovery of X-rays, Trevert[12], in 1896 measured the response of photographic film to x-rays. This method used visual assessment of the blackness of the exposed film after development. This is the first recorded

example of film dosimetry. However the result was rough because the concepts of dose unit, energy and even the film response and sensitivity were ill defined at that time. One year after Roentgen's discovery, X-rays became used in diagnostic imaging across Europe and North America.

In 1902, Dr. William H. Rollins, a Boston dentist devised a protective housing for an x-ray tube. (Hans, 1997) He placed an unexposed photographic plate against the exterior of the housing to test the shielding, measuring the fogged film after seven minutes exposure. These measurements were qualitative rather than quantitative but provided 2-D information of radiation leakage. X-ray intensities were more commonly measured using ionisation chambers to estimate the charge deposited in the detector.

The basic unit for measuring radiation exposure, the Roentgen (R), was formally adopted by the second International Congress on Radiology in 1928. This unit is defined in terms of air ionization

$$1 \text{ Roentgen} = .02083 \times 10^{11} \text{ ion pairs/cc air.}$$

It is the amount of gamma or x-rays required to produce ions depositing a charge of 0.000258 coulombs/kilogram of air under standard conditions. As a radiation exposure dose unit the Roentgen is also defined as:

$$1 \text{ Roentgen} = 1 \text{ R} = 2.58 \text{ X } 10^{-4} \text{ C/kg}$$

The Roentgen became the primary standard for radiological measurements.

The photon energy dependence of film to radiation was first discussed by Holthausen and Hamann (1932).

The optical density of X-ray film could be calibrated against known X-ray exposures to provide reliable measurements in Roentgen (R). The practical difficulties in simply making visual estimates the blackness of the film were overcome by developing simple film densitometers.

With the development of nuclear physics and experimentation with fission and fusion the need for a simple dosimeter became paramount.
In the early 1940's, military experiments were being undertaken in using film badges for personal radiation monitoring. (*Auxier*, *1980*) Sensitive film badges were commercially developed capable of compensating for the radiation energy dependence. The standard badge holds two pieces of dental X-ray film. One filtered to record only low range (20mR – 20R) and one high-range (1R-400R). These are contained in a silver or cadmium shell 1mm thick, with a window to admit beta radiation. These mass produced film badges led to cheap and effective radiation monitoring. With careful calibration, processing and measurement procedures they provided a means of mass radiation monitoring. During World War II, for testing atmospheric weapons, personnel film badges were widely used by the military. Densitometry readings of the film were also calibrated to an equivalent ionization unit such as mR. These developments lead to a better understanding of film radiation response (Auxier 1980; Pardue et al 1944)

The development of high energy radiotherapy systems in parallel with increasing use of radiography lead to an increasing need for improved quality assurance processes. Film dosimetry was first applied to radiotherapy to measure output and field dose distribution in the 1950's.

High accuracy film densitometers were developed not only for scientific and industrial radiation measurements, but also for use in radiotherapy film procedures. The key components of the simplest system are:

- A stabilised light source.
- A light sensitive detector which measures the transmitted intensity passing through the film.
- Electronics which convert this signal to an optical density.
  This electronics now produces a digital output using an A/D converter, but early systems were analogue.

It should be noted that all modern micro-densitometers physically measure transmitted intensity and film transmission. Very few of them measure density directly.

A wide variety of methods were developed to calibrate film so that it could be used reliably to checking reproducibility and signal linearity and determine radiation dose. Details of practical applications are given by *Granke, 1954*) and Dudly (1956) for high-energy electrons, (*Minet, Garsou J, Chevalier, 1965, Dutreix* 1958, Ovadia & Uhlnann, 1960, Spira, 1962, Dutreix,*1962*)

.

A key to the use of film for dosimetry lies in achieving reproducible dose measurements with an accuracy of at least ±2%. This is best achieved by films with a linear response and high dynamic range.

Considerable effort has gone into overcoming processing and other effects to produce a linear response. However film dosimetry is still unable to provide stable, uniform, and reproducible measurements to carry out absolute dose calibration, unless carefully undertaken to defined procedures.

Increasingly sophisticated. photographic densitometry techniques have been developed. Dynamically controlled film scanning densitometers became commercially available in the late 1960s Joyce, Farrow and Preston, 1960). Parallel developments in astronomy lead to automatic plate measuring machines (GALAXY, COSMOS, Super COSMOS etc) which have been successfully used to digitise plates and films up to 300mm x300mm with resolutions of 10 microns.

Computer advances since 1980 in the areas of fast processing, control systems, display technology and high intensity scanning systems allowed the development of digital scanning systems with high dynamic range accompanied by sophisticated read time and advanced image processing and analysis software,

Together with this computer development the technology associated with radiation film dosimetry has also developed rapidly. Although considerable effort has gone toward improving the reliability and reproducibility of film dosimetry many of the film dosimetry problems previously mentioned still exists.

The International Commission on Radiation Units and Measurements (ICRU) report 35 (*1984*) comments that film dosimetry is "*an empirical method, because the radiation-sensitive medium, the photographic emulsion, does not meet the general requirement for the atomic composition of the biological tissues, and the complex mechanism that transforms the absorption of energy into blackening involves many steps of a physical and chemical nature that are not thoroughly understood.*"' (*Page 92, ICRU report 35*)

The ICRP (International Commission on Radiological Protection) response clearly identifies the practical difficulties arising in the use of film. Film is influenced by many variable factors; such as emulsion halide grain quality, radiation response linearity, film exposure, energy and medium depth dependencies, processing chemical pH, temperature, artefacts, and latent image factors. Dosimetry results are also sensitive to the densitometry equipment used, warm-up factors and background signal level control etc. All of these problems make qualitative measurements difficult and negate several research results. All of these factors must be controlled if film is to be used as in dosimetry.

Chapter 3. Film Processing in Medical Imaging

3.1 Introduction

If we are to use film as an accurate and reproducible dosimeter then we must fully understand its characteristics and their effect on dose measurement procedures. As we saw in Chapter 2 considerable work has been carried and on the response of film to visible light. This work provides the basis for characterising the radiographic film response to photon and electron beams.

3.2 Film grains, sensitivity and contrast

Film Base and Emulsion

Both photographic film and radiographic film commonly take the form of a polyester base coated with either single or double emulsion. The base material is transparent providing mechanical stability for the handling. The emulsion layer is made of silver halide grains precipitated in a gelatine layer.

Silver Halide Emulsion Grains

The halide compound, AgBr is most commonly used in photographic film emulsions and was used as early in 1888 (Hans & Jashitski, 1997). The micro-crystal tabular or cubic shape grains have an average size of about 2μm in diameter and 0.13μm in thickness and embedded throughout the 0.01mm thickness gelatine layer, which can be easily penetrated by the developer and fixer.

Sensitivity is affected by grain size

The size of an emulsion grain can affect the film sensitivity to the light. Theoretically larger grain surfaces can absorb more photons to make the film faster, e.g. less exposure required to obtain the same amount of film density.

Contrast is affected by the type of the grain

Tabular and cubic grains are commonly used in most photographic and medical imaging films. Tabular grain shape present a larger projected area to the incident light so the speed is faster compared with the cubic grain emulsion. As the light absorption is more concentrated toward the surface of the emulsion layer, the tabular grain also helps to improve the image sharpness. The cubic grain can absorb light in the deeper layers of emulsion more easily as the light can more easily penetrate between the crystals. For this reason, the cubic grain can give better contrast compared with tabular grain. In medical imaging, cubic grains are used in mammography films since they give better contrast in the toe of the characteristic curve. The cubic grain also has the characteristic of uniformity and spectral sensitivity. Since 1980, other shapes of grains have been replaced by tabular and cubic especially in films designed for astronomical, photographic and X-ray use (Figure 3.1).

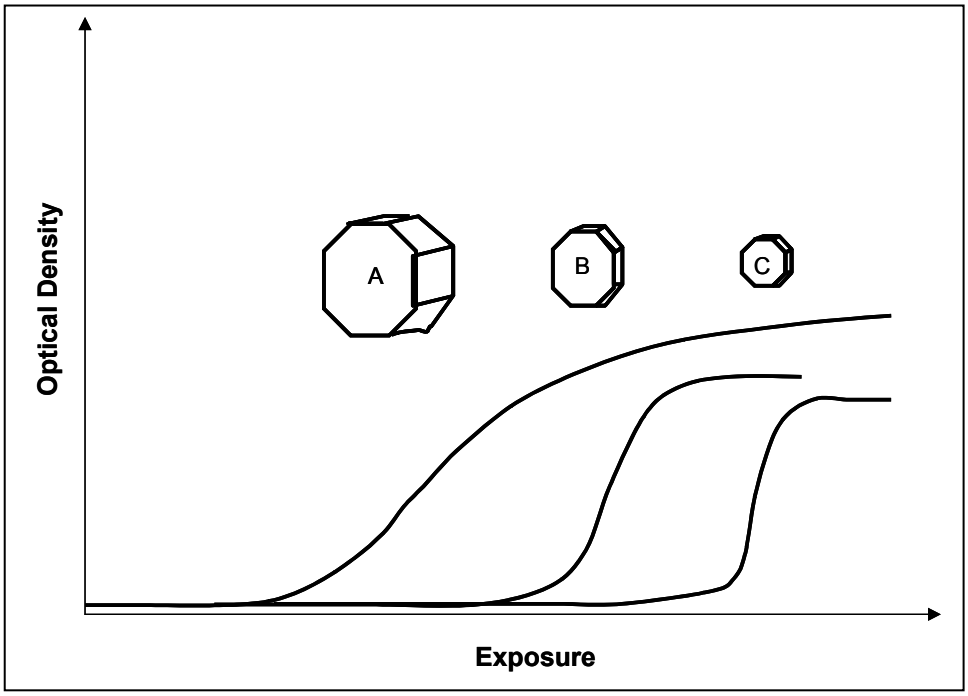

Figure 3.1 Film speed and contrast characteristic curves for tabular grain, depending on emulsion grain diameters.

3.3 The Photographic Process

The three stages of the photographic film process shown in figure 3.2 are:

- Exposure to form a latent image
- Use of chemical developer to convert the latent image to silver metal by an electron transfer reaction (reduction process)
- Use of a fixer chemical to remove the unexposed silver grains, to stabilize the developed image

Latent image process producing (Figure 3.2)

When a light photon or x-ray is interacts with a silver halide grain in the emulsion, it is absorbed into silver bromine and produces a silver ion, a bromine atom with positive charge and a mobile electron. The mobile electron becomes trapped at dislocations or at a sensitivity speck. The enhanced negative charge attracts the positive charged silver ions. The latent image formed is unstable because the electron holes can recombine and lead to the distinctions of the latent image (Figure 3.3).

Latent image with chemical development

A latent image may form a useful image by the following chemical development process:

1. Diffusion of developer reducing agent into emulsion.
2. Adsorption of developer at latent image centers.
3. Transfer of electron to latent image centres.
4. Regeneration of electron transfer agent by hydro-guanines
5. Reduction of silver halide to metallic silver.

The silver metal atoms contained in the halide grain act as a catalyst in the chemical process. The silver ions in the exposed grain are converted to black metallic silver. (Hans and Jashulski 1997)

The chemical used for developing is formed by four main components:

- Developing agents – to convert exposed grains from silver halide into metallic silver, and also maintain the pH level and the development rate
- Restrainers – to minimise fog by protecting unexposed grains
- Hardeners – to harden the emulsion to protect the film from mechanical abrasion
- Solvents – Water is used as the primary solvent in the developer solution

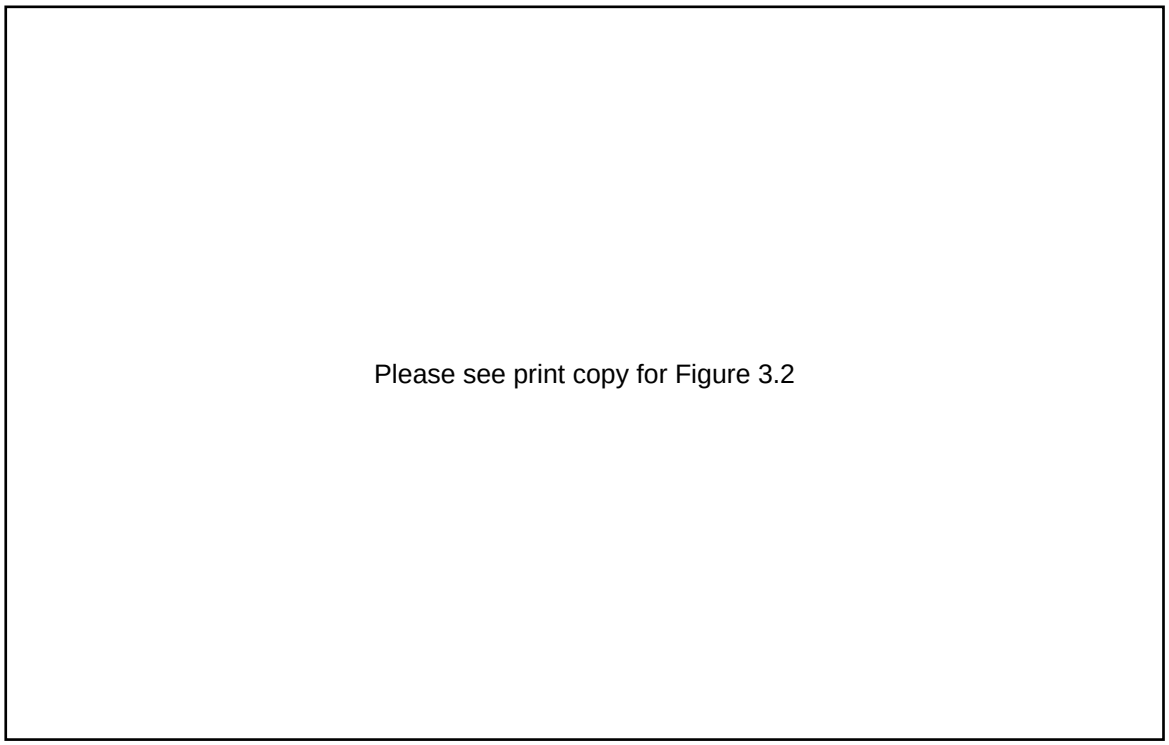

Figure 3.2 Eastman Kodak Company X-ray film processing action diagram

In a, latent image created after the exposure.
In b, metallic silver has began to produce by partial development.
In c, completed development before the fixing process.
In d, the fixing process removed the unexposed silver grain.

(Arthur G. Haus, Susan M. Jaskulski, 1997)

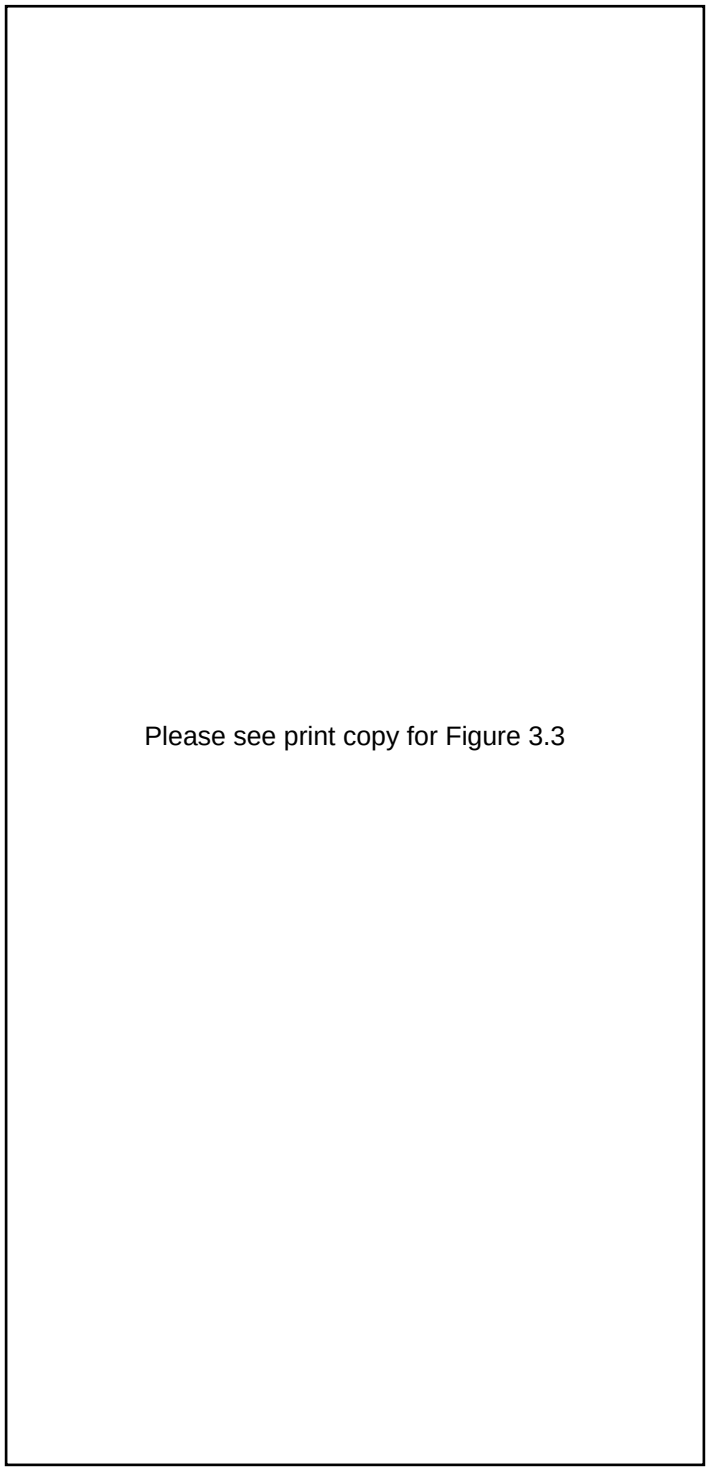

Figure 3.3 Latent image stages.

(Arthur G. Haus, Susan M. Jaskulski, 1997)

Fixation of developed image

The development sequence leaves unexposed silver halide grains which may be further exposed and blacken the final image. The unexposed silver halide must be removed using a process called fixing, leaving behind the metallic silver to form stable image. The development process must be followed by washing, fixing and drying.

The fixer consists of:

- Fixing agent – a very common fixer is sodium thiosulfate. It dissolves out the undeveloped silver ions from the gelatin.
- Preservative Agent – added to prevent some thiosulfates from oxidizing, staining the emulsion.
- Hardener – to harden the emulsion during fixing process and so reduce the water absorption during the washing stage to make for easier drying and improve the stability of the emulsion.
- Buffer - to keep the pH level more stable.
- Sequestering Agents - Some carboxylic acids are used to prevent the hydroxide forming when the film is carried from developer over into the fixer.

3.4 The effects of development and fixing process on the characteristic curve

Identical films may exhibit different characteristics if developed in different developers, or with at different temperatures or for different processing times. The manufacturer provides specific developers to optimise the film response.

The use of different developers or development procedures can change the film contrast and speed.

Processor design and Film development Quality Assurance

The latent image needs careful processing to become a visible image.

For photometric accuracy all developing, fixing, washing and drying procedures must be performed using well-designed and maintained mechanical film processors. These automatically control the processing time, speed, chemical pH and temperature etc. (Figure 3.4)

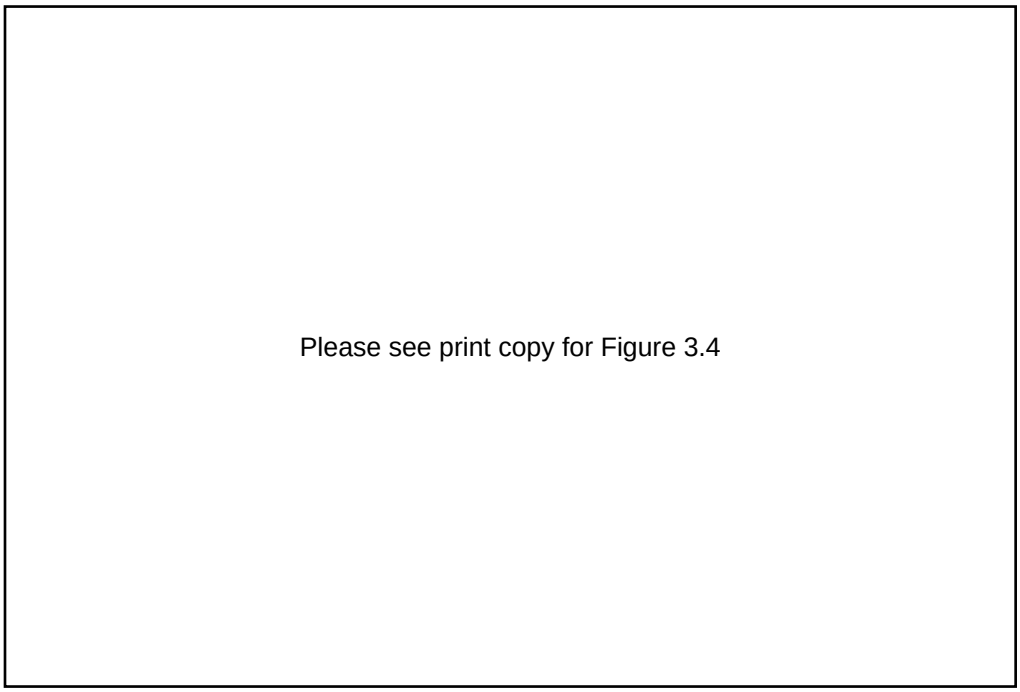

Figure 3.4 Diagram of one Eastman Kodak typical automatic film processor (Arthur G. Haus, Susan M. Jaskulski, 1997)

The maintenance and quality control of such processors are extremely important if the film is to be used for the film dosimetry. Lack of proper maintenance and QA can cause processing artefacts that reduce the photometric accuracy (Figure 3.5).

Errors introduced in processing can lead to poor calibration of the film leading to large errors in dosimetric measurements. An error of 0.1 optical densities could give about 5.0% of percentage change in dose value (Figure 3.6).

Film processing artefacts can be produced by the film rollers in the form of non uniformities such as steaks, entrance roller marks, guide shoe marks or chatter. Any of these artifacts could introduce random errors and make the film useless for QA purposes. Since each of the above artefacts has a different appearance, the performance of the processor should be monitored by processing an unexposed high sensitivity x-ray film at regular intervals.

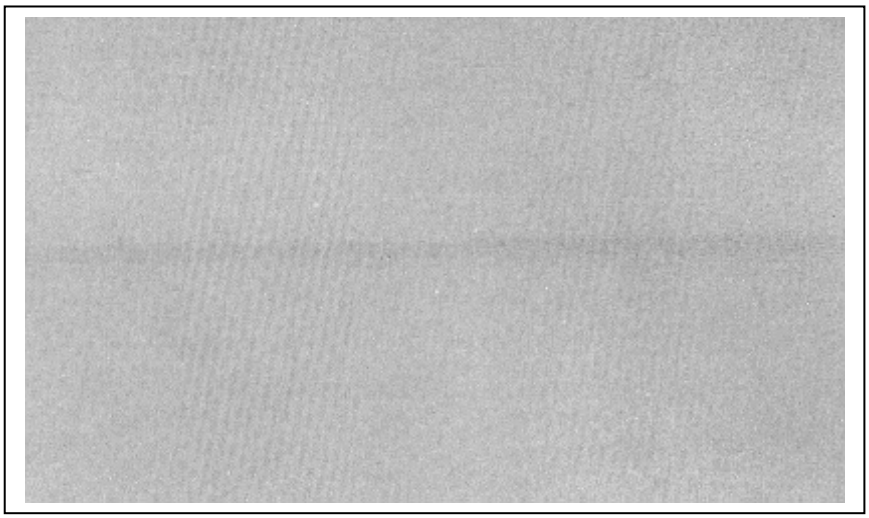

Figure 3.5 Artifact produced by processor rolling mark via film development.

The quality of the film image can also be affected by poor storage and handling of the film both before and after use. The film arrives from the manufacturer packaged in water proof wrapping. When stored it is affected by both heat and moisture which degrade opened films. Radiography film should be stored at between 10 and 21 degrees C. and at a relative humidity of between 30 to 50 percent[13]. The film should be stored on edge and not horizontally to avoid films on the bottom being weighed down by other packages or boxes. The film should also be kept away from X-ray and other radioactive materials. (Hans, 1997)

Please see print copy for Figure 3.6

Figure 3.6 An example of daily QA protocol for a darkroom and film Processor defined for radiotherapy department by this study

Chapter 4 Dosimetric Concepts in Radiotherapy

4.1 An overview of the Linear Accelerator (LINAC)

Linear Accelerators are designed for high-energy external beam radiotherapy, and their components and functions can be discussed under the following seven main parts: (Figure 4.1)

- A Klystron/Magnetron providing radiofrequency [RF] source for the accelerating waveguide. An AFC (Automatic Frequency Control) adjusts the RF frequency according to the accelerator feedback signal. The klystron is housed in the rear, fixed section of the LINAC.
- A Pulse Forming Network [PFN] in the modulator part of the LINAC generates the RF pulse.
- The electron gun and waveguide housed in the machine gantry (rotary part) provides a beam of high energy electrons. Electrons emitted by the electron gun (controlled by PFN) and injected into the waveguide, are accelerated from the injection velocity (low energy kilo-voltage) to produce a high energy beam (Mega voltage) using a vacuum microwave field.
- A bending magnet system is used to steer the beam through 270 degrees so that it enters the LINAC head and collimator system. The primary collimation system in head consists of a collimation cone which called primary collimation, beam scattering foil and flattening filter. The electron beam is further collimated by mounted electron applicator with inserting alloy cutout.

  A heavy metal target is incorporated for high-energy photon beam generation. The photon beam is collimated by the second collimator system, which consists of two pairs of collimator jaws, or a multi-leaf collimation system.
- A control console system designed for the control of machine and treatment plan delivery.
- A couch is designed to support the patient during delivery and treatment set-up.

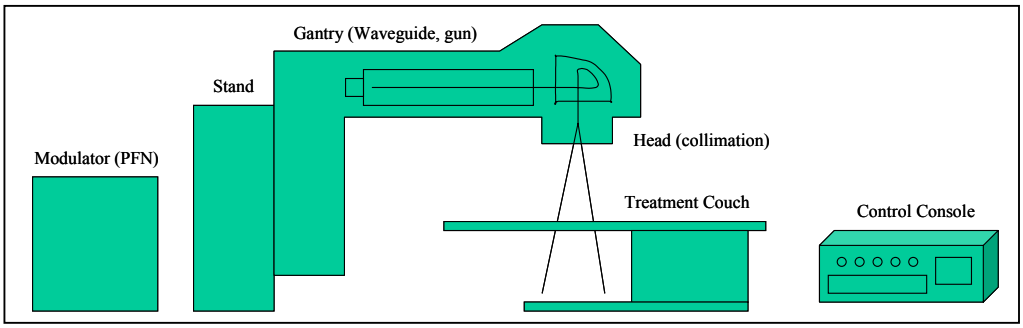

Figure 4.1 Diagram for a linear accelerator component

4.2 Quality Assurance requirement for the Radiotherapy

This chapter provides a summary to the dosimetry and quality assurance (QA) required in clinical radiotherapy.

The prime objective of radiotherapy is to deliver a lethal dose of radiation to a diseased target region while sparing surrounding healthy tissue. It is therefore important to ensure that the lethal dose:

- Is delivered to the precise target region
- Is accurate to ±3% and that the dose to surrounding tissue is below a critical level.

The sequence in a radiotherapy treatment involves:

Identifying the treatment volume from examination and medical imaging

- Choice of irradiation; photons, electrons, or a mixed field
- Choice of beam energy, field size, and number
- Selection of the number of dose fractions, dose per fraction and total dose
- Delivery of prescribed dose to within ±3% to ±5%

([21]ICRU report No. 50, 1993)

4.3 Dosimetry and Quality Assurance Procedures

In order to ensure the proper and accurate delivery of the dose required by the treatment plan we must undertake the following procedures:

- Isocentric mechanical alignment and accuracy check
- Absolute dose output calibration
- Dose distribution analysis for the radiation field

- Verification and individual check for planning dose calculation vs physical treatment delivery

4.3.1 Isocentric mechanical alignment and accuracy check – includes the alignment of the radiation beam centre with the gantry and collimator rotation centre, the laser localization system, the light vs radiation field coincidence (which the light field is a side located light source reflected to the radiation area by a mirror). Slow speed radiographic film designed for the high-energy beam verification uses is widely used for this QA work.

4.3.2 Absolute dose output calibration – Ionization measurements in a body tissue equivalent medium (water or solid phantom) refer to the Primary Reference Dosimetry Measurement (ICRU, 1976) and the clinical routine calibration protocols (IAEA, 1987; IAEA, 1997; AAPM, 1983; AAPM, 1999; IAEA, 2000)

The beam-on monitor unit must be calibrated against the absorbed dose unit in Gy (or cGy). This is commonly undertaken using an ionization chamber in a full scatter water phantom with the ionization chamber set in a reference depth in the water. The absolute dose calibration must follow the protocols provided by above documents, according to the appropriate national regulation.

4.3.3 Dose distribution in radiation field analysis - When a collimated radiation beam irradiates a medium to produce a radiation field, the intensity of the radiation dose distribution in the field varies with depth and off –axis distance.

Contours of equal dose displayed in either 2D or 3D used to represent regions of equal dose level are called isodose curves. The importance of measuring the isodose in radiotherapy is that it allows us to describe the dose distribution in treatment planning where a radiation field or a group of fields or combined beams are to be used. The isodose determines the effective treatment region based on a given maximum dose to the target region while protecting other organs and normal tissues which receive minimum dose.

The Isodose also helps the medical physicist to evaluate the beam quality, uniformity and accuracy. By checking the Isodose distribution regularly they can quality assure the radiotherapy equipment.

4.3.4 Planning dose vs physical treatment dose delivery – includes independent monitor unit calculations based on the ionization measurement data. In 3D and IMRT planning checks, point dose verification measurement is performed using by ionization or thermo luminescent dosimetry (TLD), with dose distribution for the target volume checked by film dosimetry.

It is important to define some important terms used in discussing the field dose distribution analysis

4.3.5 Tissue Air Ratio (TAR) and Tissue Phantom Ratio (TPR) - TAR (Tissue air ratio) was originally introduced for the rotational treatment before the computer planning techniques were developed. In Kahn (The Physics of Radiation Therapy, 1984), the TAR is defined as the use of dose calculation for the rotation treatment technique which the gantry rotated with a constancy isocentre but varied tissue thickness corresponding to different gantry angle position, that means the radiation source moves isocetrically with varied SSD. TAR defined as the ratio of the dose (D_d) at a given point in the phantom to the dose in free space (D_{fs}) at the same point:

$$TAR(d, r_d) = \frac{D_d}{D_{fs}}$$

It is important to determine two quantities prior to delivery of a radiotherapy dose:

- The dose in air at a given distance from the exit window
- The dose in tissue (phantom) at a fixed position when all machine parameters are constant (energy, field, fluence and collimation characteristics)

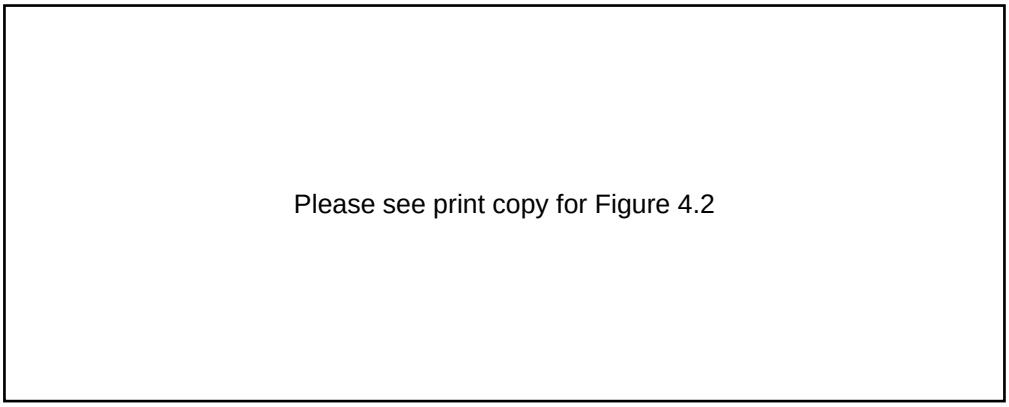

Figure 4.2, Tissue-Phantom Ratio defined by F.A. Smith, Applied Radiation Physics, World Supply, 1983

Figure 4.2 shows three setups where the beam width is the same at distance r_0. The dose at P_0 in air is D_0, the dose in the phantom (D_1 and D_2) depends on the distance between phantom and exit window (r_1 and r_2) and the TAR depends only on the field size and photon energy.

Figure 4.2 shows how TAR can be technically measured. The performance of the measurement is commonly replaced by the calculation which the relationship between PDD and TAR value can be represented by following equation:

$$PDD(d,r,f) = TAR(d,r_d) \times \frac{1}{BSF(r)} \times \left(\frac{f + d_m}{f + d} \right)^2$$

Where the TAR(d,r_d) is the tissue air ratio at same point for a field size r_d at depth d, r is the field size at the surface, f is the SSD, and d_m be the dose in free space. The TAR is commonly calculated from the PDD as the relation between point PDD and TAR using the Inverse Square Law and Back Scatter Factor (BSF). That because the TAR curve scan is more difficult to practically perform compare with PDD curve scan in a water phantom with in-consistency water surface to be vary continually with ionization chamber fixed position to the beam and accurately scan a TAR curve commonly need using point measurement technique causes measurement time significantly longer than

PDD measurement. In clinical used the TPR and TAR for each measurement point is commonly converted from PDD value for equivalent Tissue to Phantom Ratio (TPR).

4.3.6 Percentage Depth Dose (PDD or %DD)

Percentage depth dose is the beam quality and distribution in the depth of water equivalent medium. The central axis dose distribution is characterized by normalizing the dose at depth with respect to dose at a reference depth. The percentage depth dose (PDD or %DD) is defined as a percentage of the absorbed dose at any depth d to the absorbed dose at a fixed reference depth d_o along the central axis of the beam percentage depth dose is thus:

$$\%DD = \frac{D_d}{D_{d_o}} \times 100$$

For orthovoltage (up to about 400kVp) and lower energy x-rays, the reference depth is usually the surface ($d_o = 0$). For higher energies, the reference depth is taken at the position of the peak absorbed dose ($d_o = d_m$) (Figure 4.3). In clinical practice, the peak absorbed dose on the central axis is sometimes called the maximum dose, the dose maximum, the given dose, or simply the D_{max} (Figure 4.3)

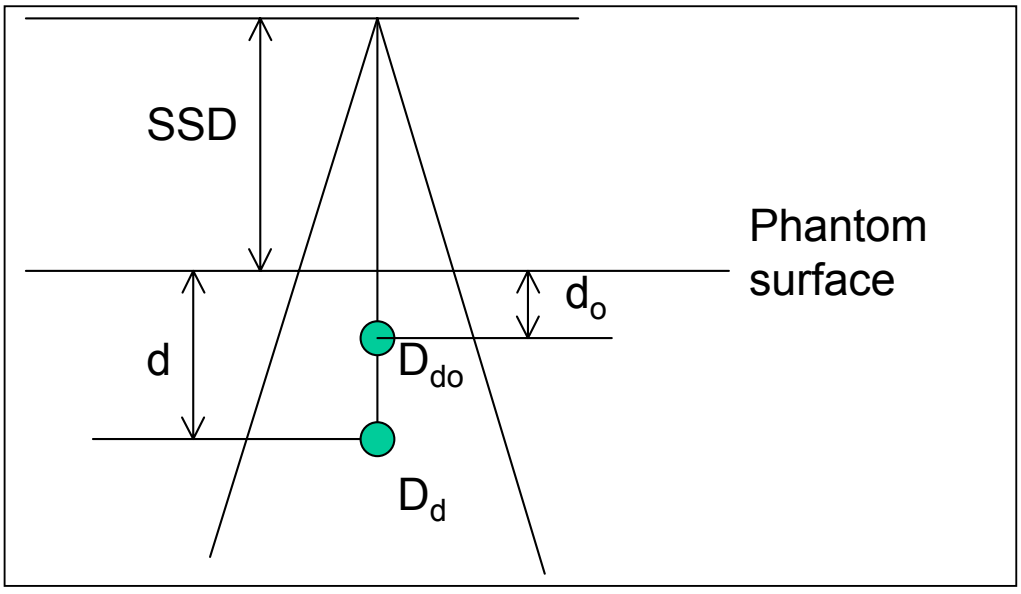

Figure 4.3 Ionization measurement setup for the measurement of percentage depth dose (PDD)

Percentage depth dose is dependent on the beam energy, source to surface distance (SSD), equivalent square field size, and medium density value. Longer source to surface distances in air cause the softer lower energy beam components to be absorbed by the air, hardening the beam proportionally and resulting in an increase in the percentage of depth dose. Smaller field sizes result in more scattering from the collimator jaws (collimator scattering factor S_c) and phantom (phantom scattering factor S_p) than larger sized fields (Figure 4.4). This increases dose at shallow depths and proportionally reduces the percentage depth dose. When the field size increases, the scatter absorbed by the phantom proportionally decreases, the build up medium influences the central-axis dose distribution, increase the percentage depth dose. However, the low energies scattered from the collimator jaw have a shorter traveling distance in the phantom medium. Therefore when the field size increases above a certain amount, this increases the build up thickness from the field edge to the central axis, and the scatter becomes a less important issue. The percentage depth dose will not increase any more.

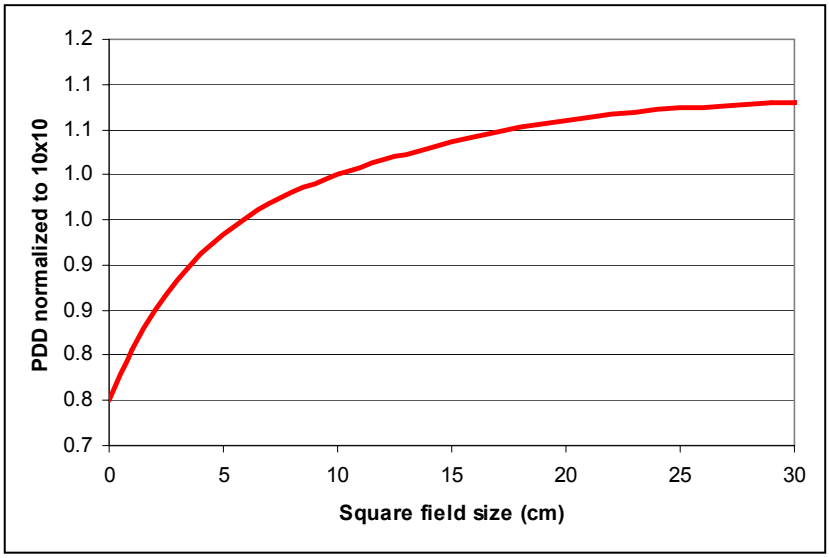

Figure 4.4 PDD value influenced by field size caused by collimator scatter in proportion causes output factor changes at dose reference measurement point

The best way to measure the percentage depth dose is by using an ionization detector to measure the dose at a number of different depths along the field central axis. This method is used for clinical planning data measurement. However, for routine quality assurance checks, the regular setting up of a water

scanning system in any radiotherapy centre means a heavy workload for the clinical physicists. The water scan is commonly only performed once a year or after a major equipment service. Although the film dosimetry is less accurate than the water scan, it easily set up and the reduction the radiation exposure delivered by the therapy equipment is an advantage. The film also provides easily visualized images. According to the AAPM (1994) and ACPSEM (1997) quality assurance practice code, beam quality should be checked at least monthly. Film dosimetry is a convenient way to carry out these QA tasks.

Percentage depth dose curve analysis

The Percentage Depth Dose [PDD] for a reference field size (e.g. 10cm x 10cm) normally is used to characterize the energy and intensity of a radiation beam and the dose variation with depth in tissue equivalent material. The PDD is clinically important in treatment dose calculation for a given depth of cancer target area. The PDD is also used in the treatment planning computer system data modeling. Comparison of the changes in PDD over time allow one to monitor the beam stability and to confirm the accuracy of planning data calculation. In analyzing the PDD curve, the following parameters / characteristics are important:

For photon beams according to IAEA protocol (Figure 4.5)

R_{100} – depth of 100% dose

R_{50} – depth of 50% dose

D_{10} – the percentage dose value at 10cm depth

D_{20} – the percentage dose value at 20cm depth

D_{20}/D_{10} – the ratio of D_{10} and D_{20}

For Electron beams (Figure 4.6)

R_{100} – depth of 100% dose

R_{50} – depth of 50% dose

R_p – practical range of the beam

E_o – mean energy of the beam determined by: $2.33 \times R_{50}$

$E_{p(o)}$ – most probable energy defined as: $0.22 + 1.98R_p + 0.0025R_p^2$

D_x – bremsstrahlung contamination of electron beam.

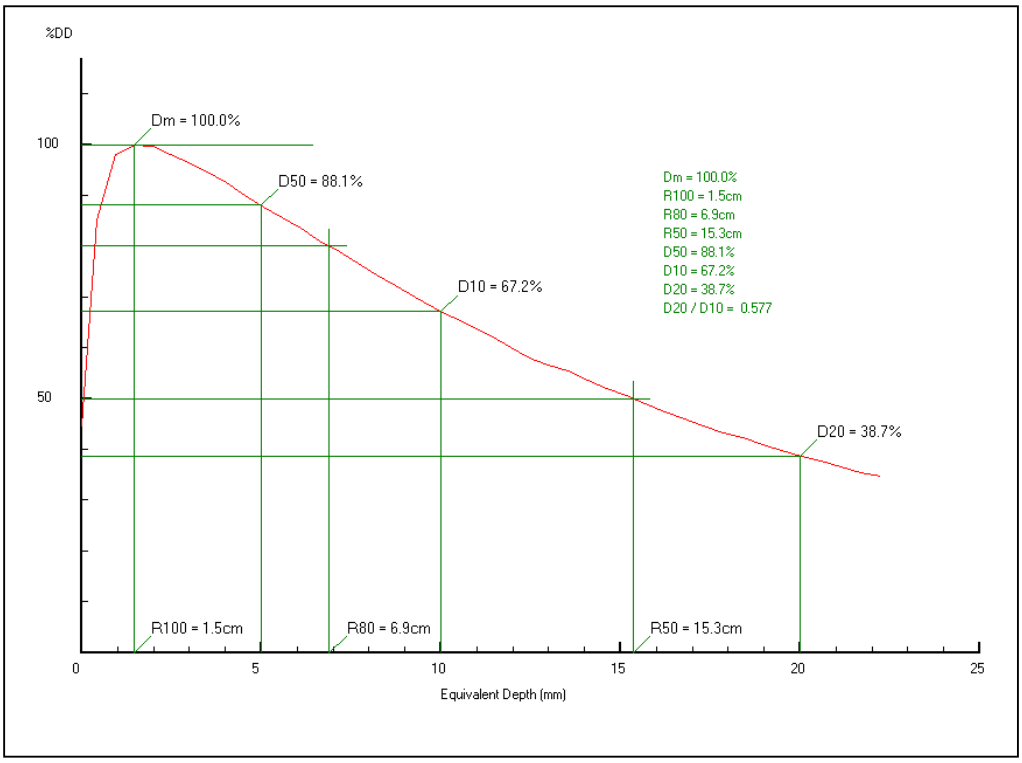

Figure 4.5 Photon PDD analysis figures

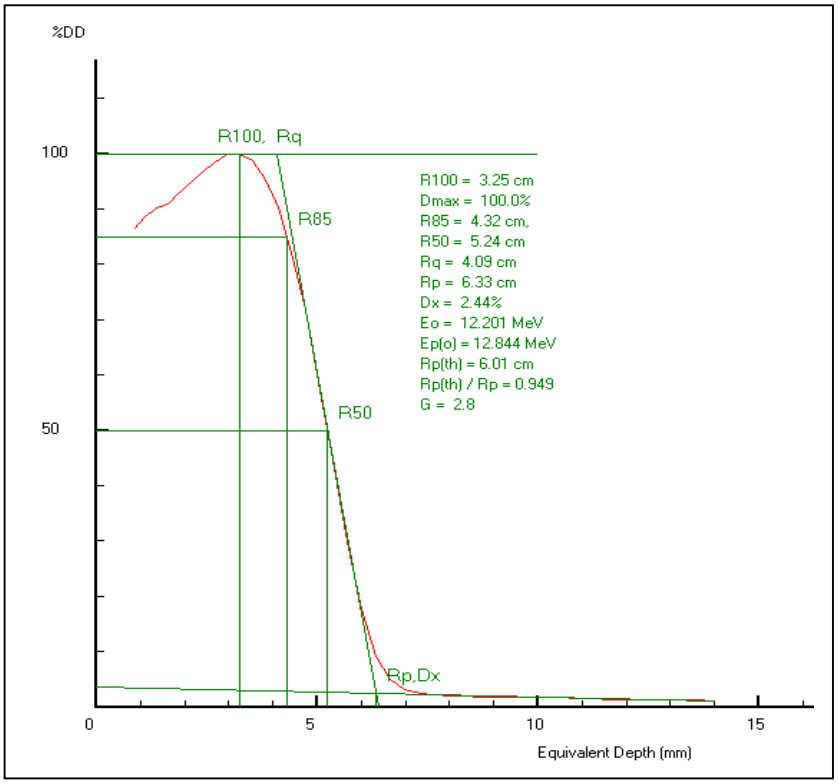

Figure 4.6 Electron beam PDD analysis figures

4.3.8 Profile Curve and Symmetry / Flatness Analysis (OAR / OCR) - It is important to check the beam profile to confirm the flatness of the dose distribution over the treatment area and the symmetry of the profile at the field edge. The radiation dose distribution in a radiation field is measured as the percentage dose along the cross-plane/in-plane beam perpendicular direction at a given depth of water, and normalising this to the reading at the beam central axis (Figure 4.7). The measurement is normally carried out using a water phantom. The profile curve is also called flatness curve (Figure 4.8).

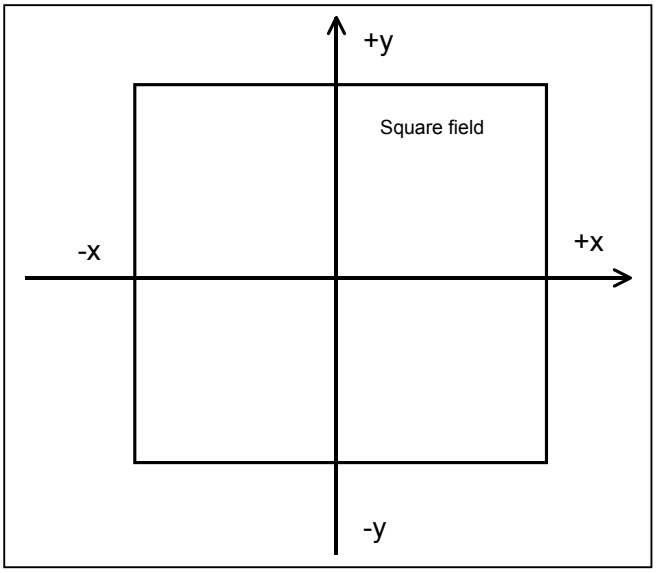

Figure 4.7 Profile scan for a square field along the central axis

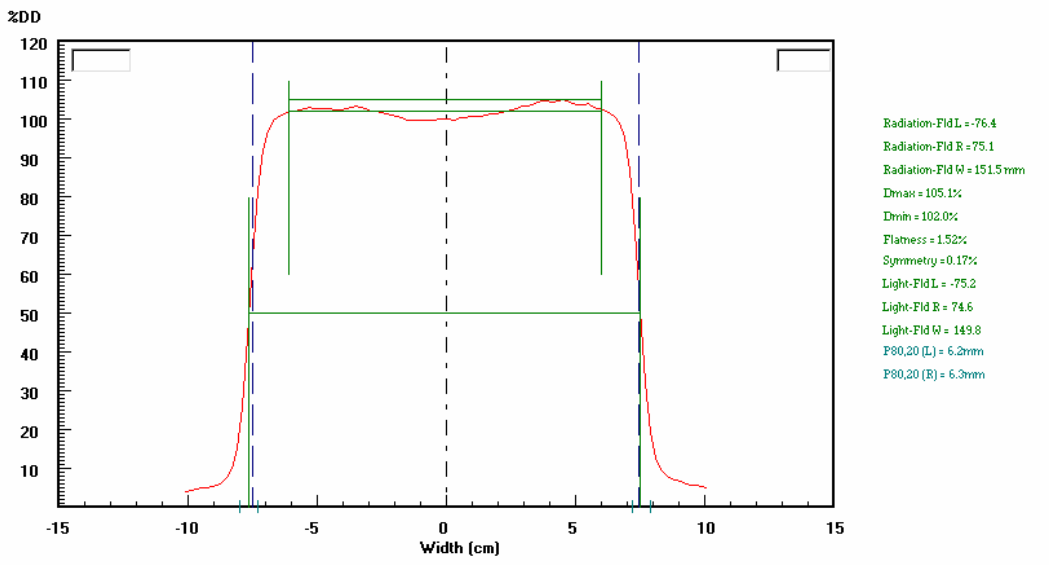

Figure 4.8 Profile curve analysis

The QA profile checks form an important part of routine work tasks for the medical physicist. For routine quality assurance purposes it can be performed using many different techniques such as multiple detector solid phantom measurement, air ionization scanning, film dosimetry or TLD point measurement arrays. The profile measurement for the planning data can also be made using an ionization detector and water scanning techniques. The analysis result includes flatness, symmetry, radiation isocentre, and radiation - light field coincidence.

Several protocols have been developed and commonly used around the world for flatness and symmetry analysis. Metcalfe and Kron (1997) in "The Physics of Radiotherapy X-rays from Linear Accelerator" addressed the most common quantitative measures following the IEC guidelines (1989)

The percentage flatness (%F) is assessed by finding the maximum (D_{max}) and minimum (D_{min}) dose point values on the profile within 80% of the beam width.

$$\%F = \left(\frac{D_{\max} - D_{\min}}{D_{\max} + D_{\min}} \right) \times 100$$

The symmetry calculation can be divided into an area under profile calculation and a mirror comparison. The area calculation is the integrated dose distributed between 80% of field size from the central axis. The formula gives:

$$\%S = \left(\frac{Area_L - Area_R}{Area_L + Area_R} \right) \times 100$$

The $Area_L$ is the area of the dose distribution range integrated the region from left size of 80% field side to the beam central axis, and $Area_R$ is for the right side of the field (Figure 4.9).

In machine maintenance and engineering checks, the IEC protocol for the mirror symmetry is also often used to compare the dose distribution percentage pair corresponding each side of measurement point.

$$\%S = \left| \frac{D_L}{D_R} \right| \times 100$$

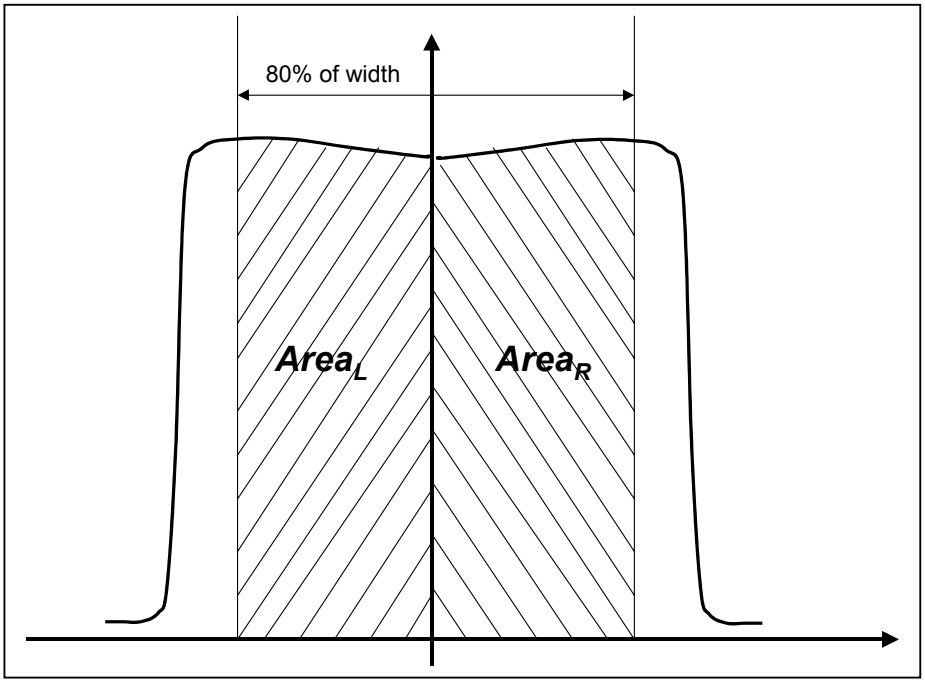

Figure 4.9. 80% of field width area compared for the symmetry analysis

Where D_L and D_R are the dose ranges compared from the left, the right side of beam with same distance off to the beam central axis (Figure 4.10).

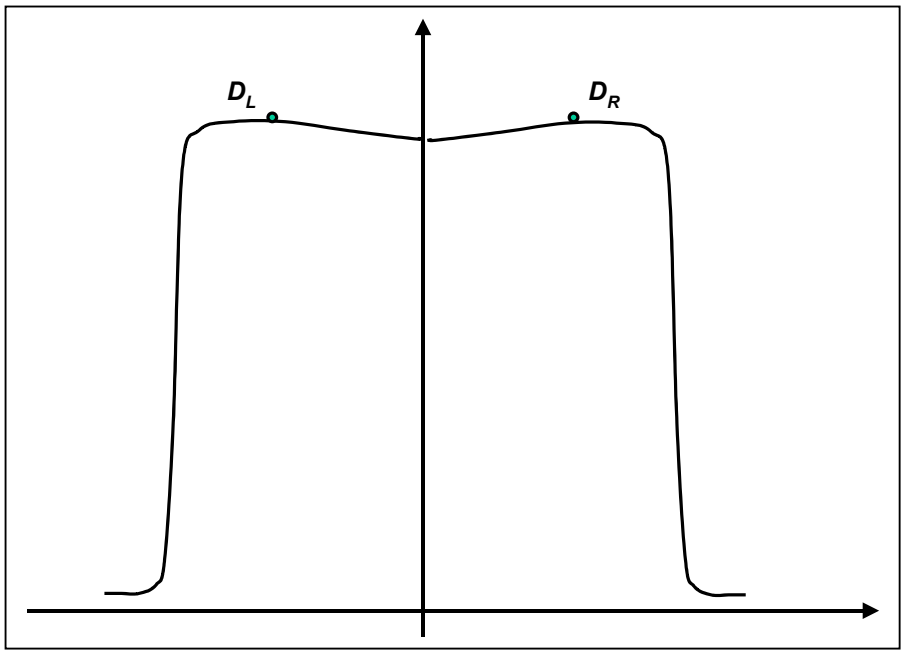

Figure 4.10 IEC field symmetry analysis corresponding dose level comparison

The uses of the beam profile for the light-radiation coincidence check is also one of the important QA checks. On most of radiotherapy treatment units, the projected light field indicates on the patient's skin where the treatment field will irradiate the patient. Aligning the light field with marks or anatomical features of the patient is an important part of the patient setup. This requires the subjective judgment of the location of the edge of the light field when positioning the treatment field and aligning the shielding blocks. The task becomes even more important when margins are decreased in the conformal treatment. In addition, the light field is of great importance a multiple beam combined fields.

The coincidence between the radiation and light field can also be checked by either water ionisation scanning or film dosimetry. The position of the edge of the light field is compared with the 50% intensity of the radiation field. The light field is set according to the machine mechanical isocentre. The radiation field edge and radiation isocentre position must be aligned to match the light. (Figure 4.11)

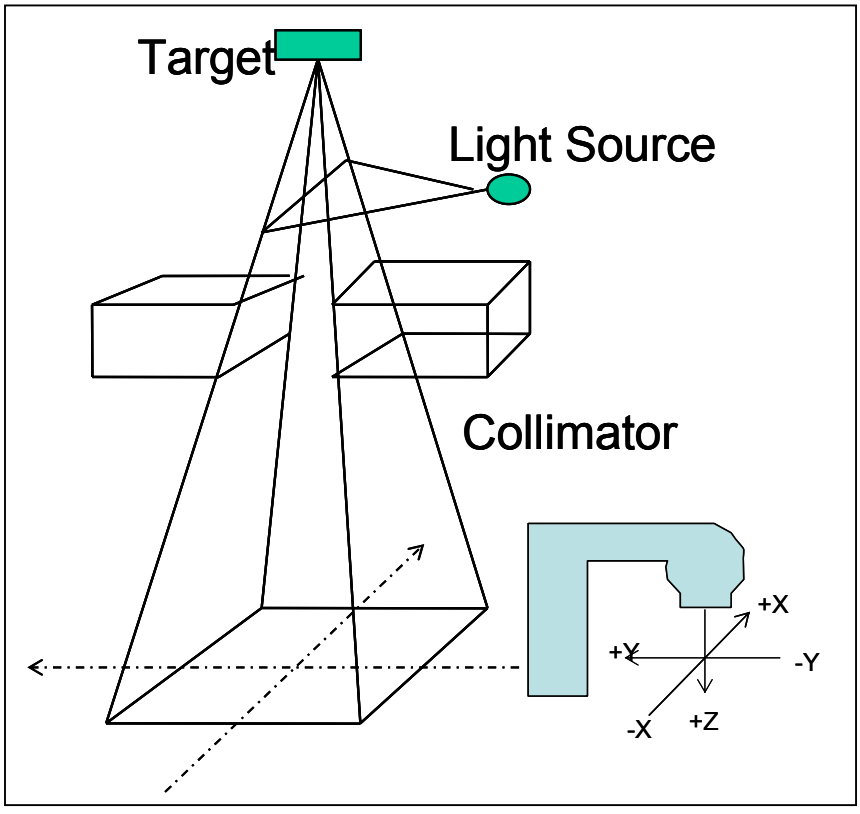

Figure 4.11 Photon-field alignments

Since this check is performed more frequently and it is a compulsory weekly or monthly QA check, film dosimetry is the most commonly used technique. The film can be analyzed visually if there is no proper film densitometry facility. The analysis of the image is very approximate and dependent on the physicist's experience, because of the difficulty in judging the 50% optical density visually. Film analysis using a densitometer or pixel scanner increases the accuracy of the alignment and can be performed by a well-designed software analysis program.

Chapter 5 Digital Densitometry Equipment - Film scanners

5.1 Introduction

This study assesses the use of desktop scanners to create a bitmap image suitable for QA procedures. Analysis of greyscale images to produce dose distribution curves (including percentage depth dose (PDD), profile and isodose distributions) allows a comparison of the dose delivered by the equipment with the Treatment Planning System (TPS) calculations. The point dose is commonly checked by using ionisation chambers. Using film dosimetry, 2-D dose distribution maps can be produced providing a powerful QA tool.

The development of film photometry systems has paralleled that of photographic science. Early photometers were based on direct visual comparison of the beam passing through the plate with a comparison beam of variable intensity. This variation was achieved by various means including neutral density filters, source distance and power delivered to a filament lamp. With the advent of electronic circuitry in the form of amplifiers and comparators and A/D converters more sophisticated comparison techniques became available. Accurate densitometers required either an exceptionally stable light source or a dual-beam system.

Forty years ago, 2-D densitometers were very specialised products and were used only by experts, mainly working in professional publishing and astronomy. Today a number of these specialist systems are operating mainly to support the digitising wide field astronomical photographic surveys (Super-COSMOS, PDS, APM, Pratt, 1974; Hambly, Mille MacGittiuray, Herd & Cornack 1998; Podd, 1972; Liwin, 2003). Their purchase price and operating costs are prohibitive and they require controlled environments and specialist maintenance.

A few x-ray film scanners and laser digitisers which give the high resolution and dynamic range necessary for radiation dosimetry have been developed

and used in hospitals for specialist research projects. However, most of them are too expensive to be easily considered by a radiotherapy department for the routine radiation field quality assurance checks.

The development of the modern personal computer has in form led to the development of low cost, desktop scanners which are both mechanically rugged and simple to use. A clinical assessment has been undertaken a technical assessment of the possibilities of using a desktop scanner for routine QA in radiotherapy.

5.2 Historical Background to Film Digitisation

All densitometers are based on the comparison of the transmitted intensity through the film with the incident intensity. This transmission value may be digitised directly or converted to an optical density. Figure 5.1 is a design of film densitometer first used by Macbeth[1] in early 1965. The higher the film optical density, the lower the amount of light is transmitted.

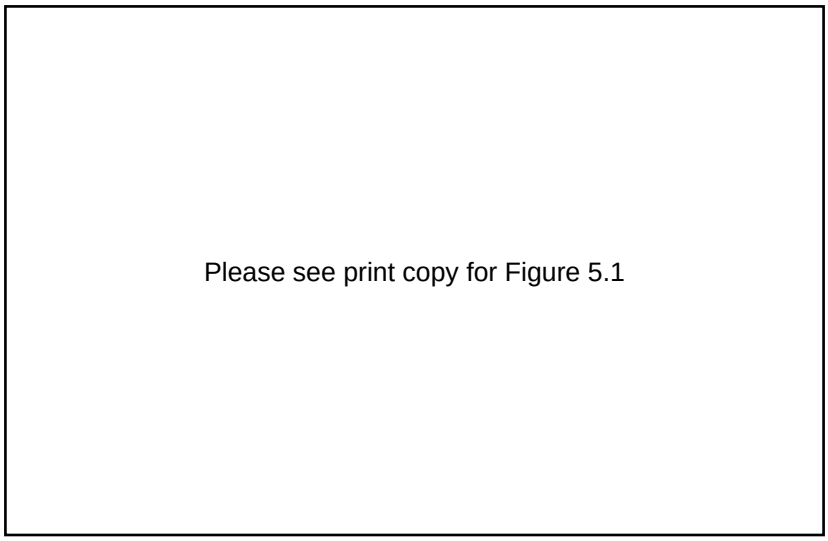

Figure 5.1, Theoretical structure of film densitometer (Macbeth, 1965)

This basic optical system has been used in number of large format 2-D film scanners commonly in use in the 1970s-1980s. 2-D digitising can be achieved by rastering the plate to-and-fro through the beam in the y-direction while driving it continuously in the x-direction.

- **Joyce Loebl Microdensitometer**

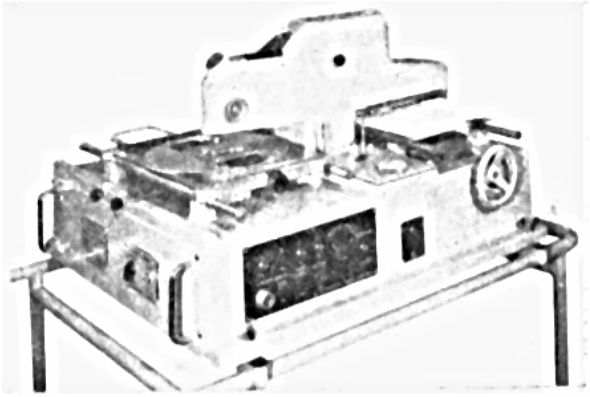

Double beam recording microdensitometer

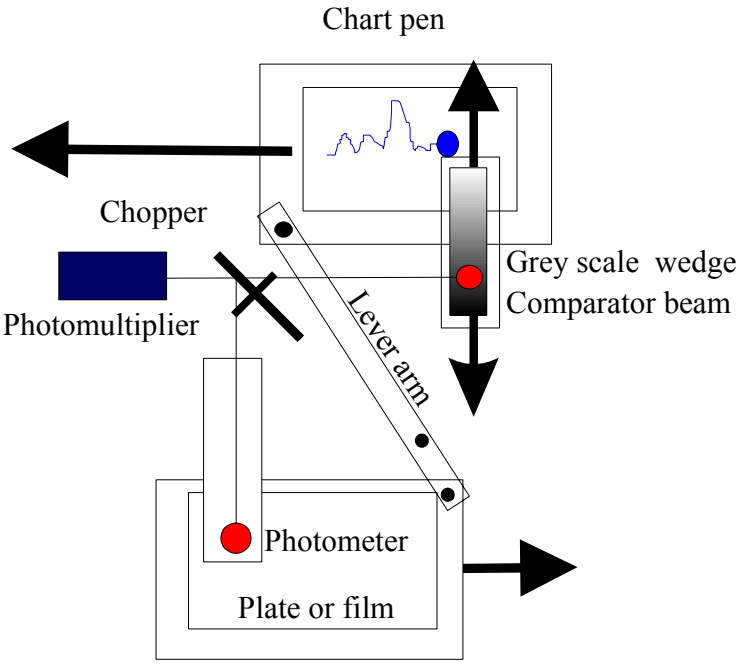

Figure 5.2 Joyce Loebl Double Beam Microdensitometer

The scanning film densitometer (Figure 5.2) developed by Joyce Loeb used a motorised drive and a mechanical linkage to move the film/plate platen linearly through the measurement beam. A comparison beam passed through a stepped density wedge which was driven by a comparator circuit.

The comparison and measurement beam fell alternately on a detector and analogue circuitry drove the comparison wedge to equalise the two

beam's intensity. The wedge position was either digitised or directly plotted using a pen which was mechanically coupled to the wedge. This is the one of the few true density measuring machines developed. These 2-D density maps were used to create profile and depth dose curves. In the 1970s this scanning densitometer found use in hospital radiation QA research.

- **The Perkin Elmer PDS Microdensitomer**

  PDS micro-densitometers have been the workhorse of the astronomical community for several decades. They played a major role in digitising sky survey plates for use in the Space Telescope Guidestar catalogues CSCI and GSCII. The densitometer uses a fixed light source projected onto the plate using microscope optics. The beam is collected, again using microscope optics, detected by a photomultiplier and digitised using a 12 bit A/D converter. The 250mmx x 250mm plate carriage can be driven in two directions using stepping motors.

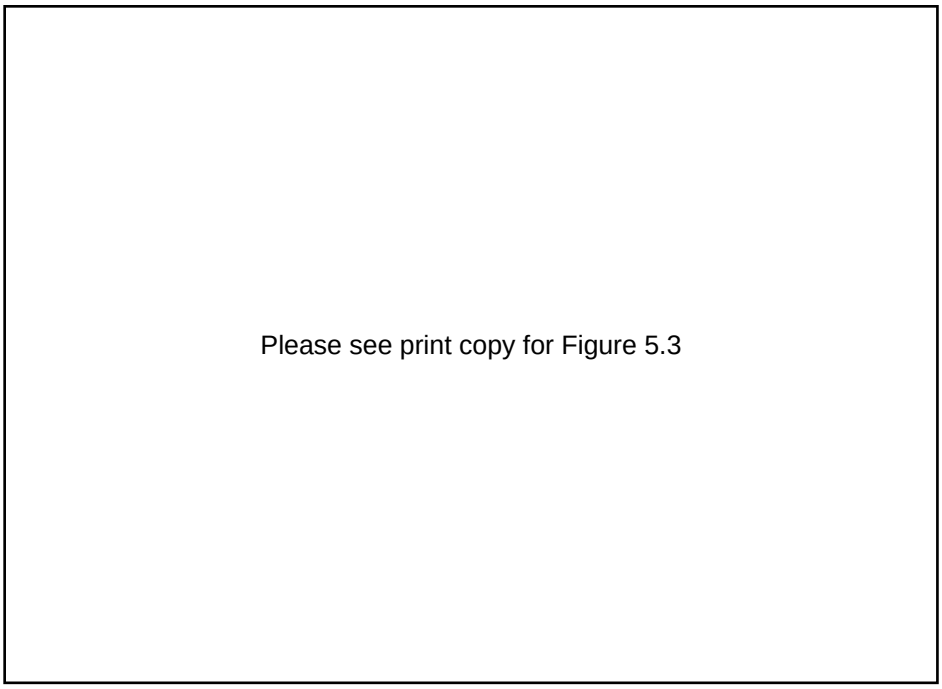

Figure 5.3 Perkin Elmer PDS
(http://www.to.astro.it/astrometry/AC_CdC/measuring.html)

- **Vidar CCD film digitiser**

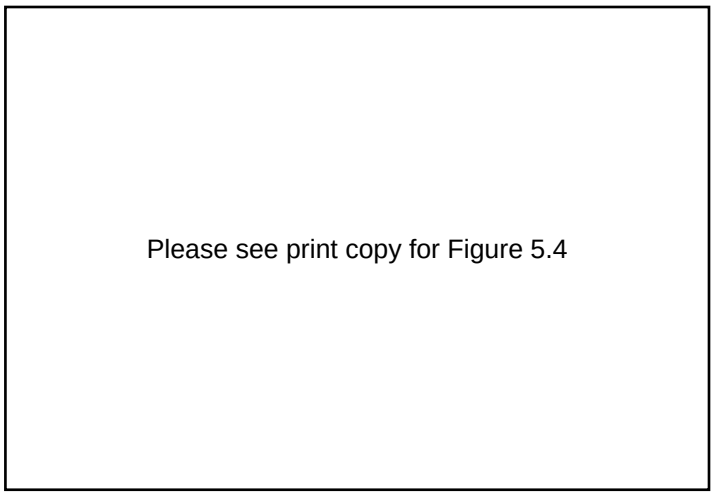

Figure 5.4 Structure of CCD digitiser
(Vidar System Cooperation, VXR Film Digitizer: TWAIN User's Guide for Windows, 1994)

A 16bit data depth scanner is made by Vidar System Corporation (Vidar System Cooperation, VXR Film Digitizer: TWAIN User's Guide for Windows, 1994). It is very similar to the normal flatbed scanner. The difference is the device uses a stabilised fixed light source. (Figure 5.4) It provides low resolution, but the signal dynamic range gives a linear, noise free effective range up to 2.5 optical density. The unit is priced in the region of $20,000.

- **Wellhofer densitometer**

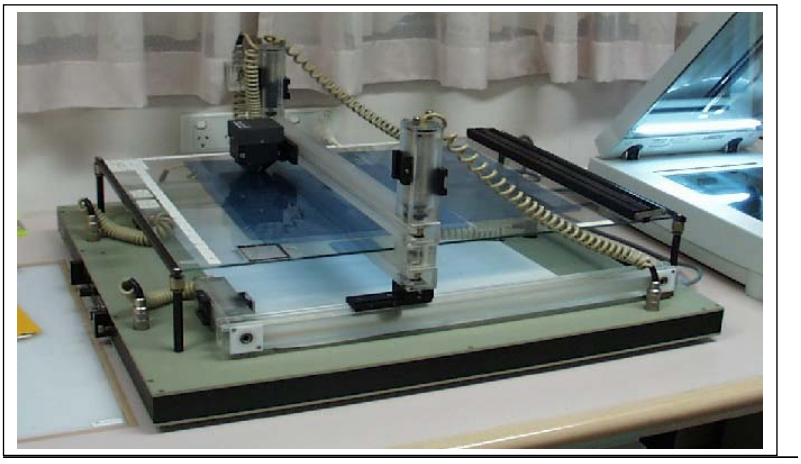

Figure 5.5, Wellhofer Scanning film densitometer

The Wellhofer densitometer designed for the film dosimetry can be adapted to the water scanning system. A light box illuminates the plate which is scanned by a small microscope photometer. The maximum size of field is 300mm x 400mm and the range of densities can effective to 4.3-4.5. The system requires careful adjustment to perform properly. In particular the glass platen must be leveled so that the detector optics moves parallel to the surface and the uneven illumination by the light box must be corrected.

The scanning-laser film digitisers

A number of digitisers which use lasers or high power flying spots to scan the film have been developed. These are generally expensive and require a purpose built controlled environment.

- **The Royal observatory Edinburgh's Galaxy, COSMOS and SuperCOSMOS measuring machines**

  From 1966 to 2000 The Royal Observatory Edinburgh developed a series of plate measuring engines capable of digitizing 500mmx500mm photographic plates to resolutions of 5- 10 microns. GALAXY and COSMOS were based on a rapidly moving spot produced by a high power oscilloscope scanning the plate orthogonal to the plate carriage motion (flying spot scanner). The signal from the photomultiplier detector was digitized and analysed off-line to produce catalogues of up to 1 million stars from each plate. This work culminated in SuperCOSMOS a fast measuring machine which utilises a laser beam, 2048 pixel linear CCD, granite table and airbearing. This system is capable of digitising a full plate to +/- 5 microns positional accuracy with a reproducibility of 0.15 μm standard error. In 2 hours SuperCOSMOS can digitise a 500mm x 500mm plate to 15 bits producing 2 gigabyte pixel maps. (Hambly, Miller, MacGillivray, Herd & Cormack, 1998)

- **Automatic Plate Measuring Machine; Cambridge**

  The Automatic Plate Measuring (APM) machine is a National Astronomy Facility operated by the Institute of Astronomy in

Cambridge. (Irwin, 2003) The system utilises a high power laser system to scan a 500m x 500mm film or plate to 7.5 μm. The 16 bit output is used to produce pixel maps or more commonly processed to produce image parameters on stars and galaxies.

- **Dempsey Laser Scanner**

  James F. Dempsey (1999) described a laser film digitiser shown in figure 5.6. A laser beam is scanned across the plate by a mirror system while the plate carriage moves orthogonally to the scan. A reference detector monitors the stability of the laser beam. The signal is detected by a photomultiplier tube (PMT) an integrating sphere before being digitised to a depth of 12 bits. The digitiser achieves a better than 5.1 optical density dynamic range.

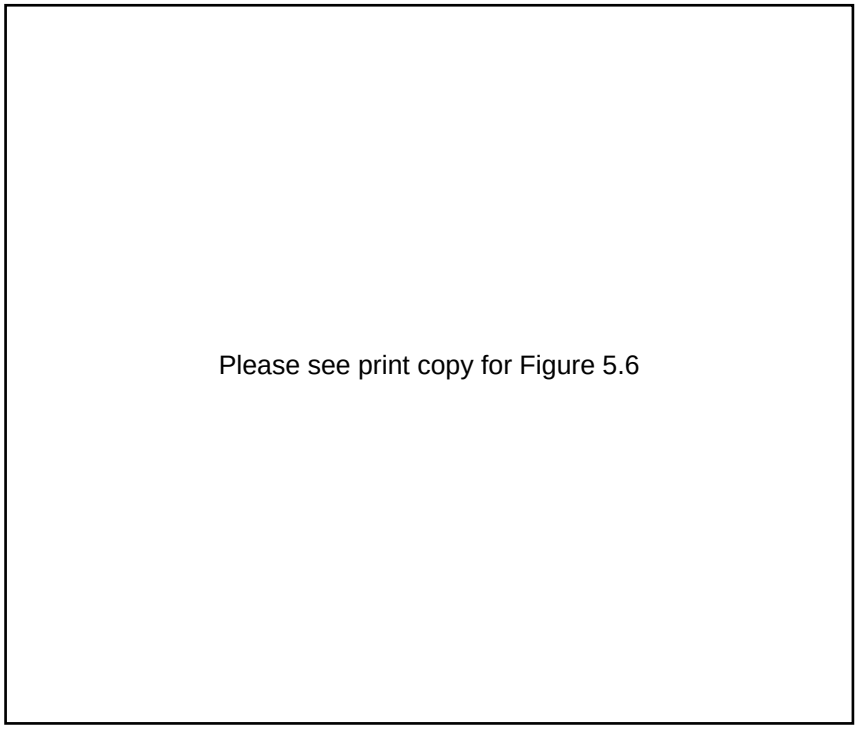

Figure 5.6 The Dempsey laser scanner

5.3 Modern Desktop scanners

5.3.1 Introduction

A flatbed scanner is similar to a photocopier in that it has a document glass which supports the film or print, a moving light source, which scans the original and a linear charge coupled device (CCD) array (Figure 5.7). Unlike a copier, the scanner digitises the image for later image processing and enhancement. The flatbed scanner has some advantages in that it has the flexibility to provide quality scanning from a wide variety of original material.

(a)

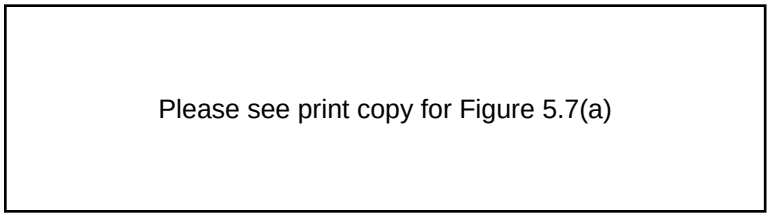

(b)

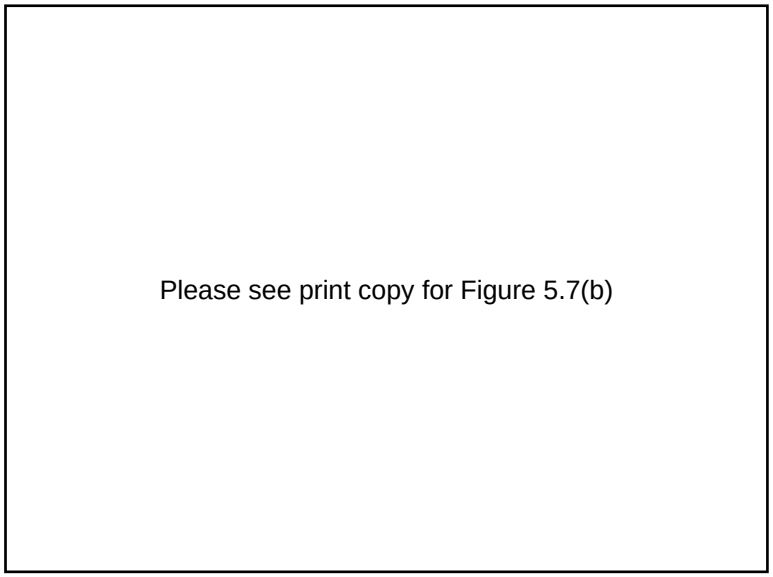

Figure 5.7 (a) The CCD detector and (b) the light bar of a desktop scanner

While rapid growth has occurred in colour scanning, all desktop scanners are capable of producing at least 256 (8 bit) greyscale output.

5.3.2 How a scanner works

Two different technologies are commonly used in building desktop scanners.

Most desktop scanners are designed to digitise reflecting prints. In these the light source is positioned on the same side of the print as the detectors. The higher quality scanners use optical reduction technology (Figure 5.8a) while the low cost scanners mostly use a contact image sensor (Figure 5.8b).

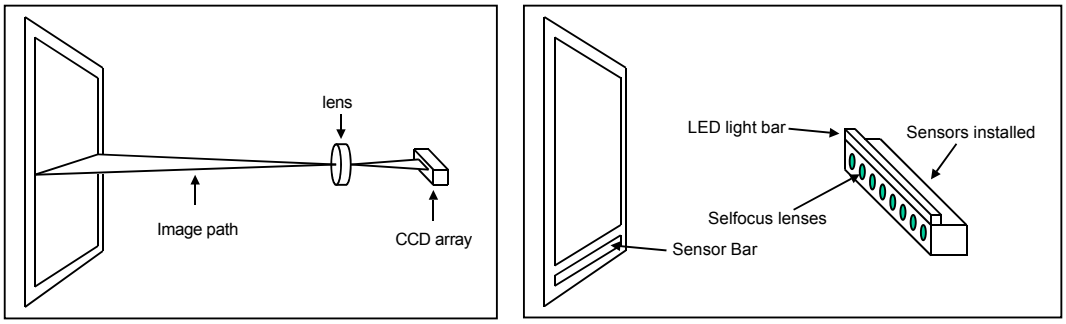

Figure 5.8 (a) Optical Reduction Scanner, image at the page is 6 to 8 times larger than the image at the CCD
(b) Contact Image Sensor Scanner, image and Sensor are the same size and there is a self-focus lens and sensor for each pixel captured.

- **Optical Reduction Scanner (ORS)**

The scanner uses a lens to reduce the image size and so that the image can be captured on a CCD. Most flatbed scanners are designed around the ORS technique since CCD arrays are usually much smaller than an A4 page.

- **Contact Image Scanners (CIS)**

A contact image sensor scanner uses a sensor that covers the entire width of the scanned area. The pixels on the CIS are roughly the same size as the scanned pixels on the page. In some CIS scanners the scan head actually touches the print/plate. In most flatbed CIS scanners, the sensor is separated from the object by the document glass. Between the object and the original are a large number of special lenses called “self-focus lenses”.

These lenses focus the light reflecting from the print so that each sensor sees only a very small part of the original.

The CIS scanner is able to be smaller and more portable than an ORS system. The scan speed can also be faster. However the sensor is often shows alignment problems, because CIS sensors are usually produced by taking several sensors and butting them up end to end. This often means that the joints between adjacent mosaic areas of the image are visible.

5.3.3 Photo flatbed scanner with Transparency adaptor

Many models of scanner are available with a transparency adaptor. These differ from the previously discussed reflected light scanners in that the light source and the CCD array lie on opposite sides of the film/plate. The light source may be a 2-D illuminated panel or a light bar which moves in parallel with the detector. (Figure 5.7a, b) Since these are usually designed for use in photo processing, the scanner has low dynamic range coupled with very high optical resolution (600 x 1200). In order to reduce the cost and increase the scan speed, some early desktop scanners only had 8bit digitization. More modern desktop scanners have optical resolution of 1600 bpi and 16 bit digitisation.

Such transparency tops allow the flatbed scanner be used as a film densitometer in film dosimetry scanning. However, compared with a dedicated film densitometer, there are some limitations.

1. The optical resolution (MTF) of the scanner may limit the detail possible.
2. Tonal resolution, signal-to-noise, and optimisation are limited. Most low cost flatbed scanners are not designed for scientific photogrammetry but for photo retouching. These are designed with limited dynamic range and digitisation depth.

However, these problems can be solved through the use of specially designed x-ray film greyscale scanners, with improved signal depth (16 bit) and illumination providing higher dynamic range, and improved signal-to-

noise. These scanners are somewhat more expensive. Table 5.1 lists a number of commercially available desktop scanners suitable for radiotherapy QA available in 2004.

Table 5.1 Some commercial desktop Scanners available for film dosimetry (http://www.proscan.com.au/brochures/1_Graphic_scanners399to4K_comparison_0411.pdf)

Please see print copy for Table 5.1

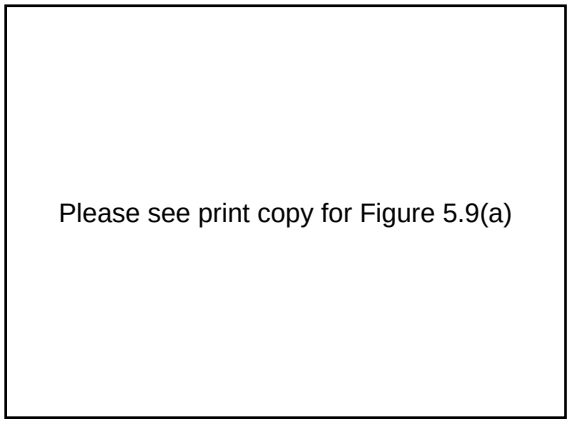

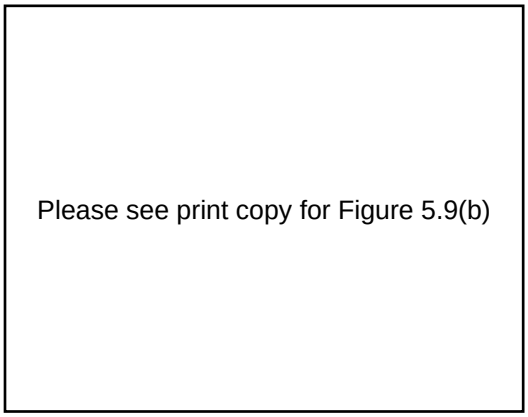

Figure 5.9 **a.** AGFA colour film desktop scanner
b. UMAX 2000 Desktop scanner transparency light source adaptor

5.4 Scanner Characteristics

For a scanner to be of use in QA we need to understand its performance in several areas:

- Spatial or Optical Resolution
- Digitisation Depth

- Dynamic Range
- Signal to Noise
- Brightness/ Contrast controls
- Reproduceability

5.4.1 X and Y direction sampling rate – Pixels Per Inch (PPI)

The resolution of a desktop scanner is given in Pixels Per Inch (PPI). This refers to the spatial sampling rate of the scanner. The sampling rate is not the only characteristic to affect the quality of the image, and therefore the use of PPI solely to describe the "resolution" is almost meaningless.

Some publications and manufacturers use DPI (dot per inch); some PPI (pixel per inch) or LPI (line per inch) to describe the scan data. In some cases professional photographers, refer to SPI (sample per inch).
DPI, and LPI are more suitable to be used in discussing the spatial resolution of an output device such as a printer or plotter. (Figure 5.10)
PPI is more often used to describe a computer screen display resolution. It seems SPI is a more reasonable term to describe the frequency of the sampled data when an image is scaled at output time.

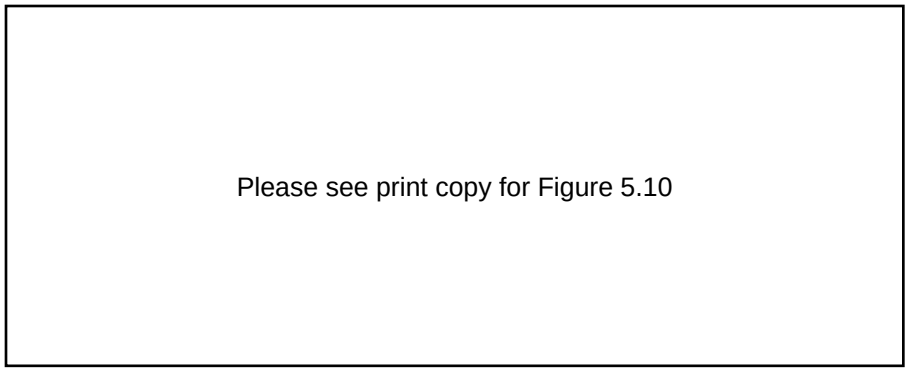

Figure 5.10 PPI and image resolution (Michael J. Sullivan, Make Your Scanner a Great Design & Production Tool, North Light Books & An Imprint of F.W Publications Inc., 1998)

If we scan at higher ppi, then the number of pixels in an image rapidly increases and large file sizes will result. Increased scanning resolution may make it impossible to display the whole region of at the full digitised resolution. For most QA procedures a resolution of between 0.1mm (250ppi

to 1mm (25ppi) is sufficient. The user does not benefit with any image quality improvement in going to higher ppi but minimises the data file size and hence processing speed.

The CCD captures a complete horizontal strip, called a “raster line” in one step. During each the step of exposure of each raster line, the scanner carriage is mechanically moved a small distance.

This distance is referred to as the y-direction sampling rate. The number of CCD elements in each raster line determines the x-direction-sampling rate. The unit used to describe the sampling rate is based on number of pixels per inch (ppi). Typical x-direction sampling rates are 300, 400 to 600 ppi for and for y-direction sampling rate around 800ppi.

Not all the manufacturers use ppi to represent the scan sampling rate. The ppi does not tell us the maximum possible resolution of a scan sampling and may not provide sufficient information to tell the actual level of scanner performance.

5.4.2 Analog-to-Digital conversion - Bit depth and density ranges

When the analog voltage from the CCD is converted to a digital number the digital-to-analog converter determines the number of grey levels available to digitise the range of transmission in the image. As example, an 8-bit A/D can achieve 2^8 256 grey levels (0 to 255). For a 24bit colour scanner, each pixel is represented by three 8bit samples for 2^{24} different colours.
In modern scanners, using a 16 bit digitisation, 2^{16} grey levels are available to the image.

Two important terms relate to ‘Bit Depth’ and ‘Density Range’ (or dynamic range).
Increased Bit Depth simply relates to increasing the number of bit levels output by the A/D (analog-to-digital) converter and hence the number of grey levels available.

‘Density Range’ or ‘Dynamic Range’ gives the range of densities which may be accurately digitised. The maximum density depends both on the strength of illumination and on the Bit Depth available. In many desktop scanners the brightness and contrast of the scanner can be adjusted to optimise the dynamic range and make the signal response more linear. This has a similar effect to an adjustment of threshold or bias voltage and gain to the A/D converter.

Increased bit depth does not necessarily lead to improved density range or reduced noise levels. The image quality obtained from a low budget 12 bit scanner may be no different from that of an older 8 bit scanner. It is necessary to compare the performance of scanners by scanning a standard density step wedge template, and measuring the dynamic range and noise characteristics at high densities.

The main importance of bit depth lies in the uncertainty in measuring the transmission. An 8 bit digitiser will produce errors of 1/256 or +/- 0.4% while a 10 bit scanner 1/1024 or +/- 0.1% errors in transmission. These uncertainties must be carried through into calculations involving optical density measurements.

Some manufacturers base density specifications on the theoretical limit at a certain density. For example, a 36bit scanner has a theoretical density limit of $\log_{10}$ (4096) = 3.6. Few, if any, really deliver this result. These specifications are probably not representative of a scanner’s performance since the maximum density measurable is limited by light source, noise, stray light and surface reflection.

In addition, limiting density values should include a spectral specification. Density specifications often ignore such information in scanners. Sadly, in today’s scanner market, manufacturers focus on reducing the costs that make the scanner more attractive to non-scientific users.

5.4.3 Signal-to-noise ratio

In most scanners, a published signal-to-noise ratio does not support density claims based upon bit depth. If a 10bit scanner has noise equivalent to the bottom 4 bits (16 counts) and then the real performance of the scanner is more like a 6bit scanner.

5.4.4 Dynamic range

Dynamic range is the total range of optical density measurable by a scanner. The dynamic range is measured using a logarithmic scale from pure white OD_{min} =0 to black a OD_{max} of between 3.5OD – 5.0OD. An increase in 1 OD unit in the dynamic range represents about ten times more potential data. If a scanner has a dynamic range of 3.2OD this scanner can handle a range of transmissions and hence intensities ten times greater than a scanner with a dynamic range of 2.2 OD.

The dynamic range is linked to the signal/noise ratio. The larger the CCD element the higher the signal/noise ratio and in general, the larger size of CCD the better dynamic range. Unfortunately, in a flatbed scanner, if the CCD element size is too large it will reduce the scanner resolution. That is why some x-ray film scanner with very high signal dynamic range have an image resolution lower than a cheap colour flatbed scanner.

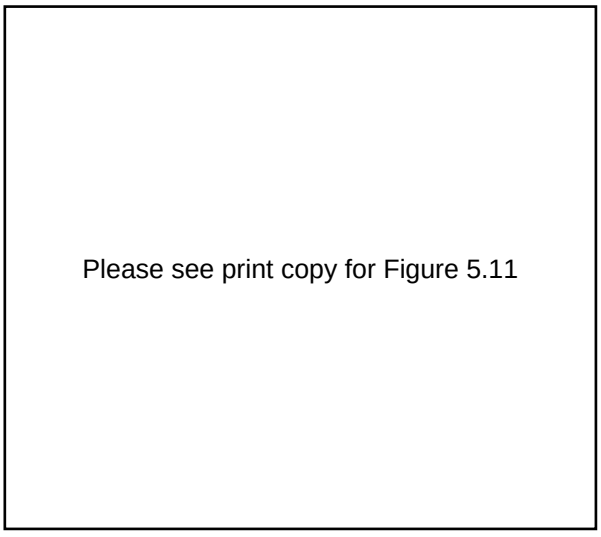

Figure 5.11 Dynamic range (Michael, Sullivan 1998)

Most flatbed scanners have an effective dynamic range (noise free) from 0.0 OD to1.5 OD or 2.2 OD but for a x-ray laser scanner, the dynamic range can reach to 3.5 OD to 5.0 OD.

Desktop scanners claiming 10bits or more of tonal resolution per colour are becoming common. The benefit from a 10bit scanner is more related to the quality of tonal transformations, like gamma correction, than they are to the increased density ranges of the scanner.

Robert G. Gann (1999) discusses two important concepts, DSNU (dark signal non-uniformity) and PRNU (photo-response non-uniformity) which are directly related to the detector and impact on image/signal depth.

The DSNU is caused by noise produced in the linear CCD elements in the absence of illumination. The DSNU is defined from the signal value (V) as the larger of V_{max} - $V_{dark\ or}$ V_{max} - V_{min} where V_{max} and V_{min} are the maximum and minimum GSV from the row in the absence of any illumination, V_{dark} is representing the darkness reading of the background value. The DSNU can be calibrated out of the scanned image by subtracting the dark noise from each detector element.

The PRNU relates to the detector elements having slightly different response to the same light intensity. The PRNU is defined as (V_{max} -V_{min}) / $V_{average}$ * 100.
The effects of spatially detector variable response can be corrected by illuminating the detector uniformly then dividing the subsequent detector output by this ‘flat field’.

Compensating for DSNU and PRNU, significantly reduces the signal/image depth in the scan.

Consider a low cost 10 bit A./D with both non uniform response and non uniform noise across the field. Some of the 10 bits are actually used to compensate for these field imperfections in the scanner. After these

corrections are made in the scan signal processing, only 8 bits may remain in the digitised image.

However, it is still important to maximise the signal depth, as it provides reduced uncertainties in the digital image. The correction of the spatial non-uniformities DSNU and PRNU reduces the overall noise. While not so important for the commercial artists, this is important for scientific users in order to provide enough density range to perform the signal linearity adjustment. For this reason most scanners designed for film densitometry have the greatest possible image depth and A/D bit number.

5.5 Screen display issues

No matter what image we have scanned, if the monitor is restricted to a 256 colour or grey scale level display, the displayed image quality will be limited.

Also, if we store an image using a simplified bitmap file as used in the GIF format , this format with only supports 256 grey scale values. Use of a JPEG file format supports up to 24-bit depth but care must be taken if the file format chosen allows image compression.

Scanners are commonly characterised by their ‘tonal resolution’. Typically, this is specified as an increased “bit depth” as in a “30-bit colour scanner”. The bit depth or bits per pixel (bpp) specification is very similar to the specification of ppi in that it tells us something about the technology in the scanner, but nothing about the quality. In fact bpp, like ppi, is becoming meaningless. A better measure of tonal resolution is the signal-to-noise ratio.

5.6 Brightness and contrast

More expensive scanners allow the user to manually override the automatic setting of brightness and contrast. The brightness control enables user to shift whole image to a lighter or darker setting. From a signal analysis viewpoint, this has the effect of adjusting the linearity of signal response curve.

Most scanner control software provides an emphasis tone map or contrast control. Although this adjustment makes very limited adjustments to the

contrast it can still be used improve the signal quality near the extremes of the region of linear response.

5.7 Image quality requirements

Professional users should consider the following as accurately characterising the scanner for scientific use:

5.7.1 Optical resolution (not PPI)

The PPI does not necessarily reflect the overall performance of the scanner. We should determine the spatial resolution of a scanner by measuring the optical frequency response of a scanner. This provides information on how well the scanner responds to high-frequency information.

The frequency response is commonly referred to as the MTF (Modulation Transfer Function). It is measured by scanning a sinusoidal bar pattern of uniform intensity and decreases in spatial frequency from one end to the other. The scanner output is analysed and the contrast, $GSV_{max} – GSV_{min} / GSV_{mean,}$ plotted against the related spatial frequency. The true optical resolution (TOR) is calculated from the MTF curve for the frequency at which the contrast drops to 20%. The MTF provides a reproducible, quantifiable value which can be used to compare the scanners.

5.7.2 Tonal resolution

The tonal accuracy of the scanner should be checked with a transparency calibration film (or standard grey scale reflectance template). For each step the optical density is plotted against GSV

$$\text{Optical Density} = \log_{10} (1/ \text{transmission})$$

e.g. an image with a transmission of 20% would get a density value of

$$\text{Optical Density} = \log_{10} (1/0.2) = 0.69$$

By performing the optical density test on each step of a step wedge calibration template film a GSV - optical density curve can be drawn.

Figure 5.12 shows a test example of transparency step wedge film measured on two different desktop scanners. One is 12 bit PTW x-ray film scanner and the other is an 8 bit HP 4/c colour scanner. This test provides the user with control over the features for tonal accuracy, dynamic range, and signal-to-noise. From this test result, we can evaluate the difference between the scanners.

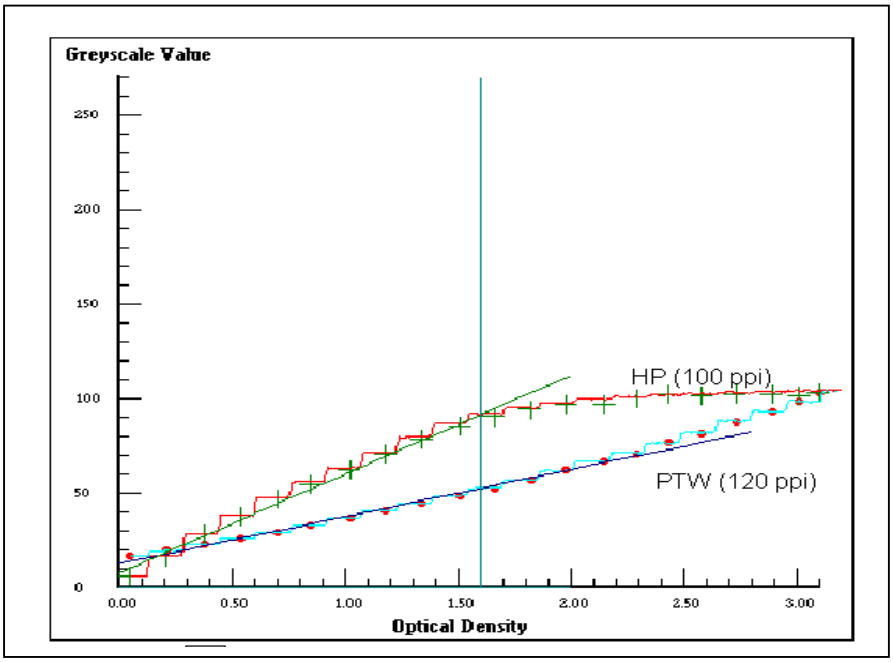

Figure 5.12 step wedge film scanned by 8bit and 12 bit desktop scanner

The 8 bit scanner has a steeper slope or contrast and good linearity for optical densities between 0.0 OD and 1.7 OD. However, the dynamic range is more restricted than that of the 12 bit scanner. The 8 bit scanner saturates at optical densities above 1.7 OD.

The 12 bit scanner has a larger dynamic range showing clear steps up to at least an optical density of 3 OD. However the GSV-OD curve deviates slightly from linearity above a 0.0 OD of 2.00 OD.

5.8 Are desktop scanners suitable for film dosimetry?

Film dosimetry techniques are not yet good enough to be used for the absolute radiation dose measurements.
Even with a perfect desktop scanner, with high spatial resolution and large dynamic range there are still too many issues influencing the dosimetry such as energy dependence, properly designed phantoms and film characteristics, (exposure, processing pH, temperature and mechanical artefacts). We have already discussed many of these fully in earlier chapters

However, if we are careful, we can use film dosimetry techniques for relative dose measurements. Film is the easiest and quickest way for us to perform routine checks of the beam, field dose distribution, and alignment. It may also be used to check photon and electron energy constancy.

The possibility of using desktop scanners to simplify the analysis of QA films will benefit the hospital physicist by simplifying routine quality assurance.

We conclude that the use of a modest cost desktop scanner with a transparency adaptor is capable of providing 2-D information at resolutions of around 100 microns in at least 256 transmission levels.
Such digitising enables the physicist to undertake 2-D dosimetry and apply corrections and signal averaging to improve the accuracy of the dosimetry..

Unlike that of a film densitometer, most scanner support software allows the user have a small amount of control over signal brightness and contrast. This gives user the ability to improve the optical density curve linearity.

All these features provide encouragement for developing procedures to for the use of desktop scanners in film dosimetry analysis.

Desktop scanners have a number of advantages over the more expensive film scanners (PDS/ Joyce Loebl) and spot densitometers (Macbeth) previously used for film analysis. These are:

Advantages:

1. Cost; the desktop scanner price is significantly lower than that of either film scanner or spot densitometer.
2. Easy set-up procedures; alignment and operation are simpler than film scanners.
3. Speed of measurement; the desktop scanner digitises an image in under a minute compared with the several hours required of a PDS system.
4. 2-D digitisation; unlike the spot densitometer which performs only single point or line scans.
5. Sample size: The desktop scanner pixel size (50 microns) is intermediate between that of a spot densitometer (1.0mm to 1.5 mm) and that of a PDS (10 microns).

Disadvantages:

1. Smaller dynamic range than PDS/SuperCOSMOS;
2. Higher signal-to-noise level than laser digitizer and analogy signal film densitometer ;
3. Light source non uniformity can affect GSV.

It is possible to develop techniques which minimise these disadvantages and allow desktop scanners to provide a valuable addition to QA methods.

The following characteristics are important in selecting a desktop scanner for Film QA purposes. While the ppi is an important issue it is not the most important. Nowadays, most scanners provide more than 400ppi, which is more than satisfactory for our purposes.

The most important characteristic is the number of greys available or image depth (bits). There is some possibility of confusion over this since a 24bit colour scanner is in reality an 8 bit grey scale scanner.

Many of the characteristics of importance to us are not readily available in the manufacturer specifications. Where possible these should be evaluated prior to purchase.

Few manufacturers provide information on the signal-to-noise levels of their scanners. However, if we going to use a scanner to perform quality film dosimetry and quality assurance, we really should request this information.
In evaluating desktop scanners we should obtain a GSV-optical density curve for the scanner. The light source distribution and stability should be also be evaluated by scanning a uniformly exposed film with a lower brightness and contrast setting.
It is important to select a scanner with some manual override of automatic scan settings of contrast and brightness.
Finally some consideration of the ease of use and the supporting software is necessary.

In the chapters which follow simple techniques are developed to allow desktop scanner images to be calibrated and corrected to provide dosimetry accurate to better than 5%.

(Note added in final proof: The performance of transparency scanners has improved significantly since this work began. 16 bit grey scale scanners with optical resolutions of 9600 x 4800 are available at a cost of under $1000.)

Chapter 6 Image Processing Technology Study

6.1 Introduction

In this section the desktop film transparency scanners are assessed in terms of

- Calibration accuracy - Optical Density (OD) vs greyscale value (GSV)
- Warm up effects
- Light source uniformity and background effects
- Signal to noise and smoothing algorithm,

Simple protocols are developed for using such scanners include:

- Background correction
- Double scanning
- Flattening

Another important improvement is the format of the signal depth. Early transparency scanners could only digitize document films. That is because the signal depth was only 8 bit. 14 to 16 bit low noise scanners are now available at reasonable prices.

However, if a desktop scanner is to be used for radiation dosimetry, calibration needs to take place first to optimize the signal response before converting the GSV into corresponding radiation dose. The GSV cannot directly be used to represent the dosimetry information. Each scanner has its own dynamic range, noise level, and signal response curve. All of these need to be optimized and calibrated to provide a correct, reproducible radiation dose corresponding to the measured GSV.

6.2 Greyscale value - optical density linearity and its optimization

6.2.1 Greyscale value and signal format depth

Currently, most computer screens are designed using 32bit signal depth to support high color quality. Most PC program languages use Red, Green, and Blue Look Up tables (RGB LUT) to build more than thousand different color

levels by the combination of 256 shades of each color. As most program coding techniques support 256 display levels e.g. RGB (0-255, 0-255, 0-255), black-white photographs are stored and displayed by synchronizing all three base color changes (R=G=B). .

The human eye is only able to distinguish a maximum of 30 different greyscale stages. Most photograph scanners support between 8 and 16 bit scanning (>>256 greyscale values). Different signal depths give different greyscale image quality (Figure 6.1). Since most computer screens are only able to display 256 greyscale levels 8bit, 16bit or 32bit greyscale images must be windowed, thresholded or false coloured using LUT tables for display

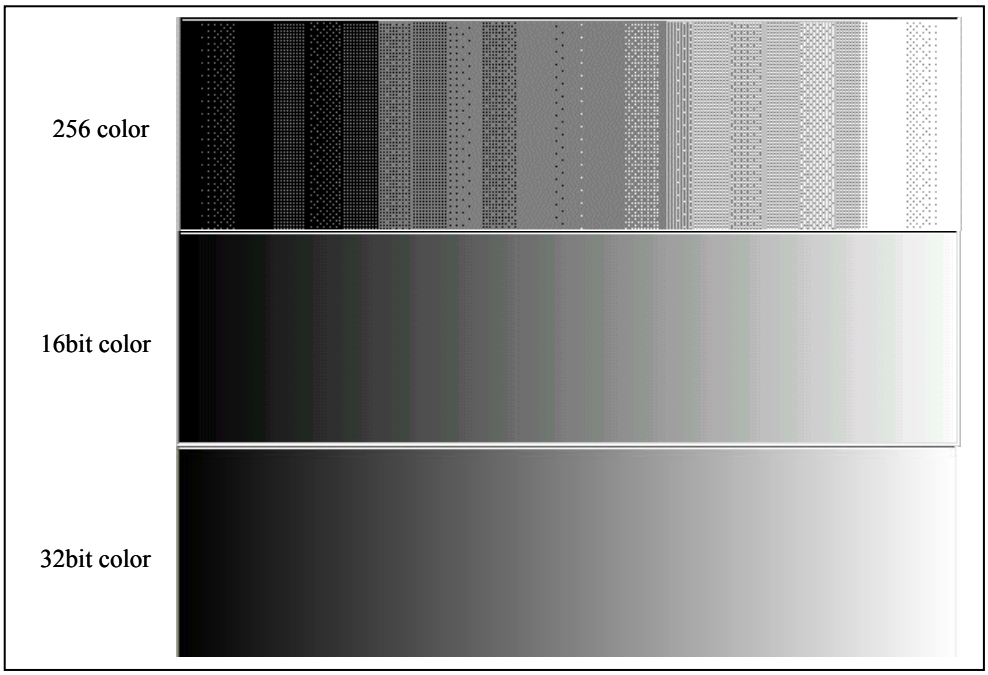

Figure 6.1 a linear density image displayed on PC screen, the image quality is affected by different screen setting

Images digitized at signal depths in excess of 16 bits require large processing memory, data storage space and fast image processing and display software making their use prohibitively expensive.

This study is aimed at the use of low cost, desktop scanners to achieve digitization of images to the accuracy and quality required of film dosimetry.

Many photographic scanners can be used for the film scanning with the addition of a transparency light source.

For film dosimetry use, we set the scanner to greyscale by software control and select scanner parameters to match the available greyscale range (usually between 256 and 65536) to the dynamic range of the dosimetry film. 256 greyscale value levels are enough for the routine film dosimetry requirement.

6.2.2 Signal depth

The signal can digitized to 8bit, 12bit, 14bit or 16bit depending on the scanner signal design. For the colour RGB desktop scanner, this value can be described as 24bit (8bit x 3) and 36bit (12bit x 3). The depth of signal is a very important figure to describe the functional ability of a scanner. The dynamic range, noise levels, contrast and brightness adjustment ranges are all dependent on the signal depth. For a desktop scanner, the signal depth is a more important technical characteristic than others.

As figure 5.12 in last chapter shown a comparison was made to compare the step wedge scans made by the HP4/c 8bit and PTW 12bit desktop scanner the step wedge film scanning curves. As it can be seen that the 8bit scan signal could only provide the effective response to around 1.5D, above that region, the response curve flattens and the signal between steps gets smaller. There is some adjustment allowing the user change to improve the linearity, it might also increase the noise and produce incorrect signal. The noise level differences between 8bit HP 4/c, and 12bit PTW transparency scanner is compared by scanning the step wedge film. At high densities, the 8bit signal become noisy, flattens and cannot distinguish steps. The scanner is not capable of measuring high intensity.

In the case of the 12bit scanner, the effective signal region is wider and the steps show a more even distribution. Each step is clearly distinguishable and the noise levels for higher densities region are low. Although response is non-

linear above 2.0D, a small adjustment can be made by user to improve this linearity (Figure 5.4)

6.2.3 Brightness and contrast setting of scanner for signal response linearity

As figure 5.12 shows a standard step wedge film can be scanned and plotted as a curve showing all the steps in the calibration wedge. This curve can be used to evaluate the scanner functional quality including sensitivity, dynamic range, and the greyscale value – optical density calibration curve (GSV-OD curve); it clear shows that the curves are not perfectly linear. Most current scanner products provide for software adjustment for the brightness and contrast settings. The reason for forcing the greyscale value to be almost linear with OD by selecting appropriate scanner software settings is to simplify the order of curve fitting required to represent the calibration curves.

The film OD-Dose response curves (especially for the commonly used Kodak XV verification film) are not linear. The GSV-OD response can be leaved with unchanged and correct the GSV-Dose curve later when the equivalent dose conversion is being performed. This will make the correction more complicated because the two non-linear curves will be combined. Since GSV-OD response is easier to linearise using the scanner software, it is simpler to get rid of one of the issues before film analysis.

Figure 6.2 shows that if the scanner brightness is adjusted, the dynamic range changes slightly. Figure 6.3 shows that adjusting the scanner contrast gives a big effect on linearity change but no dynamic range changes. If the scanner setting is unable to keep unchanged between scans (as some photograph scanner default set to the automatic brightness, contrast or colour turning while each photo scan performing), the dose value will change for the relative percentage (Figure 6.4).

The changes to brightness settings can be corrected by renormalizing all readings because the curve shape is not changed. However, if the scanner contrast setting changed, the curve shape will be affected dramatically.

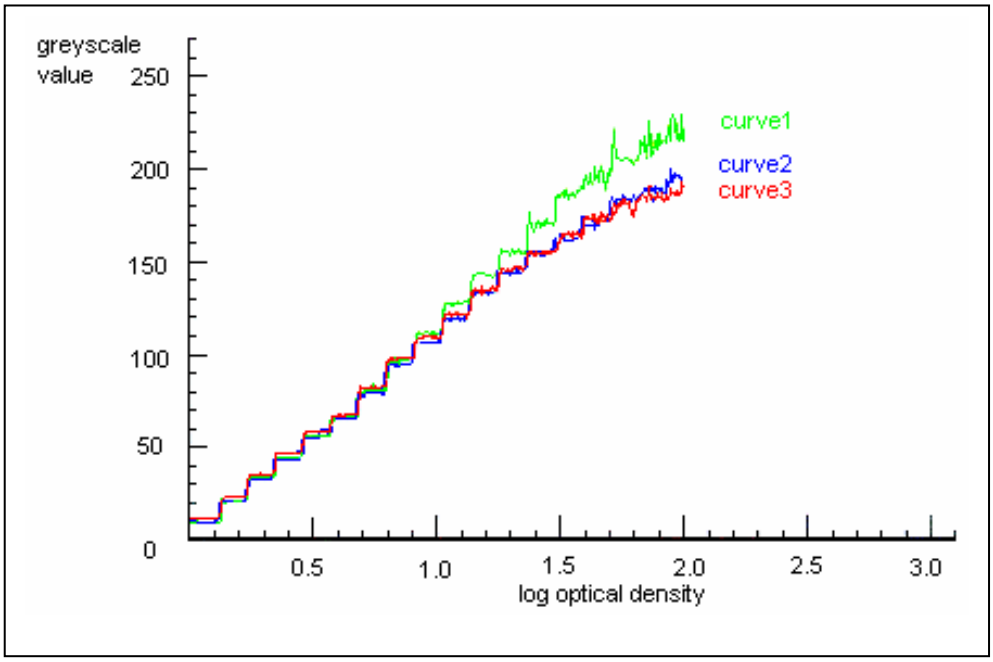

Figure 6.2 by adjusting brightness setting of scanner, the signal response range can be changed without changing the curve shape.

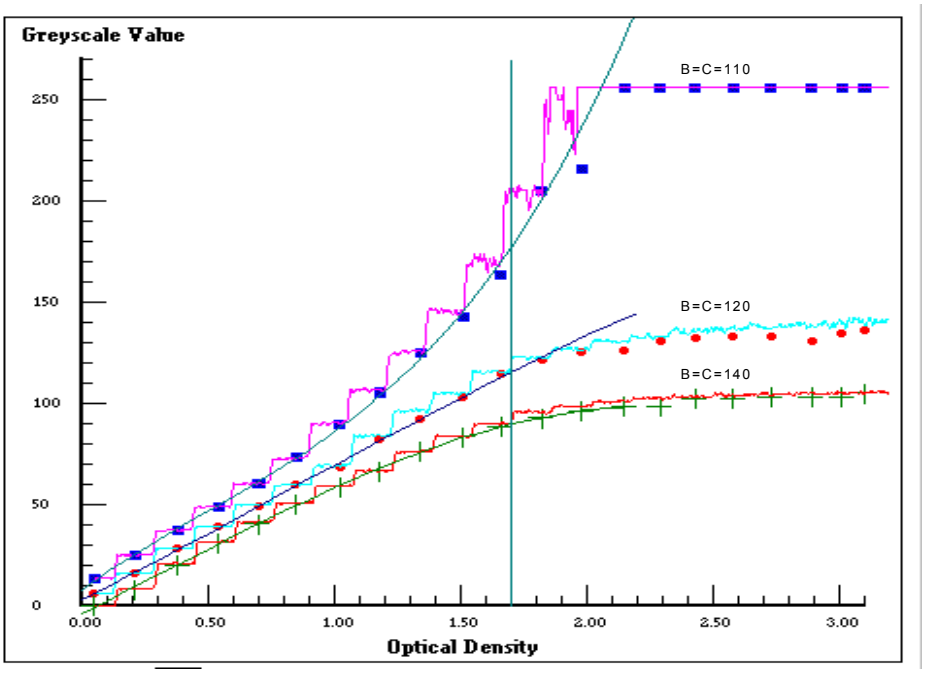

Figure 6.3. by adjusting the scanner contrast setting, the signal response linearity can be changed.

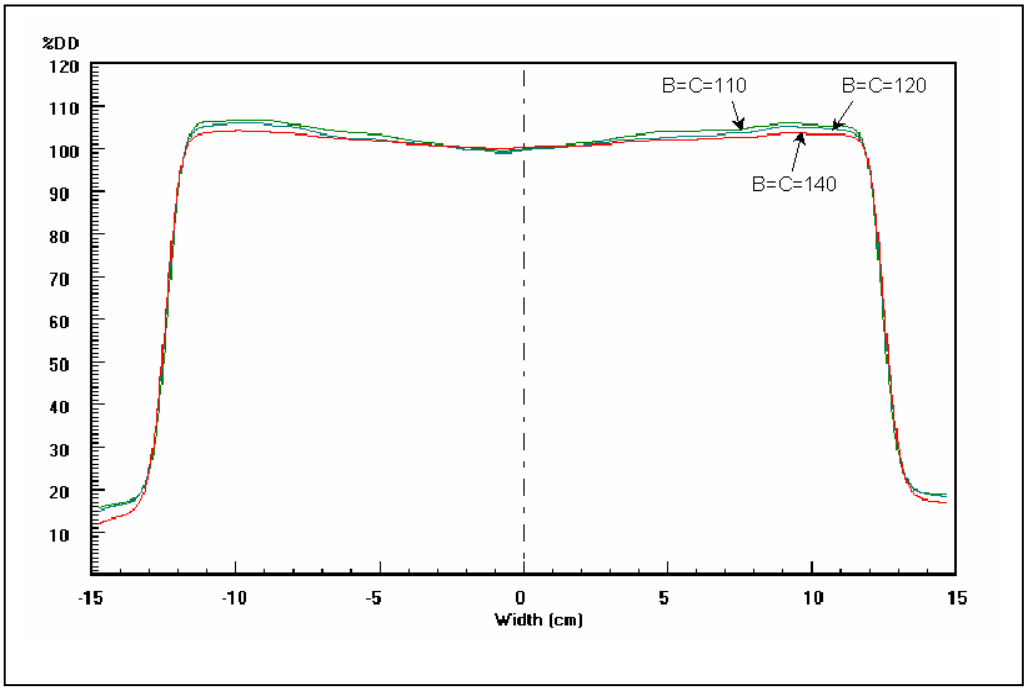

Figure 6.4 Scanner signal linearity setting change affects the film dosimetry profile curve shape

Figure 6.4 shows how the GSV-OD setting changes affect the profile shapes and subsequently the film dosimetry. So, maintaining a consistent scanner contrast setting is very important in keeping the GSV-OD response linear. The step wedge should be scanned regularly to test the scanner constancy of setting, and the GSV-OD plots archived.

6.2.4 Selection of radiation dose to optimize linearity of GSV-OD

If an 8bit scanner is the only choice to the user, the noise level can be smoothed by software. The radiation dose used to calibrate the film should be chosen to provide GSV using range within the dynamic range of the film. So, the following method to reduce noise affect may be used. Before a scanner is used for the film dosimetry, a standard step wedge film is scanned. After the the linearity of the GSV-OD is optimized by changing the scanner settings, the optimized exposure to the film should be carefully determined. A test film should be exposed to identify the radiation exposure needed to produce the optical density values in the dynamic range and within the linear region.

6.3 Scanner warm-up factor

A transparency film desktop scanner contains a light source, mirrors, CCD camera, and A/D converter. The most common light source used in a computer desktop scanner is a bar type lamp between 100 to 400 watts. The intensity of the light emitted from the light source can be slightly varied under software control. The light collected by the CCD can be influenced by changes in light source intensity. Electronics including the CCD and lamp only reach stable operating conditions after the instruments are well warmed up. Until then the output GSV will drift. Change in signal intensity affect greyscale values. When the scanner is used for the radiation film dosimetry, any adjustment of GSV made by image processing software after the image is scanned will make dosimetry difficult. In such a case, the image correctly represents the percentage of the dose distribution. It is very important for physicist to know that whether a warm-up time is required for any scanner used for the film dosimetry.

The warm up effect for a scanner can be checked by the comparing signal level changes before and after the warm up time. The film used can be a standard step wedge, or a fixed test point can be monitored on any exposed film. The film can be repeatedly measured after the scanner is first turned on, until the scan signal stops rising and reaches a stable level. After that, scans should be taken at different time gaps as 1 minute, 2 minutes, 5 minutes and 10 minutes until the signal level drops back to the standby level. Using this method the warm up time may be determined and the separation of repeated measurement optimized.

6.3.1 The investigation

Equipment and Material used

1. A HP-4c/T (8bit) desktop film transparency scanner was tested, and compared with Umax-4000 (14bit) desktop film transparency scanner.
2. X-Rite transmission single point reading film densitometer was used to measure the OD of the calibration transparency.
3. A Kodak optical step wedge was used as the calibration transparency.

4. RODOMS software was used to display Optical Density vs Screen Greyscale Value.

Method

1. Optical density range determination

The optical density values for each density step of the optical wedge film were determined using the X-Rite film transmission densitometer to read the optical density values for each step. The background value was subtracted and the zero value set on the background step.

2. Image scan for testing the scanner setting

A Bitmap image for the step wedge film was generated using the desktop scanner. The step wedge film was scanned by the HP 4c/T scanner. The scan brightness and contrast were set to achieve the best linearity which is determined by GSV-OD relationship (RODOMS) function. 100ppi scan resolution was used for the image size.

3. Film scanning times

The film image scan started from when the scanner was first turned on in the morning without any warm up. The scans were continually performed from the first scan, one after another until 20 continuous scans. After 20 scans are completed, a 10 minute gap was left before another scan is taken. Subsequent scans were taken at 15minutes, 20minutes, 30minutes and 60minutes. The step wedge film was fixed in one position without any movement and the scan area was determined without any change during the scanning procedure.

4. Image greyscale value scanning

This procedure was used to display the GSV-OD curve from X-rite densitometry readings and scanner GSV. The data manipulation was performed using the RODOMS film scan function. The GSV was read pixel by pixel along the step wedge direction (Figure 6.6). The scan position was determined accurately

corresponding to the optical density reading start and stop position on the film. 256 levels of screen GSV were inverted from B-W to the W-B (white for 0 value and full black for 256 value). An optical density vs screen GSV relationship was plotted.

Figure 6.6 Kodak step wedge film bitmap image scanned by HP 4c/T desktop scanner and pixel value scan direction

Experiment result and comments

Figure 6.7 compares two curves obtained at different scan times and we see the differences between the two curves. Figure 6.8 plots all the curves together on the screen and it is noticed that the maximum variation of the greyscale value range is up to 8 levels.

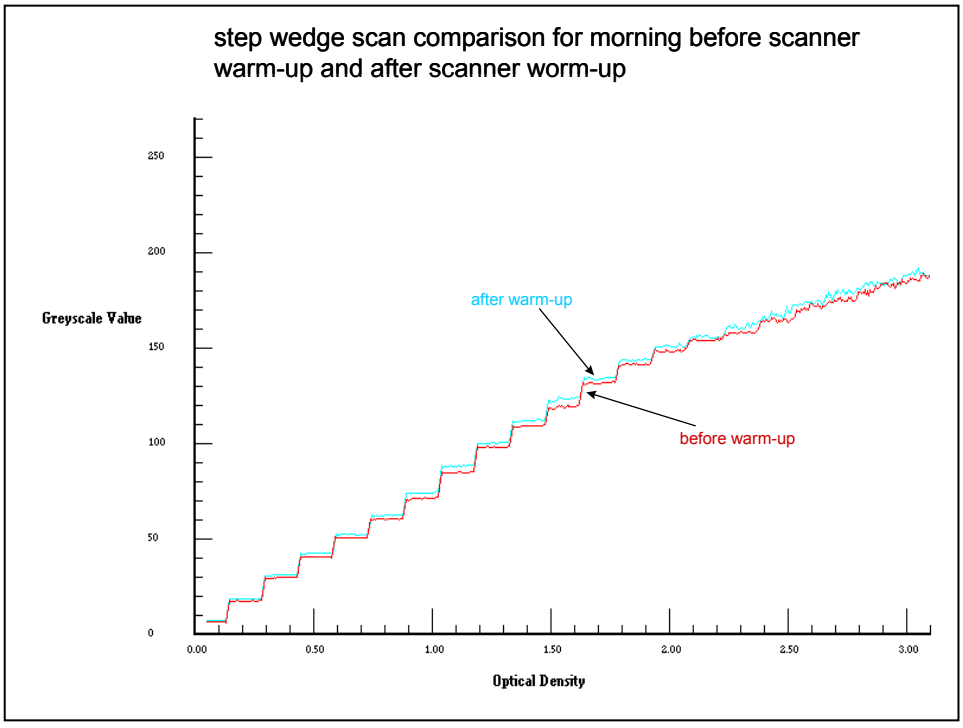

Figure 6.7, Comparison of the OD-GSV curves for same step wedge film obtained using an HP 4c/T scanner before and after a given warm up time

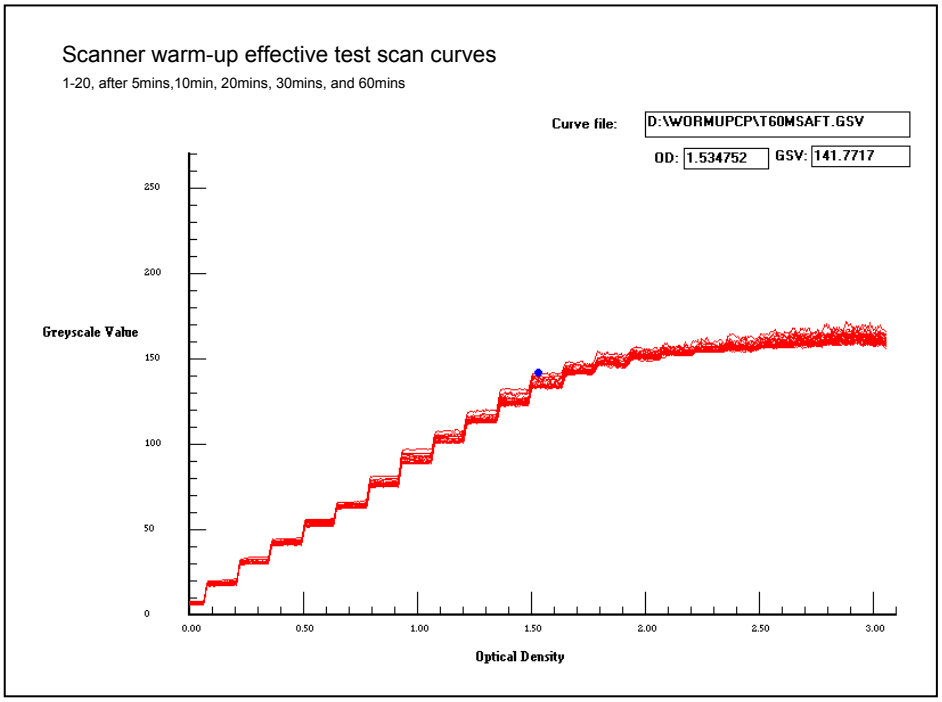

Figure 6.8, Comparison of all the curves for same step wedge film with same set-up but digitized at different times. The pixel gray scale value at OD region 1.5 is used to compare the variation in Figure 6.4.

Figure 6.9 plots the OD-GSV curve variations over the scanning times. It shows for this scanner needs 7 or 8 warm up scans to get reliable results. When the continuous scans are stopped, the signal response starts dropping in 5 or 10 minutes, and after 60 minutes, the signal level is almost back to the level before warm up. Figure 6.10 shows the warm up effect shows different effects for new generation scanner using automatic warm up control system.

This experimental result shows that the scanner warm up effect is probably common to most desktop scanners. When a scanner is used to scan a film for the film dosimetry purposes, the warm up effect must be considered. The rise time for the scanner should be determined, as well as the cool down period. The user must know the scanner reaches its operational stable condition and a program function using step wedge scan to check the warm up effect will help the scanner user to identify the optimal scanning times and perform reproducible scan experiments.

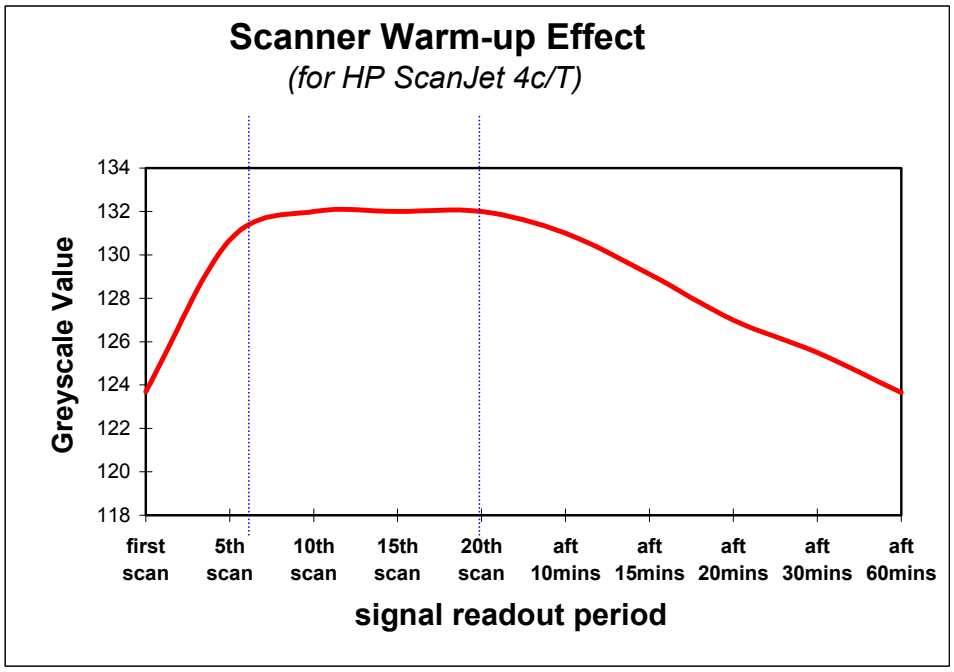

Figure 6.9, 8bit scanner grayscale value changes over different warm up times.

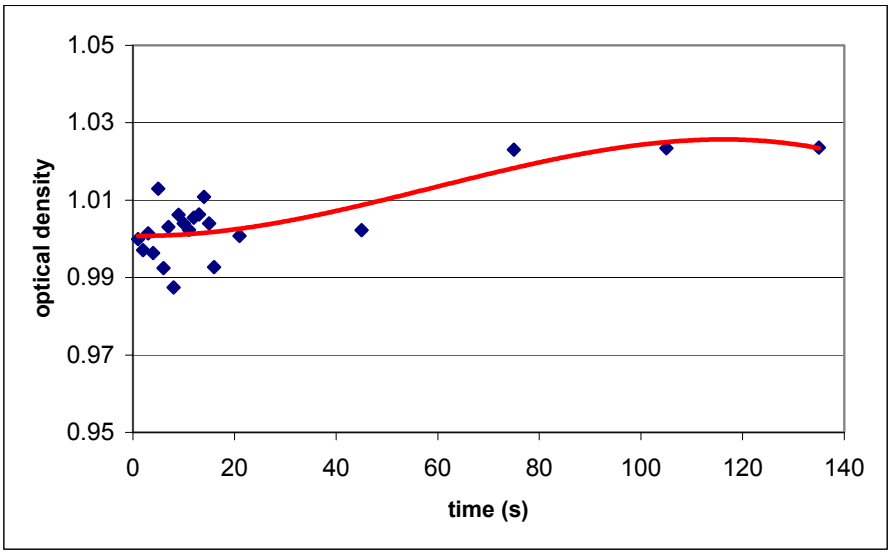

Figure 6.10 Umax Astra 4000U desktop scanner using automatic warm up control to reduce the warm up effect to scanning image.

6.4 Light source intensity distribution and background calibration

The desktop scanner is not like a film densitometer or a laser scanner. The light source does not use a point source moved in a raster when scanning a film. The light source used in most desktop scanners is a bar shaped light source, which travels in one direction along the film. This type of design could create two problems. Firstly, different scan lines over the film can receive the light from different light points within the source. If the light source is constructed very accurately, and provides uniform illumination, no problems arise. But if the light source intensity distribution is not evenly distributed along the light bar, or some part of the light source gets dirty over time, the different illumination could make the GSV incorrect. The second problem is that if the scan detector in not designed to reduce the reflected and scattered the reflection light inside the light box, some scattered light may be reflected and affect the greyscale value of several adjacent pixels. This effect could affect the pixel greyscale value slightly and might not even be noticed by naked eye (that is because most low price scanners are designed for photographic uses). However, the film analysis result could be affected by a few percent. To determine the magnitude of problems we need to scan a uniform image or the scan bed without any film on it. We adjust the light sensitivity to be suitable for the light source test, then we analyze the image pixel by pixel. The background uniformity is evaluated using iso-intensity curves and the distribution of GSV and pixel variations from the mean displayed. Figure 6.11 shows a scanner bed background scan plotted as iso-intensity curves for the HP 4/c 8bit desktop scanner. We can see the intensity distribution of the light source is good in the middle of scanning bed with flat intensity distribution within 0.5% difference, but more reflecting scattering light also made 2~3% higher, but this reflecting from this test that this scanner is good enough to be used for the dosimetry film scan, if restrict the film scan to the central area of the scanner away from the ”Reflection hot spots”.

The scanner light source intensity distribution should be checked before it is purchased for the film dosimetry. Since we may be forced to use an existing flatbed

scanner, in which after years of use the light source quality has degraded we should develop correction procedures. There are three light source intensity corrections developed and tested by this study:

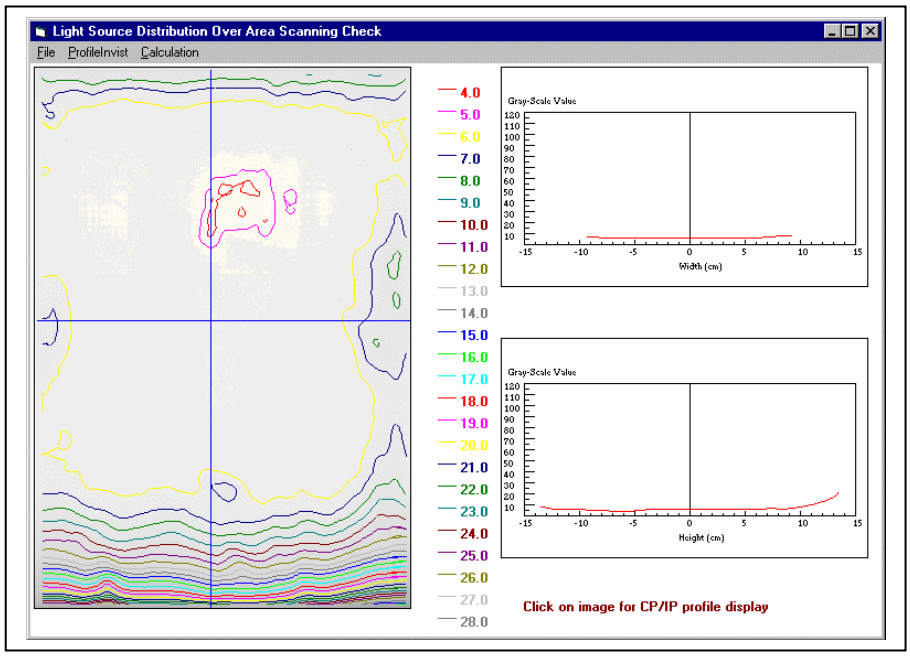

Figure 6.11 HP/4c light source distribution background scan iso-density curve

1. Background pixel curve correction

   For the travelling bar type scanner, the pixel value can be corrected by a sensitivity factor obtained from a flat field. The profile of light source intensity along the light source bar is measured by reading the GSV along the light source bar and then using the mean to give an illumination factor for each pixel position. (Figure 6.12)

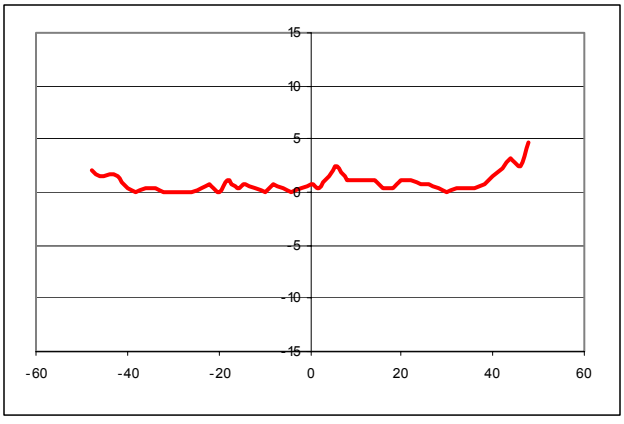

Figure 6.12 light source bar background distribution

In subsequent measurement, each pixel reading will be corrected by the corresponding illumination factor before analysis. However, this operation needs the extremely careful correspondence of the pixel positions. If the illumination factor used corrects a wrong pixel value, the scan result curve will be obviously incorrect. The background film should be scanned in registration with the measurement film with no shifting of the frames. The technical difficulties of this make it difficult to perform as a routine measurement.

2. Full background image subtraction

   For the moving light source type scanners, the uneven intensity distribution may not only come from the light source bar but be complicated by the reflected and scattered light from different parts of the scanner box. The GSV will vary in both X and Y scanning directions. This scattered background should be subtracted from the pixel readings. A full background film correction technique has been developed and tested.

   The method requires (Figure 6.13) that an unexposed background film is developed together with the exposed film. After the first film is scanned the background film is scanned without changing any scanning settings, in exactly the same position on the bed. In the film analysis program for each pixel, the background GSV is subtracted from the exposed film GSV. This method makes the proper correction for both film development and scanner background perturbations.

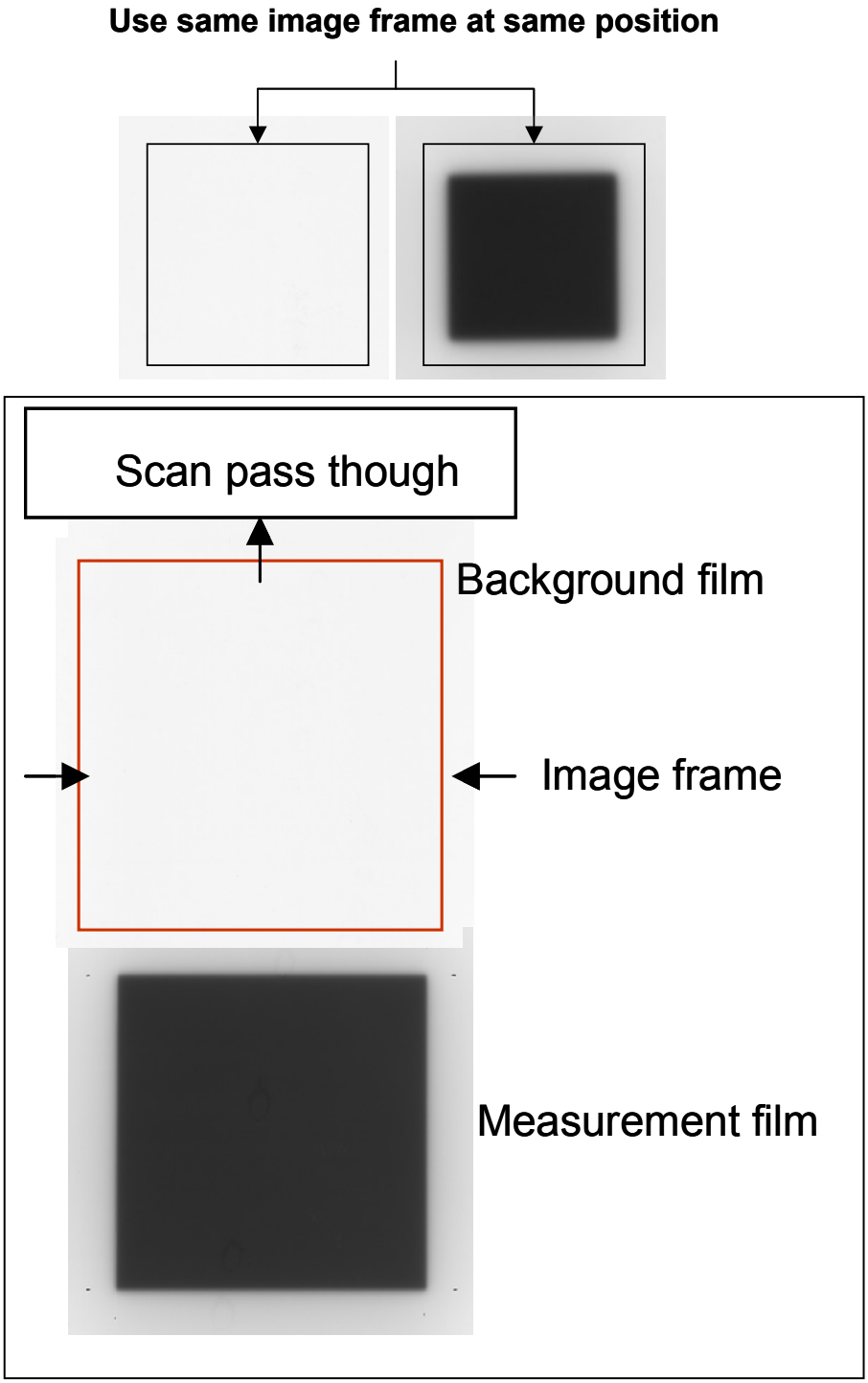

Figure 6.13 Full background film scan goes though the scanner with the scan film

Chapter 7 An Assessment of Film Dosimetry Problems

7.1 Introduction

Radiation film dosimetry normally is based on the use of industrial radiographic film. When the film is exposed and developed, the film's photo-responsive grains subtly change producing an intermediate or latent image in response to the different radiation exposure. Subsequently chemical processing produces a final image which is stable and this is analyzed using a film densitometer to provide grey scale values and optical densities. Use of a separate calibration exposure together with the QA exposure allows conversion of optical density or grey scale values to radiation dose. The resulting 2-D QA image can then be plotted as equivalent isodose curves to visualize the field dose distribution.

If the analysis is to be accurate each stage of the process from irradiation through to digitization and analysis must be reproducible and understood in detail.
As an example let's briefly consider some possible difficulties encountered at each stage of the exposure, development and measurement phases of the film QA process are considered:

- Exposure phase
  - (i) If the dose Calibration film is exposed at a different time from the main QA film, will the latent images decay sufficiently differently to invalidate the calibration?
  - (ii) How critical is it for the Calibration and QA films to be exposed to an identical energy spectrum e.g. same depth in phantom?

- Development phase
  - (i) How are dose measurements affected by film development conditions, temperature, chemical pH level, and agitation?
  - (ii) How are the measurements affected by processing artifacts?

- Measurement Phase
  (i) What is the accuracy and reproducibility of the densitometer measurements?
  Is the densitometer light source stable with time and position?
  Is the sensor stable with time?
  (ii) How much noise and uncertainty does the densitometer introduce into the measurements of dose?

With so many issues to be considered for accurate film dosimetry it has proved difficult to achieve accuracies of better than +/- 5%. This has restricted the use of film to quick, rough, visualizations of light to radiation field size coincidence.

In recent years, dynamic treatment techniques and three-D treatment planning have increased the need for a simple QA measurements providing 2-D (and indeed 3-D) dosimetry. Ionization measurements and water scanning techniques cannot easily be used for dynamic field dose distribution checks. With the use of TLD it is possible to measure the surface dose distribution over the more interesting points in the treatment area, but this still provides low spatial resolution dose information and is workload intensive.

In comparison, film can be used to rapidly provide 2-D dose distributions over large fields at resolutions of 0.01mm with low noise and a large dynamic range.
If the difficulties associated with film processing can controlled by establishing rigid protocols governing exposure, calibration, development and measurement then film dosimetry will become a more important form of dynamic treatment planning QA tool.

In this chapter the problems discussed associated with radiographic film and identify key factors affecting its use in radiotherapy QA. In particular the following problems and techniques established to overcome them are discussed:

1. **Film Calibration: optical density and dose response**

    1. OD-Dose response curve measurement
    2. OD-Dose response energy dependency
    3. OD-Dose response build-up medium dependence

2. **Latent image effects**
3. **Film processing**
    - Chemical pH and temperature effects on OD-Dose response
    - Processing marks
    - Setting-up marks
    - Handling damage

7.2 Film Calibration: optical density and dose response

Almost all densitometers measure film transmission. The Optical Density [OD] readout of the densitometer is accomplished by a logarithmic amplifier and expressed as $\log_{10}(1/T)$ where T is transmittance.

$$OD = \log_{10}\left(\frac{1}{T}\right) = \log_{10}\left(\frac{I_o}{I}\right)$$

The absolute calibration of the densitometer is made against a standard transmission tablet or optical density wedge.

The relationship between transmission and optical density is shown in the following table.

Optical Density	% Transmission	Optical Density	% Transmission
0.0	100	1.2	6.3
0.3	50	1.3	5

0.5	32	1.5	3.2
0.6	25	1.6	2.5
0.9	12.6	2.0	1
1.0	10	2.5	0.3
1.1	7.9	3.0	0.1

Before any of film products are used for the film dosimetry, it is advisable that the dynamic range and linearity of OD-Dose curve be measured to determine whether the film is suitable for the proposed use and the optimum dose rate.
Several film strips are cut from a single film. Each filmstrip is exposed to a different exposure dose using identical setups. The film strips should be developed simultaneously (or as close together in time as possible). The developed filmstrips are read using a calibrated densitometer to provide an optical density – exposure dose curve.

To minimize problems:

- All filmstrips should come from one sheet of film or at least from the same box of film, they must be all cut in the same time and packed in the same packing material.
- The beam used to expose the filmstrips should be accurately calibrated.
- The filmstrips should be exposed one after another using the same setup and the film centre must be located in the same spot under the beam.
- In order to avoid processing non-uniformity affects, all the filmstrips should be developed together simultaneously using a well maintained film processor.
- The densitometer must be stable, accurately calibrated and time allowed for warm up.

The OD-Dose response curve provides the user with details of the dose dynamic range, linearity and contrast for a particular film material. This allows the user to

determine the exposure dose for a set of QA procedures and to convert the film OD into the equivalent irradiation dose value.

Every film type has it's own characteristic OD-Dose curve and dynamic range. Using a film outside its dynamic range will clearly affect the film dosimetric accuracy.

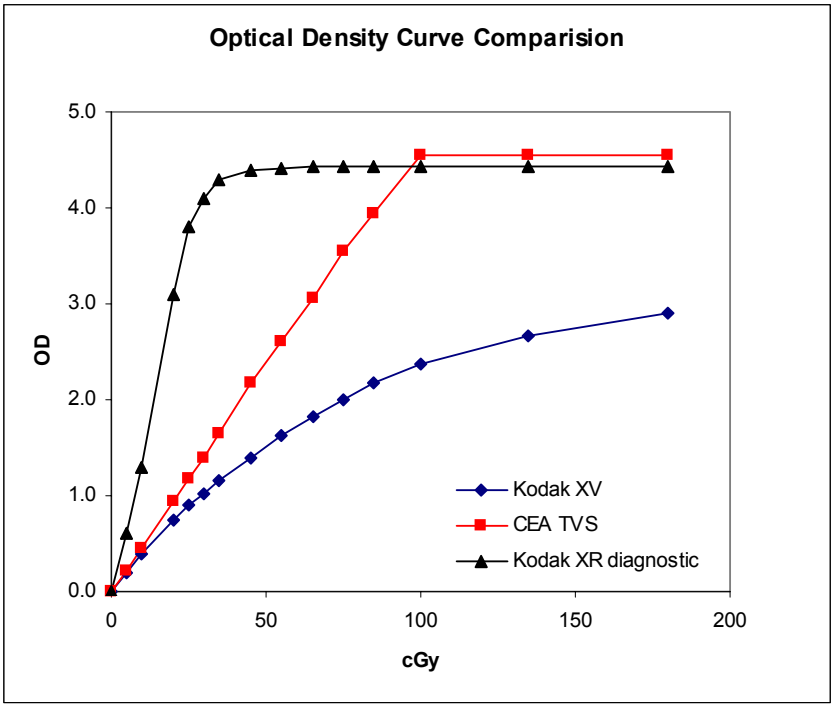

Figure 7.1 OD-Dose Response for different film types.

In this experiment, the OD-Dose response curves were compared for diagnostic, CEA-TVs and Kodak XV film. All film strips were cut from a single sheet of film [size of about 5cm x 10cm], and exposed in a solid water equivalent slab phantom with d_{max} buildup depth and 100cm SSD. The films were set perpendicular to the beam direction with 10cm x 10cm field size. All film strips were exposed on a photon beam with 6MV Siemens Mevatron-67 linear accelerator and developed using one AGFA X-ray film processor.

From Figure 7.1 the differences between three film types can be seen. The diagnostic film curve is linear over a small range of doses up to 15cGy; it provides a very high contrast image at low exposure doses but is unusable above 25cGy.
The CEA film provides a very good linearity in the dose region lower than 100cGy. It is a very good film to be used for low dose measurement and because of its linearity provides similar accurate dose conversion.

The Kodak XV-2 film is commonly used for the film dosimetry before the EDR-2 film became commercially available in 2001. The radiation response dynamic range and contrast is significant lower than EDR-2 film. For nowadays, both XV-2 and EDR-2 are concurrently used for film dosimetry. The XV-2 is more used for routine machine quality assurance such as light vs radiation field coincidence check, but EDR-2 is more used for the treatment planning verification and dose distribution checks.
Both type films are tested and compared for OD-Dose response dependent on the beam type and energy, different build-up depth, field size and beam entry angle to the film and described details in the next chapter. N. Suchowerska in 1997 (Suchowerska, N., Davison, A., Drew, J. and Metcalfe, P., 1997) and 1998 (Suchowerska, N. P Hoban, A Davison and P Metcalfe, 1999) published film calibration papers in the ACPSEM journal discussing perturbation factors and calibration. One of the important points discussed by her is that the OD-Dose response could be proportionally different at different setup depths or in different build up media. Testing the significance of OD-Dose buildup dependence helps to evaluate and determine the necessity of a correction factor for the optical density readings obtained from each film exposed at different depths in a phantom. In this experiment, the OD-Dose curves were produced at different setup depths.

7.3 Film Dosimetry Affected by Chemical, pH, Temperature

The Optical Density - Dose response is affected by film development. This may be the result of using a different processor or the same processor but under different conditions or at differing times. This study compares films exposed to radiation

beams using the same setup with the same exposure at same time but developed using three different film processors.

Equipment and materials

Three Kodak XV-2 films were exposed consecutively under a 4MV photon beam with 50MU's of calibrated output dose at 100cm SAD (five consecutive calibrations at 50MU's showed no variation in output). The film set-up used a 5cm thick perspex wedge phantom with 5cm thick base build-up, with field size of 20cm x 20cm.

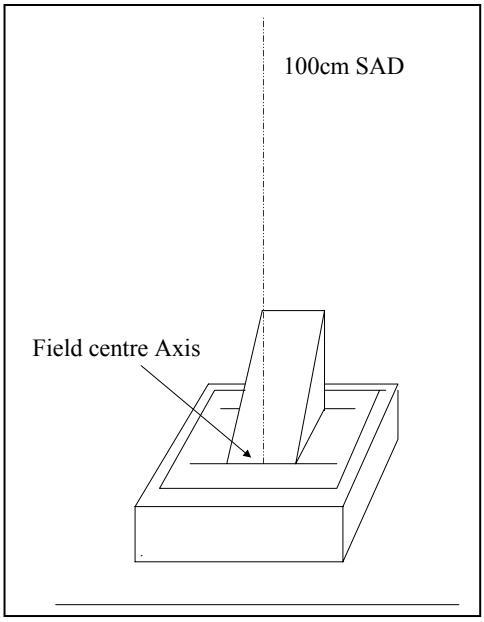

Figure 7.2 Film setup in perspex wedge phantom

Figure 7.2 shows how the perspex wedge phantom was set on the film and how the position marks were made for each end of perspex wedge in order to provide a reference point for the film distance and position setting. Three films were developed separately via different processors which were located in three different departments of St. Vincent's Hospital, Sydney (Wang Y, Cross P, 1999). Films were scanned by a HP 4c/T flat bed PC scanner after being well warmed-up. The brightness and contrast controls of the scanner were set by the greyscale signal

linearity calibration function of the RODOMS software function. Three Bitmap image files were created.

Figure 7.3 Shows the Bitmap image obtained from the HP 4c/T scanner. The image analysis was performed by the RODOMS film single curve scan function (The generation of the function details will be explained by a separate report).

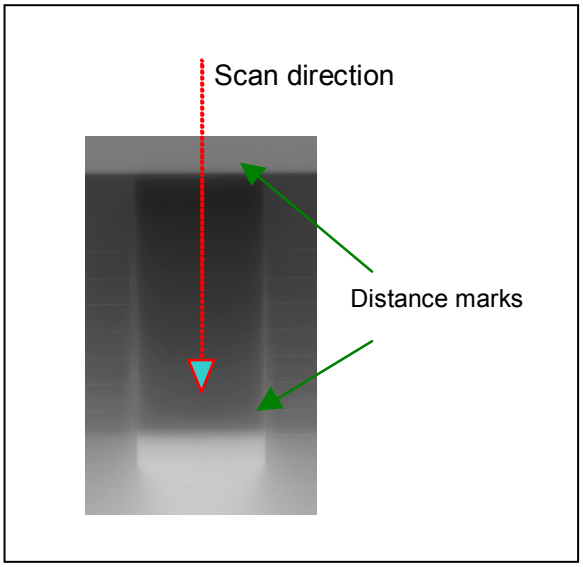

Figure 7.3 Bitmap image scanned by HP 4c/T desktop scanner

The greyscale value signal was read pixel by pixel along the image longitude axis of the wedge phantom. Each signal was converted into 256 level screen greyscale values. The scanning distance was converted into the corresponding perspex thickness at each scan point, and the thickness was also corrected by the material density factor to make the distance be the equivalent water depth. An inverse square law function was also performed in the software function to convert the corresponding perspex thickness into the equivalent depth distance.

Figure 7.4 and Figure 7.5 give the pixel value scan curves. In the Figure 7.4, The range of greyscale value for each curve is significantly different. At the D_{max} point, 120, 122, and 126 (of 256 greyscale value levels) were measured.

After a mean smoothing and re-normalizing, the three curves display no significant difference indicating that the profiles have a similar shape (figure 7.5).

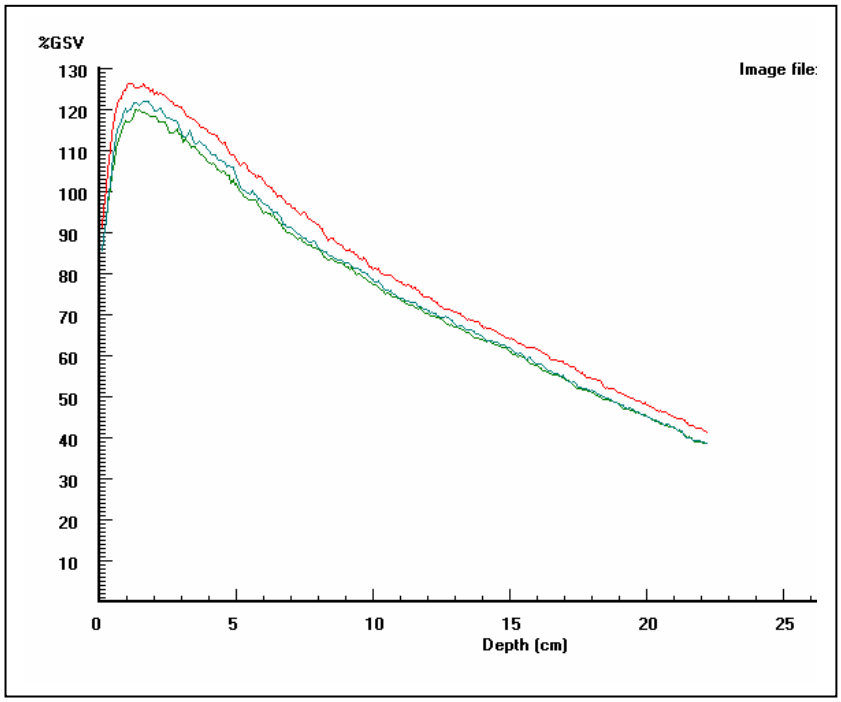

Fig 7.4 Curves for original greyscale signal read from Bitmap image

From figure 7.4 we can see that the effect of using different film processors is to cause the GSV to vary by at least +/- 5% while retaining the profile shape. Although the analysis result can be made more uniform by renormalization, this experiment result clearly demonstrates that the chemical pH and development temperature will not only affect the film development speed, but also the GSV/optical density of the final result.

Dosimetry QA films commonly have to be developed using the automatic processors in the radiology department because the small workload in the radiotherapy department does not justify their own processor. Physicists are not likely therefore to have any control over these issues. It is however important to understand that in order to maintain a reliable film dosimetry outcome, a correct film development protocol is extremely important.

As well as ensuring that the processor used undergoes regular quality assurance testing we need to develop the whole group of experimental films contiguously using a single processor.

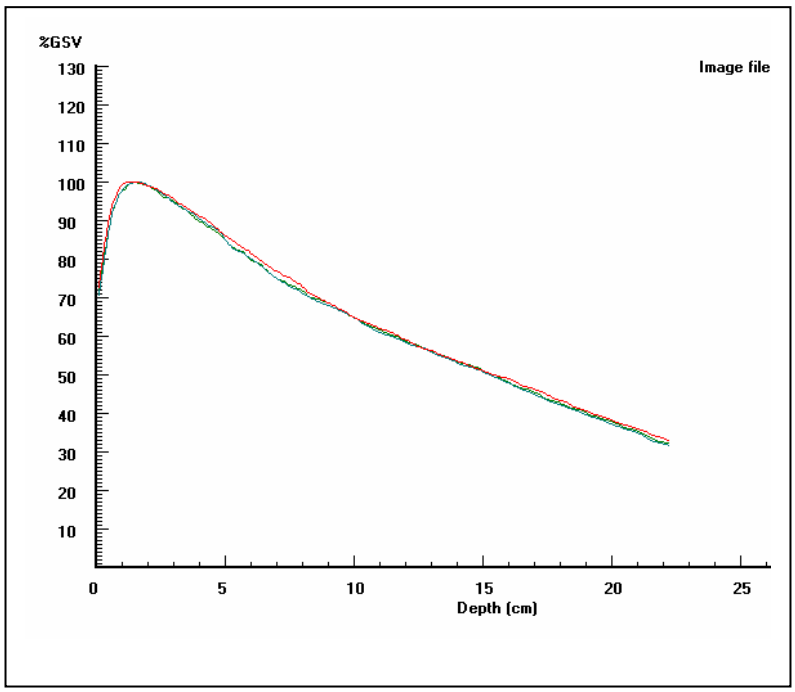

Figure 7.5 Re-normalized curves for the film developed by different film processor

From Figure 7.5, we can also see that if we renormalize three curves to the curve maximum value, the renormalized result makes the three curves almost overlie on each other. This result gives a good encouragement for using film for the relative dosimetry check. If the perturbation from processing pH and water temperature changes can be overcome, more accurate film dosimetry will result and it may even be possible to achieve absolute dose measurement using film dosimetry techniques.

7.4 Film processing artifacts

It is very important to reduce processing artifacts and reduce the film damage if we are to improve film dosimetry quality. Film-processing artifacts come from three main sources:

- *Film processing machine marks:*

  During film processing the film is placed on a film tray and is automatically fed it into the processor. It passes through a series of rollers and tanks where the film is developed, fixed, washed and dried in as little as 90 seconds. This short processing time is possible because of concentrated chemicals and high processing temperatures. The processing chemicals for automatic equipment are basically the same as for manual development although not interchangeable. After the development and fixation, a proper water wash is important for good image quality. Insufficient washing leaves marks on the film as a non-uniform base fog. Care of the rollers in the automatic processor is important to avoid film artifacts and regular cleaning of the roller racks is necessary for optimum performance. If the processor is not regularly cleaned and the roller is not washed of chemical contaminations, the roller marks can make the film unusable for QA purposes. Although the marks might not have much affect on the visual result since human eye is not be able to determine the range of 0.01 to 0.03 optical density change they could make up to 5~10% of the noise in the film analysis. So, without a professional, regular QA maintenance for the film processor, film dosimetry should not be chance to be performed in a radiotherapy department.

  The automatic processor is the essential piece of equipment in every x-ray department. The routine QA includes monitoring the performance of a processor, apart from optimum temperature and mechanical checks, chemical and sensitometric should be performed for developer and fixer. Chemical checks involve measurement of pH values for developer and replenisher, fixer and replenisher, measurement of specific gravity and fixer silver levels. Ideally pH should be measured daily and it is important to record the measurement, as regular logging provides very useful information. The daily measurements of pH values for developer and fixer can then be plotted to observe the trend of variations in these values compared to normal pH operating levels to identify problems. Figure 7.6

shows a film processor quality assurance protocol has made for Radiation Oncology Department, St. Vincent's Hospital Sydney for the routine work.

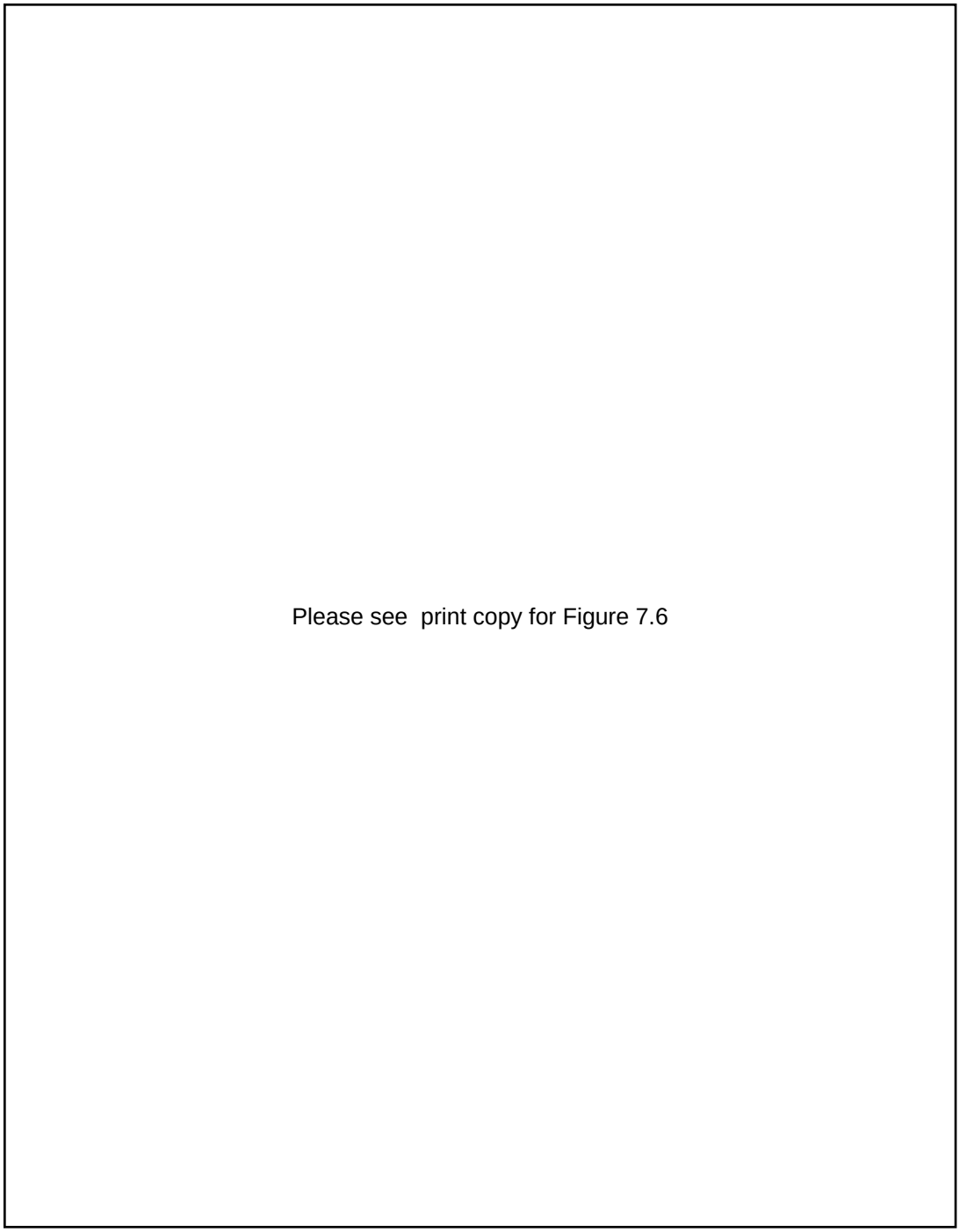

Figure7.6 Film Processor Routine QA form and protocol for St Vincent's Hospital Sydney

- *Film setup and phantom marks*

Commonly film buildup for the film dosimetry measurement is made using a solid water equivalent material slab phantom. An imperfect phantom can produce artifacts on the film image. Imperfections include:

(i) Unevenly distributed material density, un-smoothed machine quality, or bad flatness slabs.

Uneven density distribution and un-smoothed machine quality could occur on some homemade slab phantoms. The plastic material might be made by a manufacturer who is not the provider of industrial products for the dosimetry phantom material. Some plastic even contains small air bubbles. Also, when the plastic plate is cut in the workshop, scratches might be made on the surface of the plate. When the film is sandwiched between the hand-made slabs, this kind slab phantom could generate marks on the film image after the development.

(ii) bends and warps

Some phantom material could get bent into a curved shape after a few years use, especially some thin polystyrene plates with a thickness of 0.5 to 1cm. The film setup using such material may result in a small air gap.

The only way to avoid the setting up marks created by the phantom is to carefully select good quality slab phantoms, and only professional products should be used.

7.5 Latent image effects

The latent image produced in the emulsion upon exposure to radiation is unstable and will decay over time. The decay of the latent image begins immediately upon exposure. It is important therefore that any QA film be developed as soon as

possible after exposure. Thermal effects can reduce the lifetime of the latent image.

The finite lifetime of the latent image leads to a number of problems. Not least is that of calibration. Ideally QA films should be exposed and developed as near simultaneously with their calibration exposures.

The latent image lifetime is different for film types and different manufacturers. When a film is not developed directly after the exposure, the measured optical density of the film will be affected by the time between exposure and development. So, for each type of the dosimetry film, the latent image effect time should be tested.

In this study, the latent image lifetime is measured by using film exposed using the same the set up, beam, and exposure dose but developing each film after different elapsed times.

Material and method:

A 25 degree Perspex wedge phantom was set in the center of a 6MV photon beam 20x20cm^2 field with d_{max} build up depth and 100cm SSD. A 50cGy calibrated exposure dose was given, and the film developed on the same film processor after 0, 1, 2, 3, 4 and 8 days. The films were scanned using an HP4/c desktop transparency scanner (8bit greyscale value signal format). The greyscale value to optical density response linearity was calibrated by using Kodak standard step wedge film to adjust the contrast and brightness setting. The film scanner condition was checked after a full warm up to stabilize its response. The film analysis was performed using RODOMS.

Each pixel value was corrected by background value subtraction, and renormalized to the maximum value. The percentage proportion data was used for the

experiment result assessment. The central axis profile curve along the wedge angle direction for each film scanning result was plotted and overlaid.

Discussion

Figure 7.7 shows that the profile shape changes with elapsed time between exposure and development. There are almost no shape differences between the profiles for the first day and second day.

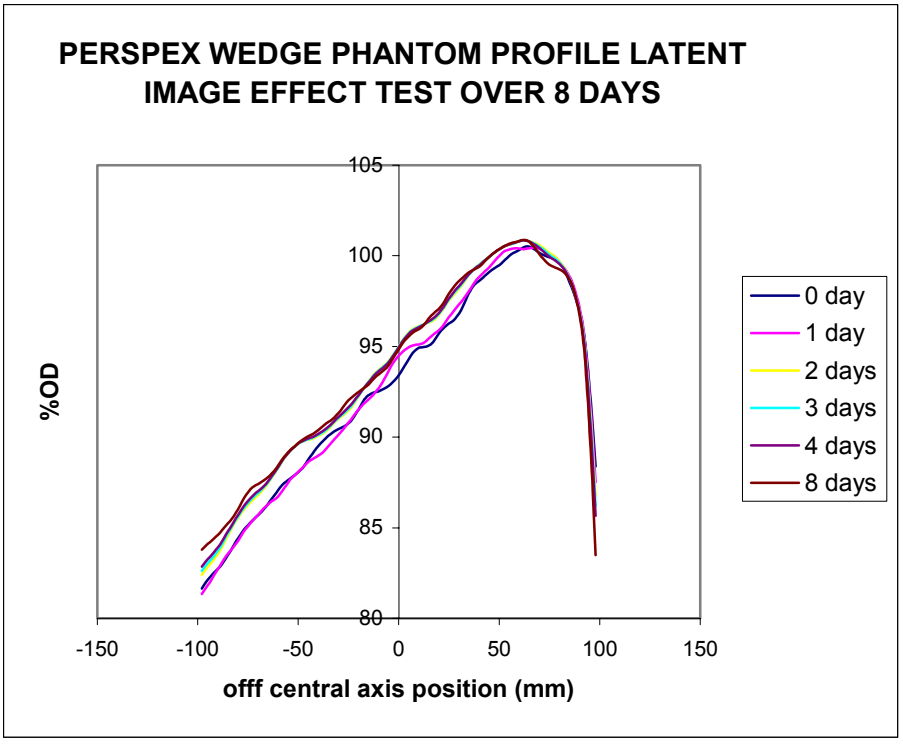

Fig 7.7, Experiment of latent image affect to the film processing. All films had the same exposure the with same set-up but at different days, then developed at the same time using same processor,

It can be noticed that the profile tail has changed and risen up slightly on third day's profile curve. This change becomes more significant after the third day's curve.

A comparison of 1day and 7days elapsed time shows that the maximum value difference is about 3% higher than after film developed in 7 days. However, no

significant curve shape changes if the film can be seen within a week period. However, as there some noticeable changes for the optical density ranges, it suggests that maximum period we should store the film before development is for 1 or 2 days. After the third day, a proportional change of the curve shape maybe affects the QA results.

7.6 Summary

EDR-2 film is commonly used for clinical planning verification. In comparison with XV-2 film type, EDR-2 has significant higher optical density response and better linearity to improve the accuracy of film dosimetry result. However, fundamentally both EDR-2 and XV-2 have similar film dosimetry problems as studied in this chapter. Almost all traditional problems such as energy dependence, beam lateral entry problem, film processing artifact etc. Nowadays, as EDR-2 film is commercially available physicists can clinically using EDR-2 film for the film dosimetry still face the same film dosimetry problems in past 20 years. The film dosimetry equipment such as film densitometer or transparency scanner are no different, the film dosimetry study in this project will still focus on the ordinary film dosimetry calibration and examine all the existing problems.

Chapter 8 Uncertainties in Film Dosimetry and Resolution Accuracy

8.1 Introduction

Film dosimetry has become more important in dose distribution checks in 3D, dynamic fields and IMRT treatment planning over recent years. Ordinary dosimetry techniques are difficult to perform compared to a film based analysis. Ionization measurements can only be taken at several fixed positions and are in a phantom and is unable to provide dose distributions for dynamic field or multiple combined field treatment plans. The TLD or in vivo techniques have been used many years to make point dose measurement for dose distribution checks but have a larger uncertainties and limited spatial resolution.

Film analysis techniques have been used in dose distribution checks since in early 1950's (Granke, Wright, Evans, Nelson & Trump, 1954). However, film dose analysis has only achieved limited use in clinical situations because the results suffer from large uncertainties. Film dosimetry is a technique which is simple to set up, is able to be used in different shaped solid phantoms and even water phantoms, and the film easily processed compared with both ionization and TLD dosimetry techniques. Over the past 40 years, many studies have been focused on reducing the uncertainty level to improve the film dosimetry results. Some techniques suggested are too complicated to perform routinely in clinical situation. So, film dosimetry is limited to routine QA checks on light-radiation field coincidence. Most people feel it difficult to overcome the issues associated with film processing artifacts, emulsion non-uniformity, beam type or energy dependence, build up medium and depth dependence, and the narrow linearity range of optical density - dose response.

KODAK XV-2 film has been used for radiotherapy physics QA in past two decades. XV-2 film has an effective dose response dynamic range around 55-60cGy. The film is commonly processed at a different time or using different film processor from the calibration film producing poor calibration. The poor linearity

of the film makes the conversion to equivalent dose from the measured optical density in error by up to 5-10%. Many reasons for this uncertainty such as processing temperature and chemical pH, and artifacts created on dirty processor mechanical system and poor calibration can be minimized or corrected by carefully designed procedures.

Other film material has better characteristics and provides some possibility to overcome the disadvantages of XV-2 film include using Gafchromic film and CEA film. However, none of those films are in general use due to either the costs or the other disadvantages. Some of the earlier Gafchromic film media are UV light sensitive and cannot retain an image for a repeat measurement.

KODAK EDR-2 became available on market in 2000. Compared with XV-2 film, EDR-2 shows a significant improvement in signal linearity, a high dose response and large dynamic range. EDR-2 film can provide more accurate dosimetry because of its good linearity and signal response at high radiation dose.

However EDR-2 film still has the characteristics of a silver halide emulsion film, such as different response to different beam type and energy. This is a problem for measuring doses at slightly different depths and different build-up media. Different field sizes used in each beam might also result in different collimator scatter to the film. This would result in higher uncertainty levels still being a problem with EDR-2 film when the film is used for the dose distribution checks for combined different beam types, energies or variable field size,.

This study focuses on the testing and comparison of the characteristics of EDR-2 and XV-2 film to suggest improvement to the accuracy of film dosimetry. EDR-2 film is increasingly used for three-D and IMRT planning dose distribution checks. EDR-2 film has a very high irradiation dose response, dynamic range and good signal linearity region comparable with XV-2 film, which has mainly used for

radiotherapy QA in past two decades. Film dosimetry has been viewed for many years as an unreliable technique, with a high uncertainty in analysis results.

In order to address the film characteristics to improve the reliability of EDR-2 film a comparison of EDR-2 and XV-2 film has been made. In characteristic curves of Optical Density vs Dose have been measured and the dependence of optical density on beam type, energy, build-up in a solid phantom, and field size investigated.

The dose distribution at different beam angles and orientation were also performed for both EDR-2 and XV-2 films. A comparison of the characteristics of EDR-2 and XV-2 films provide us with some clear ideas on how to improve the calibration accuracy in film dosimetry and the implementation of film based dose distribution checks.

8.2 A comparison of EDR-2 and XV-2 film

Several experiments were carried out to compare the characteristics and evaluate the calibration uncertainties, beam type and energy dependence, build depth dependence, field size dependence and beam to film entry angle dependence for EDR-2 film.

8.2.1 General Experimental Details

EDR-2 film and XV-2 film characteristic curves (OD vs Dose) were compared (Figure 8.4). The film was cut into the strip size 5x10cm^2 and packed using black paper. RW3 white solid slab phantom was used for the set-up of build-up depth dependence check, beam type and energy dependence check, field size dependence check and optical density calibration. Two specially designed rod phantoms different diameters were used for the beam to film entry angle dependency checks. The radiation source used is the 6MV photon beam on Varian Clinac-2100C.

The exposed film was developed using a Konica SRX-701film processor with a processing temperature 35^{o}C and 90 seconds processing time. All filmstrips were stacked together on the large film before send into the processor. All films in each experiment group were processed at same time using same processor in order to reduce the film processing uncertainties.

The film was scanned using an Umax Astra-4000U desktop scanner with transparency adaptor, 14bit grayscale and 100dpi image resolution. Scan linearity is adjusted using the contrast and brightness controls to provide a linear GSV-OD relationship using the WellHofer standard step wedge. The adjustment resulted in a GSV-OD deviating by ±1.0% from a linear relationship. The resulting dynamic range reached to an optical density of 3.19D. Scans were saved as bitmap files, and analyzed procession a subset of RODOMS.

The scanned grayscale values were converted into the optical density value using the calibration. A smoothing algorithm was applied where the value of each pixel was an average of the neighboring pixel values in a 3x3 matrix with the two highest readings and two lowest readings removed.

The depth dependence

A slab phantom and film was setup as shown in Figure 8.1 to 100cm SSD, on the top of 6cm thickness slabs for a backscatter build-up.

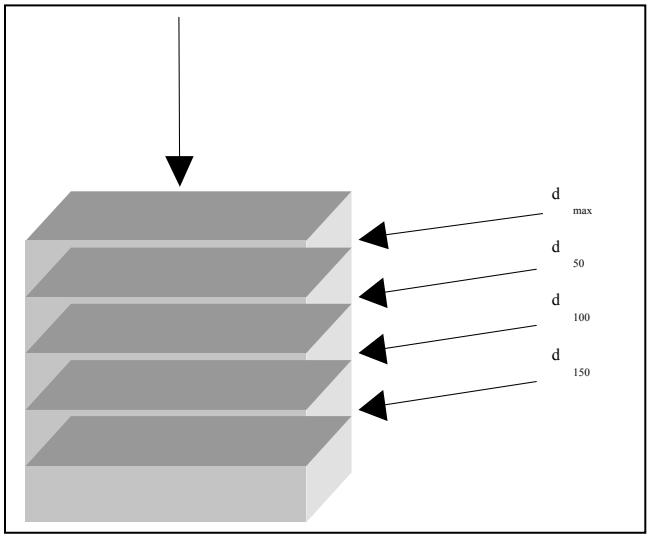

Figure 8.1 Film strips set-up in solid water phantom

Absolute dose rates were calibrated to different build-ups for d_{max}, $d_{5.0}$, d_{10}, d_{15} and d_{20}. For each build up, EDR-2 film was exposed at doses of 50, 100, 200, 300, 400, 500, 600 and 700cGy to each strip. The exposure 50, 100, 150cGy were given for the XV-2 strips. Both film types were mounted as one single strip with the experiment group and developed along with a background film.

Field size dependence

The same set-up was used for the build-up dependence check, with film strips set at d_{10} depth. Doses of 60cGy were given to XV-2 and 350cGy to EDR-2. The measurements were performed using filmstrips at the centre of the beam without change in the build-up and beam distance, the field size was varied for each exposure from 1x1, 2x2, 3x3, 4x4, 5x5, 10x10, 20x20, and 30x30cm^2 square fields (Figure 8.2). Two different depths were compared between d_{max} and d_{10}. Both films were developed together and the optical density value normalized with reference to the 10x10cm^2 field. The comparison with an ionization measurement was performed with the same set-up using a small volume ion-chamber. Three curves are overlaid in figure.

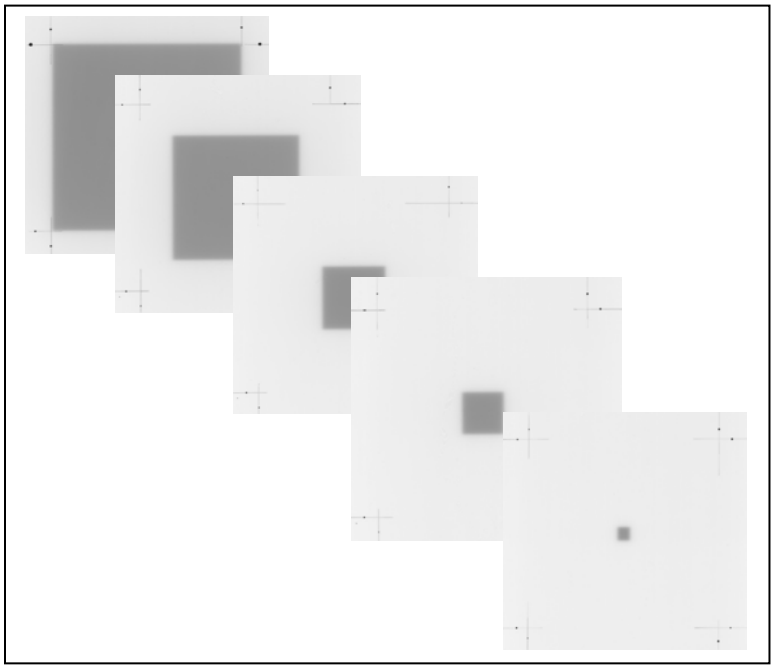

Figure 8.2, Film taken at $d_{10,}$ 100cm SAD and given 60cGy to XV-2 and 350cGy to EDR-2 film for different field size

Beam-type and energy dependence

The film strips were set up in the same slab phantom (Figure 8.2), but set at 100cm SSD on the build-up slab surface. All strips had a build-up at d_{max} thickness according to the d_{max} thickness required for each beam type and energy. The calibrated dose to expose XV-2 film was 60cGy and 350cGy for EDR-2 film.

Beam to film entry angle dependence

Two cylindrical RW3 material phantoms were set up isocentrically with the gantry rotation centre, one of 25cm diameter and another one of 8cm diameter (Figure 8.3).

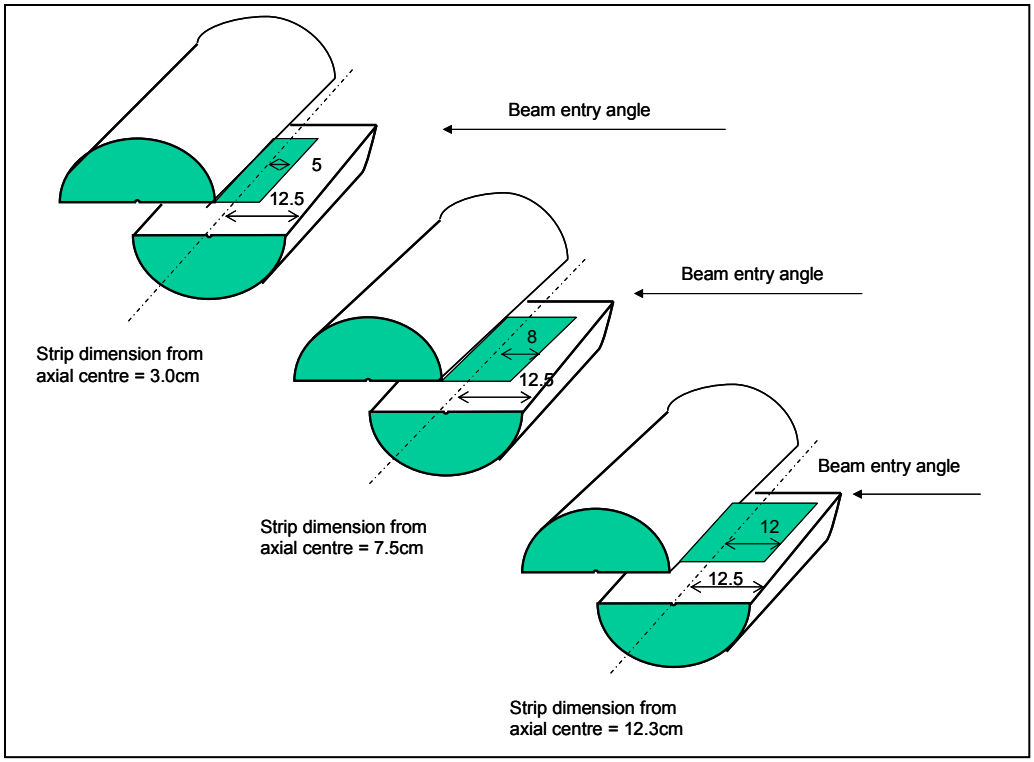

Figure 8.3, The filmstrip set at the centre of the rod phantom. For the lateral beam entering the film parallel to the beam central axis, three different size filmstrips were compared to test for the lateral scatter.

Both rod phantoms were cut into two semi-circle cylindrical sections though the cylinder axis line. Black paper packed filmstrip was located at the central axis of the rod and the central axis point marked on the film pack. In order to

reduce the air gap, plastic electrical tape was used to tightly bind the two pieces of semi-cylinder together on both ends. The film loaded cylinder was set up to align the central axis line to the gantry rotation isocentre, and the film was lined-up to be horizontal using both side wall lasers. A 60cGy exposure dose was applied to the XV2 film and 350cGy for the EDR2 film, calculated for the cylinder centre depth. The gantry was set to different angles for each exposure from 0^o to 80^o with a 15^o step. A 1^o small angle change step was made from 80^o to 90^o gantry angles.

8.2.2 Results

The beam type and energy dependence test result shows by the table in Table 8.1. High energy electron beams give higher optical density response from the film at the dose distribution peak value depth. The difference in OD between the lowest and highest energy electron beams is more than 0.1D.

There is no significant difference in the OD and beam energy for the two beam types for EDR-2 film and XV-2 film.

Beam type and Energy	EDR-2 Film Average OD for 350cGy at dmax	XV-2 Film Average OD for 60cGy at dmax
6MeV Electron	1.79	1.54
9MeV Electron	1.81	1.55
12MeV Electron	1.87	1.59
16MeV Electron	1.92	1.63
20MeV Electron	1.97	1.63
6MV Photon	1.78	1.50
10MV Photon	1.81	1.51

Table 8.1 Comparison of EDR-2 and XV-2 beam type and energy dependence.

The optical density - dose curves for EDR-2 and XV-2 films are shown in Figure 8.4. The optical density response is varied in both film types. Although the response for EDR-2 and XV-2 are different and also in different linearity, the relative range changed by beam type and energy could be similar.

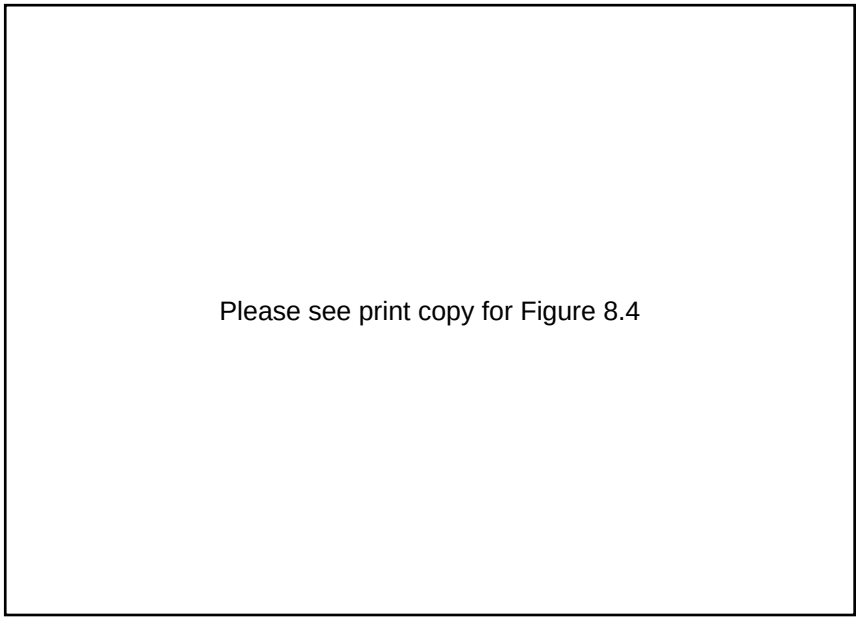

Figure 8.4, Optical Density - dose response for EDR-2 film and XV-2 film (Wang, Zealey, Cross, 2003)
.

The build-up dependence results are shown in Figure 8.5 for the EDR-2 film and Figure 8.6 for XV-2 film. Those two figures show that the build-up is insignificant for exposures in the linear region of the response curve. This result helps us to determine the effective dose response range for both films. As we can see from the figures there is no significant perturbation from different build-up depth for exposures of between 350-400cGy for EDR-2 film and 55-60cGy for the XV-2 film. Above these values buildup effects become evident.

The film field size dependence results are shown in Figure 8.7 for the build-up of d_{max} and Figure 8.8 for the build-up of d_{10}. The Field Size Factor [FSF] is the dose normalized to the 10mmx10mm field dose of the EDR-2 film. Comparison of the FSF results obtained by film dosimetry with those measurement carried by the ionization chamber, shows significant differences. For the d_{max} build-up, there is maximum 2% discrepancy in the FSF between EDR-2 and XV-2 films, but the discrepancy between film and ionization measurement shows a 15% difference for small field sizes. The d_{10} build up, shows a 5% maximum

difference in FSF between EDR-2 and XV-2 films. Again in small fields ionization measurements differ from this by a maximum of 20%.

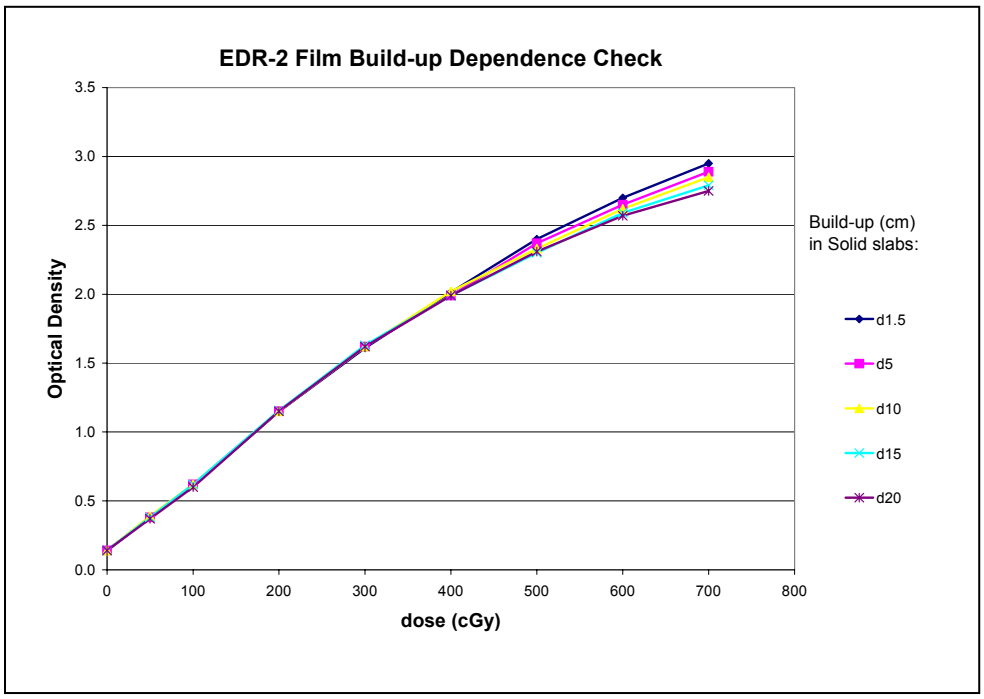

Figure 8.5, Build-up depth dependence check for EDR-2 film in solid RW3 slab phantom with 6MV x-ray, 100cm SSD, and 10x10cm^2 field size.

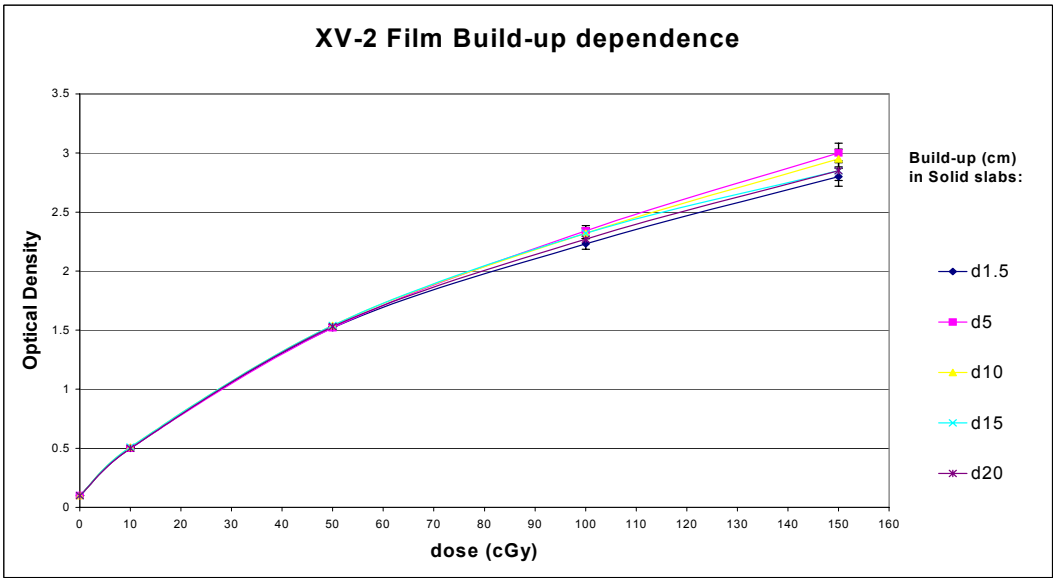

Figure 8.6, Build-up depth dependence check for XV-2 film in RW3 slab phantom with 6MV x-ray, 100cm SSD, and 10x10cm^2 field size.

When the field size is decreased, the differences in FSF between films and ionization measurements become larger.

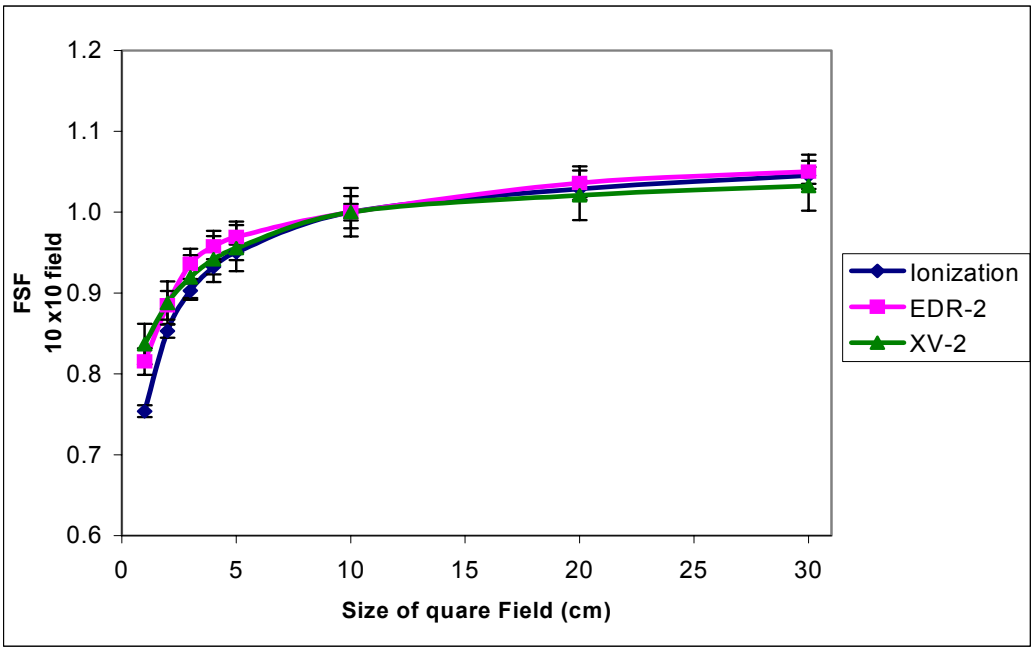

Figure 8.7, Field size dependence check for 6MV X-ray at d_{max} build up. The readings are normalized to the 10x10cm^2 field.

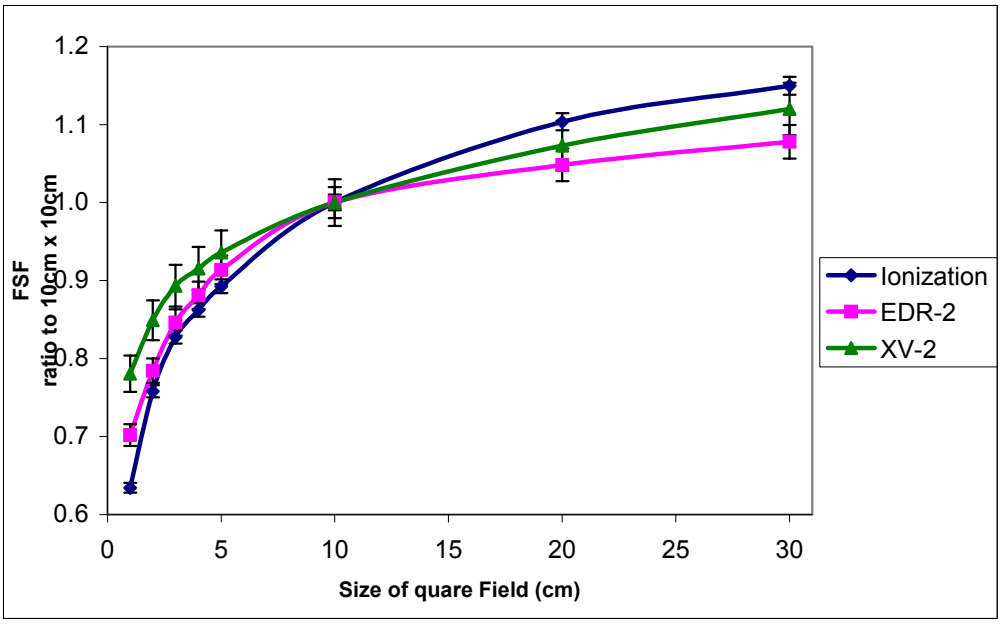

Figure 8.8, Field size dependence check for the d_{10} build up. The readings are normalized to the 10x10cm^2 field.

The beam to film entry angle dependence test result is shown in Figure 8.9, and different rod phantom diameters are compared in Figure 8.10. There is no obvious difference in results between EDR-2 and XV-2 film. Both films give broadly similar results. The GSV vs Dose entry angle curves show no difference if the beam to film entry angle lies between 10^{o} to $80^{o.}$ However, for beam entry angles smaller than 10^{o} and lateral entry beams, the results become noisy, and the OD rapidly increases with angle when the film is almost parallel to the film. This effect is stronger if the beam entry distance is larger.

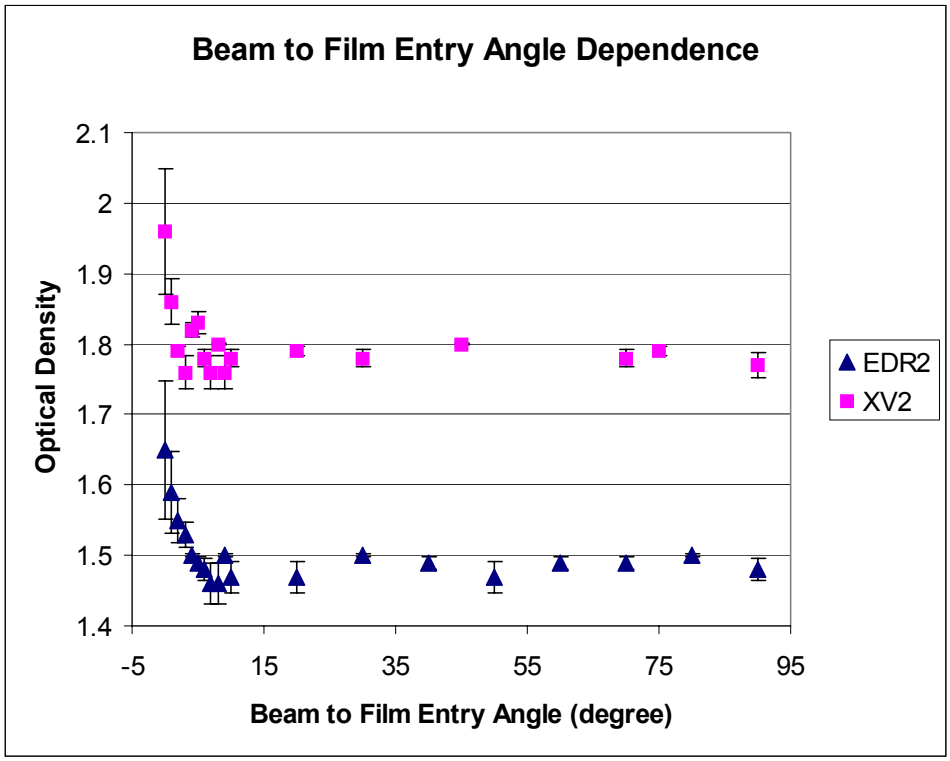

Figure 8.9, 6MV X-ray beam entry angle to the RW3 rod phantom central axis from 90^{o} to 0^{o} to the film and exposure to filmstrips centre are 60cGy to the XV-2 film and 350cGy to the EDR-2 film

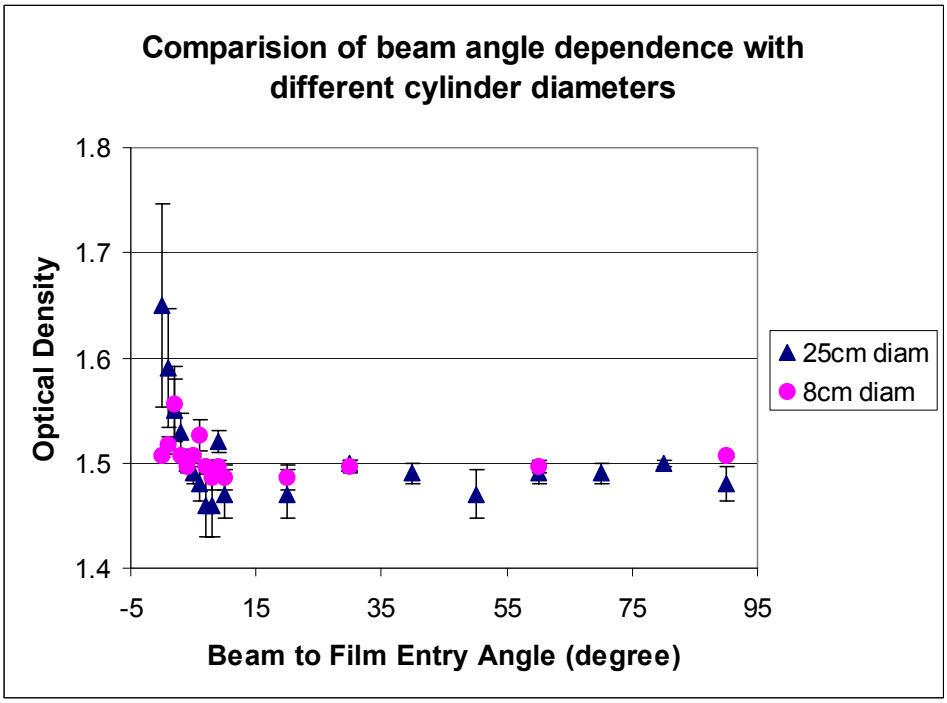

Figure 8.10, Beam entry angle test for different diameters of RW3 cylindrical phantom. The comparison made between 25cm and 8cm different diameter build-up. The central axis dose is calibrated same to 350cGy to the EDR-2 film.

8.2.3 Discussion

Film response to different beams and energies

Giving the same dose using a different beam and energy is expected to produce very different OD vs Dose response curves. Comparison of the 60cGy dose level for XV-2 and 350cGy dose level for EDR-2, shows the dose conversion must use separate OD vs Dose response curves created for each beam type and energy. However, the experiment results also show that the optical density responds to changes in dose in a similar way for different beam type and energy.

This allows the possibility of renormalizing the curves from different energies and beam type to the same value point. All curves overlay each other with very little difference. In this case, we might possibly use only one common OD vs Dose response curve but calibrated with different renormalization values for each beam and energy.

Film response to the processing

Uncertainties are generated by processing variations between films developed at different times, with different processors, temperature and chemical pH. The film analysis result most affected by these effects is the OD-Dose response curve. If we only use the OD-Dose calibration film exposed at the same time and processed together with the test film, using same film processor, the uncertainty level will be reduced effectively. However, this is technically impossible.

We can however minimize effects due to processing by undertaking QA on the film processor and exposing a single film to a fixed calibration dose for every test film.

Film response beam entry angle dependence

There is no significant difference between results for the beam angles from 90 degree (perpendicular) to 10 degree beam angle to the film. The OD increases steadily for angles smaller than 8 degrees and the differences. When the beam lies almost completely parallel to the film (<3 degrees) the OD increases by more than 0.1 OD above the OD for high angles. This result is similar for both EDR-2 and XV-2 films. This variation in response is significant because in film isodose analysis it could cause a 5 to 10% result difference in dose estimation. From the comparison of film set in different diameter rod shaped phantoms, larger diameter phantoms cause even larger increase in OD. We consider that the larger diameter phantoms are closer to the clinical situation with regard to film set-up depth.

The reason for the increase is complicated, It could be caused by the air space between the film and phantom surface, the film packing material, and the secondary scatter generated by the film emulsion silver grains. From this experiment, we recommend that the lateral angle beam entry angles to the film should be greater than 7-10 degrees.

Film response build-up depth dependence

The beam energy spectrum hardens with build-up depth. The shallow build-up includes more low energy photons/electrons and these will provide high levels of scattered radiation. The film has a high response to such low energy scattered radiation and will have an elevated OD as a result.

This enhanced exposure is negligible for low buildup depths. When the build depth increase, the beam contains less lower energy scattered radiation, and the film exposure is lower. At interim buildup depths there is a peak in scattered radiation and an over response in the film. The amount of response difference depends on the machine design and consequently the film calibration would need to be calibrated for a specific machine.

However, the data can be used from the EDR-2 film and XV-2 film to determine the dose for a given depth and reduce incorporate into the film measurement.
This experimental result also suggests that increasing the build up thickness could help to reduce the optical density variations caused by low energy scatter. This is often experienced in the field profile measurements if we use film taken with little or no build-up and is seen in the form of an over-response in the flatness curve compared with that obtained using a water ionization scan

Field size dependence

The experimental results show that the film response to different field sizes could get different value for the ratio compared with ionization measurements. The differences are also depending on the film type and build-up depth.

Both the FSF vs Field size curve shapes vary for different films and the ionization measurements. The curves are steepest for small field size and flatten towards larger fields. As we know silver halide film has an energy dependent behavior and an over response to the low energy scattering.

Different field size beams have varying components of low energy scattered radiation resulting from different build-up depths. The different field sizes contain different proportions of scattered radiation reflected by collimation system. The surface dose also could contain more lower energy components than a deeper build-up region. Hence we expect a higher response for film than an ionization chamber for small fields.

It should give consider if that when a film dosimetry check is performed for a 3-D plan or IMRT. different field sizes could affect the result.

If the test film result is calculated using the output factor given by the ionization measurement, a level of uncertainty will exist in the dose distribution analysis results due to the films response to low energy scattered radiation. There is need to consider this issue and develop procedures to improve the film analysis result for the IMRT QA.

8.3 Summary

The result of this study has helped to gain a better understanding of the EDR-2 film characteristics. Compared with XV-2 film, the EDR-2 film has higher effective dynamic range with good signal response linearity. However, the film shares beam type and energy dependence characteristics with the XV-2 film. If the film is directly used in film dosimetry for checks on planning dose distributions without further careful correction the uncertainty levels of the dosimetry could still be high. This is especially true for multiple beam and small size field in some IMRT planning dose distribution quality assurance.

This study suggests that film calibration correction factors should be used instead of simply using the ionization chamber correction factors. The film exposure should be corrected by the factor measured from film optical density curve.

Calibration of the film can be simplified by using a correction table established for different beam energies containing with different build-up depth and field sizes instead of using a single OD-Dose response curve to convert the equivalent dose.

The curve shape appears not to depend on the film type, although the OD range does, the response curves can be renormalized to a control reference reading for converting the optical density to equivalent dose. The process needs to be performed before the isodose analysis processing take place. Implementation of this method would not be easy in routine clinical work unless the film analysis software is specially designed to manage these complicated corrections.

In order to reduce the uncertainties associated with film processing, a control reference exposure taken with the testing film.

Acknowledgement

All the appreciation for when experiments has performed in Ballarat new cancer centre and greatly thanks to the Physicist group of Radiation Oncology Victoria especially to the William R. Patterson, chief medical physicist of ROV for providing effective support on the experiment facilities and film processing.

Chapter 9 Radiation Oncology Dosimetry Management System [RODOMS] - the Development of a QA Protocol

9.1 Introduction to the RODOMS QA Protocol

The use of radiographic film can simplify day-to-day QA procedures. The use of any form of film for radiation dosimetry requires careful calibration, development and measurement under controlled and reproducible conditions. If film is to be used then a detailed protocol for its use, measurement and analysis is required.

RODOMS has been developed over the past 6 years from a basic set of calibration procedures to a level where it can be used for full QA. It has been extended further for use with IMRT and Brachytherapy, in Sydney St. Vincent's Hospital, Geelong Andrew Love Cancer Center, Ballarat Austin Radiation Oncology Center and Sydney the Mater Hospital.

In earlier chapters we have shown that the following measurements are important in radiotherapy QA.

1: Scanner Setup and Calibration

- Linearization
- Flat fielding and scattered light correction

2: Dose Calibration

3: Percentage Depth Dose (PDD or %DD)

4: Beam Profile

9.2: A Software Overview

This section provides an overview of the RODOMS software. We discuss the software development in detail in Chapter 11. The software is driven via a GUI interface and programmed in Visual Basic.

The main software modules deal with:

1. Input of GSV data from scanned film images
2. Output of images, charts and data to printer
3. Image display
4. Dose calibration
5. Signal correction factors and data interpolation
6. Signal smoothing functions
7. Curve drawing and curve fitting
8. Conversion from pixel to physical coordinates
9. Isodose data tracking, isodose curve plotting and profile display
10. Three-D chart graph display
11. Data save and retrieval

The film dosimetry is one of the important part of RODOMS software (Figure 9.1) providing clinical quality assurance for quick dose distribution analysis. The program analyses digital images scanned from film using a film scanner or a high dynamic range desktop scanner with transparency adaptor. The software can import bitmap images created by different scanners (Figure 9.2).

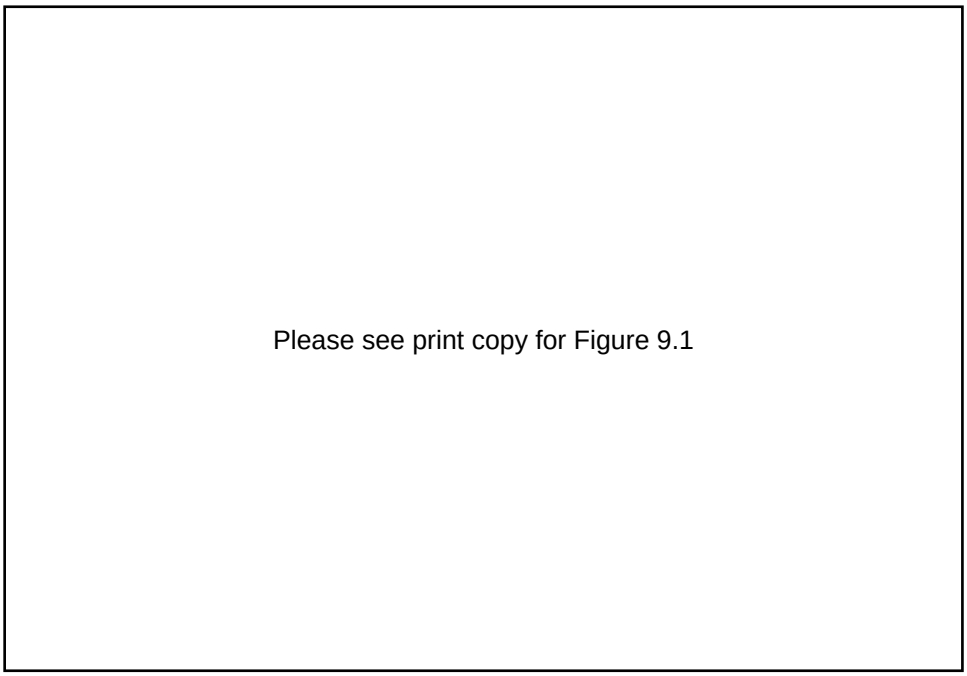

Figure 9.1 RODOMS Main menu face

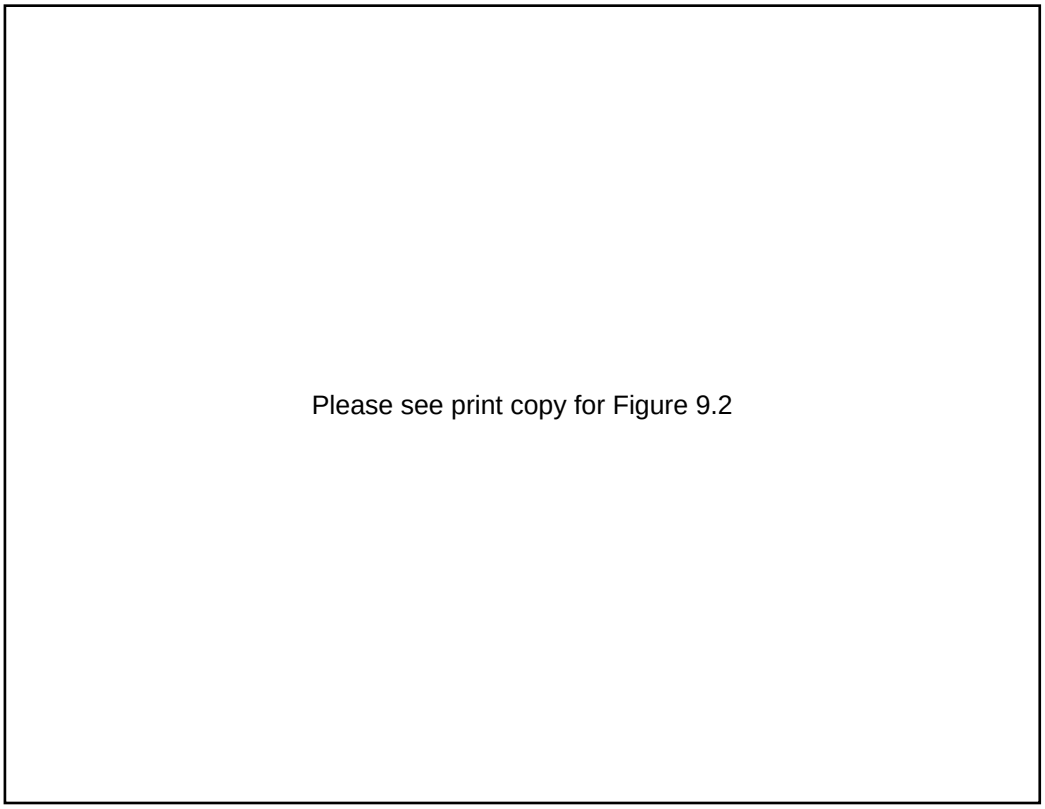

Figure 9.2 Film dosimetry main menus.

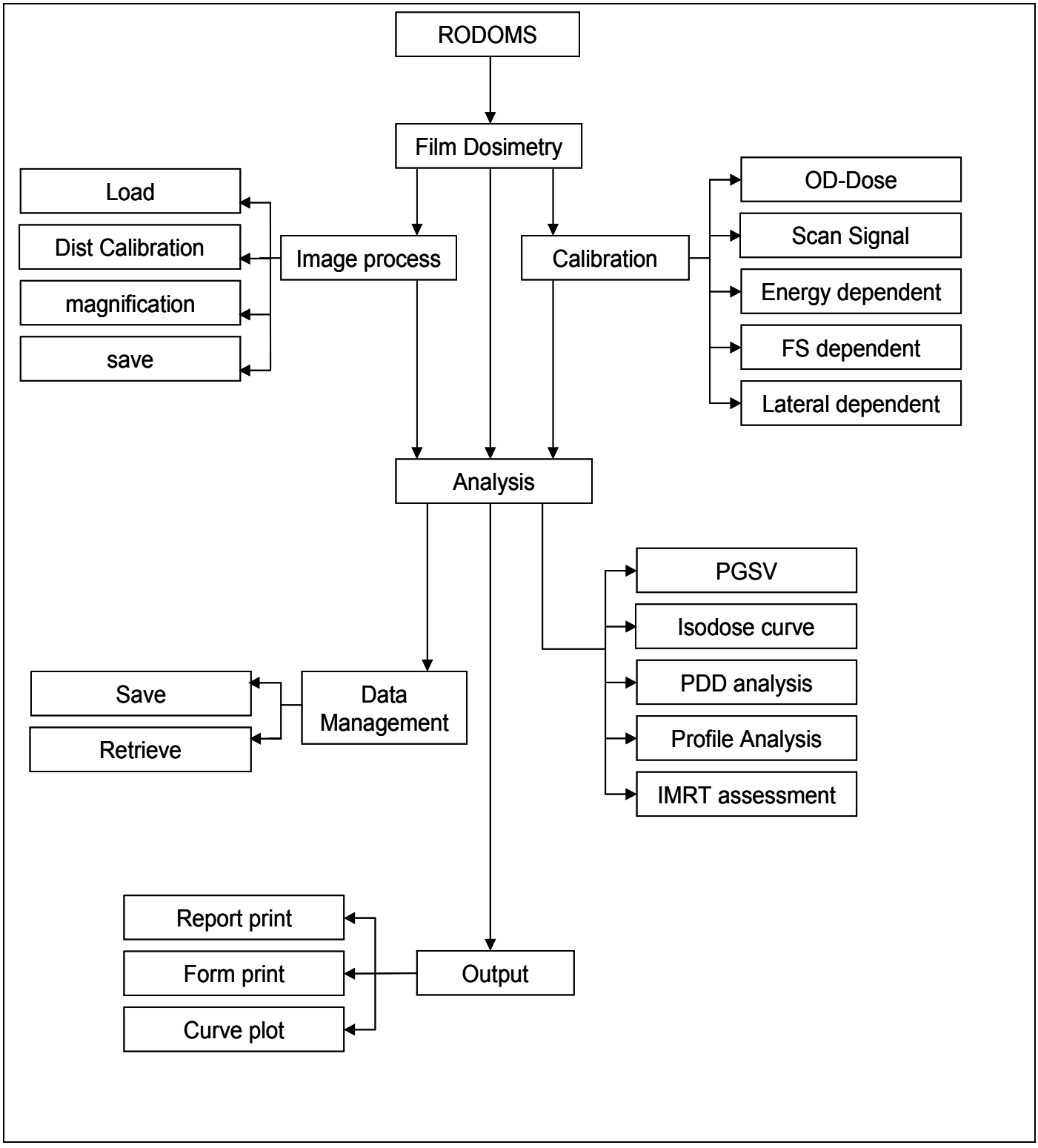

Figure 9.3 RODOMS film dosimetry functional flow diagram

The following procedures are incorporated into the software

Image process: includes loading and storing of a bitmap file generated by film scanner (.bmp, .JPG, .Gif) into the analysis form (Figure 9.4, 9.5).

Subsequent procedures allow the user to

- Mark-up the image to calibrate distance measurements and magnification (Figure 9.5),
- Restore other images created by the program such as Isodose distribution map, curves and darkness intensity map (virtual film).

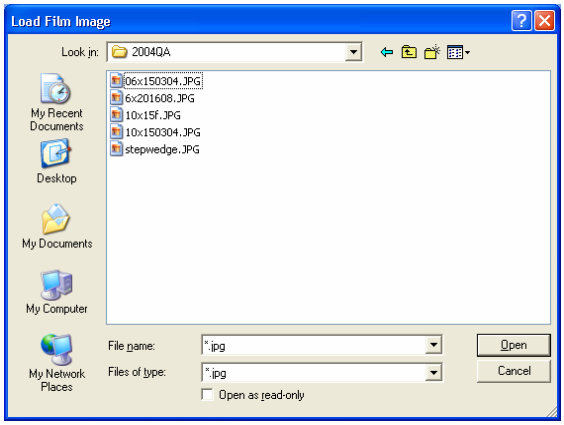

Figure 9.4 image file load

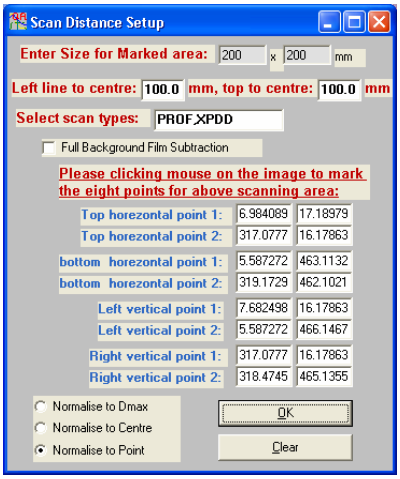

Figure 9.5 film analysis forms.

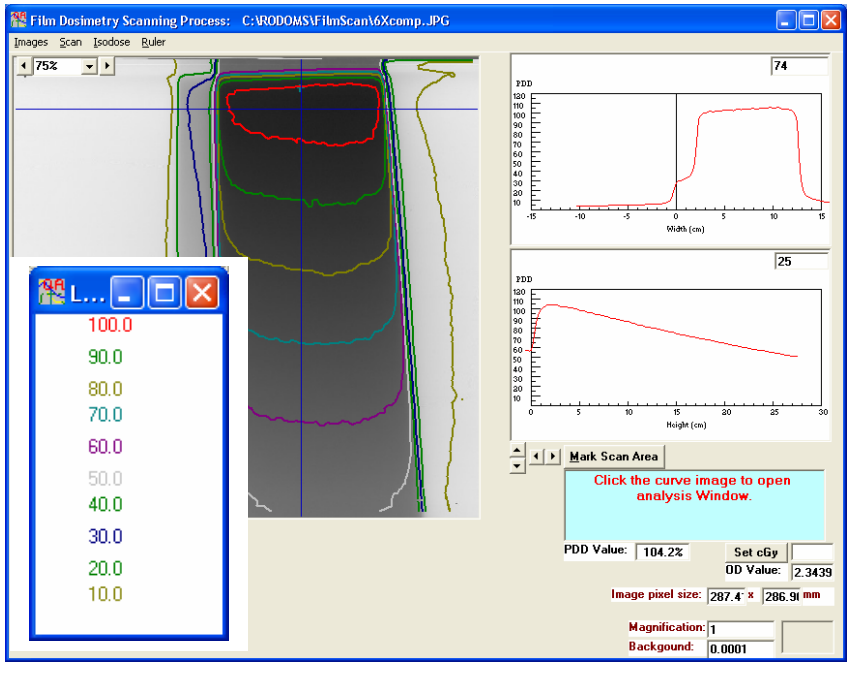

Figure 9.6 distance mark

Calibration: includes analysis of calibration film-strips to generate OD-Dose calibration curves (Figure 9.7) and the step-wedge reference film to calibrate the scanner signal to optimize the scanner performance e.g. uniformity, dynamic range, and linearity (Figure 9.8). The calibration function also allows the user to check the OD-Dose response for energy/beam type dependence (Figure 9.9), field size dependence (Figure 9.10), and beam-to-film entry angle dependence (Figure 9.11).

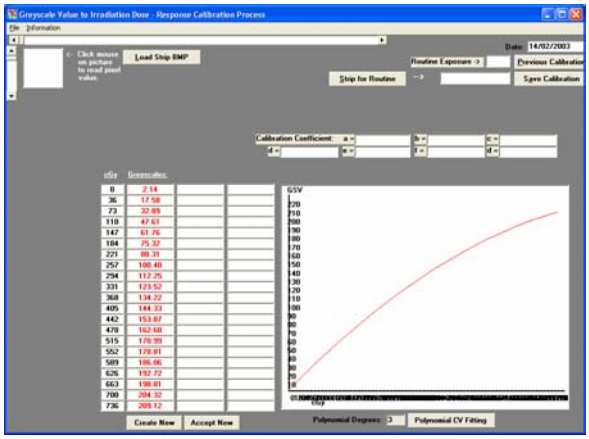

Figure 9.7 film strip OD-Dose calibration

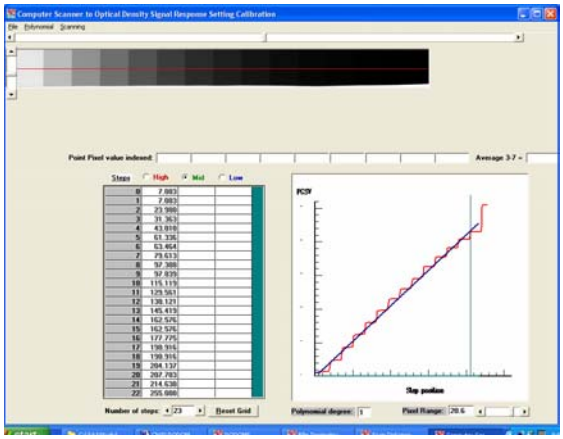

Figure 9.8 Scanner signal calibration

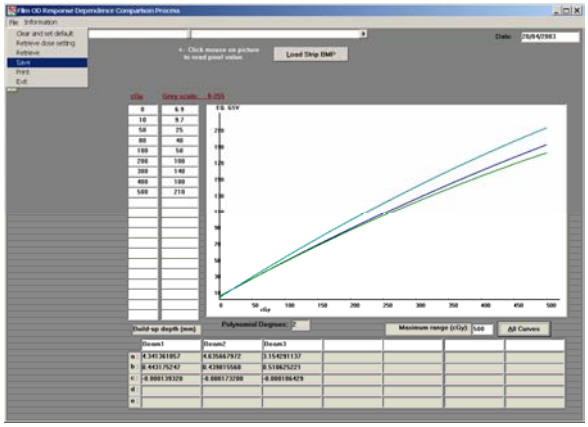

Figure 9.9 Energy dependence check

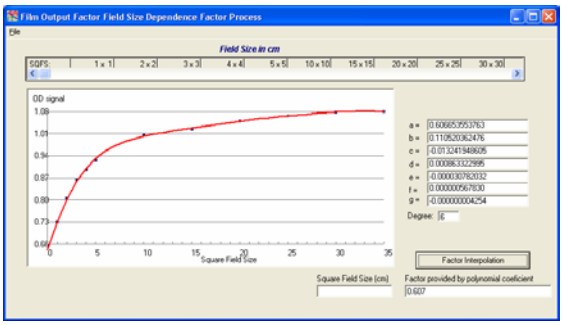

Figure 9.10 Field size dependence check

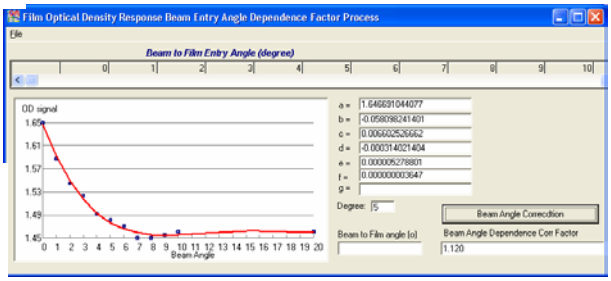

Figure 9.11 beam to film entry angle dependence check

Analysis: this function is designed for reading the image pixel greyscale value, converting GSV into equivalent dose by using calibration data, plotting the Isodose curves (Figure 9.12, a, b, c), and inspecting PDD/profile curves over an analyzed film image along the X/Y axis with parameterized curve analysis result (Figure 9.13, a, b).

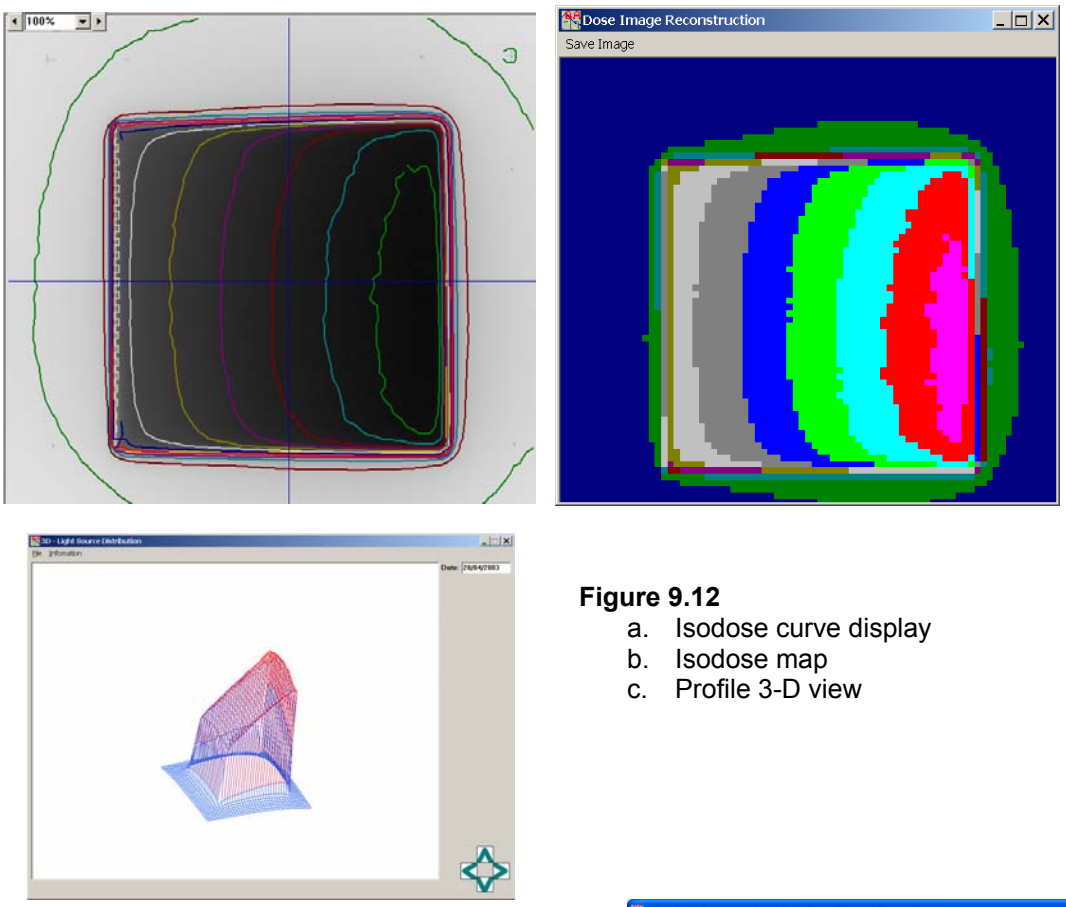

Figure 9.12
a. Isodose curve display
b. Isodose map
c. Profile 3-D view

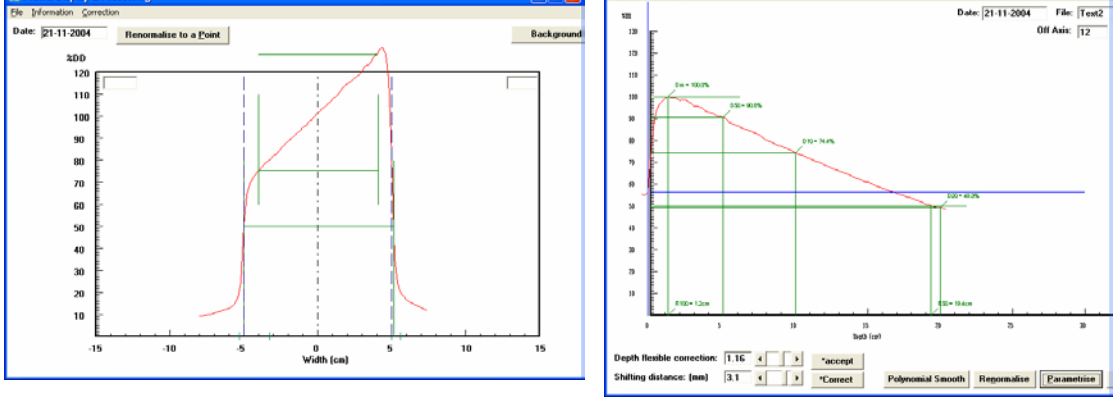

Figure 9.13 a. profile analysis. b. %DD analysis

The function can perform the analysis for both single image and combined film images. In the latter the film is exposed sequentially to radiation fields of different beam energy/types. The separate and corrected analysis results can be re-combined into a single field analysis result (Figure 9.14). This function helps the user to overcome the film dosimetry beam energy/type dependence.

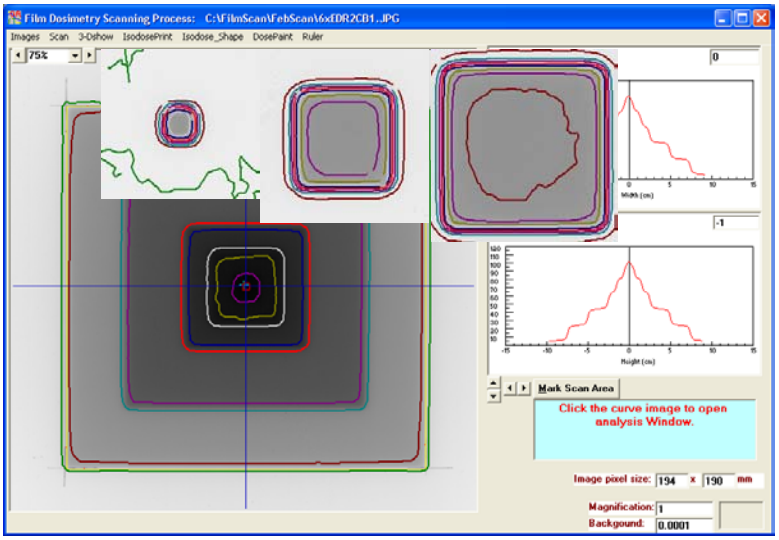

Figure 9.14 multiple beam re-combination analysis

The isodose overlay function is developed for 3D and IMRT treatment planning verification for the dose distribution check. It allows the user to overlay selected isodose curves for film analysis and planning calculation results. An analysis function calculates and reports the discrepancy between the isodose area and edges (Figure 9.15 a, b). This requires that the planning dose distribution be loaded into the program.

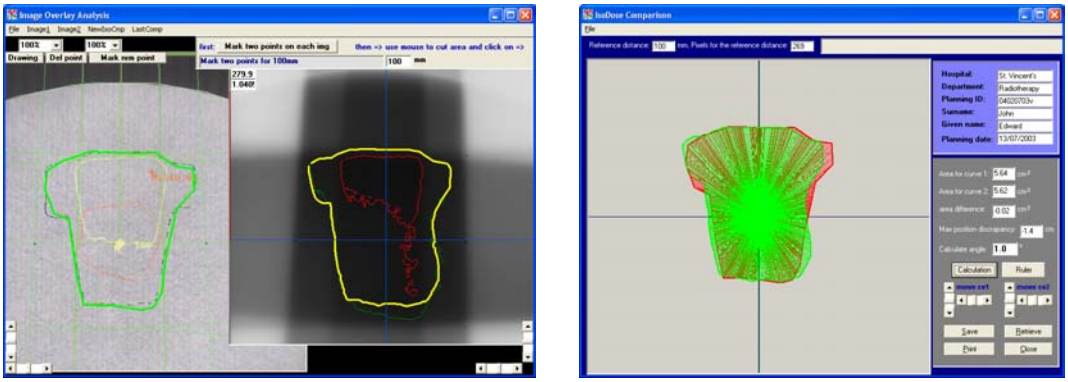

Figure 9.13 a, film analysis result overlay with planning calculation
b, selected isodose curve overlay analysis and report

Data management: provides data saving and retrieval functions for storing images, analysis curves, calibration data and analysis results (Figure 9.14).

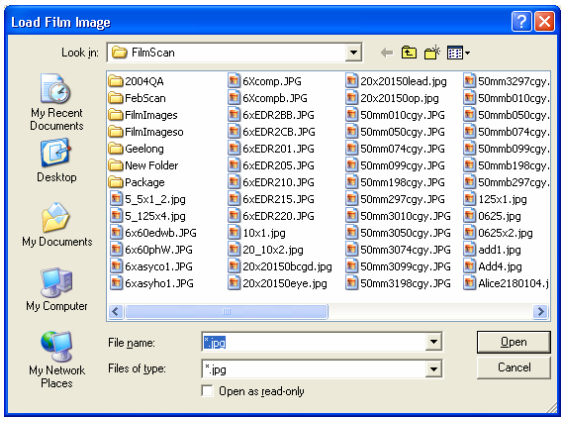

Figure 9.14 File management

Output: provides hard copy output of data tables, forms and curve plots. It also provides for screen captures.

Summary

The RODOMS software was designed to help radiation oncology physicists in reducing their routine daily workload by use of standardized protocols incorporating correction procedures. The protocols discussed previously are designed to allow the radiotherapy Quality Assurance (QA) and Quality Control (QC) to be performed in a way guaranteed to match the national and international standard and regulations. In past 10 years, the RODOMS has been continuously developed and upgraded to include functions of routine dosimetry, mechanical and isocentric alignment, absolute output calibration, film dosimetry and planning point monitor unit checks. The RODOMS software has been tested and used by many hospitals across Australia and South-East Asia.

Chapter 10 Software Development and Functional Design

10.1 Introduction

The RODOMS software provides tools which allow a user to perform QA measurements using radiographic (or radiochromic) film. The basic tools as discussed in chapter 4, the measurement and display techniques commonly used in QA. In subsequent chapters described methods of implementing the QA procedures using film and a desktop scanner to achieve maximum accuracy. It should be noted that the basic concepts could also be applied to QA images obtained in digitized form. In this chapter describes the software in detail under the following subheadings:

1. GUI interface
2. Bitmap image display
3. Pixel value read from bitmap image
4. Signal correction factors and data interpolation
5. Signal noise smooth function
6. Curve drawing and curve fitting
7. Scan physical distance convert calculation and coordinate determination
8. Isodose data tracking, isodose curve plotting and shape printing
9. Three-D chart graph display
10. Data saving and retrieving
11. Result output processing

10.2 Programming language

The language used for the software development is Visual Basic. The version started with 5.0 and then upgraded to version 6.0. Visual Basic is a GUI (Graphic User Interface) object oriented Windows programming language. A simple point-and-click interface provides access to a wide variety of graphics and data processing tools. The language also supports program development tools including error handling and debugger procedures. Compared with C++ or Delphi, Visual Basic is a language which provides physicist‘s with a simple windows interface, allowing them to process complex graphical data with less coding and link the data with multiple format objects.

The program can be run on all Windows based computer operation system including Windows-95, 98 and NT, and XP the program can be run form from any compact disk drive.

10.3 API interface

Using the API (Windows Application Programming Interface) to provide many powerful functions can extend the programming capabilities. The program developed is then run as a normal Windows application. The basic development function 'Form' provides a window on the computer screen which can be allocated to several functional procedures (or objects) such as:

Text box – data entry box.
Label box –displays the title of the entry box or item.
Picture box – loads and display the bit map image and plot data curves.
Command button –start a sequence of coding which performs a particular function.
File dialog box –opens and saves data as an imported/exported data file.
Communication dialog box –connects to the series port to provide the computer link for the data transmission to/ from external equipment (e.g. scanner).
Message box –displays operational messages e.g. help text in message box to provide hints or error handling while the program in operation.

10.4 Image formats

BMP

With the advent of CGA, EGA and then VGA monitors capable of displaying up to 256 different colours, the simple black and white bitmap was no longer adequate. The bit-depth was increased to match the improved performance of the printer. With two bits you can define four colours, 8-bit images provides 256 levels. New formats, including Microsoft windows BMP were developed to support the demands of the new monitors. Microsoft BMP format defines a pixel value by storing its associated index number rather than the much longer RGB value with up to 256 colours. This allows each pixel

to be stored as an eight bit number. This can be done in Red, Green and Blue components are stored separately – RRRRGGGGBBBB – or – RGBRBGRGBRGB –.

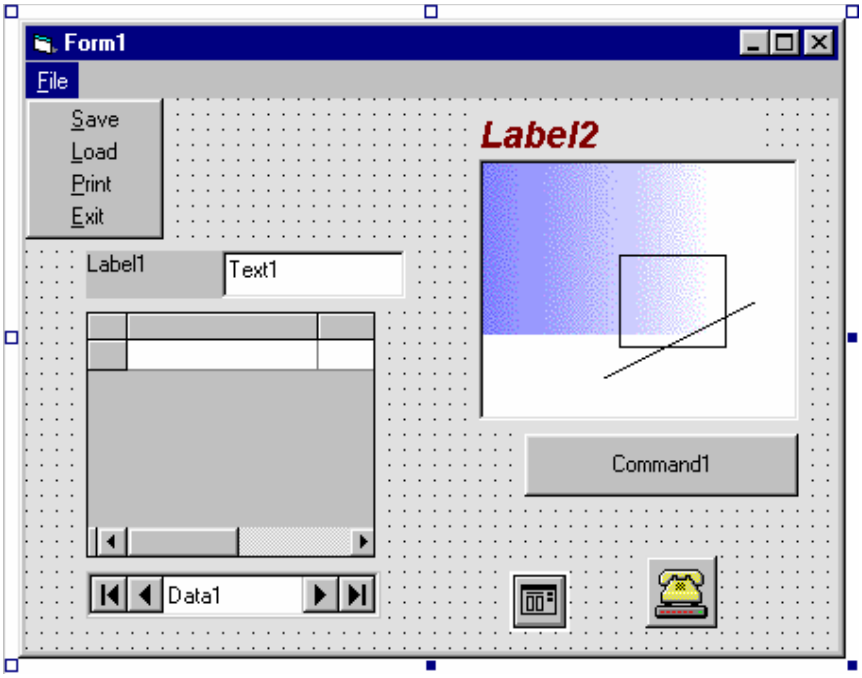

Figure 10.1 Window form object

TIFF

Whereas the BMP format uses a fixed header with fixed fields followed by sequential data, the TIFF has a much more flexible structure. A simple 8-byte header points to the position of the first Image File Directory (IFD) tag. The IFD also indicates where image data which need not be stored sequentially) is stored in the file.

GIF

The TIFF's flexible nature is not suitable for Web work where every byte counts. Instead the GIF (graphic interchange format) containing a maximum of 256 colours with an 8-bit palette is commonly used. Unlike other formats, this takes full advantage of storing fewer colours at low bit-depths. For a typical 8-bit image, GIFs can be losslessly compressed by 40% or more for inclusion in Web pages.

JPEG

The JPEG is widely accepted since that can be compressed by 50% with little loss of quality. JPEG is flexible in that it allows the use of extensions.

10.5 Image files handling

The import/export of image files (BMP, .JPG, or .GIF format) are accessed via a common dialog window (Figure 10.2) provided from Visual basic library. This allows us to list all relevant image file names by file extension. The user can select the required image from the display menu by mouse.

```
‘~~~~~~~~~~~~~~~~~~~~~~~~~~~~~~~~~~~~~~~~~~~~~~~~~~~~~~~~~~~~~~~~~~~~~~~
On Error Resume Next
'ChDrive "K:\"
'ChDir "K:\Radio\Physics\FilmScan"

CmDialog1.DialogTitle = "Load Film Image"
CmDialog1.CancelError = True
CmDialog1.FileName = "*.jpg"
CmDialog1.DefaultExt = "jpg"
CmDialog1.Filter = "Image files(*.jpg)|*.jpg|*.bmp"
CmDialog1.Flags = OFN_FILEMUSTEXIST Or OFN_SHOWHELP
‘~~~~~~~~~~~~~~~~~~~~~~~~~~~~~~~~~~~~~~~~~~~~~~~~~~~~~~~~~~~~~~~~~~~~~~~
```

Since the file open or save command dialog window function is dealing directly with computer disks, an error handling procedure is used to handle any of disk or file fault and display the error message and help message. The program is programmed to escape from the function without crashing.

When a name of bitmap file is selected, the windows clipboard object is called to load the image data from the bit map file into the clipboard buffer. The picture box located on the form is determined for the image display. It will acquire the image data and display each pixel according to the pixel position X and Y value and the value for the RBG colours.

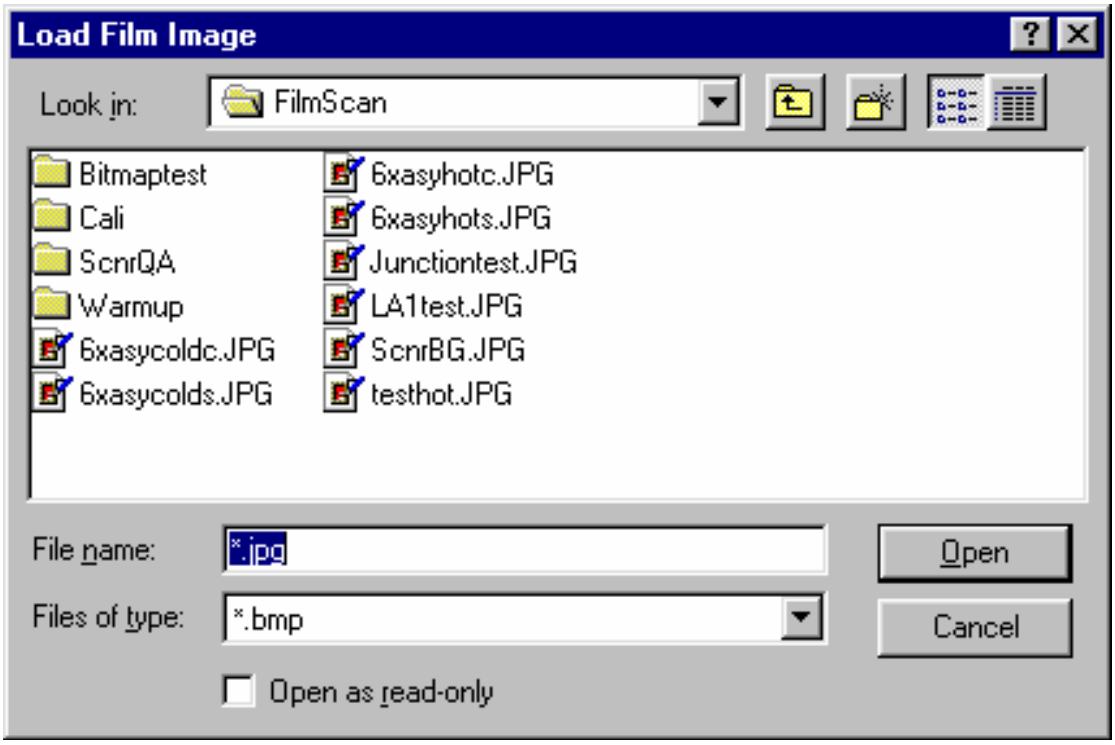

Figure 10.2 File open/retrieve dialog box

The size of picture box and display resolution in this program is determined according to the film dosimetry scanning size and steps. The value of picture size can be selected either by entering the frame's physical size into the text box or clicking the mouse on the reference marks on the image picture.

The software routine follows below:

```
'~~~~~~~~~~~~~~~~~~~~~~~~~~~~~~~~~~~~~~~~~~~~~~~~~~~~~~~~~~~~~~~~~~~~~~~~~~~~
CmDialog1.Action = 1
If Err = 32755 Then
 Exit Sub
Else
 FileName = CmDialog1.FileName
End If


Text6 = "Wait for image loading……"
Text6.Visible = True
```

```
Picture2.Visible = True
Picture3.Visible = True
VScroll1.Visible = True
HScroll1.Visible = True
Command1.Visible = True
DoEvents

Clipboard.Clear
Unload Disset
Call clrscrn_Click

Clipboard.SetData LoadPicture(FileName)
Picture1.Picture = Clipboard.GetData()
Filenamebuf$ = FileName
Picture1.Left = 50
Picture1.Top = 50
Picture1.DrawWidth = 2
If Picture1.ScaleWidth / 2 > 600 Then
   MsgBox "Warnning: Image is too large for the calculation size."
End If

Text3 = 1
Text4 = Picture1.ScaleWidth
Text5 = Picture1.ScaleHeight
orgX = Picture1.ScaleWidth
orgY = Picture1.ScaleHeight
rsz = 0

c0 = 6
Nway = 0
Disset.Top = Picture2.Top
Disset.Left = Picture2.Left - 250
Disset.Text4 = "PROF, PROF"
Scflg = 0
Disset.Show
Text6.Visible = False
‘~~~~~~~~~~~~~~~~~~~~~~~~~~~~~~~~~~~~~~~~~~~~~~~~~~~~~~~~~~~~~~~~
```

10.6 Bitmap image storage and background value subtraction

Pixel values are read from the displayed image (Figure 10.3) by using the ‘Point (X, Y)’ function. The primary reading from a bit map pixel is stored as a long integer representing the RGB (Red, Green, and Blue base colours). For the film dosimetry, the greyscale value is displayed using identical values across all the three basic

colours. The Point (X, Y) object function allows 256 greyscale values to be obtained by the calculating the cubic root as this function returns a long integer number to represent the multiplication of three (RGB) 0 ~ 255 greyscale for each pixel data unit as:

$$GSV_{pixel} = \sqrt[3]{PV_{RGB}}$$

Which GSV_{pixel} is the greyscale value for a pixel between 0 and 255, and PV_{RGB} is the pixel RGB total number the program read from a pixel point.

The pixel information is stored in an array as X and Y position and the pixel greyscale value. After the bitmap pixel value scan is completed, a two dimensional loop is entered to subtract the background from the image. In this program, the background value can be either use an average value calculated from the centre of background film or a pixel by pixel subtraction using values from the double scanning image of the background film.

The software routine follows below:

```
‘~~~~~~~~~~~~~~~~~~~~~~~~~~~~~~~~~~~~~~~~~~~~~~~~~~~~~~~~~~~~~~~~~~~~~~~~
'scanning over the image area
yc = 0
For j = 1 To Picture1.ScaleHeight - 1 Step 2
   xc = 0
   For i = 1 To Picture1.ScaleWidth - 1 Step 2
      cbuf = 0
      nv = 0#: n = 0
      For l = -1 To 1
         For k = -1 To 1
            cbuf = Picture1.Point(i + k, j + l)
            If cbuf >= 0 Then
               nv = nv + cbuf ^ (1 / 3)
               n = n + 1
            End If
         Next k
      Next l
      If n > 0 Then
         sx(yc, xc) = i
         sy(yc, xc) = j
         sd(yc, xc) = 255 - nv / n - Val(Text8)
```

```
            xc = xc + 1
        End If
    Next i
    yc = yc + 1
Next j
'~~~~~~~~~~~~~~~~~~~~~~~~~~~~~~~~~~~~~~~~~~~~~~~~~~~~~~~~~~~~~~~~~~~~
```

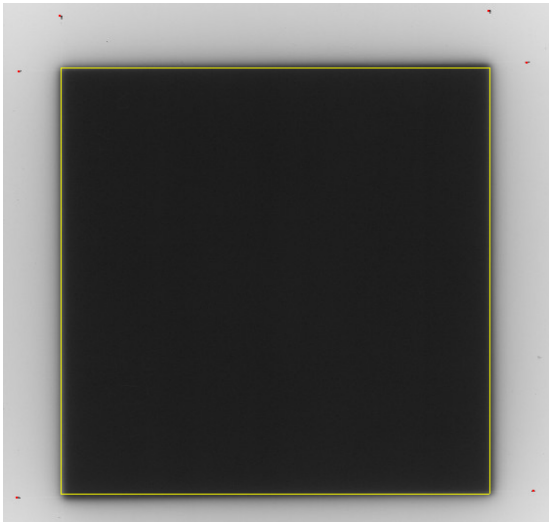

Figure 10.3 a bitmap image loaded with marks of distance and field edge

10.7. Signal correction factors and data interpolation

The scan pixel value is converted into the relative dose percentage value by re-normalization. The re-normalization functions determined in this program provide four different options for different clinical dosimetry requirements. The user can perform re-normalization by using

- the maximum data value
- the value from the field centre
- the value from any point on the image picked by user clicking mouse on the image
- any value entered form the keyboard type

The re-normalization calculation is performed by using a two dimensional array to convert the pixel value into the re-normalized percentage value and store this back into the variable array.

```
‘~~~~~~~~~~~~~~~~~~~~~~~~~~~~~~~~~~~~~~~~~~~~~~~~~~~~~~~~~~~~~~~~~~~~~~~~~~~~
       For j = 0 To yc - 1
          For i = 0 To xc - 1
             sd(j, i) = (sd(j, i) - Bsd(j, i)) * Bsc(j, i)
          Next i
       Next j

'renomalise
For j = 0 To yc
   For i = 0 To xc
      sd(j, i) = sd(j, i) / (Gnrm - 1#) * 100#
   Next i
Next j

For j = 0 To yc - 1
          For i = 0 To xc - 1
             For k = 0 To 19
                If Gv(k + 1) <= 0# Then GoTo 117
                If sd(j, i) > Gv(k) And sd(j, i) <= Gv(k + 1) Then GoTo 117
             Next k
117
If Gv(k + 1) <= 0# Then
                Gds(j, i) = Gd(k)
             Else
                Gds(j, i) = Gd(k) + (Gd(k + 1) - Gd(k)) * (sd(j, i) - Gv(k)) / (Gv(k + 1) -
Gv(k))
             End If
          Next i
       Next j
‘~~~~~~~~~~~~~~~~~~~~~~~~~~~~~~~~~~~~~~~~~~~~~~~~~~~~~~~~~~~~~~~~~~~~~~~~~~~~
```

10.8 Signal/ Noise and smoothing procedures

From a practical viewpoint, the film analysis result is highly dependent on the signal to noise of the digitized data. For higher energy verification X-ray film images, there are three main noise sources

- Artifact noise – dependent on the film quality, phantom quality and quantum mottle of the beam.
- Chemical processing noise - related to the variable conditions at the time of processing.

- image scanning and data processing noise - related to the image density data readout, correction and normalization

Artifact Noise

Film Grain - Within an emulsion, Film grains are built up from the original silver halide crystals which are often individually no larger than 2.0 microns, although larger groupings are formed by the uneven distribution of grains in the emulsion layer.

Random fluctuations of density are generally called 'white noise', because it has the same noise amplitude at all spatial frequencies. *Phantom quality* - is due to uneven distribution of the surface phantom build up and material density distribution. This is not usually a very large factor if the phantom is made of high quality. However, it could be variable due to scattered radiation created from uneven build up and any air gap between the solid pieces in a slab phantom (Poisson distribution).

Quantum mottle - is caused by the random arrival rate of X-ray photons and becomes significant on film with a high conversion efficiency in which few X-ray photons are required to form the image.

$$N = \overline{N} \pm \sqrt{N}$$

Because quantum mottle originates outside the film, its effects are modified by the sharpness and contrast settings when the film is scanned.

Film processing and data scanning effects

A film processor should be maintained in a good processing quality and working conditions to avoid artifacts. Chemical conditions such as temperature level and pH value will significantly affect the film density and contrast. A ±2.0^{o}C temperature change or a 0.2 pH value change can make produce ±10% density value change. This effect could occur over the whole image. Small variations of temperature and pH

changes, which produce a uniform density change between films, could be overcome by entire signal re-normalization.

Artifacts are unwanted density variation in the form of blemishes in the radiograph that arise from improper handling, exposure, processing, or housekeeping. Artifact marks created by poorly maintained film processor can create large problems in film dosimetry. Many films are made unusable for QA by the artifact marks created on the film image by mechanical and chemical processes. More often, a poorly maintained film processor produces striping on the film image, which follow the processing direction. Some marks are visible by eye but other less visible artifacts will have significant effect on the film dosimetry.

Film scanned by a computer scanner, densitometer, or digitizer commonly use a light source to light the film. The signal is collected from the other side of the film corrected for the light illumination level. The signal corresponds to an optical density value $T = \log_{10} (I/Io)$. Unlike single point densitometry reading, the light source is dynamically moving with the detector changing the sampled position on the film during a scan. The physical design of the scan equipment can give an uneven light density distribution in the scanning area. This results in incorrect, but repeatable errors in transmission value unless corrected.

Smoothing methods

Three methods are used in RODOMS functions in order to perform the signal smoothing for different purposes.

Running Mean - Mean smoothing is used to correct the original image signal, the background scan and the factor data curve. The pixel value for each measurement point is made up by an average of pixel greyscale values, which are located within 1 mm^2 square area. For the background correction factors, such as those factors for a background film and scanning illumination area background distribution, the curve needs to be smoothed to represent the common values of these correction factors.

For this purpose, the methods to average values with the neighbour points are simply performed in the smoothing function as the following algorithm:

Buffer array <- curve array

1. Sorting value index
2. Take off unacceptable value (e.g. remove lowest and highest readings)
3. Average remaining data
4. Loop while curve array <- the number of buffer array

Median smoothing - In most signal applications, a linear smoothing (or a linear filter) is used to eliminate the noise-like components of a signal. Some signals might lie too far off a trend-line indicating that the signal is not representative of the measurement data. A simple linear fit might not be adequate in this case. As shown on Fig. 10.6, points at x=2 and x= 4 might be considered to lie outside the relationship predicted by a linear fit.

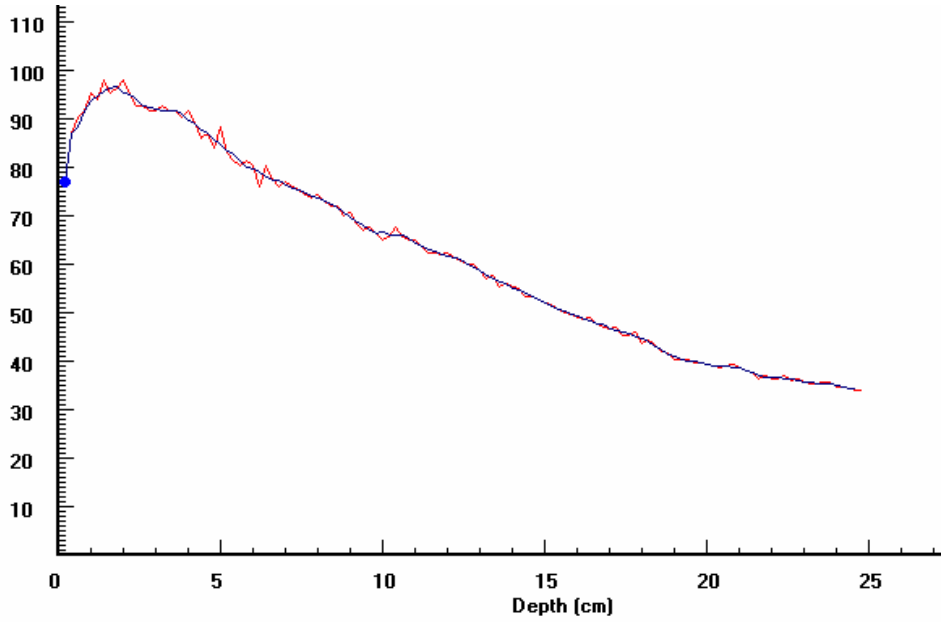

Figure 10.4 A film for PDD check. The film was scanned via an 8bit HP document scanner. The original curve contains high noise levels. The curve was smoothed using the median + polynomial smoothing.

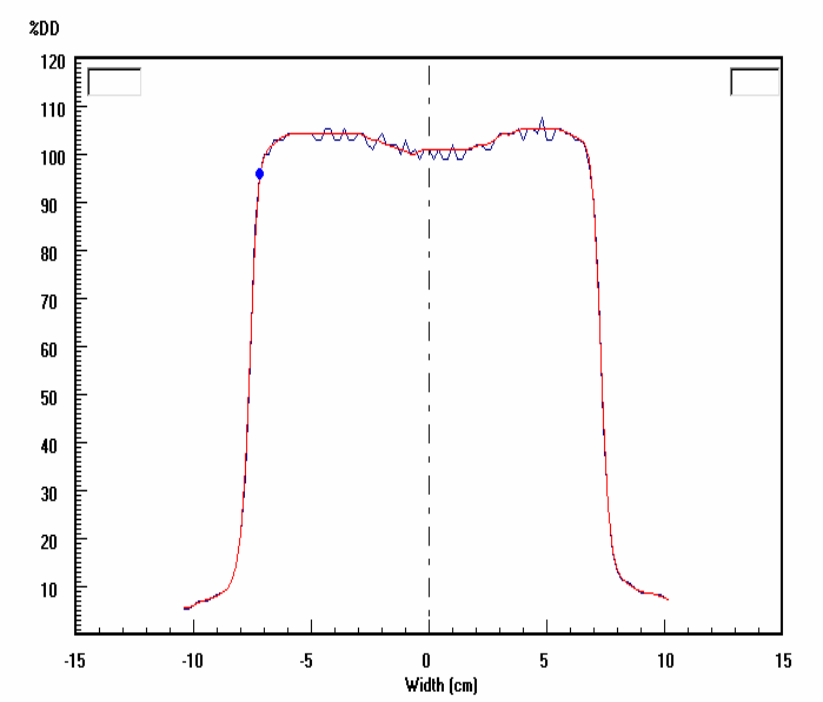

Figure 10.5 A film for profile check. The film was scanned via an 8bit HP document scanner. The original curve contains high noise levels. The curve was smoothed using the median + polynomial smoothing.

For such cases, a nonlinear smoothing filter can be used before the linear smoothing. This nonlinear smoothing preserves signal discontinuities yet filters out large errors.

A non-linear smoothing algorithm using a combination of running medians can be used to take the place of the linear smoothing.

The basic concept of median value is that each pixel is replaced by the median value of its nearest neighbors. The function performs following steps:

- Select nearest neighbors
- Sorting (rank) the group value into an ascending or descending sequence.
- Pick the median value (middle) of the group and store into a series variable array.
- Link the median value for each group and copy the value into the curve data array variable.

A programming scheduled code is as follows:

```
If n > 0 then
    For l = 0 to n
        For c = l to n
            If signal (c)   < signal (l) then
                Signal (c) swap with signal (l)
            End if
        Loop
    Loop
    Signal = signal (n / 2)
End if
```

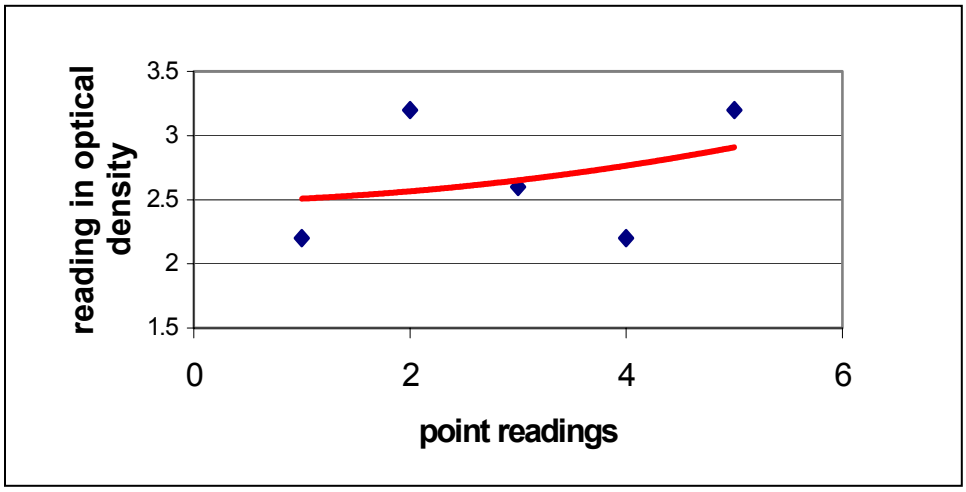

Figure 10.6 Median smoothing

Linear-Polynomial smoothing -Compared with other curve fitting algorithms such as logarithm and exponential, the polynomial least square method can provide a good fit to complex curves by using several degrees of fit. In this study, the curve fitting breaks the data into small sections using a program looping function.

Linear polynomial smoothing is performed in the final adjustment of a curve fitting process. In order to keep the curve's original shape, the curve is broken up into small data groups. Each group might contain 3 or 4 points. A low order linear polynomial is

applied to each individual group. The point value is recalculated using the linear polynomial factors of the group.

Using the power series polynomial function to fit the curve data into a quadratic curve, the function used like:

$$y = \sum_{n=0}^{N} C_n \cdot X^n$$

The linear function for the group can be described as:

$$f(X) = a + bX + cX^2 + \ldots + NX^n$$

All the data is uniformly spaced data points so it can be calculated to the quadratic curve from a group of consecutive data points.

The coefficients, a, b, c, d etc., are computed using the method of least squares fit to a polynomial described in “Data reduction and error analysis for the physical sciences”, Philip R. Bevington, McGraw Hill 1969.

Which

$$\begin{aligned}
&\sum X_i^0 Y_i = a\sum X_i^0 + b\sum X_i^1 + c\sum X_i^2 + \cdots\cdots + C\sum X_i^n \\
&\sum X_i^1 Y_i = a\sum X_i^1 + b\sum X_i^2 + c\sum X_i^3 + \cdots\cdots + C\sum X_i^{n+1} \\
&\sum X_i^2 Y_i = a\sum X_i^2 + b\sum X_i^3 + c\sum X_i^4 + \cdots\cdots + C\sum X_i^{n+2} \\
&\cdots\cdots \\
&\sum X_i^n Y_i = a\sum X_i^n + b\sum X_i^{n+1} + c\sum X_i^{n+2} + \cdots\cdots + c\sum X_i^{n+n}
\end{aligned}$$

n – degree of the polynomial order

C – coefficient factors as a, b, c …… C_n

Consider the equations, we can get:

$$X_{11} = \sum X_i^0 \qquad X_{12} = \sum X_i^1 \qquad X_{1n} = \sum X_i^n Y_i$$

Determinants to the matrix as:

$$\begin{vmatrix} x_{11} & x_{12} & \cdots\cdots & x_{1n} \\ x_{21} & x_{22} & \cdots\cdots & x_{2n} \\ & \cdots\cdots & & \\ x_{n1} & x_{n2} & \cdots\cdots & x_{nn} \end{vmatrix}$$

Evaluated to:

$$\begin{vmatrix} 1 & x_{12} & x_{13}\cdots\cdots & x_{1n} \\ 0 & 1 & x_{23}\cdots\cdots & x_{2n} \\ 0 & 0 & 1\cdots\cdots\cdots & x_{3n} \\ 0 & 0 & 0\cdots\cdots\cdots & x_{nn} \end{vmatrix}$$

Then solved for: a, b, c

The algorithm is performed by a visual basic function as follows:

Pseudo-code of programming function:

for n -> N

define the degree of polynomial

for j=0 to degree

for I=0 to degree

$$P_1 = \sum_{j=0}^{\deg ree} \sum_{i=0}^{n} d^{j}_{\deg ree} \cdot D_i$$

$$P_2 = \sum_{j=0}^{\deg ree} \sum_{i=0}^{n} d^{j}_{\deg ree}{}_{i}$$

Loop I

Loop j

for j=0 to degree

for I=0 to degree

$$\sum_{k=0}^{i} \frac{P_1(i)}{P_2(i)}$$

$D_{smoothed}$ =

Loop I

Loop j

Loop n

Results and discussion

Figures 10.7 and 10.8 show the comparison of an original scanning signal curve for a 4MV photon 15 x 15cm field profile and depth dose curves from measurements in the RODOMS water phantom. The comparison shows the fully smoothed curves by the noise fitting function.

In most of signal processing applications a linear smoothing function is used to eliminate the noise-like components of a signal. For some processing applications, it is desirable to eliminate most wave shapes created by artifacts from the film processing. However, linear smoothing might not be completely adequate due to the type of data being smoothed. Too small an angle or too large a number of the data points in the group may change the curve shape.

Running means and medians generally preserve discontinuities in a signal curve. A better compromise is to apply a polynomial fit to small sets of data and interpolate to

get a value for the central data point, mean smooth could is considered to be used as to determine the common flow of the curve such as a correction factor curve

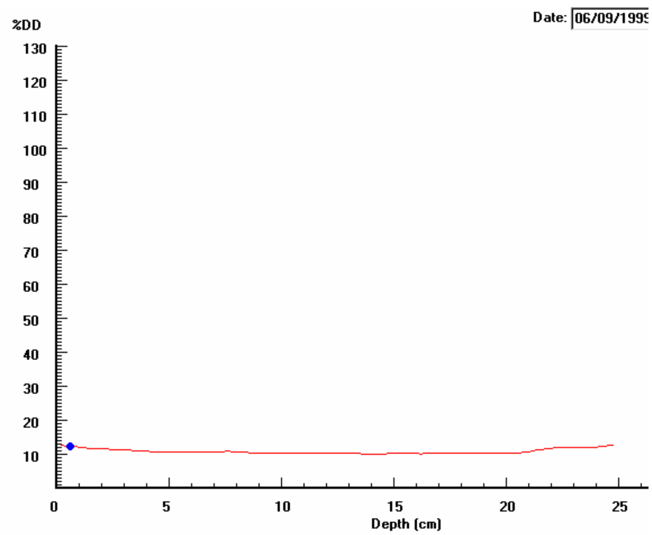

Figure 10.7 Mean smoothing used to obtain a film scanning background correction factor curve.

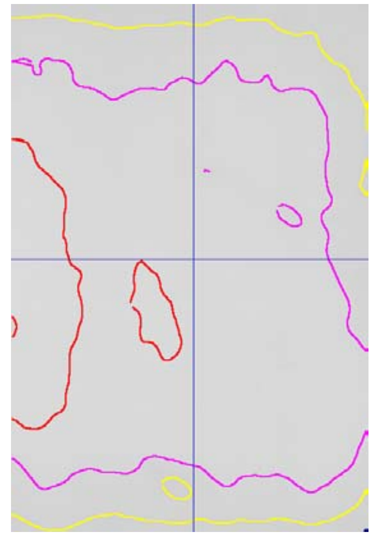

Fig 10.8 Background film scanned on HP 8bit desktop scanner.

10.9. Film setup to beam direction angle distance correction

A trigonometric method is used to correct the equivalent depth for the film setup angle in both the solid wedge phantom or water phantom. The pixel position X and Y on the image is converted into the physical distance representing the equivalent build up depth. The film setup angle, the phantom surface distance, and the exposed field size are entered by the user via the data entry text boxes. Each pixel position located on the image corresponds to a different depth, off centre axis distance, attenuation by phantom material and inverse square law effect. To work out the effective distance for each pixel, the angle between the film and beam direction is calculated. Each pixel to be corrected conversion of the pixel dots into equivalent distances, stored as array variables. The function group used for the geometrical and trigonometrical calculation is controlled by a logic flag set for different beam type (Photon or Electron) and setup type (SSD or SAD)

'~~~~~~

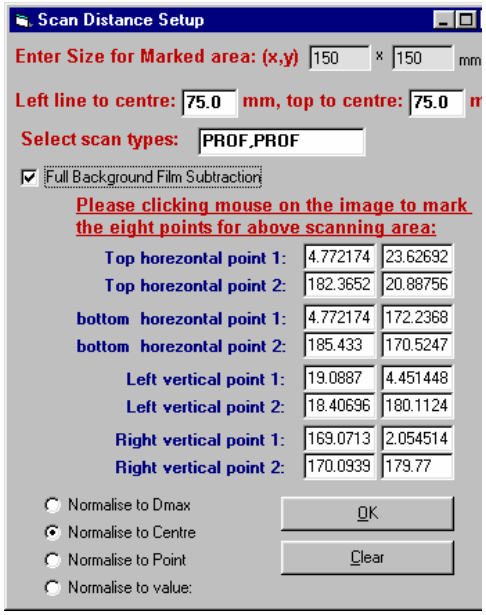

Figure 10.9 Scan Distance Determination Window.

```
'water phantom film folder angle and material correction

  Dim xi As Double, si As Double, xi0 As Double
  Dim w As Double, af As Double

'  If Wtrfolder.Checked = True Then
'    If phantom.Text1 = "" Or phantom.Text2 = "" Or phantom.Text3 = "" Or phantom.Text4 = "" Then
'      Wtrfolder.Checked = False
'      GoTo 150
'    End If

'    af = Val(phantom.Text1)
'    w = Val(phantom.Text2) / 2#
'    xi0 = w * Tan(af * 3.1415626 / 180#)
'    If Scflg = 1 Or Scflg = 2 Then
'          For i = 0 To xc - 1
'             si = prfx(i)
'             xi = si * Sin(af * 3.14159 / 180#)
'             xj(i) = xi0 - xi
'             di(i) = si * Cos(af * 3.14159 / 180#)
'             prfx(i) = di(i)
'          Next i
'    ElseIf Scflg = 3 Or Scflg = 4 Then
'          For i = 0 To yc - 1
'             si = prfy(i)
'             xi = si * Sin(af * 3.14159 / 180#)
'             xj(i) = xi0 - xi
'             di(i) = si * Cos(af * 3.14159 / 180#)
'             prfy(i) = di(i)
'          Next i
'    End If
```

```
'     If phantom.Text5 <> "" And Val(phantom.Text5) > 0.5 And Val(phantom.Text5) < 1.5 Then
'       If Scflg = 1 Or Scflg = 2 Then
'         For i = 0 To xc - 1
'           prfx(i) = prfx(i) * Val(phantom.Text5) + Val(phantom.Text6)
'         Next i
'       End If
'       If Scflg = 3 Or Scflg = 4 Then
'         For i = 0 To yc - 1
'           prfy(i) = prfy(i) * Val(phantom.Text5) + Val(phantom.Text6)
'         Next i
'       End If
'     End If
'   End If

    ' Dim af As Double, bt As Double, ox As Double, fs As Double

     '*******************************************
     ''v-dis=val(phatom.text2)-15
     'ox=(v-dis)*tan(val(phantom.text1))
     'af=atn(SSD/ox)
     'af = Atn(1000# / ((Val(phantom.Text2) - 15#) * Tan(Val(phantom.Text1) * 3.14159 / 180#))) * 180# /
3.14159
     'bt = 90# - Val(phantom.Text1)
     'fs = 1000# / Sin(af * 3.14159 / 180#)

      ' Dim si As Double, fi As Double, thtai As Double
      ' Dim di0 As Double, di1 As Double, di2 As Double, di3 As Double, di4 As Double

     'If scflg = 1 Or scflg = 2 Then
     '  For i = 0 To xc - 1
     '    si = prfx(i)
     '    di0 = si * Sin(bt * 3.14159 / 180#)
     '    di1 = fs * Sin((af + bt) * 3.14159 / 180#)
     '    di2 = Sqr(fs ^ 2 + si ^ 2 - 2# * fs * Cos((af + bt) * 3.14159 / 180#))
     '    di3 = di1 / di2
     '    thtai = Atn(di3 / Sqr(1 - di3 * di3)) * 180# / 3.14159
     '    di4 = Sin((180 - bt - thtai) * 3.14159 / 180#)
     '    di = di0 / di4
     '
     '    'density correction
     '    Dim ds1 As Double, ds2 As Double
     '    ds1 = Val(phantom.Text3) / Sin(thtai * 3.14159 / 180#)
     '    ds2 = ds1 * Val(phantom.Text4)
     '    If di > Val(phantom.Text3) Then
     '      prfx(i) = di + dsc
     '    Else
     '      prfx(i) = di
     '    End If
     '  Next i
     'ElseIf scflg = 3 Or scflg = 4 Then
     '  For i = 0 To yc - 1
     '    si = prfy(i)
     '    di0 = si * Sin(bt * 3.14159 / 180#)
     '    di1 = fs * Sin((af + bt) * 3.14159 / 180#)
     '    di2 = fs ^ 2 + si ^ 2 - 2# * fs * Cos((af + bt) * 3.14159 / 180#)
     '    thtai = di1 / Sqr(di2)
```

```
'    di3 = Atn(di3 / Sqr(-di3 * di3 + 1))
'    di4 = Sin((180 - bt - di4) * 3.14159 / 180#)
'    di = di0 / di4
'    'density correction
'    prfy(i) = di - (1 + Val(phantom.Text4)) * Val(phantom.Text3) / Sin(thtai * 3.14159 / 180#)
'  Next i
'End If
```

10.10 Curve drawing and curve fitting

The curve plotting performed in the program uses the 'Line(X0,Y0) – (X1,Y1), RGB colour' function to connect one pixel position to another by drawing a line between two positions. The type and width of the line can be determined either via windows edit screen or using Draw width and Draw type. The line draw used for the depth-dose curve or the profile curve is performed by two-D array loops. Each line draw start and stop position is swapped by the current loop array pointer. The X or Y data is used to determine the coordinate value and percentage data is used for the range value.

Low order polynomial curve fitting is used to perform the data smoothing over small data sets to reduce the noise without changing the curve shape.

```
'~~~~~~~~~~~~~~~~~~~~~~~~~~~~~~~~~~~~~~~~~~~~~~~~~~~~~~~~~~~~
For i = 0 To 20
  If Text4(i) = "" And i <= 20 Then Exit For
Next i
mc = i
If mc < 1 Then Exit Sub

dg = 3 'Val(Label3)
For j = 0 To dg
   xy = 0
   For i = 0 To mc - 1
      xy = xy + Val(Text3(i)) ^ j * Val(Text4(i))
   Next i
   xyx(j) = xy
Next j

For j = 0 To dg * 2
   xx = 0
   For i = 0 To mc - 1
      xx = xx + Val(Text3(i)) ^ j
   Next i
   xxx(j) = xx
Next j

n1 = 0: n2 = 0
For i = 1 To dg + 1
   For j = 1 To dg + 1
      X(i, j) = xxx(n1): n1 = n1 + 1
```

```
    Next j
    X(i, dg + 2) = xyx(n2): n2 = n2 + 1: n1 = n2
Next i

For k = 1 To dg + 1
    For i = k To dg + 1
        xk = X(i, k)
        For j = k To dg + 2
            X(i, j) = X(i, j) / xk
        Next j
    Next i
    If k > dg Then GoTo 1101
    For i = k To dg
        For j = k To dg + 2
            X(i + 1, j) = X(i + 1, j) - X(k, j)
        Next j
    Next i
1101
Next k

a = 0#: b = 0#: c = 0#: d = 0#: e = 0#: f = 0#: G = 0#

If dg = 6 Then
    G = X(7, 8)
    f = X(6, 8) - G * X(6, 7)
    e = X(5, 8) - G * X(5, 7) - f * X(5, 6)
    d = X(4, 8) - G * X(4, 7) - f * X(4, 6) - e * X(4, 5)
    c = X(3, 8) - G * X(3, 7) - f * X(3, 6) - e * X(3, 5) - d * X(3, 4)
    b = X(2, 8) - G * X(2, 7) - f * X(2, 6) - e * X(2, 5) - d * X(2, 4) - c * X(2, 3)
    a = X(1, 8) - G * X(1, 7) - f * X(1, 6) - e * X(1, 5) - d * X(1, 4) - c * X(1, 3) - b * X(1, 2)
End If

If dg = 5 Then
    f = X(6, 7)
    e = X(5, 7) - f * X(5, 6)
    d = X(4, 7) - f * X(4, 6) - e * X(4, 5)
    c = X(3, 7) - f * X(3, 6) - e * X(3, 5) - d * X(3, 4)
    b = X(2, 7) - f * X(2, 6) - e * X(2, 5) - d * X(2, 4) - c * X(2, 3)
    a = X(1, 7) - f * X(1, 6) - e * X(1, 5) - d * X(1, 4) - c * X(1, 3) - b * X(1, 2)
End If

If dg = 4 Then
    e = X(5, 6)
    d = X(4, 6) - e * X(4, 5)
    c = X(3, 6) - e * X(3, 5) - d * X(3, 4)
    b = X(2, 6) - e * X(2, 5) - d * X(2, 4) - c * X(2, 3)
    a = X(1, 6) - e * X(1, 5) - d * X(1, 4) - c * X(1, 3) - b * X(1, 2)
End If

If dg = 3 Then
    d = X(4, 5)
    c = X(3, 5) - d * X(3, 4)
    b = X(2, 5) - d * X(2, 4) - c * X(2, 3)
    a = X(1, 5) - d * X(1, 4) - c * X(1, 3) - b * X(1, 2)
End If
```

```
If dg = 2 Then
   c = X(3, 4)
   b = X(2, 4) - c * X(2, 3)
   a = X(1, 4) - c * X(1, 3) - b * X(1, 2)
End If

If dg = 1 Then
   b = X(2, 3)
   a = X(1, 3) - b * X(1, 2)
End If

Picture2.DrawWidth = 2
'put curve data onto the chat
For i = Val(Text3(0)) To Val(Text3(mc - 1))
   lx = x0 + i
   r = y0 - (a + b * i + c * i ^ 2 + d * i ^ 3 + e * i ^ 4 + f * i ^ 5 + G * i ^ 6)
   If i > Val(Text3(0)) Then Picture2.Line (X1, Y1)-(lx, r), QBColor(11)
   X1 = lx: Y1 = r
Next i

Text8(0) = Format(a, "###0.00000000")
Text8(1) = Format(b, "###0.00000000")
Text8(2) = Format(c, "###0.00000000")
Text8(3) = Format(d, "###0.00000000")

Picture2.ForeColor = QBColor(0)
Picture2.FontSize = 6

'put curve data onto the chat
   ld(l + 2) = a + b * pos(l + 2) + c * pos(l + 2) ^ 2 + d * pos(l + 2) ^ 3
   ls(l + 2) = pos(l + 2)
   If pos(l + 2) < 1# And pos(l + 2) > -1# Then ld(l + 2) = dos(l + 2)
Next l

'store data
For i = 0 To sc
  dos(i) = ld(i)

Next i

'print curve
For i = 1 To sc - 1
   Line (x0 + 300 + pos(i - 1) * ap, y0 - dos(i - 1) * 3)-(x0 + 300 + pos(i) * ap, y0 - dos(i) * 3), QBColor(1)
Next i
DoEvents
```

10.11 Physical distance calculations and coordinate determination

Conversion of pixel size to the physical distance is possible within the program. The simplest option is to enter the physical image size in mm via the text box. The program will determine the calibration between pixel and physical mm scales. However, this

method depends on the resolution of the scanned image. If the scanned image or screen image is small, the distance error could be as large as +/- 3mm.

The second calibration option allows the user to mark the fiducial positions on the film before scanning the image. The user then needs to mouse-click on the fiducial marks and enter the separation of the two marks.

```
'~~~~~~~~~~~~~~~~~~~~~~~~~~~~~~~~~~~~~~~~~~~~~~~~~~~~~~~~~~~~~~~~~~~~
Dim slbuf As Single, srbuf As Single
Dim stbuf As Single, sbbuf As Single
slbuf = (Val(Text2(4)) + Val(Text2(5))) / 2
srbuf = (Val(Text2(6)) + Val(Text2(7))) / 2
SW = Abs(slbuf - srbuf)

stbuf = (Val(Text3(0)) + Val(Text3(1))) / 2
sbbuf = (Val(Text3(2)) + Val(Text3(3))) / 2
SH = Abs(stbuf - sbbuf)

ix = Int(Val(Filmscan.Text4) * Val(Text1(0)) / SW)
SL = slbuf * ix / Val(Filmscan.Text4)
SR = srbuf * ix / Val(Filmscan.Text4)

iy = Int(Val(Filmscan.Text5) * Val(Text1(1)) / SH)
ST = stbuf * iy / Val(Filmscan.Text5)
SB = sbbuf * iy / Val(Filmscan.Text5)

Filmscan.Picture1.ScaleWidth = ix
Filmscan.Picture1.ScaleHeight = iy
Filmscan.Text4 = ix
Filmscan.Text5 = iy

Filmscan.Label6 = "mm"
Filmscan.Picture1.DrawWidth = 1
Filmscan.Picture1.Line (SL, ST)-(SR, ST), QBColor(14)
Filmscan.Picture1.Line (SL, SB)-(SR, SB), QBColor(14)
Filmscan.Picture1.Line (SL, ST)-(SL, SB), QBColor(14)
Filmscan.Picture1.Line (SR, ST)-(SR, SB), QBColor(14)
```

10.12 Isodose tracing, isodose curve plotting and printing

The first step in isodose tracing is to determine the range of isodose values of interest. As an example in the program, a 10% to 150% isodose range with 10% steps is defined by the user.

A dual loop is used determine isodose contours pixel by pixel for each step of isodose level. Two data points will be loaded into the loop each time. If one pixel is tested great er than the current isodose level and the other one is less or equal to the current isodose level, the loop will be exited and an interpolation function will be performed to

calculate the proper position of the isodose point. The isodose point data will be stored in two X and Y, 2--D arrays which represent the isodose level and the point count number. The tracing is performed independently for both X-axis and Y-axis.

After isodose point tracking completed, a new two-D loop is run again to perform the isodose point sorting for all points with the same isodose level. The strategy is to start from the first isodose point, and compare the trigonometrical distance to all other points related to that isodose. To find the nearest distance point, store the last point into the isodose curve variable, then start new check for the found point until all the points are sequenced into a continuous curve.

The third step is using the line draw function to plot the isodose curve on the screen over the film image picture (Figure 10.10). Each isodose curve will be plotted using different line colour.

Isodose shading (Figure 10.11) is of use to clinicians in viewing planning dose distributions. Although isodose shading provides a less accurate representation than isodose curves, it is preferred by medical staff. In the program, a separate window is opened with identical size format as the isodose area. The line draw function loop is run, but instead of linking the isodose points, each pixel in the particular isodose area is plotted as a square dot with a colour determined by the isodose level.

```
'~~~~~~~~~~~~~~~~~~~~~~~~~~~~~~~~~~~~~~~~~~~~~~~~~~~~~~~~~~~~
l = 0: more = 0: nomore = 0
stp = 10#
For lv = 10# To 150# Step stp
   If nomore > 5 And more = 1 Then Exit For
   nomore = nomore + 1
   p(l) = 0
   For j = 0 To yc - 1
     For i = 1 To xc - 1
       If sd(j, i) >= lv And sd(j, i - 1) < lv Or sd(j, i) < lv And sd(j, i - 1) >= lv Then
          pdx(l, p(l)) = sx(j, i - 1) + (sx(j, i) - sx(j, i - 1)) * (lv - sd(j, i - 1)) / (sd(j, i) - sd(j, i - 1))
          pdy(l, p(l)) = sy(j, i - 1) + (sy(j, i) - sy(j, i - 1)) * (lv - sd(j, i - 1)) / (sd(j, i) - sd(j, i - 1))
          p(l) = p(l) + 1
          more = 1
          nomore = 0
       End If
     Next i
   Next j
   For i = 0 To xc - 1
```

```
      For j = 1 To yc - 1
        If sd(j, i) >= lv And sd(j - 1, i) < lv Or sd(j, i) < lv And sd(j - 1, i) >= lv Then
          pdx(l, p(l)) = sx(j - 1, i) + (sx(j, i) - sx(j - 1, i)) * (lv - sd(j - 1, i)) / (sd(j, i) - sd(j - 1, i))
          pdy(l, p(l)) = sy(j - 1, i) + (sy(j, i) - sy(j - 1, i)) * (lv - sd(j - 1, i)) / (sd(j, i) - sd(j - 1, i))
          p(l) = p(l) + 1
          more = 1
          nomore = 0
        End If
      Next j
    Next i
    If p(l) > 0 Then
      plv(l) = lv
      l = l + 1
    End If
  Next lv
  cl = 12
  For j = 0 To l - 1
    For i = 1 To p(j) - 2
      dis1 = Sqr((pdx(j, i) - pdx(j, i - 1)) ^ 2 + (pdy(j, i) - pdy(j, i - 1)) ^ 2)
      For k = i To p(j) - 1
        d1 = Abs(pdx(j, k) - pdx(j, i - 1))
        d2 = Abs(pdy(j, k) - pdy(j, i - 1))
        dis2 = Sqr(d1 ^ 2 + d2 ^ 2)
        If dis2 < dis1 Then
          lx = pdx(j, i): ly = pdy(j, i)
          pdx(j, i) = pdx(j, k): pdy(j, i) = pdy(j, k)
          pdx(j, k) = lx: pdy(j, k) = ly
          dis1 = dis2
        End If
      Next k
    Next i
```

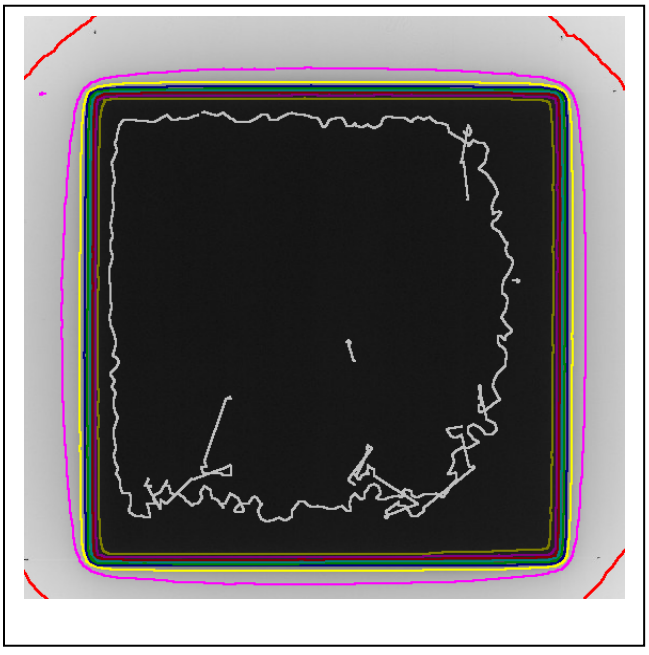

Figure 10.10 20x20cm^2 flat field isodose plotted over the film scanned image,

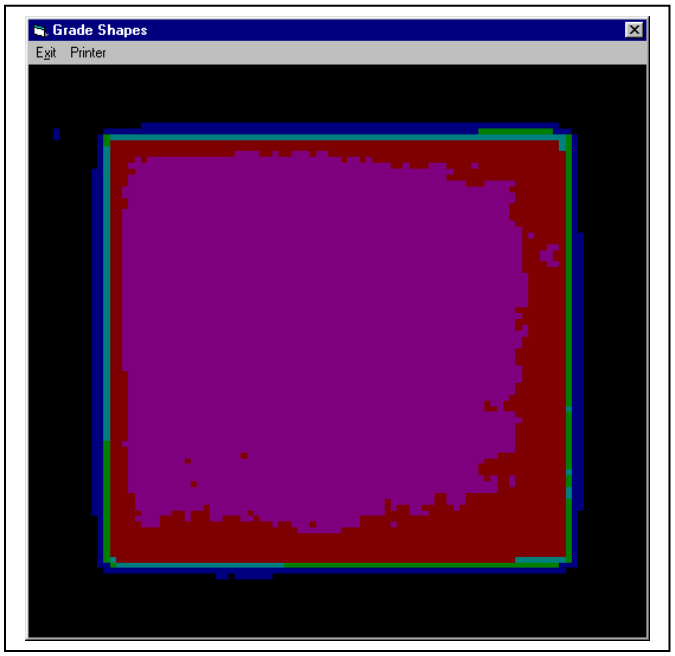

Figure 10.11 20x20cm^2 flat field isodose map displayed using colours,

```
            If Abs(pdx(j, i - 1) - pdx(j, i)) < 20 And Abs(pdy(j, i - 1) - pdy(j, i)) < 20 Then
               Picture1.Line (pdx(j, i - 1), pdy(j, i - 1))-(pdx(j, i), pdy(j, i)), QBColor(cl)
            End If
         Next i
         If Abs(pdx(j, p(j) - 1) - pdx(j, 0)) < 20 And Abs(pdy(j, p(j) - 1) - pdy(j, 0)) < 20 Then
            Picture1.Line (pdx(j, p(j) - 1), pdy(j, p(j) - 1))-(pdx(j, 0), pdy(j, 0)), QBColor(cl)
         End If
         ptx = Filmscan.Width - 1000
         pty = VScroll1.Top + VScroll1.Height + (j + 1) * 300
'        Filmscan.Line (ptx - 300, pty + 50)-(ptx - 50, pty + 50), QBColor(cl)
         Filmscan.CurrentX = VScroll1.Left
         Filmscan.CurrentY = pty
         Filmscan.ForeColor = QBColor(cl)
         Filmscan.Print Format(plv(j), "##0.0")
         DoEvents
         cl = cl + 1
         If cl > 14 Then cl = 1
      End If
   Next j
   Shape printing
   ShapeFrm.Top = 1
   ShapeFrm.Left = 100
   AutoRedraw = -1   ' Turn on AutoRedraw.
   a = 80
   ShapeFrm.Width = xc * a
   ShapeFrm.Height = yc * a
   ShapeFrm.ScaleWidth = ShapeFrm.Width
   ShapeFrm.ScaleHeight = ShapeFrm.Height
   BackColor = QBColor(15)

'       For i = 0 To xc - 1
'          Write #1, Int(sx(1, i) - (SL + SR) / 2 + 0.5),
'       Next i


      For j = 0 To yc - 1
         For i = 0 To xc - 1
            If Gds(j, i) < 0 Then Gds(j, i) = 0
            Frc = Int(Gds(j, i) / 5 + 0.5)
            If Frc < 0 Or Frc > 15 Then Frc = 15
            ForeColor = QBColor(Frc)
            Line (i * a + 1, j * a + 1)-(i * a + a, j * a + a), , BF ' Red box.
'            MsgBox Str$(j) + "," + Str$(i) + "," + Str$(Frc)

         Next i
      Next j
'~~~~~~~~~~~~~~~~~~~~~~~~~~~~~~~~~~~~~~~~~~~~~~~~~~~~~~~~~~~~~~~~
```

10.13 3-D displays

A film scan analysis (Figure 10.12a) result represents two-dimensional data (Figure 10.12b), and can be plotted as many profile curves or depth dose curves along both X and Y direction. It is possible to plot all the curves together on the screen, as a multiple chart picture which provides a 3-D view of the data. This function is useful

clinically to provide a quick view of the dose distribution for some special radiation field QA checks such as electron cut-out, multiple field junction, and compensation block shielding fields.

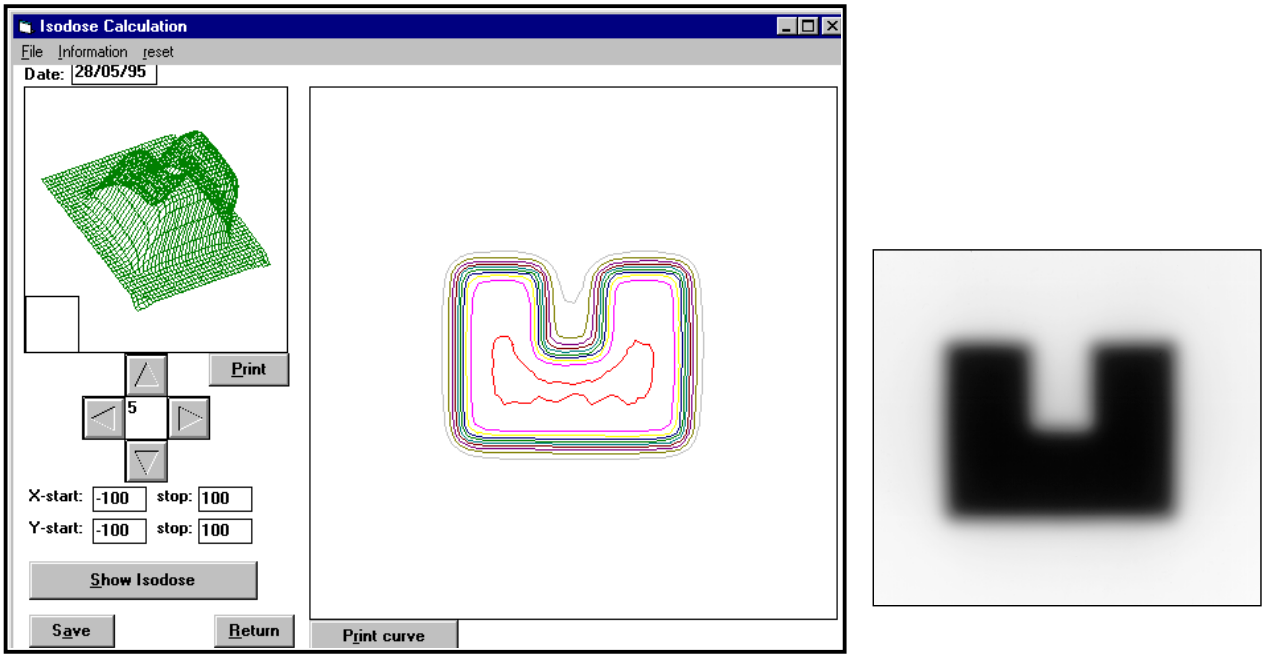

Figure 10.12 a. 2-D isodose curves and profile curves in 3D display
b. an irregular field film scanned image.

The first step is to determine a picture box on the design display window to display the three-D chart. Since the number order for the pixel layout is from 1 to n, the curve data position value needs to be converted for the centering.

The second step sends the centered point values to an X, Y and Z data buffer. As each picture rotation receives an angle number by either mouse clicking or array key press, each X, Y, and Z value will be modified by the triangle function:

$$Y = Y0 \times \cos A - Z0 \times \sin A$$
$$Z = Z0 \times \cos A + Y0 \times \sin A$$

As an example (Figure 10.13) the required rotation angle along the X axis, the point Y and Z will be changed by above function calculation for a given angle “A”. The function

loop is used to continue to call the triangle modification object to modify the curve points one by one.

Each rotation direction and rotation axis is determined as function objects. When the rotation signal has been received, appropriate function object will be called according to the rotation angle and axis.

The picture box clear function object will be called to clear the current curves before drawing the new modified the curves. The 'DrawSxSySd' curve drawing function object is called to draw the new curves.

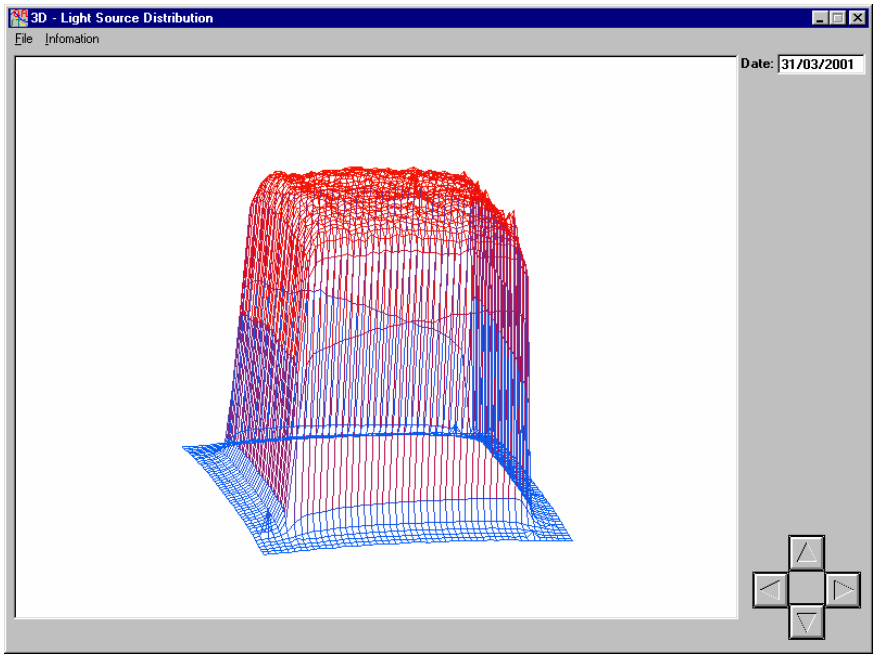

Figure 10.13 Line draw profiles displayed in 3-D view for a square field, the image can be rotated and shifted by mouse control

```
'~~~~~~~~~~~~~~~~~~~~~~~~~~~~~~~~~~~~~~~~~~~~~~~~~~~~~~~~~~~~~~~~~~~~~~~~
If xc < 1 Or yc < 1 Then Exit Sub
nrm = sd(Int(yc / 2), Int(xc / 2))
v = 0
For j = 0 To yc - 1 Step 2
   h = 0
   For i = 0 To xc - 1 Step 2
      ix(v, h) = sx(j, i) - sx(j, xc - 1) / 2
      iy(v, h) = sy(j, i) - sy(yc - 1, i) / 2
      iz(v, h) = 200 * sd(j, i) / nrm
      cd(v, h) = 255 * sd(j, i) / nrm
```

```
        h = h + 1
    Next i
    v = v + 1
Next j

Dim Nx As Double, Ny As Double, nz As Double
For j = 0 To v - 1
    For i = 0 To h - 1
        Ny = iy(j, i) * Cos(3.14159) - iz(j, i) * Sin(3.14159)
        nz = iz(j, i) * Cos(3.14159) + iy(j, i) * Sin(3.14159)
        iy(j, i) = Ny: iz(j, i) = nz
    Next i
Next j

fw = Picture1.ScaleWidth / 2
fh = Picture1.ScaleHeight / 2
Call Picture4_Click
Call Picture7_Click
Call Picture4_Click
Call Picture7_Click
Call Picture4_Click
Call Picture7_Click

Private Sub Picture4_Click()
Dim Ny As Double, nz As Double
For j = 0 To v - 1
    For i = 0 To h - 1
        Ny = iy(j, i) * Cos(5 * 3.14159 / 180) - iz(j, i) * Sin(5 * 3.14159 / 180)
        nz = iz(j, i) * Cos(5 * 3.14159 / 180) + iy(j, i) * Sin(5 * 3.14159 / 180)
        iy(j, i) = Ny: iz(j, i) = nz
    Next i
Next j
Call DrawSxSySd
End Sub
'~~~~~~~~~~~~~~~~~~~~~~~~~~~~~~~~~~~~~~~~~~~~~~~~~~~~~~~~~~~~
```

10.14 Data saving and retrieval

The window object common dialog box is loaded to provide the data store and retrieval function. The coding to support the dialog box include file extension definition, default file name determination, film name list filter, file management action type and error handling etc.

The data file format used in this program is ASCII format. The consideration for the file format type is that to allow the use different proprietary software to directly display or convert the format to a different work sheet format without extra coding.

When a file name is selected, the user can click on the ‘OK’ command or double click on file name like normal window function to save or retrieve the file. The file ‘open’ command is called with file type, file number and action type to open the file from the determined disk directory. For the data savings, a group of coding will perform a directory checking before the file save. If the file already exists, a message box will be opened and user will be asked to decide either overwrite the old data file or withdraw one step back to change another file name.

```
‘~~~~~~~~~~~~~~~~~~~~~~~~~~~~~~~~~~~~~~~~~~~~~~~~~~~~~~~~~~~~~~~~~~~~
Private Sub savechart_Click()
If scaninf.Text1(0) = "" Or scaninf.Text1(1) = "" Then
  scaninf.Show
  Exit Sub
End If

99 On Error Resume Next

CmDialog1.CancelError = True
CmDialog1.DialogTitle = "Save 3-D Curve File"
If cvfile <> "" Then
   CmDialog1.FileName = cvfile
Else
   CmDialog1.FileName = Mid$(scaninf.Text1(0), 1, 2) + Format$(scaninf.Text1(2), "00") +
Format$(Now, "mmyy") + ".cht"
End If

CmDialog1.DefaultExt = "cht"
CmDialog1.Filter = "3-D Curve data files(*.cht)|*.cht"
CmDialog1.Flags = OFN_FILEMUSTEXIST Or OFN_SHOWHELP
CmDialog1.Action = 2
If Err = 32755 Then
 Exit Sub
Else
 cvfile = CmDialog1.FileName
End If

On Error GoTo 100
If Dir(cvfile) <> "" Then
   asw = MsgBox("Data file is already exist. Overwrite?", 3, "File Exist")
   If asw = 2 Then
      Exit Sub
   ElseIf asw = 7 Then
      GoTo 99
   End If
End If
Close #1
Open cvfile For Output As #1
    Write #1, Text1
   For i = 0 To 10
     Write #1, scaninf.Text1(i)
```

```
    Next i
      Write #1, v, h
   For j = 0 To v
      For i = 0 To h
        Write #1, ix(j, i), iy(j, i), iz(j, i)
      Next i
   Next j
   Close #1
Exit Sub
100 If Err And Err <> 32755 Then MsgBox ("Error " + Error(Err) + " has found.")
    Close
    Resume 101
101
End Sub

Private Sub reteives_Click()

On Error Resume Next
CmDialog1.CancelError = True
CmDialog1.DialogTitle = "Load 3-D Line Chart Data"
CmDialog1.FileName = "*.cht"
CmDialog1.DefaultExt = "cht"
CmDialog1.Filter = "3-D Chart files(*.cht)|*.cht"
CmDialog1.Flags = OFN_FILEMUSTEXIST Or OFN_SHOWHELP

CmDialog1.Action = 1
If Err = 32755 Then
 Exit Sub
Else
 cvfile = CmDialog1.FileName
End If

On Error GoTo 210
ReDim inbuf(20) As String
 Open cvfile For Input As #1
     Input #1, buf1
   Text1 = buf1

   For i = 0 To 10
    Input #1, buf1
    inbuf(i) = buf1
   Next i

   Input #1, v, h
   For j = 0 To v
      For i = 0 To h
        Input #1, ix(j, i), iy(j, i), iz(j, i)
      Next i
   Next j
   Close #1
   For i = 0 To 11
    scaninf.Text1(i) = inbuf(i)
   Next i

  Call DrawSxSySd
 Exit Sub
```

```
210 If Err And Err <> 32755 Then MsgBox Error(Err)
Close
Resume 211
211
End Sub
```

10.15 Image and Graphical Output

The film analysis result and curve output function is developed to organize the document A4 size paper layout. ‘Printer’ objects command is used to send both text data and curve data to the computer determined default printer. The printing font, font size and font colours are determined for each text display requirement. Using a normal Windows program output function, all the text and curve drawing will be allocated to the printing page pixel. The horizontal position of text layout is controlled by the ‘TAB(n)’ function call. The line spacing is controlled by the ‘Printer’ command to send an empty line to the printer. If one text in a screen text box is multiple line formatted, the ASCII character command ‘CHR$(n)’ is used to load a window’s ASCII code for the line feeding or spacing.

Printing graphical charts is more complicated since the page output pixel size for both cross plane and in plane has to be calculated to fit on A4 format. Size In the software implementation, the scaling for printing must be calculated separately from that used for monitor display resolutions. So, the line drawing and colours between screen display and printing to be determined separately.

```
‘~~~~~~~~~~~~~~~~~~~~~~~~~~~~~~~~~~~~~~~~~~~~~~~~~~~~~~~~~~~~~~~~
Private Sub IsoPrint_Click()
If I < 1 Then Exit Sub
If scaninf.Text1(0) = "" And scaninf.Text1(1) = "" Then
   MsgBox "Set-up information then select print again."
   scaninf.Show
   Exit Sub
End If

On Error GoTo 390

Printer.FontName = Printer.Fonts(fnt)
Printer.FontBold = False
Printer.FontSize = 12
Printer.Print: Printer.Print: Printer.Print: Printer.Print
Printer.FontUnderline = True
Printer.Print Tab(12); "ISODOSE CURVE PRINT"
```

```
Printer.Print
Printer.FontSize = 10
Printer.FontUnderline = False
Printer.Print Tab(15); "Machine: '" + scaninf.Text1(0) + "'";
Printer.Print Tab(35); "Beam type: "; scaninf.Text1(1);
Printer.Print Tab(60); "Energy: "; scaninf.Text1(2) + " " + scaninf.Text1(3);
Printer.Print Tab(84); "Field size: "; scaninf.Text1(6) + "mm x " + scaninf.Text1(7) + " mm"
Printer.Print
  Printer.FontSize = 9
  Printer.Print Tab(15);
   For i = 0 To 90
      Printer.Print "_";
   Next i

   Printer.FontSize = 7
   Printer.DrawWidth = 5
   a = 38
   x0 = 30 * a: y0 = 3000

cl = 12
For j = 0 To l - 1
   If p(j) > 1 Then
      For i = 1 To p(j) - 1
         If Abs(pdx(j, i - 1) - pdx(j, i)) < 20 And Abs(pdy(j, i - 1) - pdy(j, i)) < 20 Then
            Printer.Line (x0 + pdx(j, i - 1) * a, y0 + 10 * a + pdy(j, i - 1) * a)-(x0 + pdx(j, i) * a, y0 + 10 * a +
pdy(j, i) * a), QBColor(cl)
         End If
      Next i
      If Abs(pdx(j, p(j) - 1) - pdx(j, 0)) < 20 And Abs(pdy(j, p(j) - 1) - pdy(j, 0)) < 20 Then
         Printer.Line (x0 + pdx(j, p(j) - 1) * a, y0 + 10 * a + pdy(j, p(j) - 1) * a)-(x0 + pdx(j, 0) * a, y0 + 10 *
a + pdy(j, 0) * a), QBColor(cl)
      End If
      Printer.Line (x0 + 9500, y0 + j * a * 10)-(x0 + 9800, y0 + j * a * 10), QBColor(cl)
      Printer.CurrentX = x0 + 9000
      Printer.CurrentY = j * a * 10 + 3000
      Printer.ForeColor = QBColor(cl)
      Printer.Print Format(plv(j), "##0.0")
      cl = cl + 1
      If cl > 14 Then cl = 1
   End If
Next j
Printer.Line (x0 + (SL + SR) / 2# * a, y0)-(x0 + (SL + SR) / 2# * a, 13500), QBColor(1)
Printer.Line (x0 - 200, y0 + (ST + SB) / 2# * a)-(9600, y0 + (ST + SB) / 2# * a), QBColor(1)


Printer.CurrentX = 1000
Printer.CurrentY = 230 * a + 6500
Printer.ForeColor = QBColor(0)
Printer.FontSize = 11
Printer.Print "Signature: _____      Date:   " + Format$(Now, "dd/mm/yyyy")
'Printer.NewPage
Printer.EndDoc

Exit Sub
390 If Err Then MsgBox (Error(Err))
   Close
```

```
    Resume 391
391
End Sub
```

10.16 Summary

The RODOMS film dosimetry program developed to be based on the film dosimetry analysis protocols from radiotherapy clinical quality assurance. It uses Microsoft windows development techniques such as GUI programming language involved with graphic image and chart processing, data mathematics calculation process, data store and retrieving processes etc. As VB-6 language can be used as an object oriented software development tool, the functions developed within the project as function group package, can be re-used to different application processes.

The RODOMS software has been developed for radiotherapy medical physicists and can be run it as a normal PC windows application software, it can be stored and runs on different Microsoft Windows operating system such as Win 95/98, NT, 2000 and XP.

Chapter 11 Phantom Design for the Film Dosimetry

11.1 Introduction

The use of film for QA requires the development of phantoms designed for specific procedures. Reproducible results require that the phantom is aligned in accordance to standard protocols discussed in previous chapters.

Phantoms are commonly used in the following procedures:

1. Radiation and light field coincidence checks.
2. Beam profile flatness and symmetry checks.
3. Depth dose curve measurements.
3. Radiation beam energy measurements.

Since the 1950's, film has become increasingly used in radiation field quality assurance. The film is exposed to radiation in a water tank or in a phantom made from such as perspex, polystyrene, or solid water equivalent plastic material. These materials are chosen because they have similar radiation characteristics to tissue and are easily shaped and machined. These phantoms may be simple homogenous, geometric shapes (cylindrical, spherical or wedge) or more complex, like the anthropomorphic phantom which has inserts of varying attenuation which mimic abdominal structures.

In this thesis we develop procedures which utilise both solid and water phantoms for use with film QA procedures.

The use of a solid phantom for beam energy studies started in the early 1960's. Solid plastic slab phantoms are used in both ionisation dosimetry and film dosimetry. Nowadays film is commonly used for radiation and light field coincidence checks because it is easy to set up, and is easily analysed by eye.

However simply sandwiching film between two solid water slabs aligned parallel to the beam has many technical problems. Dutreix and Dutriex (1969) described the influence of build up on the depth dose curve and also discussed the effect of the thin air gap between the film and slab. Since this issue has proved hard to overcome using simple setup techniques, the use of film for the beam energy measurement has been ignored for many years.

A slab phantom is used in this study to derive profile dose distribution and, percentage depth dose profiles. The measurement and analysis procedures associated with the phantoms include corrections which allow more accurate dosimetry than previously. These procedures include corrections for field dependence, energy dependence, build-up depth dependency, latent image effects, and incorporate signal smoothing, and scanner signal linearity adjustments.

11.2 Depth Dose Curves

- **Slab phantoms**

For a depth dose check, the verification film is set vertically along the beam direction parallel and coincident with the beam axis (Figure 11.1).

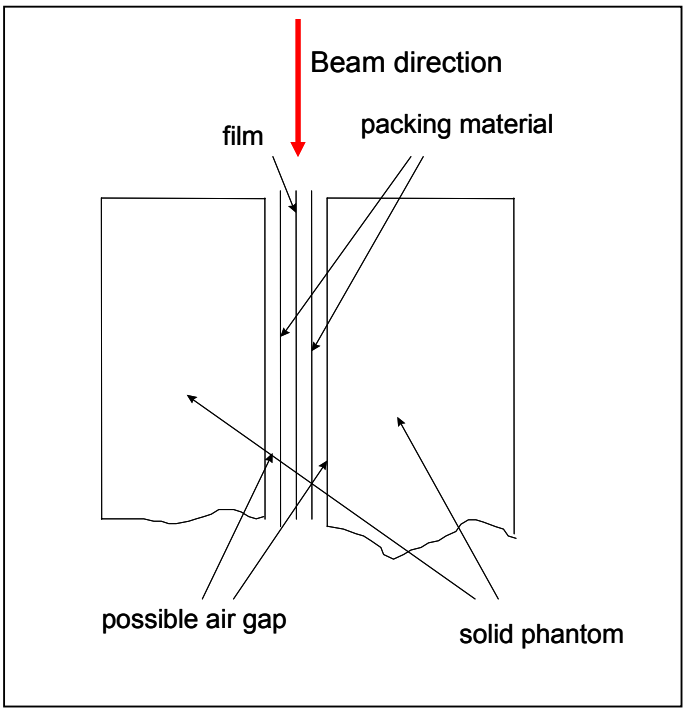

Figure 11.1 Lateral Film set up in solid slab

1. Typical results are shown in Figure 11.2 (Dutreix, and Dutreix, 1969).The film is pre-packed and the packing material density is a lot lower than that of the build up phantom.

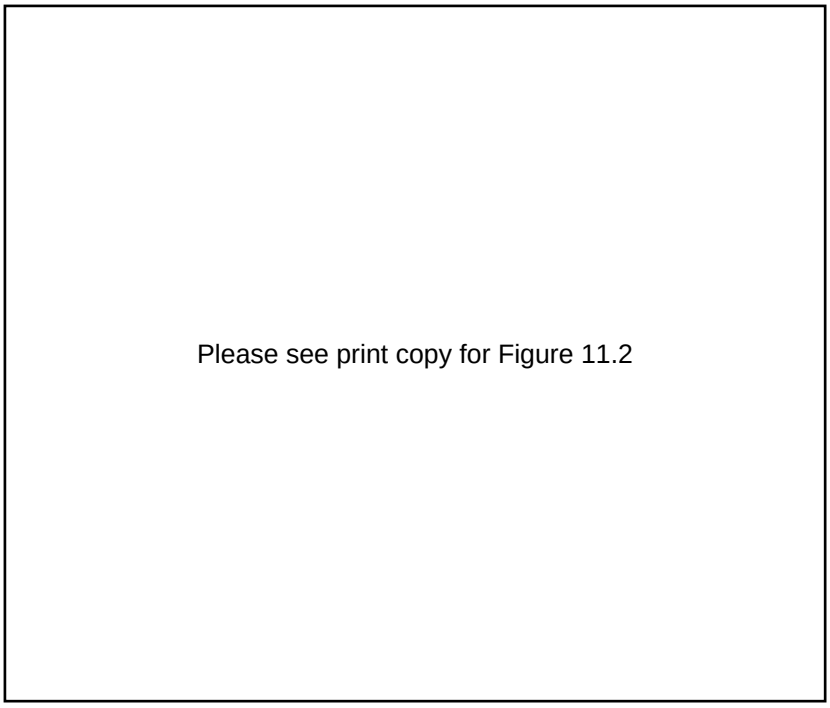

Figure 11.2 set-up influence, film exposed in sandwich set-up in slab phantom (Dutreix, J. and Dutreix, A., *Film Dosimetry of High-Energy Electrons*, Annals New York Academy of Sciences 161 Article 1, 1969)

In performing a depth dose measurement where the film is usually set vertically, the packing material can become compressed in very localised regions resulting in possible air gaps between the envelope and phantom. This results in a lower density build-up and will significantly affect the measurement readings.

Note that for the beam profile checks, where the film is placed horizontally, this density difference can be safely ignored because the packing material is very thin and the film is set perpendicularly to the beam axis.

In this experiment, different angles of orientation of the slab phantom to the beam are tested. Figure 11.4 shows the four different depth dose curves in which films are set in different angles to the beam direction. Figure 11.3 shows the setup with 0, 5, 10 and 15 degrees. The result shows that the curves for angles of 5, 10, and 15 degrees differ only slightly.

However, there is a clear difference between these three curves and that obtained with a vertical setting (0 degree). The edge on film result gives higher %GSV. This is because the equivalent build up is affected by the packing material. Intended to solve this problem, this experiment has compared the beam energy check analysis calculation. Table 11.1 gives a summary of the analysis results.

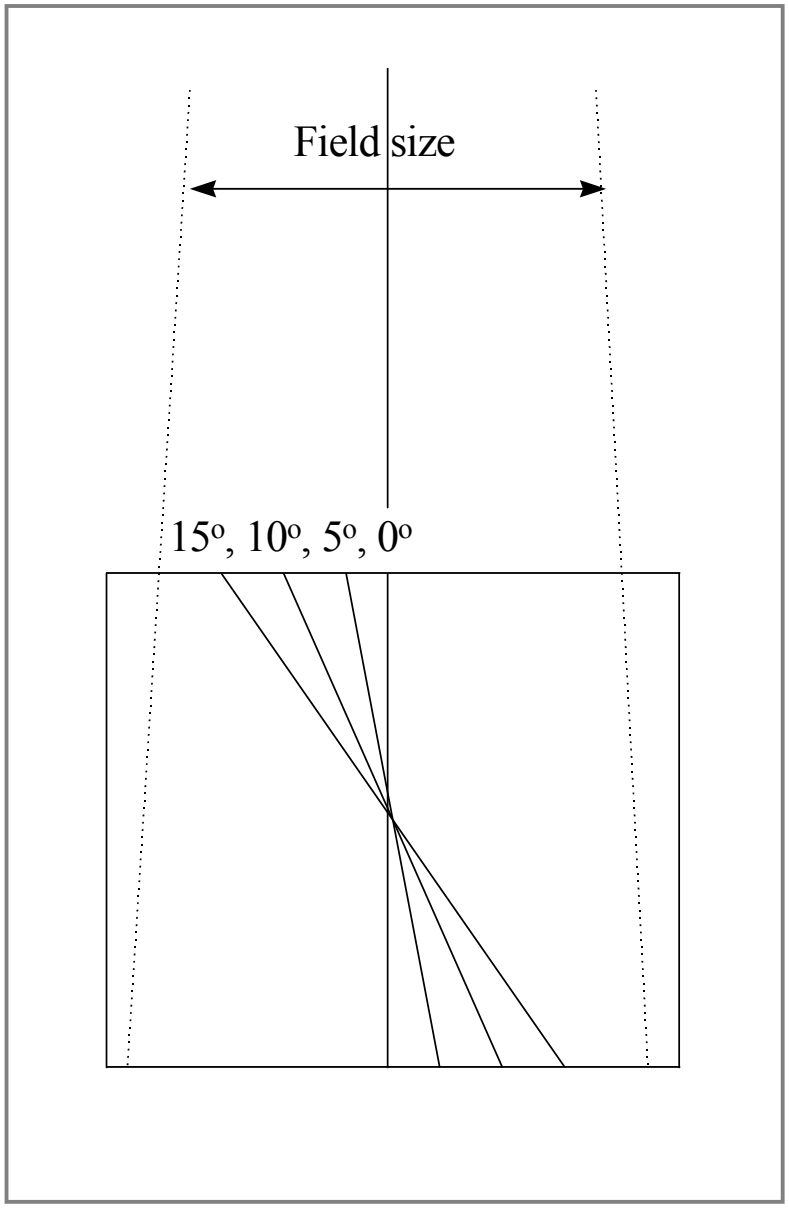

Figure 11.3 Films set different angles in water phantom

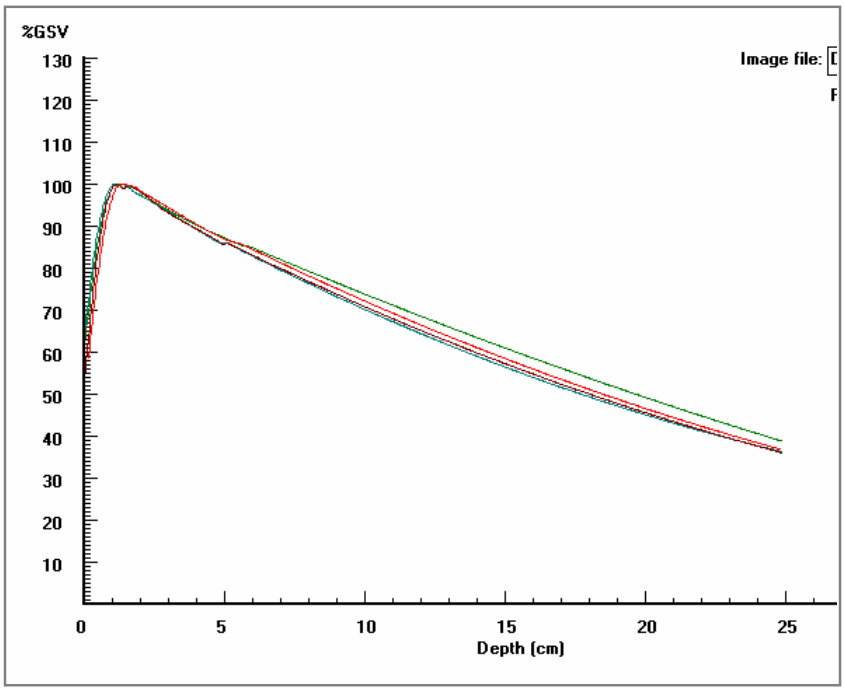

Figure 11.4 PDD curve for different film setup angles

Figure 11.5 displays the D200/D100 ratio variation from 0° to 15° film set up angles. It shows that the ratio has dropped between 0 and 5 degree setting. After that each angle made the ratio increase slightly. That would be caused by the physical distance which is changed slightly by the diverging angle.

Film angles ->	0°	5°	10°	15°
R_{100}	1.2	1.2	1.2	1.3
R_{50}	19.7	17.9	18.0	18.5
D_{50}	87.2	86.1	85.7	85.9
D_{100}	73.8	70.2	70.9	70.2
D_{200}	49.2	45.1	45.6	45.9
D_{200}/D_{100}	0.667	0.643	0.644	0.645

Table 11.1 PDD curve analysis result for different film set-up angles

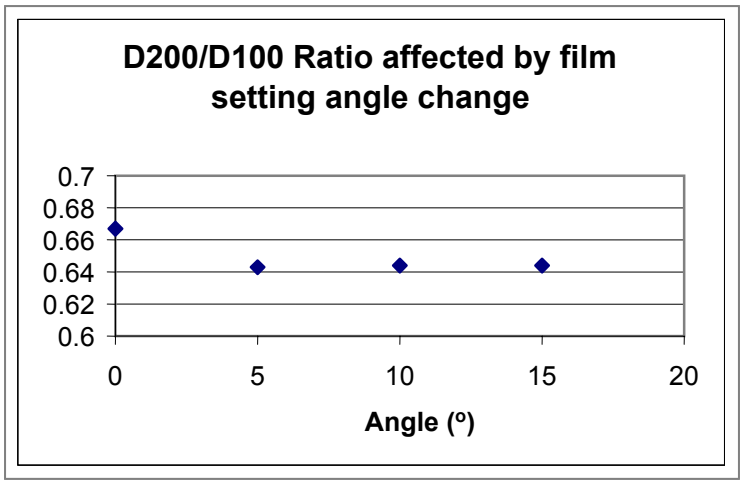

Figure 11.5 D200/D100 ratio changed via different film set up angle scanning

The experimental results from the slab phantom show increased noise and artefact levels in the build up region can be higher up to ±10% in comparison with ionization measurement result. This is due in part to the slab material uniformity. In order to avoid the grosser effects due to air-gaps we recommend that an inclined setup water phantom is used. We have designed such a phantom and incorporated corrections for beam angle (equivalent depths) into the RODOMS software.

- **Water Phantom**

Water phantoms normally are commonly used for absolute dosimetry measurement. As noted above the noise in the build-up region when using a slab phantom can be high. We can avoid this problem and those relating to uneven compression of packing material by using a water phantom. However water tanks are unwieldy and difficult to use for daily QA.

A special film holder was designed and built for the depth-dose profile film measurements. The film is tightly sandwiched between two 3mm perspex plates set into a holder (Figure 11.6). This is set in a 30x30x30cm^3 perspex water tank filled to the level of film holder top surface. The film edge extends beyond the top of perspex holder above the water surface.

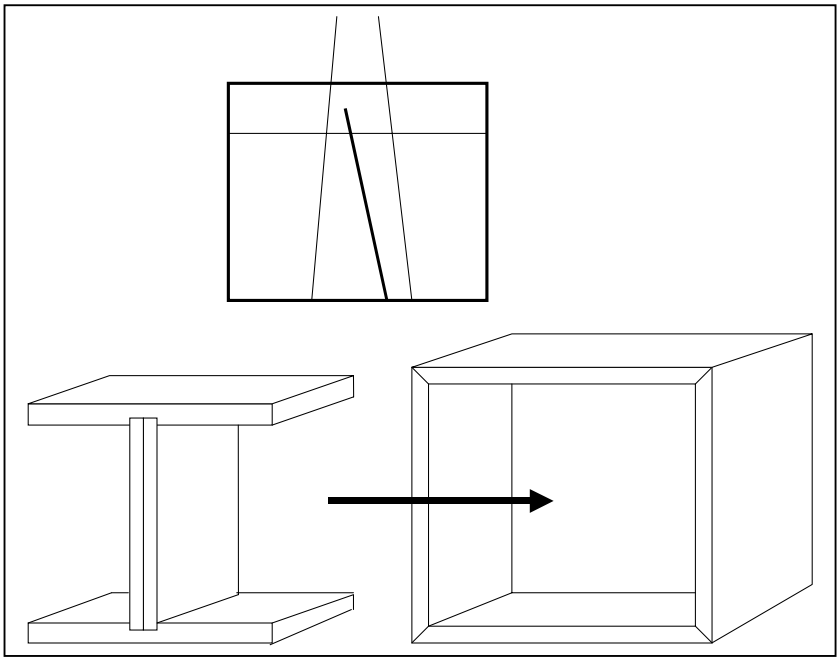

Figure 11.6 Sandwich film holder inserted into a water phantom

It is necessary to convert the depth to equivalent distance. This is incorporated in the RODOMS procedure which is based on the following trigonometric model.

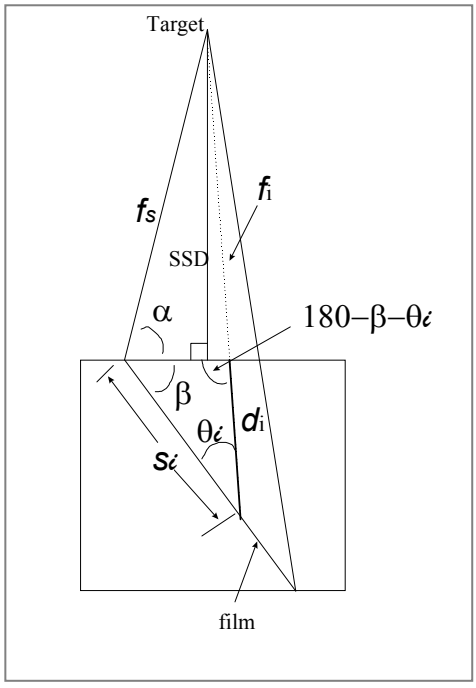

Figure 11.7 Equivalent depth calculated for a measurement point on film

The slope angle will be corrected by a trigonometry based mathematical conversion calculation (Figure 11.7).

The film is set at an angle (β) to the surface of a water phantom whose field centre is placed at a distance SSD from the target and is perpendicular to the beam axis. The distance from the top edge of film to the target is f_s. The line joining the target and film top edge makes and angle α to the water surface. In scanning along the film, the scan distance S_i at any point forms the angle θ_i between the beam and the film. The physical SSD f_i and equivalent depth d_i need to be calculated for the test point S_i as follows:

From the sine rule, the relationship between the angles is:

1. $$\frac{d_i}{\sin \beta} = \frac{s_i}{\sin (180 - \beta - \theta_i)}$$

2. $$\frac{f_e}{\text{Sin } \theta_i} = \frac{f_i + d_i}{\sin (\alpha + \beta)}$$

and also from the cosine rule:

3. $$\cos (\alpha + \beta) = \frac{f_s^2 + s_i^2 - (f_i + d_i)^2}{2 \cdot f_s \cdot s_i}$$

from equation 3 we get: $$f_i = \sqrt{f_s^2 + s_i^2 - 2 \cdot fs \cdot si \cdot \cos (\alpha + \beta)} - d_i$$

Substitute 3 into 2: $$\theta_i = \frac{f_s \cdot \sin (\alpha + \beta)}{\sqrt{f_s^2 + s_i^2 - 2 \cdot f_s \cdot \cos (\alpha + \beta)}}$$

and substitute 2 into1, we can get the equivalent depth d_i corrected as:

$$d_i = \frac{s_i \cdot \sin \beta}{\sin \left[180 - \beta - \sin^{-1} \left(\frac{f_s \cdot \sin (\alpha + \beta)}{\sqrt{f_s^2 + s_i^2 - 2 \cdot f_s \cdot \cos (\alpha + \beta)}} \right) \right]}$$

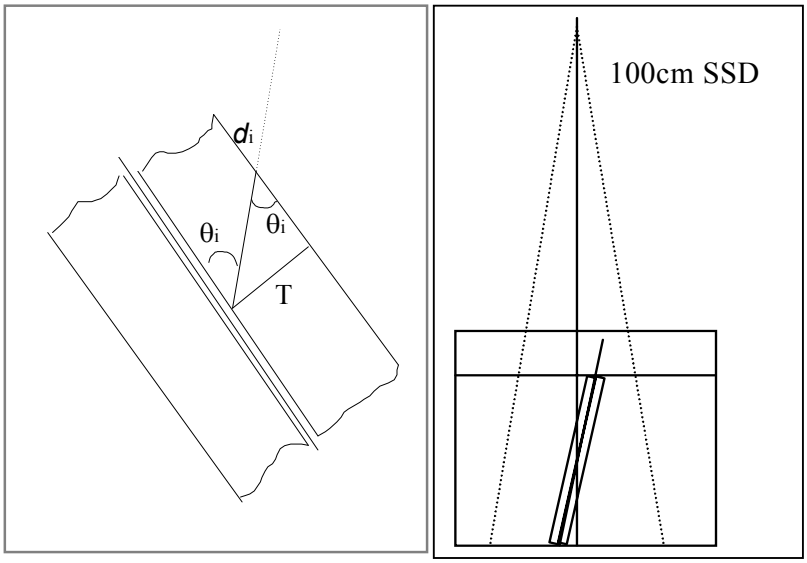

Figure 11.8 Equivalent depth correction for film holder material density

To hold the film in the water phantom and keep the film in a stable position, a non-equivalent water density material (perspex) is be used inside the water phantom. In order to increase the accuracy of the film scan result, an equivalent distance is also corrected by the following (Figures 11.6 & 11.8).

T is the thickness of the folder material with a density of ρ. The angle between the beam and the film θ_i is derived from the depth correction formula. So, the equivalent depth di can be corrected by:

$$d_i = d_i - \frac{T}{\sin \theta i} + \frac{T}{\sin \theta i} \rho$$

Both solid slab and water phantom for this study design are used as angled beam entry, in order to avoid the surface effect which is mentioned by Dutreix[42] etc., if the verification film packing envelop is of water proof material the use of a water phantom can achieve better a quality dose-depth measurement.

11.3 Beam Energies

- **Wedge Phantom Design for Electron Beam**

Electron energy checks cannot be easily performed routinely because the complexity in measurement setup. Routine Electron beam energy check is unable to use the method for photon beam energy routine check, to compare two readings from two different depths. Electron energy is characterised by the surface mean

energy (E_o), 50% dose level depth (R_{50}) and practical range (R_p). For most machines with different electron beam energies the R_p is low, but the measurement is sensitive to the accuracy of the set up distance causes the difficulty to use either cylindrical or plane parallel ionisation chambers for the fixed point setup. The best way to measure the electron beam energy is using water scan techniques. Although by scanning the ionisation chamber in the water tank we can obtain reliable electron beam percentage depth dose curves, the water tank is not suitable for regular weekly use.

An alternative means of providing depth dose information can use varying thicknesses of solid water or water equivalent materials to attenuate the beam intensity. A wedge phantom and film can provide such attenuation and the dose along the wedge can be converted into equivalent percentage depth dose.

Islam et al (1993) designed the first Perspex wedge phantom and used it for the electron energy measurements. By using multiple ionisation chamber detectors under the wedge phantom to collect several off -axis readings, an equivalent depth dose curve was made by linking the renormalised signals. Since the size of ionisation chamber could not be made very small in size, the gap between each centre of detector was as large as 1.5cm; and the depth dose curve obtained was very rough. The cost to make the multiple ionisation chamber line and multi-channel electrometer was also very expensive.

The perspex wedge phantom used here is designed with the following considerations. Firstly, the wedge should span 80% of the field width at 100cm SSD to avoid the beam profile shoulder. This requirement in the present case yields a 2cm gap between the wedge toe and the field edge of the 25 x 25 cm^2 applicator. This gap is useful in that it minimises the contribution of electron scatter from the side walls to the build up region of the film density/distance curve. Secondly, the thick end of the wedge at the 80% field width limit should correspond to the practical range R_p, for the highest electron energy in use. For example if the “console” energy is 20MeV, the thickness required is around 10cm to get enough build up for the tail of R_p curve. The wedge angle required is roughly about 30 degrees. An extension of the wedge beyond the field width limit at the heel end is of no consequence since the ray path thickness becomes increasingly greater than R_p

and so the beam in this region becomes completely absorbed and beam penumbra and collimator scatter are not seen.

The geometrical calculation carried out as part of RODOMS to convert each physical point on the film into equivalent depth distance uses the following trigonometrical functions Figure 11.9 a, b, c):

1. <u>The range of film scan distance determination</u>

   Off_X - variable of physical distance from beam center to the tail of the wedge phantom.

   α - variable of wedge angle at the tail end.

   β - variable of angle made by divergent field edge with the wedge at the heel end.

   $$\beta = 180 - \tan^{-1}\left(\frac{SSD}{EFR}\right)$$

   EFR - effective field range at 80% profile.

   ScD - film scanning distance.

   $$ScD = (off\_X + EFR) \times \frac{\sin(\beta)}{\sin(180 - \alpha - \beta)}$$

2. <u>Convert scan pixel number to physical distance</u>

   DFtr - variable of distance conversion factor.

   Dist - distance measured between the film marks.

   $$DFtr = \frac{Dist}{Pixels}$$

   P_i - variable array of scanning point physical distance

   $P_i = Pixe_{li} \times DFtr$

3. <u>Projection of film scan point to the position of phantom surface</u>

   SPD_i - variable array of phantom surface scan point projecting distance

   $SX_i = P_i \times \cos(\alpha) - off\_X$

   TDi - variable array of phantom vertical thickness for the scan point

   $TD_i = P_i \times \sin(\alpha)$

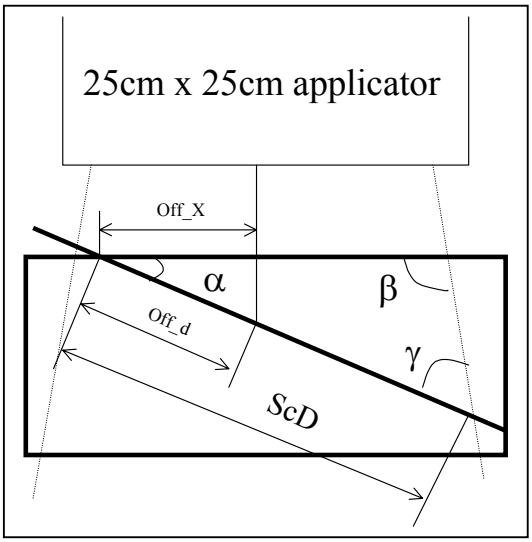

Figure 11.9a One piece of Perspex Block cut into two pieces to make a wedge phantom for SSD set up, and sandwich film between the block

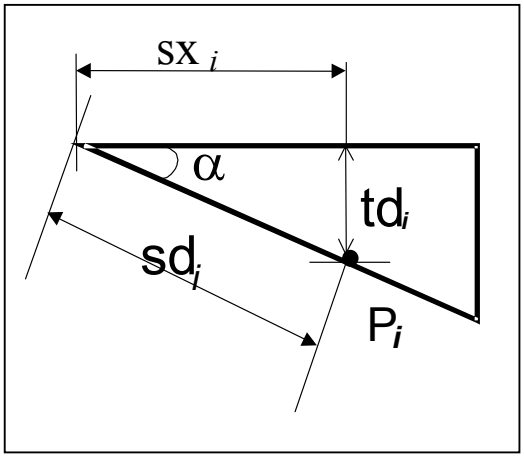

Figure 11.9b triangle distance conversion from the tip edge of the phantom to the beam set up centre

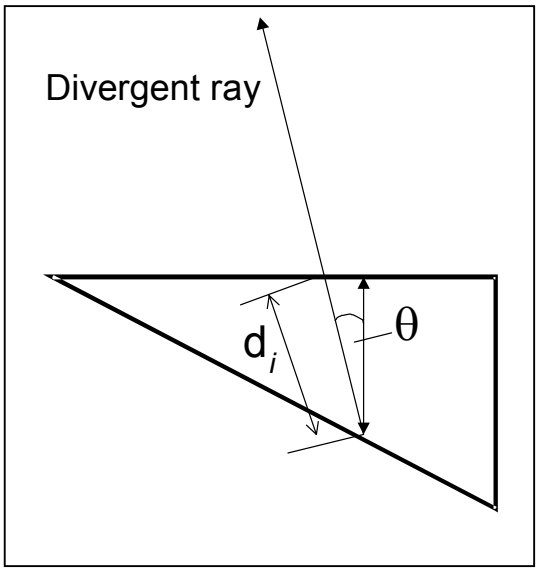

Figure 11.9c triangle distance conversion from vertical thickness to a diverted distance along the beam entry direction

4. Phantom thickness beam direction divergent angle correction

θ_i - correction angle for each projected scan point

$$\theta_i = \tan^{-1}\left(\frac{SXi}{SSD + TDi}\right)$$

5. Scanning equivalent depth

D_i - variable array of scanning equivalent depth

ρ - phantom material density

$$Di = \rho \times \frac{TDi}{\cos(\theta i)}$$

The film set up in the wedge phantom showed in the following pictures:

Gantry 100cm SSD set up for gantry 0^o and gantry rotated to perpendicular to the wedge angle.

- **Wedge Phantom Designed for the Photon Beam**

Although photon energy can be routinely checked by ionisation measurement at different depths, we designed a wedge phantom and a properly corrected film dosimetry technique to perform the photon energies. Compared with the ionisation measurement technique, the film is a lot easier to set up in a solid phantom, beam-on time will be saved significantly, and the result will provide a fully visualised, equivalent percentage depth dose curve.

The phantom design and set up for the photon energy check, should be easier than that of the electron beam because:

- There is less concern about the collimator scatter contribution to the surface dose;
- The percentage depth dose curve does not fall off in the same way as the electron beam in air. Therefore the phantom wedge angle can be made larger to the surface direction, and the field size to cover the wedge can be made smaller.

- Film can be set to 100cm SAD constant distance to the film or SSD to the phantom surface, not limited like the setup for electron beam as a photon beam has no applicator insert on the collimator as in an electron treatment.

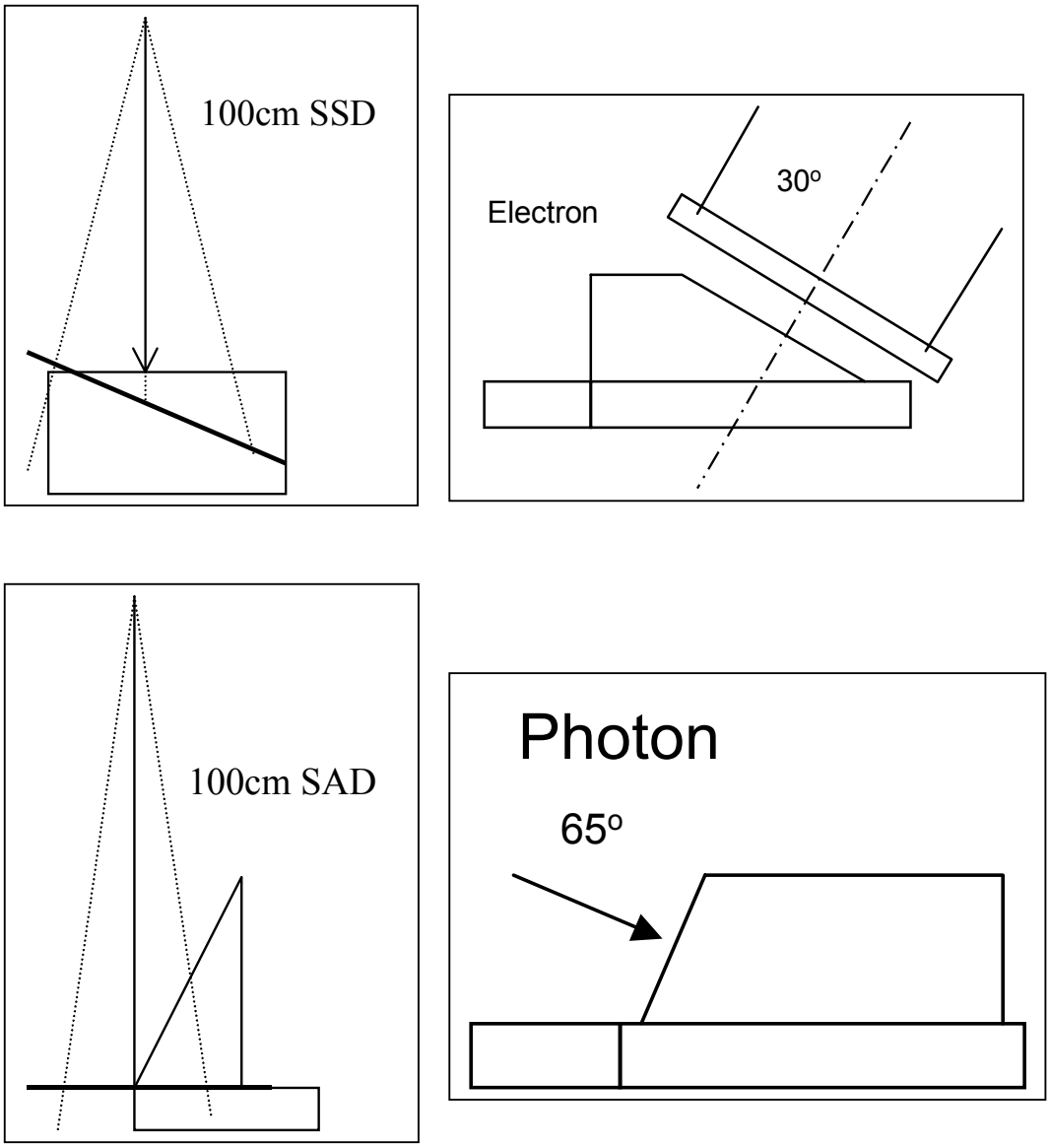

Figure 11.10 a comparison between different solid wedge phantom designs used in RODOMS development for both photon and electron energy checks.

11.4 IMRT Phantoms

- **Cylindrical plastic phantom**

A cylindrical solid phantom was designed for the rotational dynamic radiation beam field treatments achieved by rotating gantry. Normally, we can perform a radiation isocentric check by taking a star shot film. Using a very narrow beam made by the jaws almost closed, and a film in the plane of rotation, the gantry is rotated to different angles. The star shot image can be visually compared with the physical mark of mechanic isocentre. In recent years, dynamical treatment planning and stereotactic treatment techniques used in the radiotherapy technique have increased the importance of the star-shot film check. In addition, film has become important in comparing the planar measured dose distributions with planning calculations as part of 3-D treatment QA.

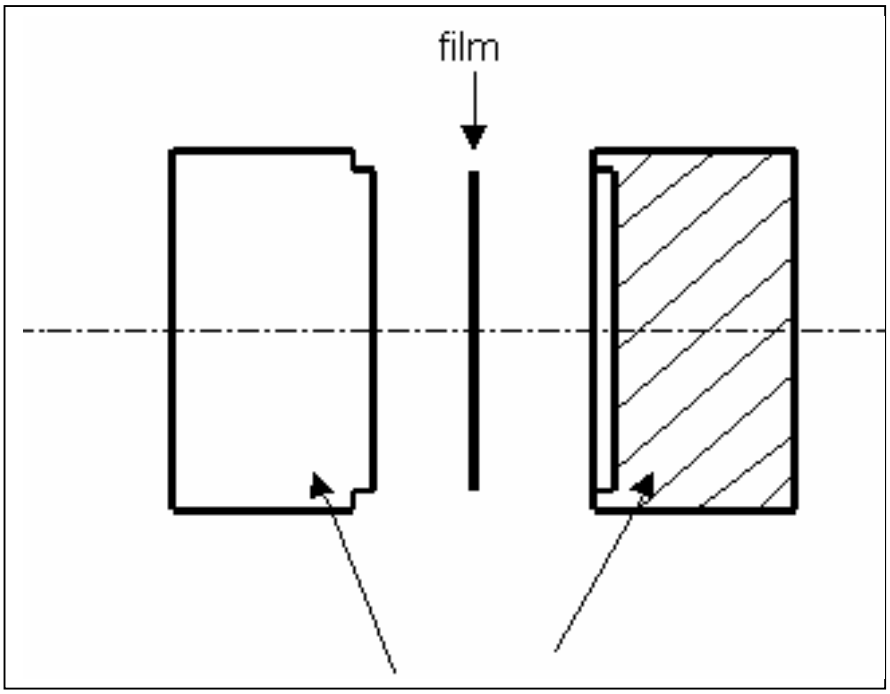

Figure 11.11 A lateral view of cylindrical phantom design. A circle shape cut film is sandwiched in between two pieces of cylindrical blocks.

Since the difficulties of using ionisation measurements or water scanning techniques to check the dynamic field dose distribution, a 16 cm diameter cylindrical film dosimetry phantom is designed for use with radiographic film. Figure 11.11 shows the physical shape of the phantom component made from by

two cylindrical, black plastic blocks. One piece is made as male and the other piece made as female with about 1cm shallow recess in order to stop the light leakage to the film. The film is cut into a circular shape to fit into the phantom, and sealed in by black sticky tape. All assembly has to be done in the dark room.

In order to check the coincidence of radiation beam centre and gantry rotation isocentre, the phantom centre is set to the gantry rotation centre, aligned by the three calibrated treatment room lasers. The jaw size can be opened to the treatment field size according to the treatment planning (figure 11.12 to 11.14). After the film is developed, the film can be scanned by a desk top transparency scanner and the scanned image analysed by the film dosimetry software and the equivalent dose distribution data and the isodose curves displayed.

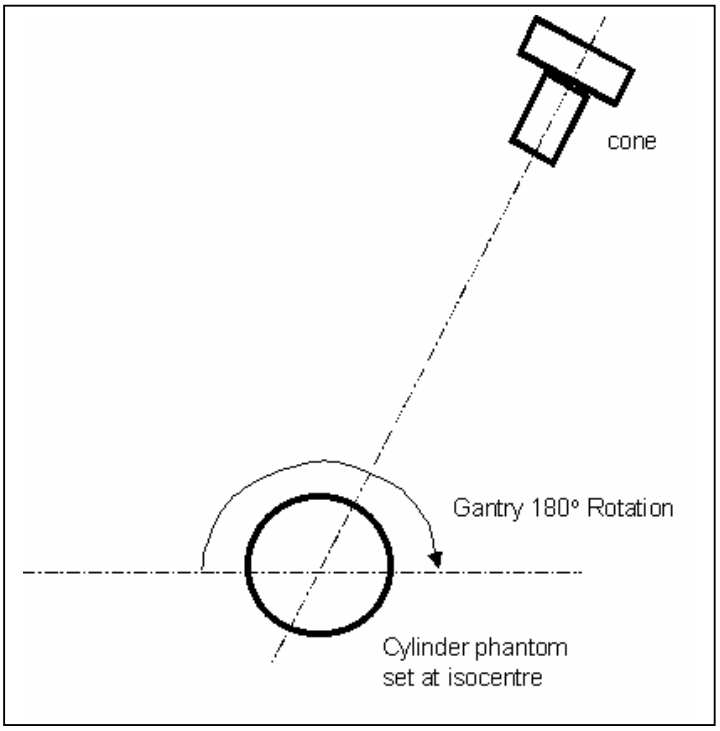

Figure 11.12 a front view of cylindrical phantom showing to the beam isocentre. The gantry is rotated around the phantom centre.

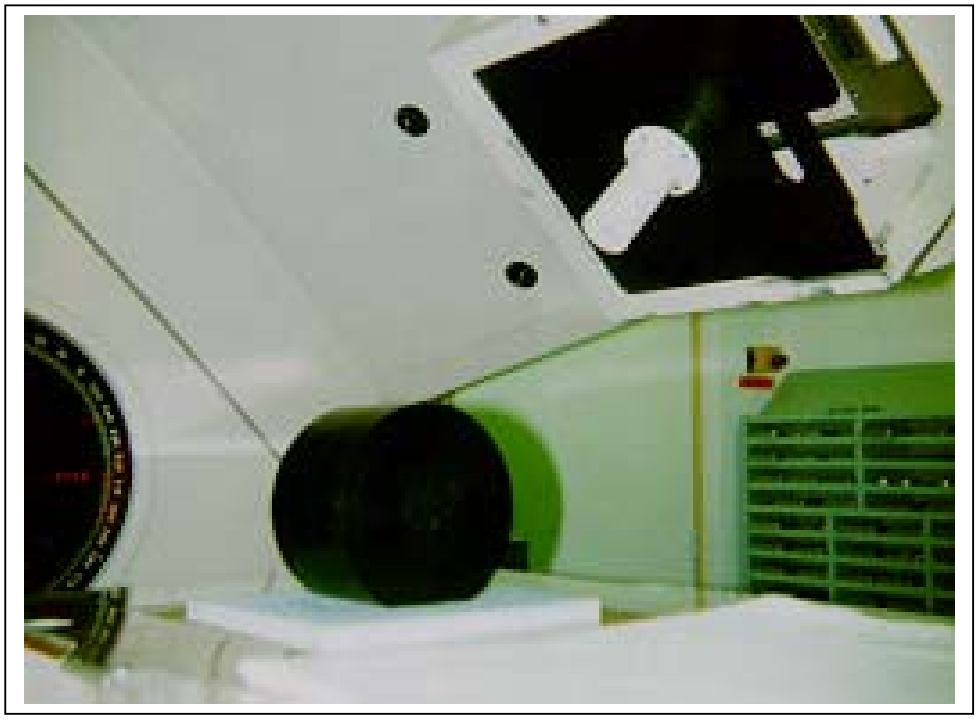

Figure 11.13 cylindrical phantom set up under a treatment unit

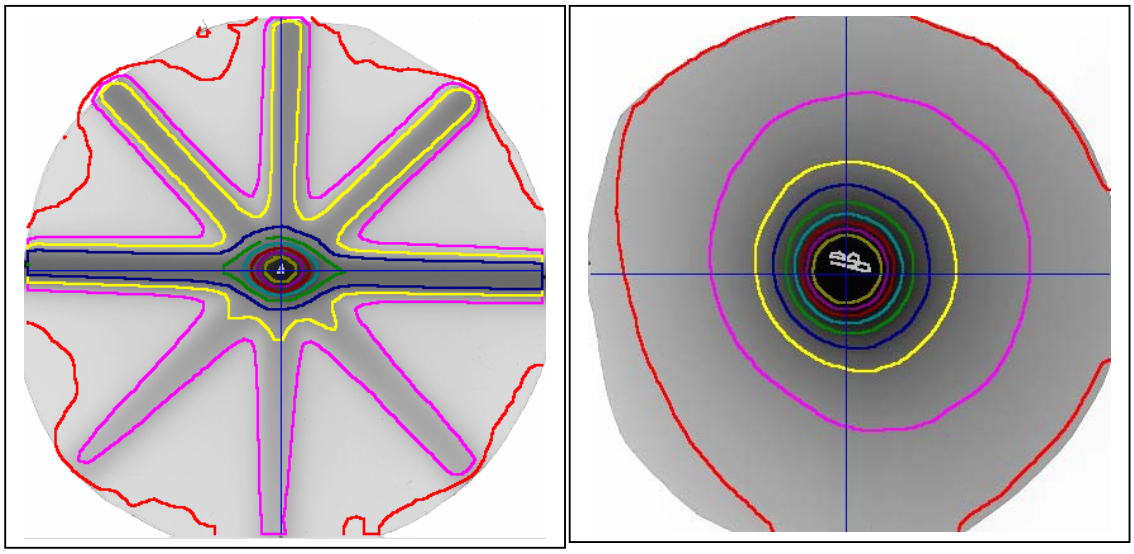

Figure 11.14 Isodose curves are scanned by RODOMS,
for both star shot exposure and 360^{o} rotation exposure

Chapter 12 An investigation into the source of low energy scattered radiation of significance in film dosimetry and correction technique

(Presented at the EPSM-2000 conference and published in APESEM journal in 2001)

(Wang Y, Cross P, Zealey W, An investigation of unexpected background value correction in film dosimetry, Conference Australian EPSM-2000 (Engineering Physics and Science in Medicine), Newcastle, NSW, Australia, Nov 2000)
(Wang.Y, Zealey.W, Cross.P, An investigation into the source of low energy scattered radiation of significance in film dosimetry, APESM, vol. 25, September 2002)

Please see print copy for Abstract

Key words

Film dosimetry, background, scatter, optical density, Cerenkov radiation

12.1 Introduction

Film dosimetry is a common technique used to quickly obtain dose distribution information for radiation field checks. The technological advance made in successive generations of film scanners and digitisers has improved film analysis accuracy significantly over the past five years. The resulting dose distributions, in carefully calibrated cases, have increasingly matched the profiles obtained from ionisation scans in water.

However, there are many issues affecting reliability and reproducibility in film dosimetry. The film analysis result can be influenced by such as latent image, energy dependence, build-up medium dependence and physical and chemical processing artifacts. These perturbing effects can be produced by film batch variation, product quality, film developing technique, image processing technique and exposure operation factors. This study is focused on the origin and nature of film background and developing an accurate corrective method for it.

The concept of background correction in film dosimetry is subtraction of the fog value created by the film base and emulsion. Since the fog value has no relation to the radiation dose, this value should always be subtracted from the image optical density value. The simplest and most common way to deal with unwanted background is to evaluate the fog levels of a film by measuring a point optical density reading from somewhere outside the irradiated field. With Reference to Figure 12.1, Point 1 is a typical point chosen for background subtraction. Removing the offset in this way has the effect of “pulling the curve down” and changes the relative proportions of the data points. (From Circle 1 we can see that even when the depth dose from the film tail region matches flat of the water scan curve, in the penumbral tail, there is a discrepancy in the curve shape over the rest of the penumbra.) If the selected point is too close to the irradiated field area (Point 2), an unrealistic zero or negative background value can be given by the when fog is subtracted (Circle 2). This method is therefore an approximate background correction, where the corrected curve derived from the film may not represent the actual dose profile after conversion to derived dose (DD).

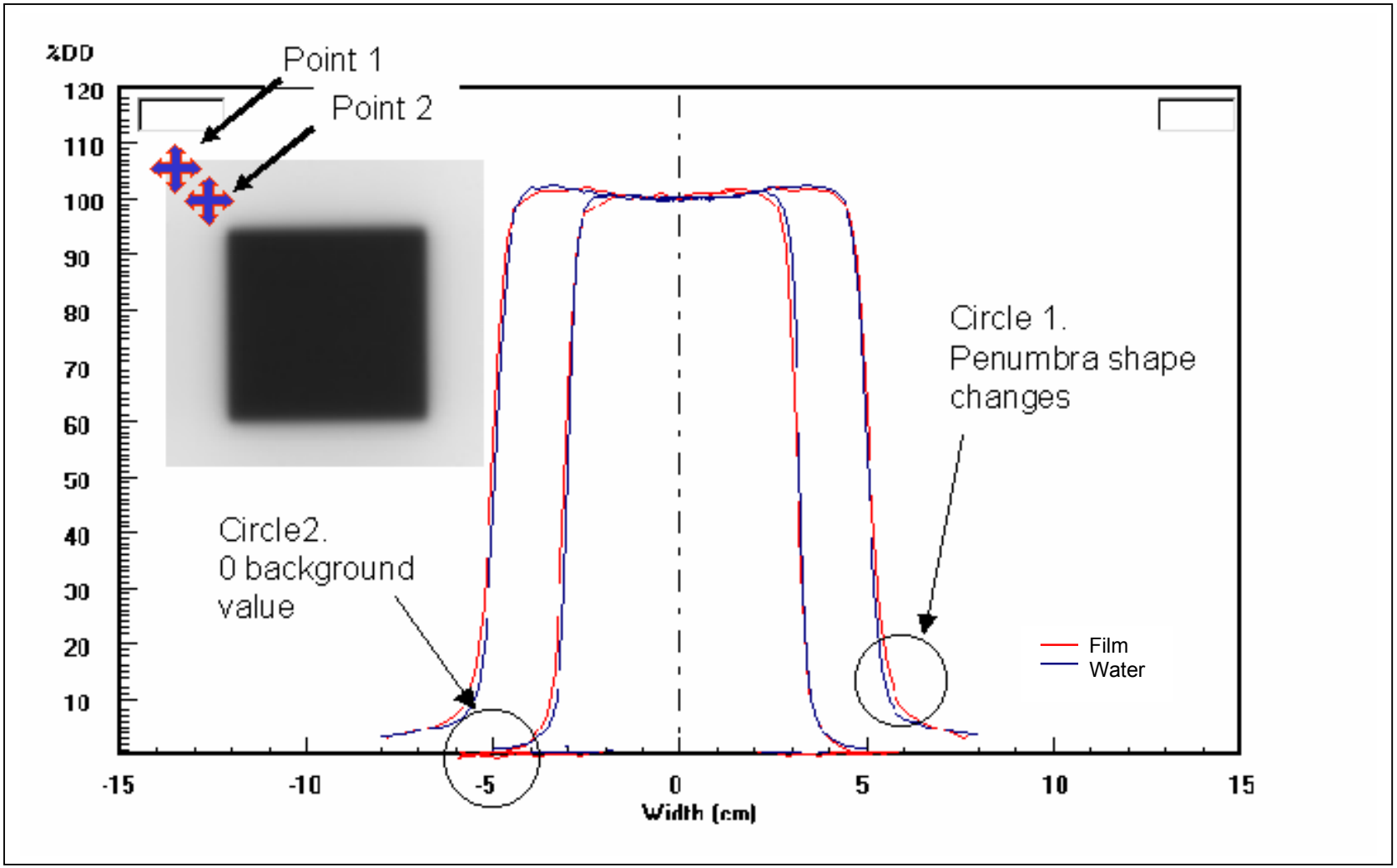

Figure 12.1. *Comparison of profiles for 5MeV Electron beam obtained using film and water scans when the background fog value is evaluated from the same film outside the irradiated field. Circles 1 and 2 show the discrepancy in the penumbra regions when Points 1 and 2, respectively, are used to obtain the background value.*

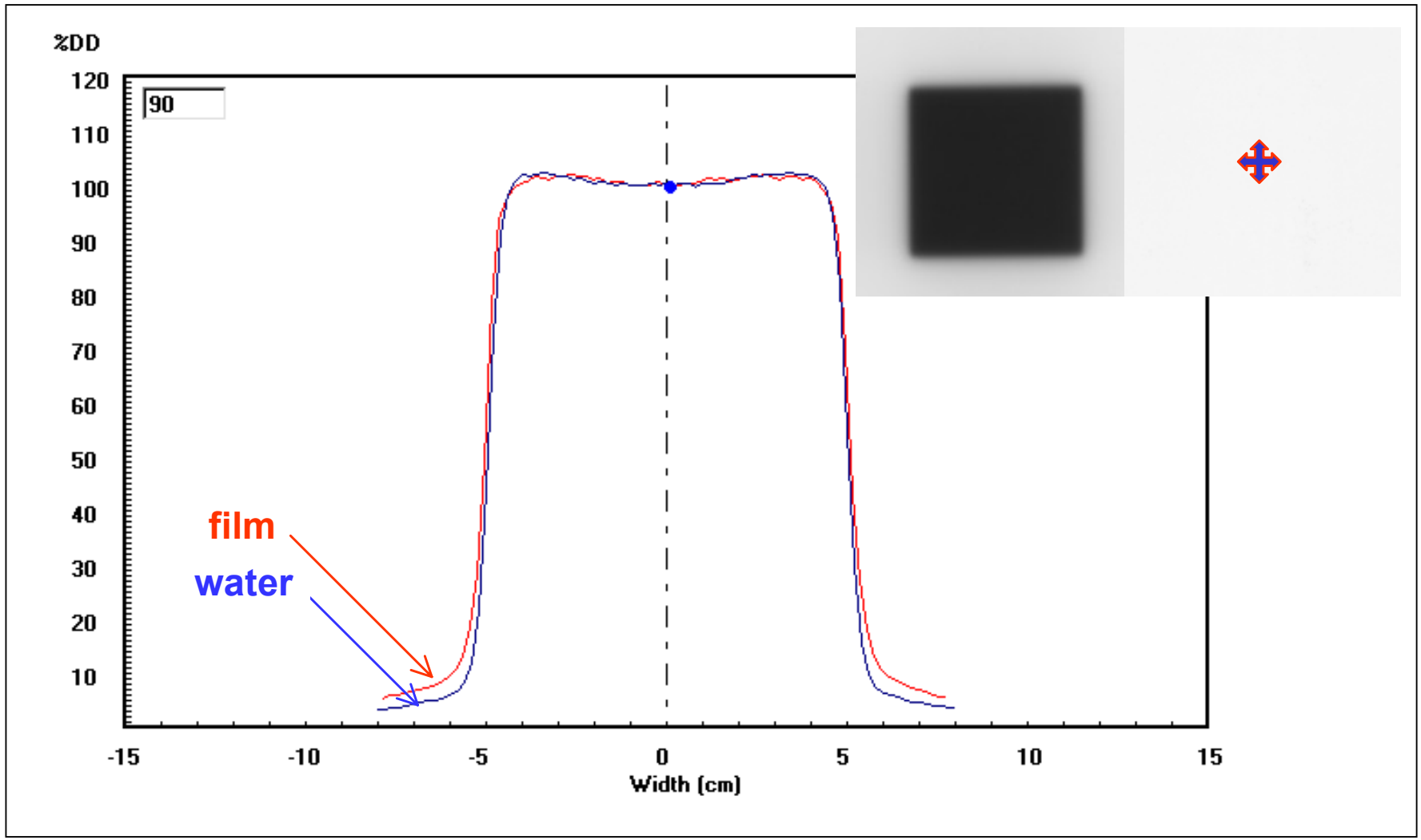

Figure 12.2*Comparison of profiles 5MeV Electron beam obtained using film (desktop scanner) and water scans when background fog values are subtracted using a separate background film (Equation 1).*

Computer desktop scanners enable us to perform a pixel-by pixel background subtraction using a separate background film from the same package, which is developed at same time as the irradiated film. The apparent dose outside the field edge obtained using this technique often appears unexpectedly higher compared to the in-water ionisation scans. Figure 12.2 shows the film profile analysis using background subtraction resulting in a background value of 3-5% higher than for water scans. This is especially evident in the penumbral tail region.

The purpose of this investigation is to achieve more accurate film dosimetry results by taking into account the unexpected background. In considering a corrective method, it is first necessary to examine the origin and nature of the radiation producing the background. Some possibilities suggest themselves and give guidance on the experiments to perform.

The first possibility to consider is that of visible light being produced by electrons in the medium, thus increasing the darkness on the film emulsion (Cerenkov effect). In 1969 Dutreix and Dutreix reported a 5% increase in OD due to Cerenkov radiation (Jelly, 1958). on a bare film exposed in a transparent Lucite phantom. Cerenkov radiation was first discovered by Mallet in 1926 and studied by Cerenkov from 1934 – 1938 It can be summarised as a high velocity charged particle moving through a dielectric medium causing local, non-isotropic polarisation in the atoms of the dielectric. These atoms return to normal states by emitting a blue visible light. This light can be destroyed if the particle velocity becomes less than light's phase velocity in the medium, otherwise the light remains due to constructive interference. It has been reported that if a bare film is exposed in a transparent medium, some additional blackening arises due to Cerenkov radiation.

The second possibility to be considered is that due to interactions producing characteristic x-rays or Auger electrons. The probability of producing a K-shell characteristic photon (the fluorescence yield) is defined as

ω_K = (Number of K x-ray photons emitted) / (Number of K shell vacancies)

and (1-ω_K) is then the probability of emitting an Auger electron. For tissue-equivalent materials the K-shell binding energy is about 0.5keV. Any resultant characteristic radiations will be locally absorbed, thus not contributing to the measured dose profiles. For the silver atom (Z=47), the K-edge is 25.5keV and ω_K is 0.82 (18% of interactions produce Auger electrons). The film emulsion will locally absorb the low kerma characteristic x-rays and Auger electrons thus contributing to the observed increased background as compared to ionisation profiles measured in water.

12.2 Experiments

Material and method

The change in optical density produced by irradiating stacks of film as compared to a single film is used to determine whether the Cerenkov effect, characteristic X-radiation or Auger electrons could be responsible for the enhanced background observed in film dosimetry.

Strips of Kodak X-Omat V verification film were cut in the darkroom to a strip size of about 5cm x 10cm each. All strips including the background strip had similar exposure to the safe light. The filmstrip packs with their appropriate inter-leaving were sealed in black paper wrapping. The packs were irradiated in a 30cm x 30cm solid acrylic slab phantom at the d_{max} build-up depth for each beam type and energy. A field size of 10cm x 10cm was used for both the electron (5MeV, 7MeV, 9MeV and 12MeV) and 300kV (3.5mm Cu) x-ray beams with 100cm SSD for the electron beams and 50cm FSD for the x-ray beam. A dose of 20cGy was given for each exposure for both electron and x-rays. This dose value was chosen to be within the linear region of the film's optical density to radiation dose response characteristic curve. In the darkroom, the irradiated filmstrips were attached to a piece of header film with metallic polyester tape and then fed through the automatic processor for simultaneous development.

Four experiments where using X-rays and electron beams devised to determine the characteristics of the observed enhanced background effect. (Figure 12.3)

- Experiment 1 irradiates film strip stacks placed at d_{max} in a solid phantom. The stacks comprise 1,2,3,4,5 and 6 films and are exposed with same dose. The optical density readings for each stack are compared. Electron were used to study the energy dependence of the effect.
- Experiment 2 was a repeat of the first experiment but with a piece of black paper inserted between each of the filmstrips in stacks of 2,3,4,5 and 6 films. Exposures were made using 5MeV electron and 300kV (3.5mmCu) photon beams. Inserting a piece of black paper in between the filmstrips tests whether visible light contributes to the optical density readings on the film.
- Experiment 3 also tests for visible light by exposing stacks of 6 films and comparing, the readings between stacks of film only, black paper inserted between films, and overhead transparency sheet inserted between films. A 300kV (3.5mmCu) x-ray beam was used for the exposures.
- Experiment 4 compared a single film with a stack of 6 pieces of black paper on top of a film to determine whether the scatter is coming from the original beam, the build up medium or from the film itself.

An X-rite 331 film densitometer was used to read the exposed filmstrips. Three measurements were made for each film in a stack. The background fog value was determined from an unexposed filmstrip, which was cut from the same film and developed together with other strips. For comparative purposes, optical density readings were also taken using the densitometer from a large volume water tank dosimetry system (Scanditronix RFA300). The average reading of each filmstrip pack was processed and plotted as trend charts in MS-Excel. The optical density readings were rescaled by the value read from the single film stack. Exposures and readings for the 6-filmstrip stack were repeated as a reproducibility check.

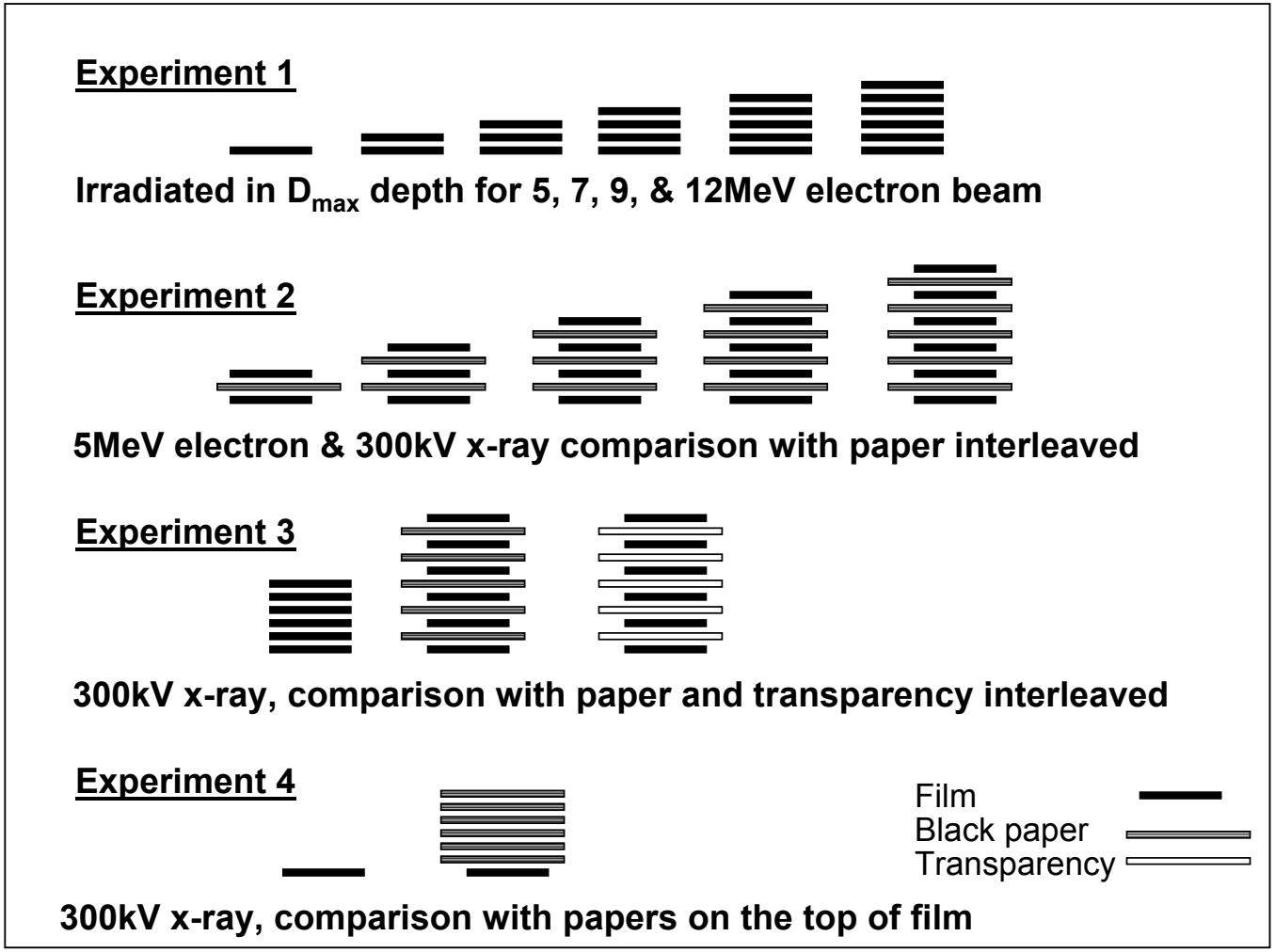

Figure 12.3 *Experiments to determine the characteristics of the observed enhanced background effect using a series of film strip stacks interleaved with black paper and overhead transparency sheet. All stacks are irradiated to 20cGy at d_{max} in a solid acrylic phantom.*

Results

The results of Experiment 1 are shown in Figure 12.4. Optical density (OD) readings for the stacked films were averaged and then normalised to the single film reading. Normalised OD readings were plotted against the number of filmstrips in a stack for each energy. The charts show an increased sensitivity to perturbation as the beam energy decreases, and an increased sensitivity from the thicker film packs (stack number) for each energy. With increase in energy the stack number dependence becomes less pronounced. The observed increase in OD with increasing film stack number indicates that there is a scattered radiation produced in the films, which creates an increased dose response in adjacent films. The energy dependence of the OD increase is consistent with the production of characteristic and Auger radiations rather than Cerenkov radiation.

The results of Experiment 2 are plotted only for the 5MeV electron beam since this energy exhibits a sensitive response. The 300kV chart produces a similar curve shape. Figure 12.5 shows a film stack comparison between bare film in the stack and films interleaved with black paper irradiated with exactly the same set-up and dose. The differences between the two curves are significant. The scatter from neighbouring films is almost completely absorbed by a single piece of black paper. This indicates that the scatter is either visible light or a very low energy radiation.

The 300kV beam results from Experiment 3 are shown in Figure 12.6 in which OD readings for the individual films in the 6-film stacks are plotted for the different packing configurations. The chart values 1 to 6 for the abscissa relate to the position of the film in the stack, with Position 1 being the topmost and Position 6 being the bottom film in the stack. A significant increase in response (~20%) is observed in the stacks with bare film as compared to the interleaved films, indicating that the scatter is absorbed in the paper and transparent sheet. There is only a little difference in response (~2%) between the film stacks interleaved with black paper and those with transparent sheets. This result strongly suggests that visible light is only a small component of the excess scatter observed. In all cases there is reduced response in those films at the top

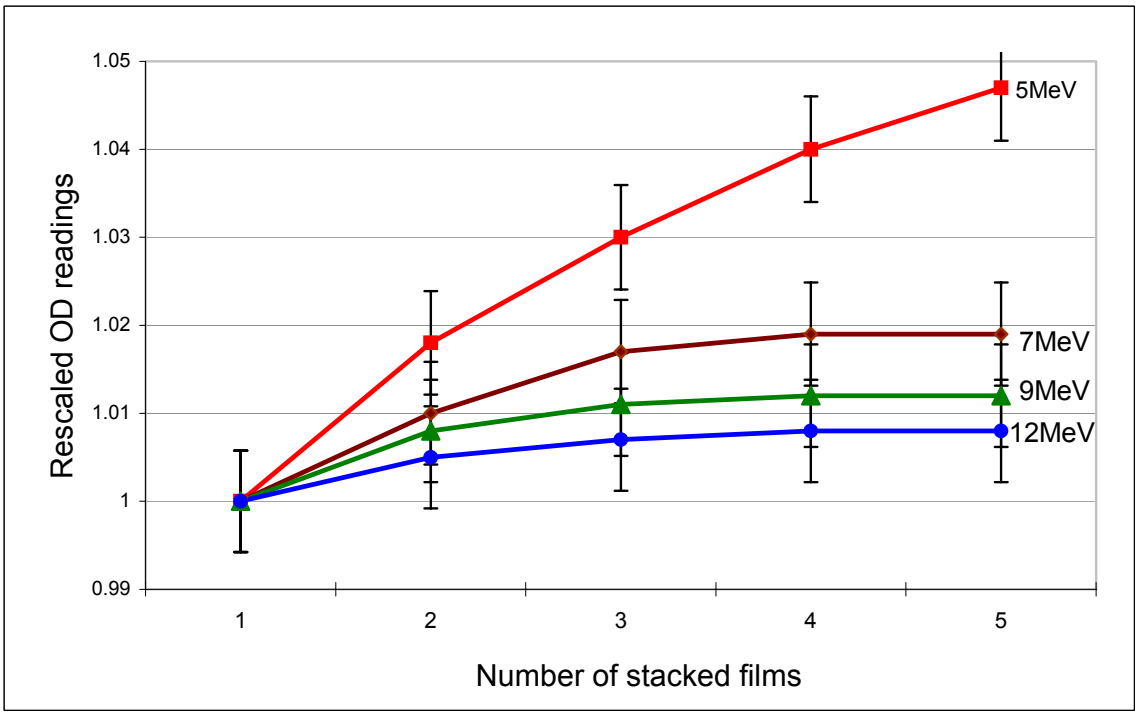

Figure 12.4 *Results of Experiment 1, the effect of the number of filmstrips per stack and electron beam energy on average optical density. Ratio of OD reading / OD 1 film stack*

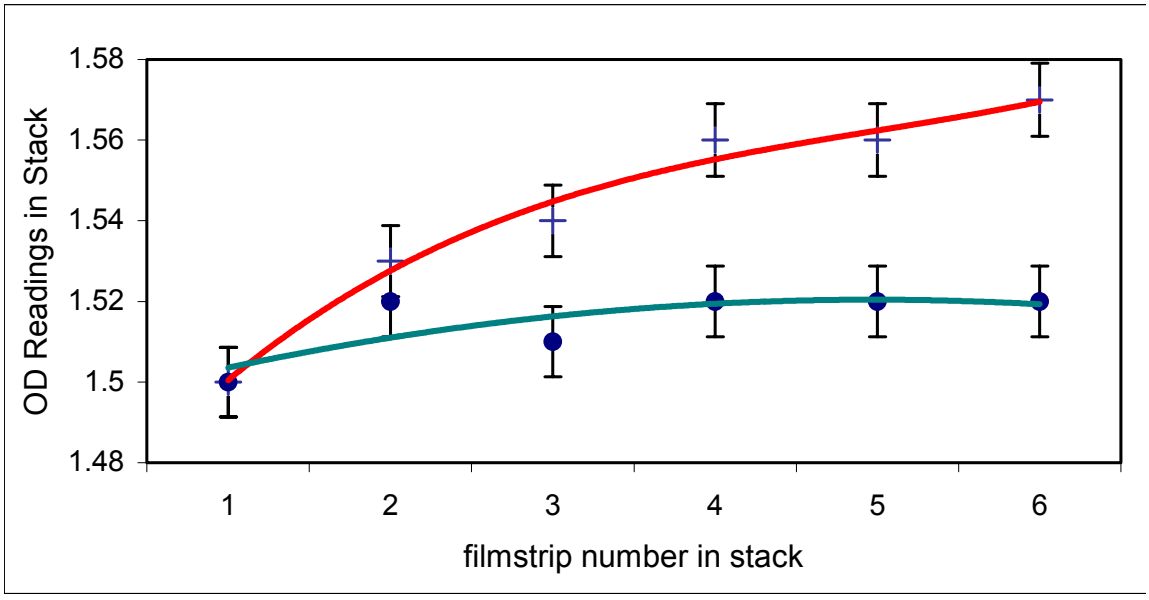

Figure 12.5 *Results of Experiment 2, the effect of inserting black paper between the filmstrips in the stack on the optical density of each filmstrip. The mean error range is calculated as ΔOD ±0.01, estimate as 0.01/√n (n – number of readings repeated in stack*

(Position 1) and bottom (Position 6) of a stack. This result shows that the filmstrips on the outside of the stack were less perturbed than the strips in the middle. Positions 2 through 5 show similar OD values. The scatter then appears to be isotropic in direction rather than backscatter or forward scatter. Films in the centre of the stack receive a flux from two sides while those at the edge receive a flux from one side only. *(Figure 12.6)*

There was no OD reading difference between the single bare film and the single film with 6 sheets of black paper placed on the top of the film in Experiment 4. This result indicates that the observed OD increase is not created by the overlying material but rather is the result of the beam interacting with the surface of the film.

The processing and polynomial curve fitting maximum error range is $\pm$2%. Since the average trend values are steadily reproducible, the noise interruption is considered negligible.

12.3 Enhanced background correction technique

An empirical approach can now introduce to determine an additional correction term to apply for background subtraction in film dosimetry. A common technique for background correction in film dosimetry using a desktop scanner is to subtract the background fog values obtained from a separate unexposed film on a pixel-by-pixel basis. The corrected optical density value is determined by:

$$OD_{corrected} = OD_{reading} - OD_{background} \quad (1)$$

where $OD_{reading}$ is the measurement optical density reading and $OD_{background}$ is the optical density reading at the same position for the unexposed film.

As shown in Figure 2, this simple subtraction technique results in an over-prediction of dose outside the field edge by 3-5% as compared to water scanning results.

In the new procedure as well as a separate unexposed background film, a single and a dual strip package is exposed immediately after the film and to the same dose. The effect of the additional scattered background is incorporated into a total correction term according to the expression below.

$$OD_{corrected} = OD_{reading} - \{OD_{background} + (OD_{single} - OD_{dual})\} \quad (2)$$

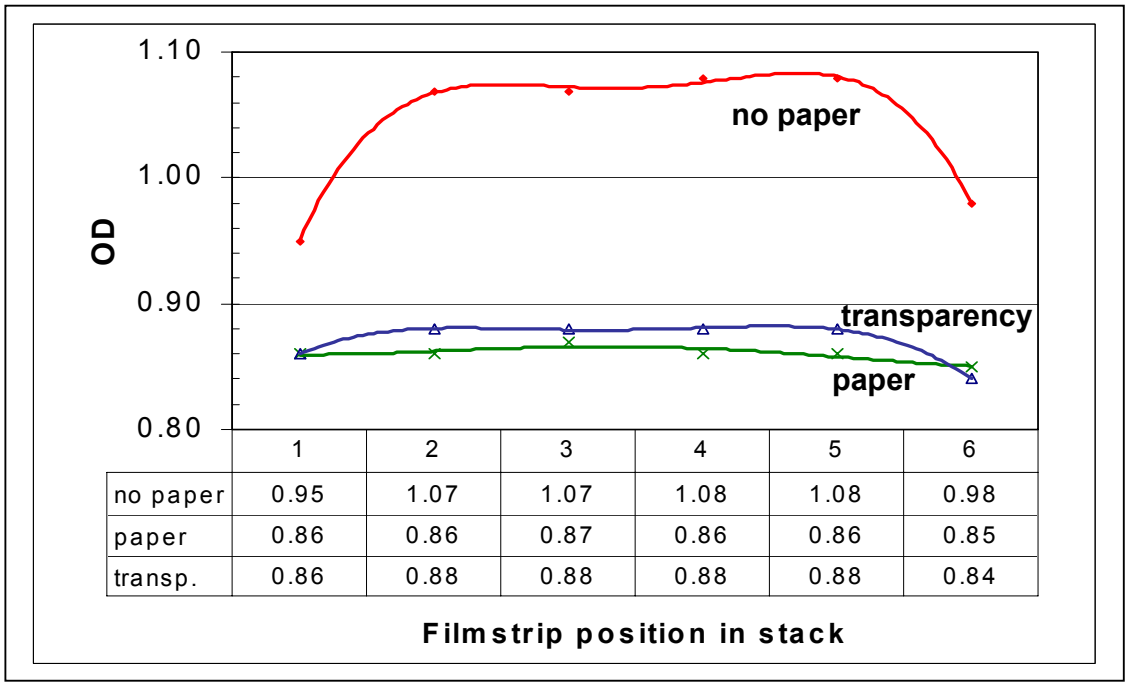

	1	2	3	4	5	6
no paper	0.95	1.07	1.07	1.08	1.08	0.98
paper	0.86	0.86	0.87	0.86	0.86	0.85
transp.	0.86	0.88	0.88	0.88	0.88	0.84

Figure 12.6 *Results of Experiment 3 (300keV), the effect of inserting black paper and overhead transparency sheet between the filmstrips in the stack on the optical density of each filmstrip.*

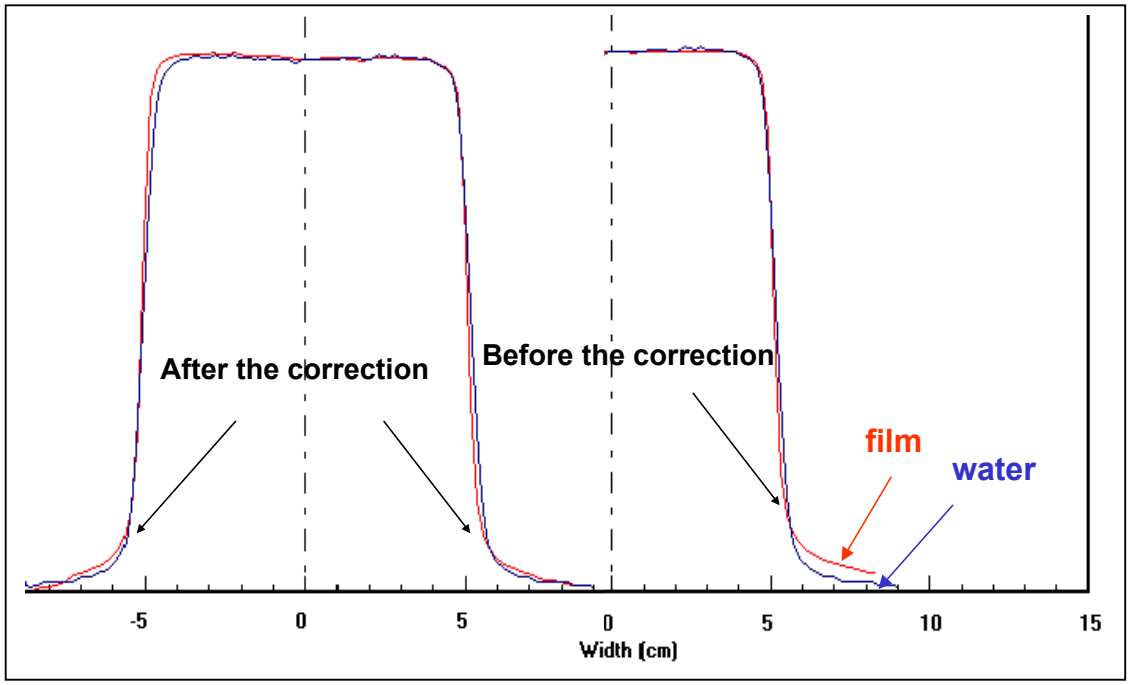

Figure 12.7 *Comparison of 10MV X-ray profiles obtained using film (desktop scanner) and water scans before and after applying the additional background subtraction term to the film analysis (Equation 2).*

where OD_{single} and OD_{dual} are the average optical density readings for the single and dual film test strip packages respectively.

Equation 2 has been applied in an implemented as part of an in-house developed software package. Figure 7 shows the improvement in beam profile matching with this extra correction term.

12.4 Discussion

Our experiments clearly show that the measured dose outside the field edge is of the order of 3-5% higher in film dosimetry than for in-water ionisation scans. These also show the following characteristics of the radiation producing the increased background values:

- Intensity decreases with increasing beam energy
- Low energy radiation absorbed in both opaque and transparent media
- Emitted in all directions
- Created in the film, not the phantom

These contrast with the characteristics of Cerenkov radiation which increases in intensity with particle energy, is a form of visible light (therefore not absorbed in transparent media) and is emitted in a forward direction.

Figure 12.6 shows that the experimental results indicate that low energy secondary radiations such as characteristic x-rays or Auger electrons. Dominate effects due to visible Cerenkov radiation, since we would consider a significant contribution of the Cerenkov radiation should be produced in the phantom material. If so, the film seems unlikely that it is responsible for the observed dose increases where the film used is sealed in an opaque packet. The results of Experiments 2 and 3 indicate that a small proportion of the radiation absorbed by a sheet of black paper is transmitted through the transparent medium and may then be visible light. The determination of the spectral characteristics of this radiation would require a more detailed study with sophisticated instrumentation.

12.5 Conclusion

This study has shown that there is an additional source of radiation background influencing the results of film dosimetry. The low intensity, energy dependent background has been revealed through the digital analysis to film dosimetry. Only a small component, if any, of this can be attributed to Cerenkov radiation. The characteristics of this background are consistent with low energy secondary radiations produced in the film. Further study is required to quantify its spectral characteristics. The methods suggested by this study can improve the film dosimetry accuracy is shown by the profile curve penumbra and tail regions, it is relatively improved by incorporating an additional term in the background subtraction formula to account for this effect.

Chapter 13 Dynamic Radiation Field Film Dosimetry

13.1 Introduction

Dynamic treatment fields include photon and electron arc-therapy technique, dynamic wedge field, stereotactic isocentric rotation field, dynamic multi-leaf conformal treatment and intensity modulation radiotherapy (IMRT) treatment techniques. Since water scanning techniques cannot currently be used for the dynamic field dose distribution measurement, dynamical field dose distribution is measured by ionization chamber dosimeter measurements or by comparison with Monte Carlo calculations. The planning dose distribution quality assurance is commonly carried out by ionization point dose measurements, TLD readings, film dosimetry or gel dosimetry.

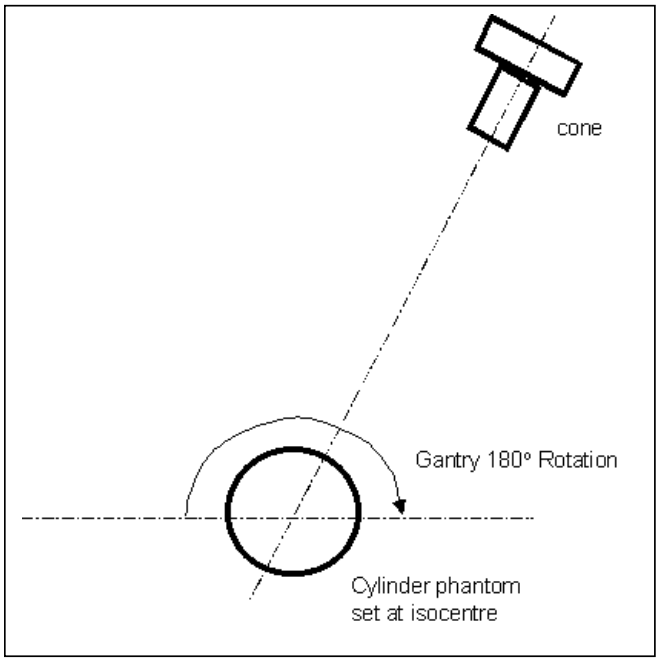

Figure 13.1 Cylindrical plastic phantom set up for the stereotactic treatment field checks.

Ionization measurements can only be performed at a few points as part of a dose check. The accuracy of measurements in small stereotactic or multi-leaf conformal fields can be influenced by the fact that the air cavity of the ion-chamber occupies part of the target region. The measurement effective point,

d, in the small beam could also be influenced by a rotated exposure. So, the calibration of ion-chamber measurement can become unreliable.

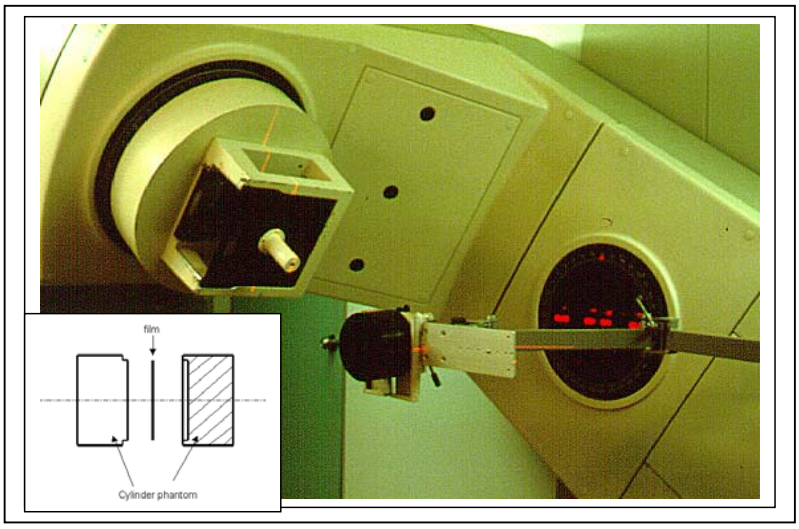

Figure 13.2 Film sandwiched in plastic cylindrical phantom and isocentrical setting for the linac checks Cylindrical

TLDs can be used take more simultaneous point readings, but the dose distribution check is rough and time consuming to perform.

Three-dimensional dosimetry using polymer gel and magnetic resonance imaging applied to the verification of conformal radiation therapy in head-and-neck cancer, has developed as an alternative IMRT dosimetry technique to film and TLD. (Lbbott etc, 1997; De Deene, De Wagter, Van Duyse, Derycke, De Neve and Achten, 1998) Special developed Polymer Gel material can be fitted into different shaped cavities inside a body inhomogeneity phantom. The electron density of this Gel material can be checked by the phantom CT scan to simulate complicated IMRT conformal planning and treatment. The Gel material is designed to be sensitive to the radiation beam and change in colour and transparency due to the radiation dose. However, the current technique still has a high uncertainty and the gel technique is still not mature enough to be used clinically.

The film dosimetry technique currently is the easiest way to use to visualise the dose distribution. The film can be set in phantom at different angles to the beam direction. However as we have seen the film has it own complexity and

limits. Firstly, for these special treatment field checks, the phantom needs to be designed and machined properly for the film set up. Secondly, the verification film has a non-linear dose response and is energy dependent. The goal of this study is to develop a film dosimetry technique for dynamic radiation fields which is both reliable and reproducible.

In this chapter two investigations are presented:

- QA assurance procedures to determine the isocentre and wedge dosimetry in a dynamic radiation field
- Dynamic Field and 3D Planning Checks using a Spherical Phantom

13.2 Quality assurance (QA) procedures to determine the isocentre and wedge dosimetry in a dynamic radiation field

Method

Kodak X-Omat XV-2 film is used for the initial experiments. Since 2001, Kodak EDR-2 film became available from the market with higher density dynamic range and with good linearity up to 3.0. Later experiments, especially the IMRT planning QA checks, have used EDR-2 film for the isodose reconstruction test.

Film dosimetry was undertaken in the following dynamic radiation situations:

- A dynamic wedge using a photon field
- A star-shot of a small sized isocentric field for photon beam.
- 180^{o} gantry rotation field isodose distribution

In each case the film was set in different specially designed phantoms such as solid slab, water tank, and cylindrical plastic etc. as described in Chapter 11. The film was exposed to different beam types and energies generated by a linear accelerator. Exposed film was developed using automatic film processor and the film was scanned using a computer desktop scanner with transparency light source adaptor. The scanned image was saved as Windows bitmap file and loaded into the film dosimetry program interface, which was specially developed for this project.

The dynamical wedge field profile check was performed with the film using solid slab phantom either perpendicular or almost parallel (at a very small angle) to the beam direction. The profile for different build up depths was analysed. The photon beam arc therapy field and a stereotactic field dose distribution were checked by setting the film in the cylindrical plastic solid phantom (Figure 13.1) and the film was cut into a circular shape (Figure 13.2).

The GSV - Dose calibration was obtained, as previously, by using strip-films in a slab phantom with 10cm x 10cm field 100cm SSD and d_{max} build up depth. A control film with the same film strip set up was taken when the testing exposure was performed.

Three films were used for each film dosimetry measurement:

- A test film for the field measurement
- A control film for the existing OD-Dose response curve range calibration.
- An unexposed film, developed with test film, using the same film processor for scanning background value correction.

The RODOMS film dosimetry software developed for this project analysed the image GSV obtained over the film area. Each pixel value read from the image is subtracted by the corresponding pixel value read from the background film; the pixel value is converted into an equivalent dose value by interpolation using calibrated OD-Dose response curve. Then a re-normalisation function is performed to calculate the equivalent dose value into the percentage dose value for each pixel. The percentage dose value over the image area is then traced by isodose tracking function to process the isodose curve. The profile curve (or percentage depth dose curve) for both cross-plane and in-plane directions can then be investigated by the user shifting the mouse over the image area.

The analysis function provides the parameterised result for the profile (or PDD) analysis result. The results and curves can be output to the graphic printer, saved to disk and retrieved later to the screen interface.

Results

Figure 13.3 and 13.4 show the different angles dynamic wedge measured for the Siemens 6MV photon beam 10cm x 10cm field size at 10cm build up depth. Since it is not possible to make a simple comparison with a water scanning result, the point dose ionisation measurement was compared and resulted in a +/- 1% discrepancy.

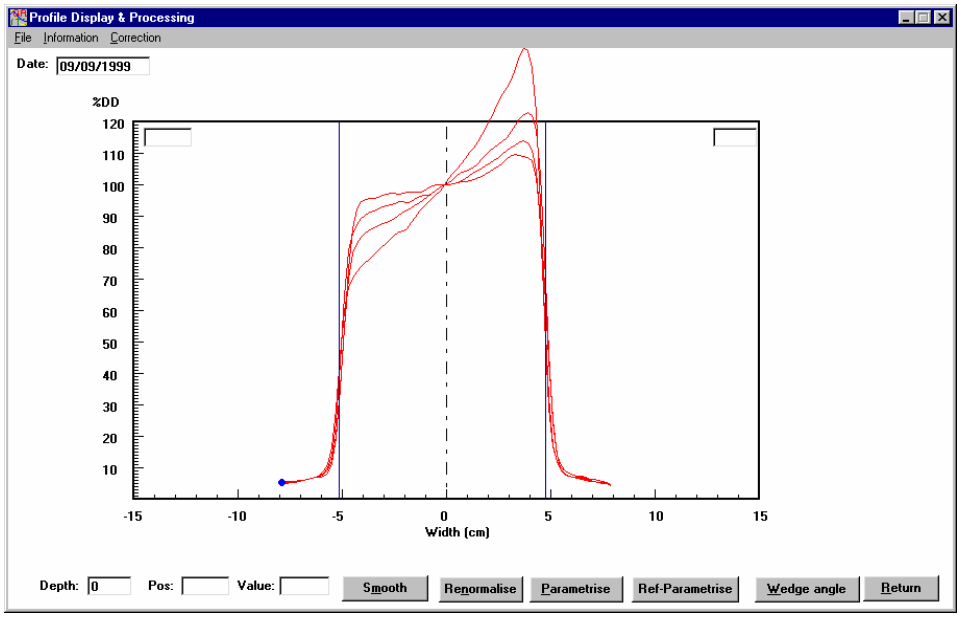

Figure 13.3 dynamic wedge field profile taken by film dosimetry 15°, 30°, 45°, and 60°

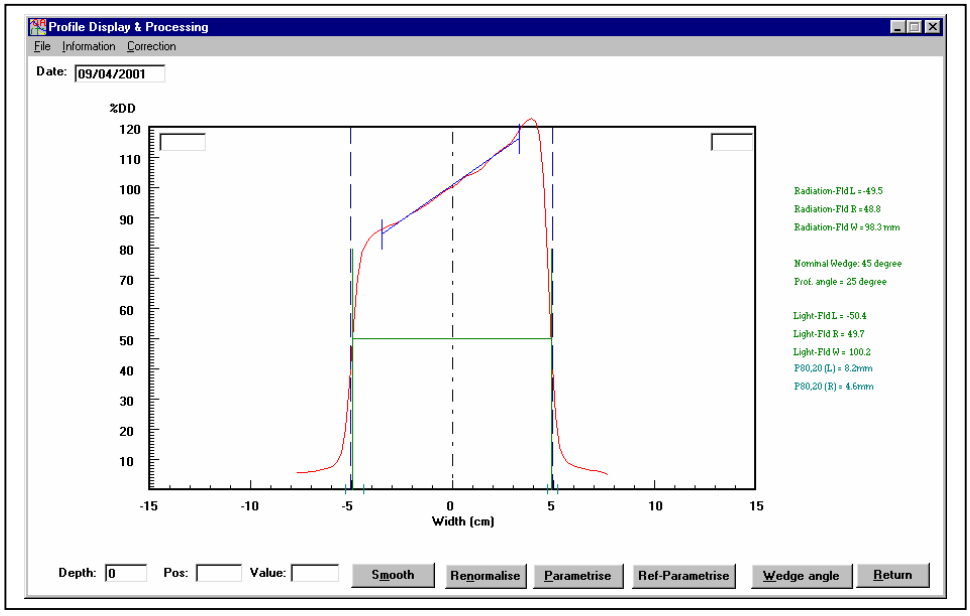

Figure 13.4 profile curve analysis for dynamic wedge field film dosimetry

Figure 13.5 shows a star shot of a small sized isocentric field to compare the beam rotation centre with the marks of the gantry mechanical rotation centre.

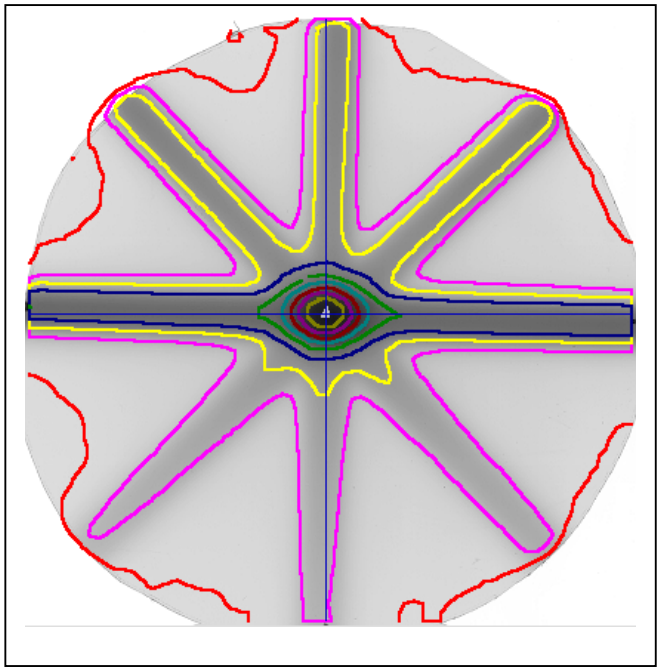

Figure 13.5 2.0cm diameter narrow beam star shot film isodose curve centre compared with gantry mechanical rotation centre mark.

Figure 13.6 shows the isodose distribution of a 2cm jaw open and 180^{o} gantry rotation field with the film was taken by using the cylindrical plastic phantom. The profile across the beam centre is also plotted.

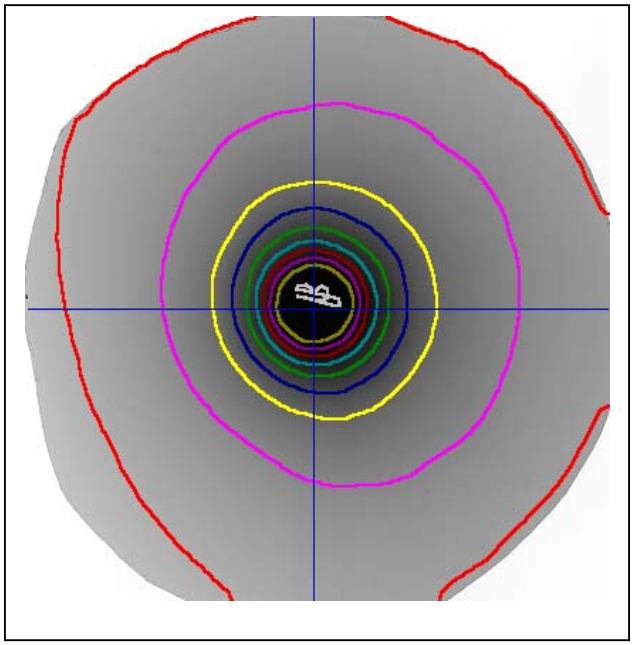

Figure 13.6 180^{o} gantry rotation 4cm jaw open field isodose tracking.

Discussion and Conclusion

The film analysis results give a significant improvement in reliability and reproducibility. In this study, we used several films to make one measurement test on film dosimetry dose distribution check.

The control film used for the optical density response calibration in this study is extremely important.

The film response to the irradiation dose is not linear, and the curve is curved at different exposure dose region. The film's GSV/Optical Depth depends on processing time or processing equipment. If simply use an existing OD-Dose response curve to perform the dose convert calculation, the GSV will give an incorrect dose.

Although three films are used for one film dosimetry measurement, compared with TLD or gel dosimetry results, the time efficiency, operation simplicity and cost are still significantly better. Compared with the ionisation measurement techniques, dose distribution can be easily visualised using film dosimetry techniques.

The film dosimetry performed in this study uses more than one film to perform one measurement. The calibration of OD-Dose response curve and full background value subtraction improve the reliability and reproducibility of the film dosimetry technique.

Since there are currently no mature techniques of dynamic treatment planning QA technique available to the clinic, the possibility of using film dosimetry is significantly improved by this study result. To make a greater possibility that film dosimetry is used for the dynamical field planning QA checks.

13.3 Dynamic Field and 3D Planning Checks using a Spherical Phantom

13.3.1 Overview

Work on the application of film dosimetry used for planning QA technology development discussed in 13.2 led to the development of a new film based technique for viewing the isodose distribution over a layer in a treatment

plan with different orientations. A special ball shaped phantom was designed for extended film dosimetry calibration performance. The phantom and software functions have been in clinical use since July 2002. This section will present the phantom design, experimental performance, calibration test, software functions and examples cases of clinical treatment planning tests.

Many techniques have been developed to deliver optimised treatment and in recent years we have seen the development of numerous three-dimensional dynamic techniques. Currently, dynamic wedges using multi-leaf collimators (MLC), three-dimensional stereotactic and intensity modulated radiotherapy (IMRT) beams are becoming more common in clinical use.

Compared with the traditional treatment techniques, the implementation of quality assurance procedures to the dynamical field, three-D plan and IMRT treatment techniques is more complicated. The ordinary measurement and scanning techniques are difficult to perform. As an example of IMRT, the quality assurance tasks include isocentric mechanical alignment, absolute dose measurement for three dimensional distribution fields in one plan, and evaluation performance for the hot/cold spot created by combined beam junction. Any treatment plan may involve combination of mechanical movement or multiple fields combined with different beam energies and different entry orientation. It is therefore not possible to simply use either point measurements or single scanning techniques to obtain QA information for routine purposes.

A combination of ionization measurement, TLD dose monitoring, and film dosimetry are commonly used in carrying out QA tasks. Most of these measurements can only be performed by using solid phantom. The design of such a solid phantom effectively is the common challenges to many QA study projects but particularly to IMRT QA.

There are many solid or water phantoms becoming available now for the IMRT QA (Figure 13.7). However, most of these are designed for either point dose measurement or fixed orientation of film settings. Although some phantom designs have combined film and ionization set up, there are no

successful ways to perform a relative calibration between the point absolute dose and film iso-density. The new EDR-2 film product provides higher dose response, dynamic range and better signal linearity than previous films, making the film dosimetry easier to perform for quick dose distribution checks.

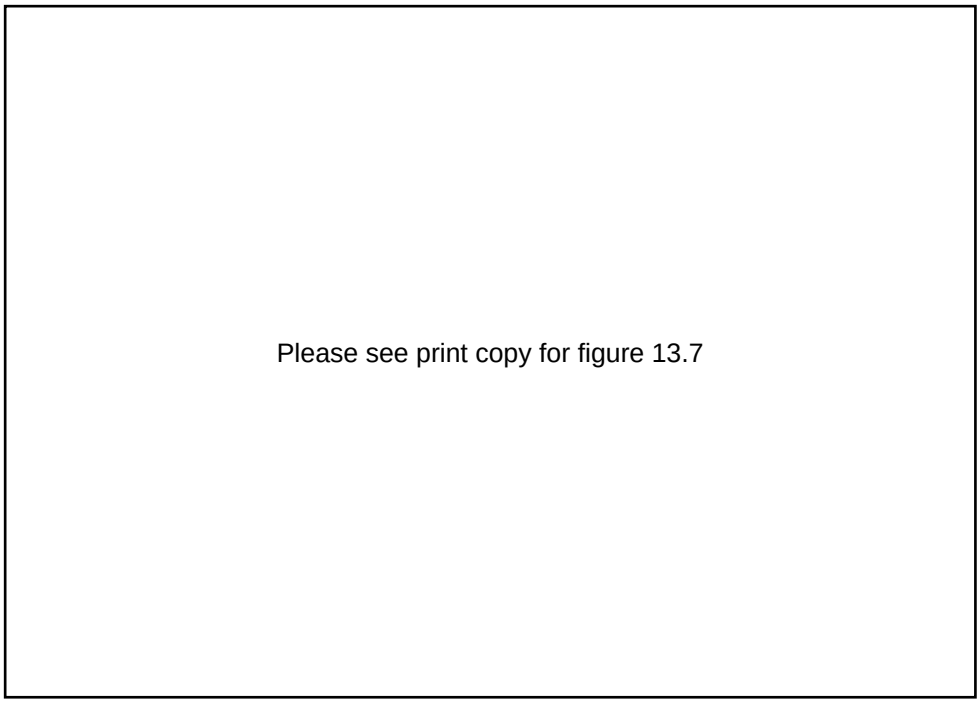

Figure 13.7 Some IMRT QA Solid phantom on the market in 2003

However, there are still a few problems to be solved such as the need to set up the film accurately in three dimensional orientation and the orientation of the film for different beam entry angles, designing a phantom with a build-up to reflect the real dose distribution for a 3-D treatment plan.

13.3.2 Experimental design

A ball shaped phantom was developed in order to combine the measurement in 3-D dose distribution using film dosimetry techniques, TLD technique, and ionisation dosimetry technique. (Figure 13.8, 13.9, 13.10, 13.13) Isodose analysis software for film dosimetry was developed to accept, analyse and generate results from the three dosimetry techniques.

The solid ball shaped phantom consist of two separate hemisphere shapes with three disk replaceable central holders which swap the disks in the middle position without changing the ball outline diameter and shape but changing the holder for use with an ionisation chamber, TLD rod chain and a circular shaped film cassette. The design is intended to allow the following:

1. Isocentric absolute dose calibration using standard absolute dose calibration according to IAEA and ACPSEM protocols.
2. Calibration using a TLD carrier of by ionisation chamber calibration
3. Use of TLDs distributed in a different shapes and orientations to perform not only the point dose checks, but to be able to provide equivalent curve information such as depth dose and profile curves.
4. Simpler set up of film in a range of different orientations relative to the isocentre
5. Combinations of Ionisation chamber, TLD, and film dosimetry techniques to be able to check, alignment, and calibration against each other.

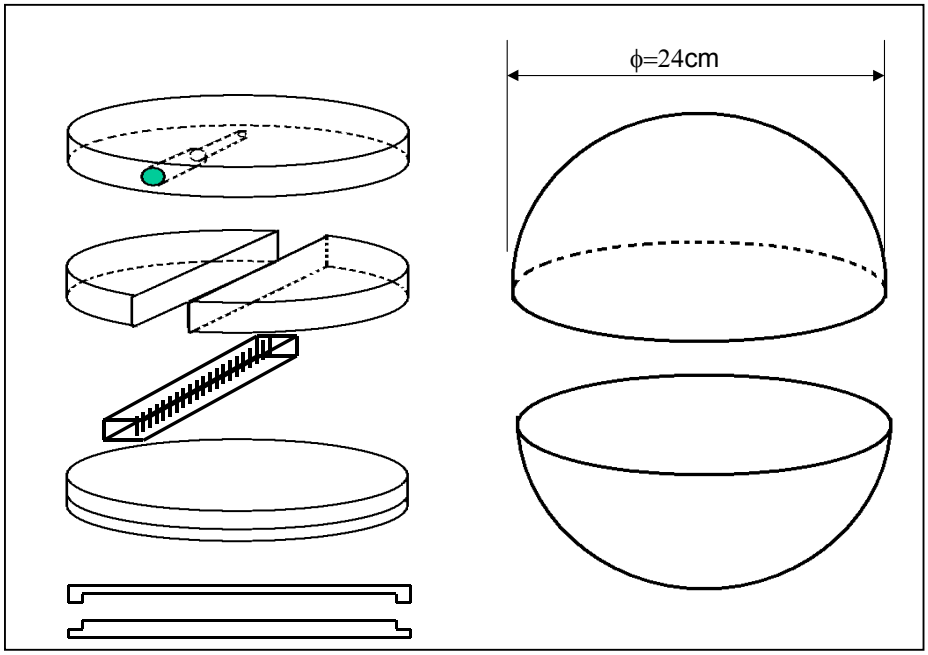

Figure 13.8 Ball shaped phantom combined for ion-chamber setup, TLD setup and film cassette

Additional isodose analysis software was developed to support the film dosimetry in this study.

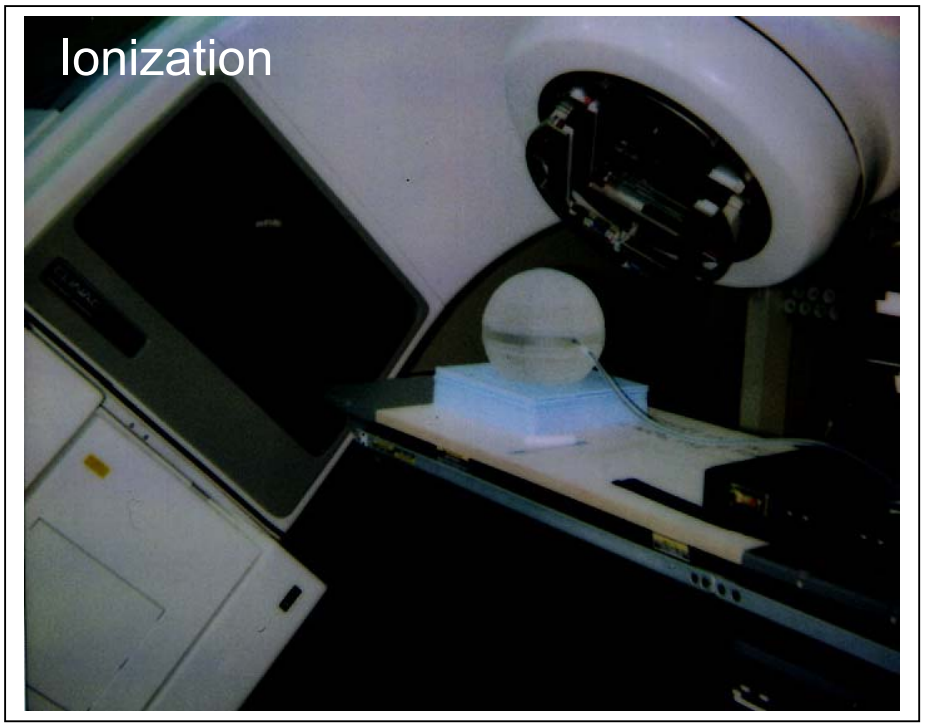

Figure 13.9 Ball phantom Ionization measurement set up.

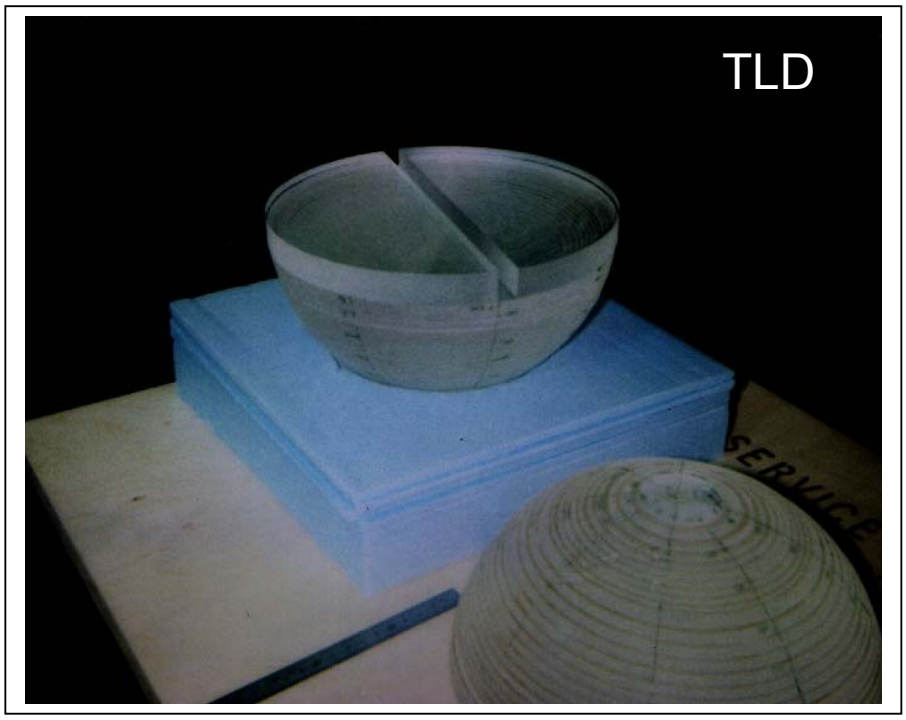

Figure 13.10 Ball phantom TLD measurement set up.

Figure 13.11 Ball phantom Film disk setup with different angle in three-D orientation.

13.3.3 Calibration procedures and early test results

The following experiments were performed to compare the dose measurements from ionisation chambers, TLDs and film using the spherical perspex phantom:

Ionisation Chambers:

1. An ionisation chamber was inserted into the spherical perspex phantom and the water equivalent depth of phantom surface to the ion-chamber's effective centre for different angles was calculated.
2. The ionisation measurement dependence on beam angle was studied by comparing measurements made at different gantry angle settings to the phantom centre (table 13.7)

Table 13.7 Spherical Phantom Ionisation Measurement Gantry Angle dependence

Gantry Angle	average reading	Deviation (%) from average
0	9.350	0.96
5	9.300	0.42
10	9.300	0.42
15	9.317	0.60
20	9.300	0.42
25	9.300	0.42
30	9.250	-0.12
35	9.200	-0.66
40	9.200	-0.66
45	9.233	-0.30
50	9.250	-0.12
55	9.200	-0.66
60	9.200	-0.66
65	9.283	0.24
70	9.250	-0.12
75	9.250	-0.12
80	9.250	-0.12
85	9.267	0.06
90	9.250	-0.12
Maximum	**9.350**	**0.96**
Minimum	**9.200**	**-0.66**
Average	**9.261**	**0.00**
Standard Deviation	**0.046**	**0.50**

After isocentrically mounting the ion-chamber perpendicular to the beam, the gantry angle is rotated around the ion-chamber axis, and the dosimetry readings compared for different angles and different coordinates. A better than ±1.0% standard deviation was observed indicating that the phantom quality is acceptable for subsequent QA use.

3. Absolute dose calibration for the phantom was performed using water tank measurements, solid slab phantom measurements and ball phantom measurement in order to calibrate the phantom scatter factor for the ball (Figure 13.12). these measurements provided:
    - Calibration of the different scatter factors between water and solid slabs.
    - Comparison of isocentric dose measurements ball and slab phantoms to calculate the phantom scatter factor for the ball.
    - Measurement of the output factor which include both phantom scatter and collimating scatter to the ball for different field sizes.

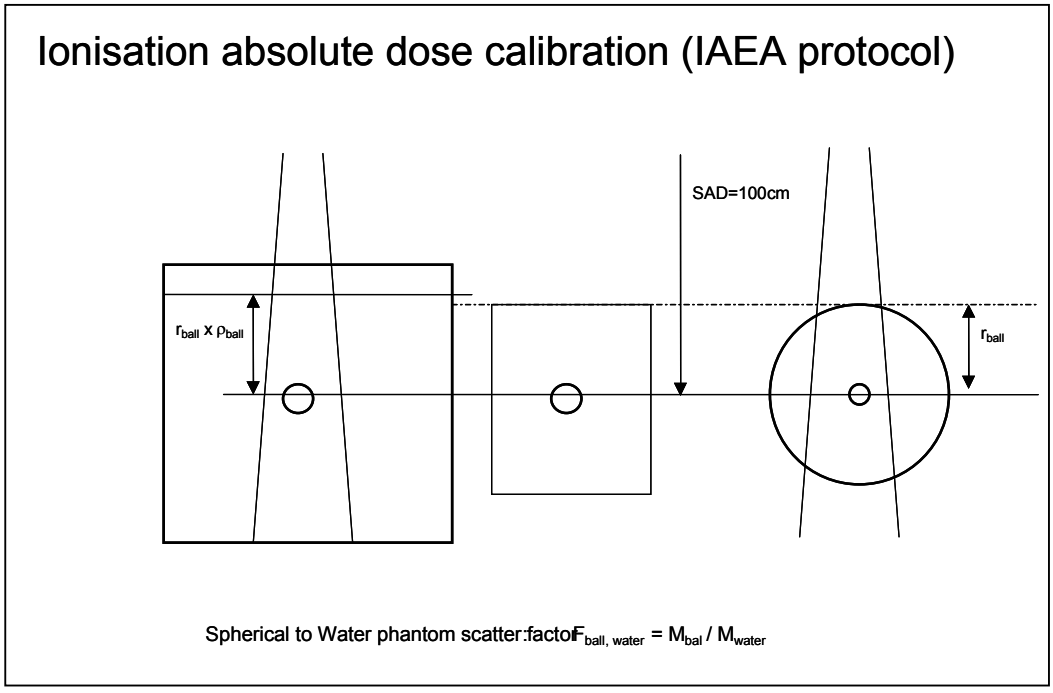

Figure 13.12 Absolute dose calibration and phantom scatter factor measurement

TLD measurements:

The spherical phantom was designed to take a TLD rod carrier which was used to:

- Calibrate TLD rods at ion-chamber effective point by giving calibrated doses and making individual sensitivity correction factors (Figure 13.13).

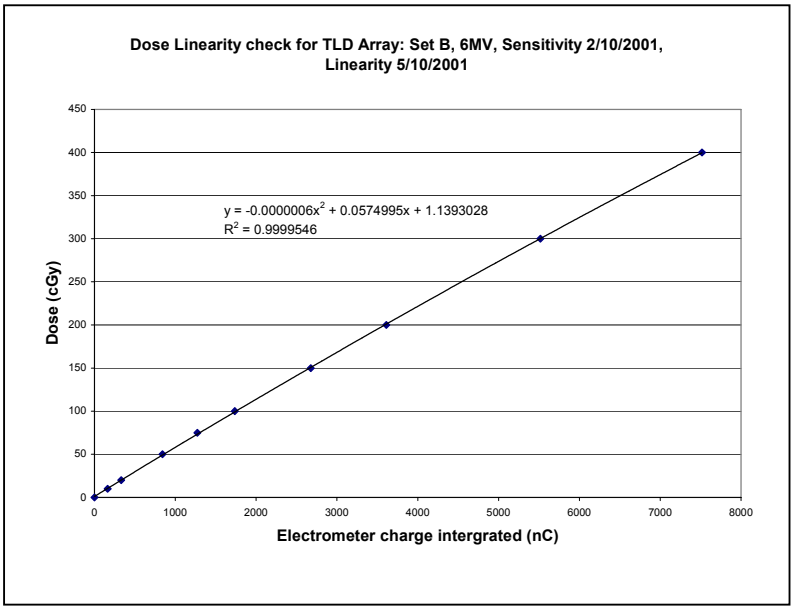

Figure 13.13 TLD measurement calibration and dose linearity

- Undertake a gantry angle dependence check of TLD readings and calculate phantom correction factors. ((Figure 13.14 and 13.15)

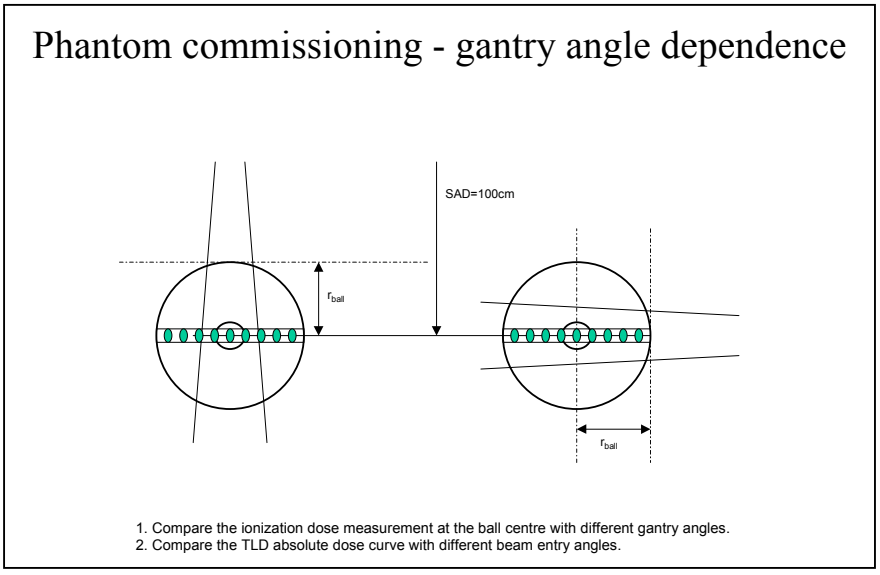

Figure 13.14 TLD reading gantry angle dependence check

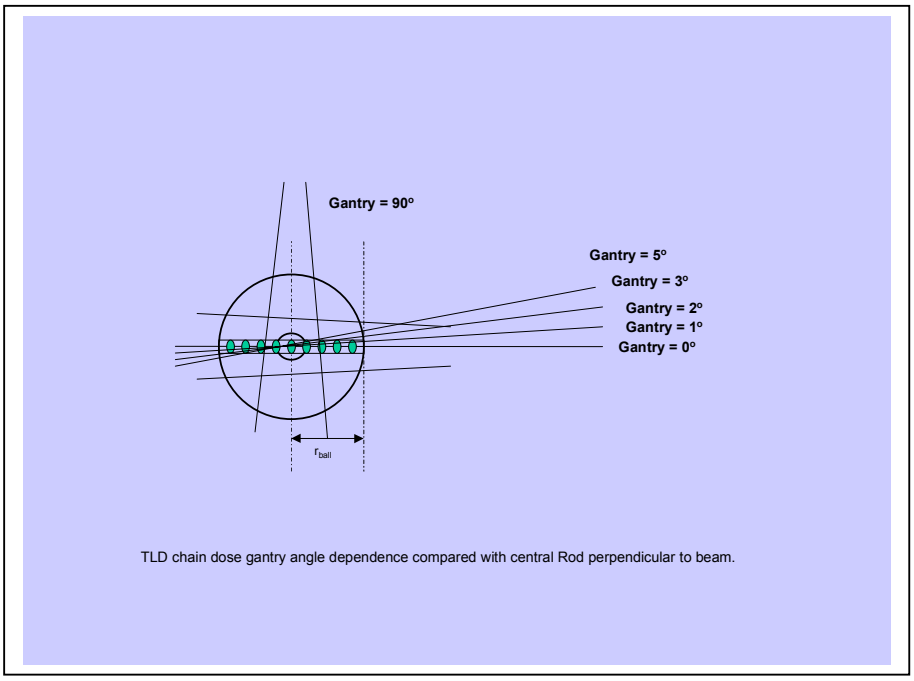

Figure 13.15 TLD readings compared for small lateral angles.

- TLD array beam profiles and TPR with polynomial curve fitting. (Figure 13.16, 13.17, 13.18, 13.19)

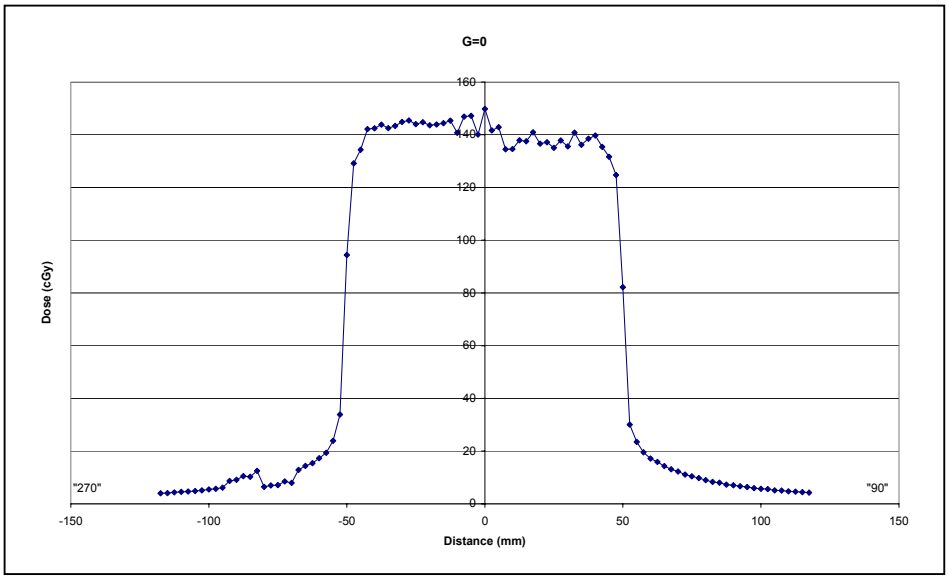

Figure 13.16 An example of a beam profile curve measured by TLD rod chain in the spherical phantom. Note the high noise level.

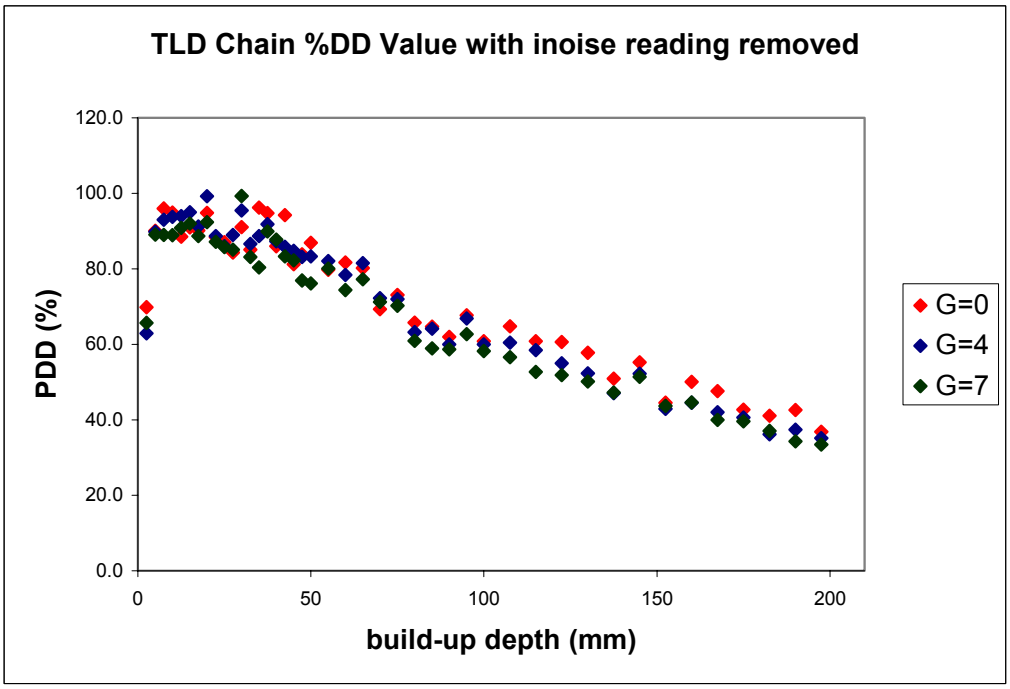

Figure 13.17 The original TLD readings for 0, 4, and 7 degree beam entry angles.

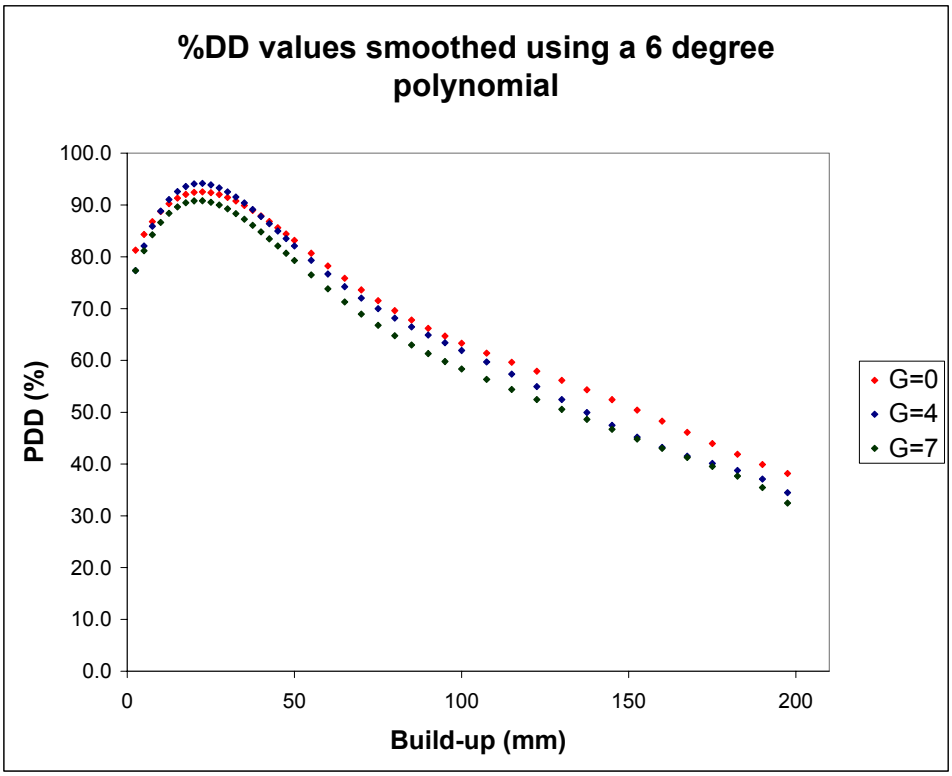

Figure 13.18 TLD measurements for lateral beam angles 0, 4, 7 degrees. After perform polynomial curve-fitting process.

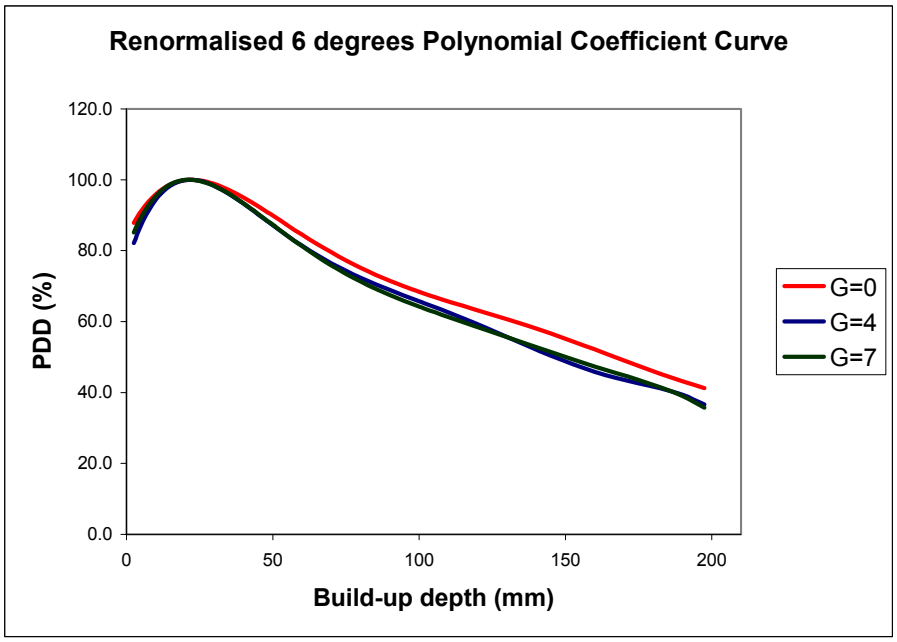

Figure 13.19 TLD measurements for lateral beam angles 0, 4, 7 degrees. After polynomial curve fitting and renormalize process.

The sensitivity test to each individual TLD rod was repeated with standard deviation of up to 8%. Polynomial smoothing was performed in the curve fitting.

It is to be noted that a dependence beam entry angle is observed.

- Phantom CT scan image and Digitally Reconstructed Radiograph [DRR] image generation. (Figure 13.20, 13.21)

  The CT spherical ball phantom was scanned in a 2.0mm slice step with the film cassette inserted. The images were digitized and transferred into CMS FOCUS planning system and contours outlined for each slice. The Digital Reconstructed Radiograph was generated by the RODOMS planning DRR function.

Figure 13.20 Spherical phantom CT scan image and contoured by the CMS Focus planning system.

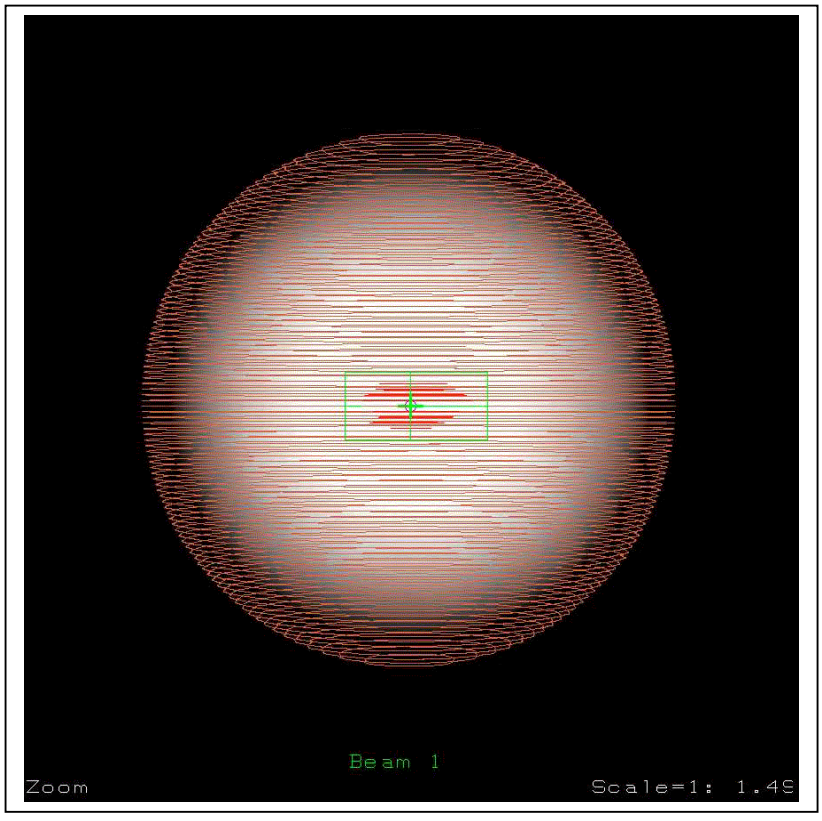

Figure 13.21 The Digital Reconstructed Radiographic (DRR) image generated utilising the phantom material electron density.

Figure 13.20 shows the CT scanned ball phantom with the film cassette inserted, and the images loaded into the treatment planning system, a simulating target is contoured. Also Figure 13.21 shows a DRR image (Digital Reconstructed Radiograph) to display the phantom material density for showing an equivalent X-ray image on the screen. The mass density is converted from the electron density which calibrated from the Hounsfield numbers of the CT image pixel by pixel, calculated for each CT slice but interpolated between CT slices to make the image displayed as a reconstructed radiograph.

13.3.4 Treatment Planning QA Tests

Three treatment plans were compared using calibrated film and TLD profiles. Both small square fields and IMRT fields are simulated by using both forward and inverse treatment planning technique.

Treatment Plan 1. Small square fields at the phantom isocentre combined with three different gantry and couch angles were used to make the dose planning calculation for a three-D oriented planning report. The monitor unit to the centre of phantom was checked by ionisation chamber measurement. (Figure 13.21, 13.22, 13.23, 13.24, 13.25, 13.26b)

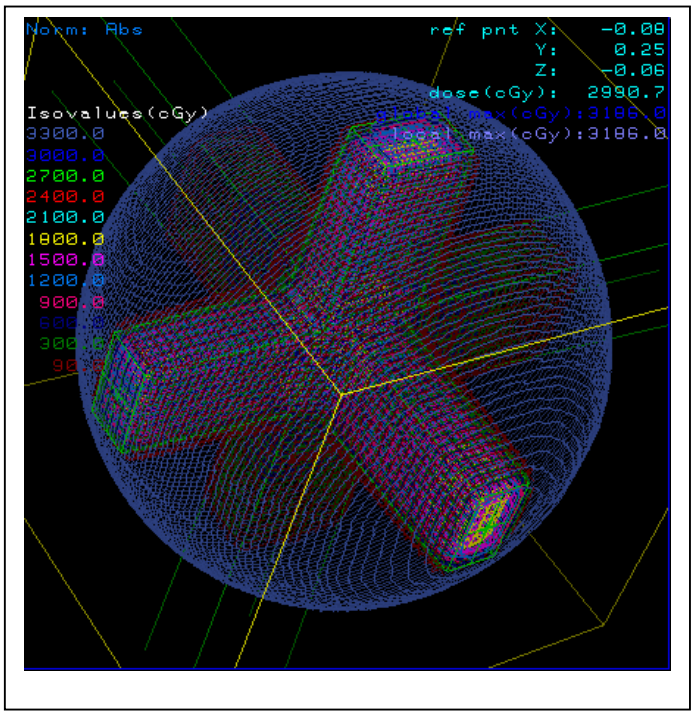

Figure 13.21 A simple case of 3-D planning example, planned for spherical phantom using CMS FOCUS.

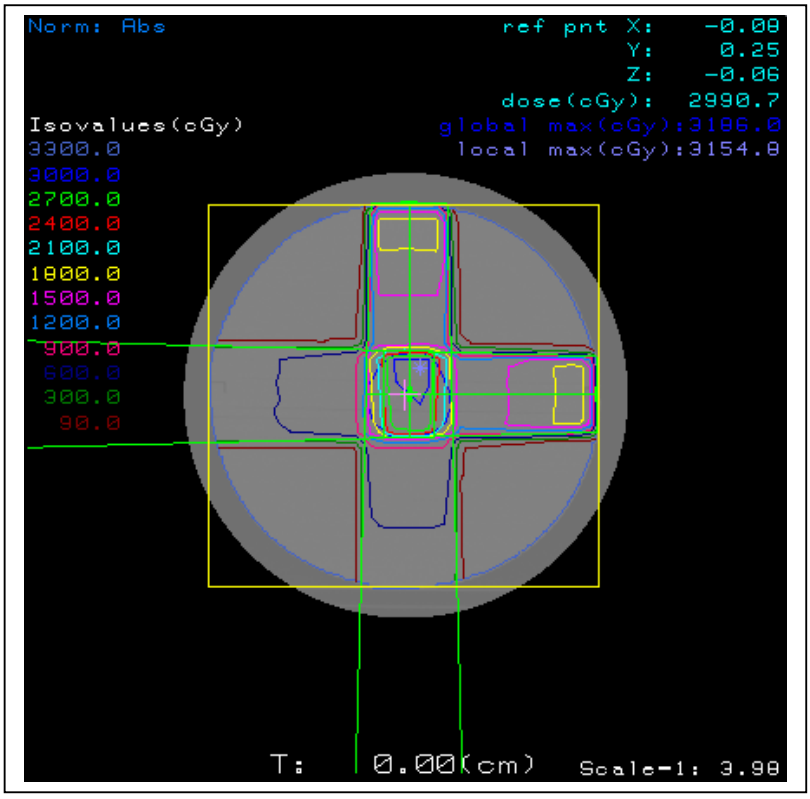

Figure 13.22 A simple case of 3-D planning example, planned for spherical phantom using CMS FOCUS.

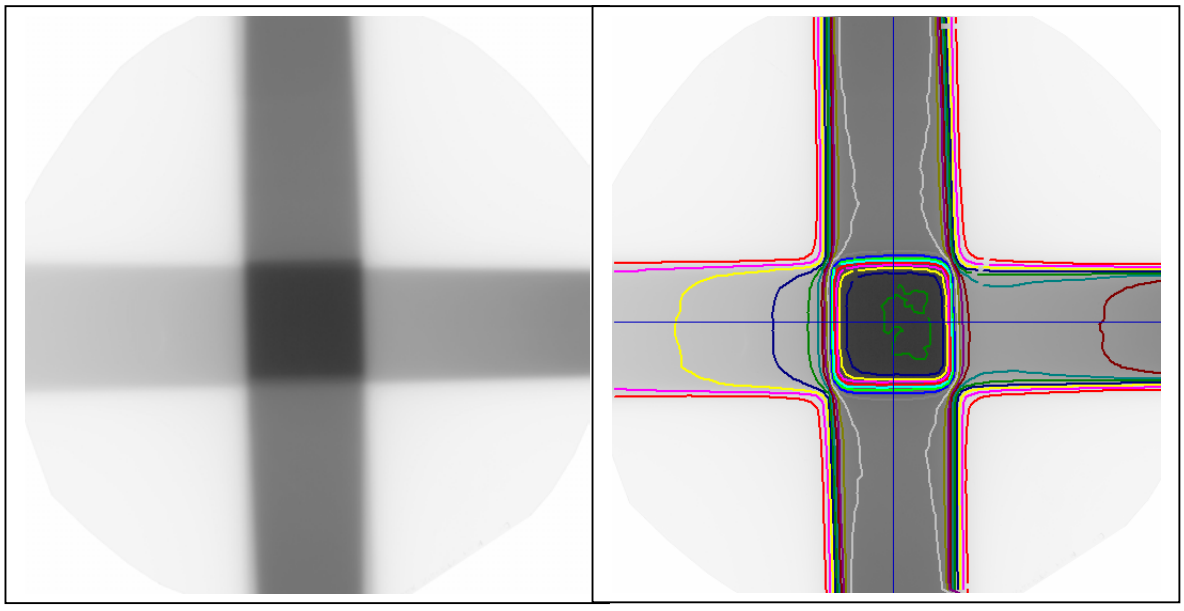

Figure 13.23 a. A film taken to check the plan dose distribution.
Figure 13.23 b. Isodose curve generated by analysis software.

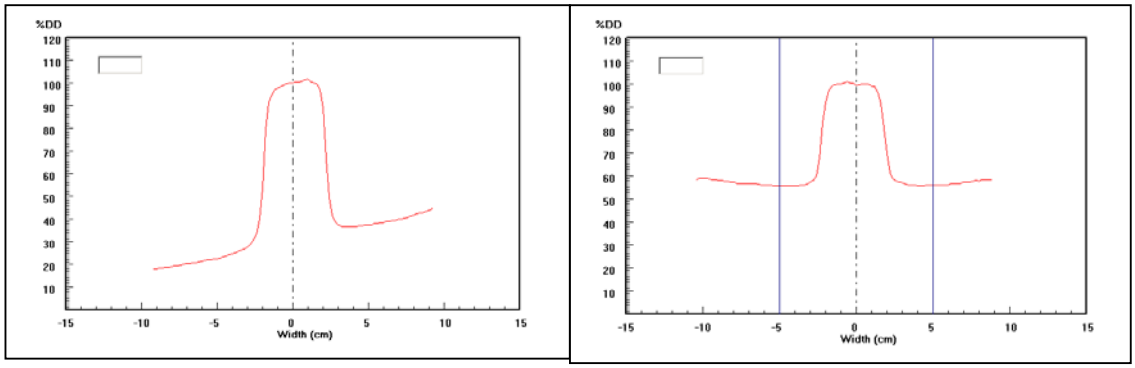

Figure 13.24 Profile curves obtained from isodose distribution results.

a. Cross plane displayed the profile for the vertical beam but the intensity attenuated from right to left by a combined lower energy lateral beam entry.

b. The profile for lateral beam in Figure 13.23 combined with a high energy vertical beam, the profile background level shows high but less attenuation compare with low x-ray

Treatment Plan 2, An Gross Target Volume (GTV) is contoured to simulate a kidney shape surrounding a sensitive organ contoured at isocentre. Nine fields are given by the inverse plan conformal to the PTV. The plan was evaluated by the Dose Volume Histogram (DVH).

Treatment Plan 3, Two lateral tangent fields opposite to cover a long curve shaped GTV on the side of the Ball phantom with a simulated sensitive organ next to the GTV. The isocentre of plan has shifted to the PTV centre near one side of phantom.

In each film exposed, the following procedure was implemented:

- Testing the film scanner signal setting used different angle physical wedge field exposed and scan the profile using film scanner and compared the profile shape and angles with Wellhofer water scan data at the depth 10cm (as routine scanner signal QA check).
- EDR-2 film was cut into a circular shape to fit into the inserting disk film cassette of the Spherical Ball phantom. The disk was inserted

into the phantom centre as a replacement for the ionisation chamber and TLD holder.

- The Ball phantom was setup with the film disk face on to the gantry and target direction so that the film was parallel to the cross orientation, making the film parallel to the beam when the gantry is rotated 90 degrees. The exposure of each field was given by the planning calculation but with the monitor unit corrected by beam to film entry angle dependence correction factor.

Film dosimetry signal calibration

- Pixel GSV signal to corresponding dose inspecting
- Signal noise polynomial smoothing
- Build-up dependence and field size dependence correction

Film dosimetry analysis processing

Bitmap image pixel signal to equivalent dose converting on 3-D treatment planning system:

- Isodose tracking and curve plotting
- Profile curve inspection and analyses
- Use DRR to build dose distribution volume.

Results and discussion

In both Plan 2 and plan 3, the isodose curves were plotted by pixel value to dose convertion. The results show that the film analysis provided excellent agreement with both planning curves and the TLD profile measurements with a standard deviation of 1-3% after renormalisation. Some individual points had discrepancies of up to 5%. These higher deviations were associated with points at the junction between the fields or the edge of the fields.

Discrepancies between the dose planning, TLD and film measurements may arise from:

1. Experiment physical alignment and surface errors in the hand made phantom (+/-1%).
2. TLD measurements do not fully sample the radiation field. The distance between the TLD rods is larger than both planning and film pixels. Field edge and junctions falling between rods could provide the observed deviations of up to +/-2%.
3. The air gap in the TLD rod holder and the fact that TLDs are not tissue equivalent could also add to the observed deviations.
4. The planning calculation result is more theoretically smoothed unlike the film analysis.

However, the experimental result is impressive in that it shows that the film curves can more accurately represent the dose distribution than the TLD technique. By carefully calibrating the film scan signal and analysis process, the comparison measurements can be carried out using EDR-2 film with high reliability.

The spherical ball shape phantom allows the film to be set in different orientations in a 3D which is convenient for the isocentric planning three-D data commissioning check.

However, the use of the spherical phantom is still limited at this stage for settings that are isocentric. To perform the ionisation measurement for a weight point different to the isocentre, different ionisation chamber holders need to be made if the point dose measurement is required for IMRT field for some different segment size involved in a combined field. As there is no inhomogeneity medium incorporated in the phantom this made testing possible only for water equivalent tissue.

As an example of lateral film dosimetry used for the 3-D treatment planning dose distribution verification, the figures 13.25 and 13.26 show a multiple combined beam field by given beam though three different entry angle and each single field combined with more than one segments. The film analysis result overlays a chosen isodose curve with planning calculation result. The

RODOMS performed an overlay comparing shape, equivalent area and maximum discrepancy of the curve edge.

Figure 13.25 phantom lateral film dosimetry analysis result compare with planning calculation result

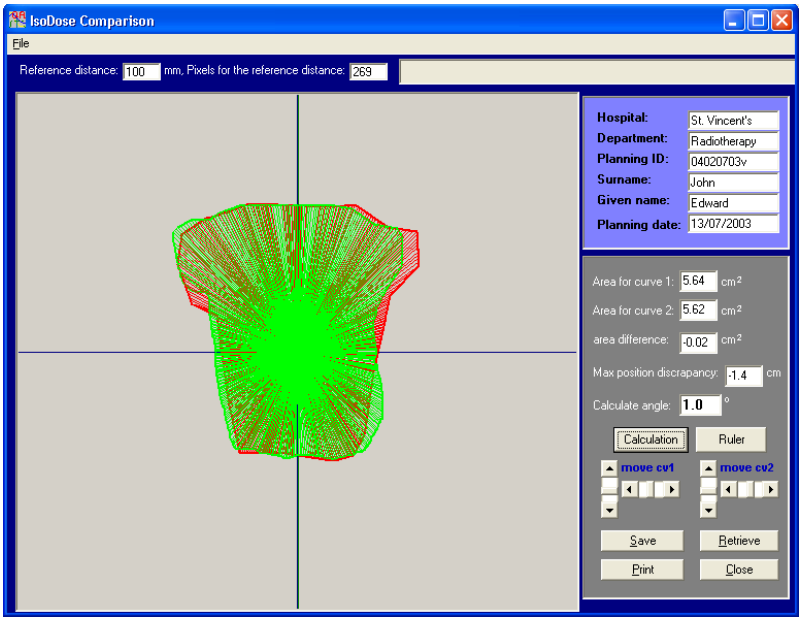

Figure 13.26 overlay analysis for planning calculation and film dosimetry result used for IMRT dose distribution check. Analysis include comparing dose distribution shape, calculated area, and maximum edge discrepancy

13.4 Summary

Although it is too early to fully justify the accuracy of IMRT film planning checks, the cases of some simple three-D plan checks performed with this study have given a great encouragement to using this design. Extensions to this study are continuing. Using the film calibration technique and software developed in this project, very effective QA checks have been performed for a complicated 3-D treatment plans combined with beam centre absolute dose checks against the monitor unit calculated by the planning system The film analysis result can be compared and calibrated with TLD multiple point dose measurements with same set-up in the phantom. The TLD readings can be absolutely calibrated using ionisation chamber measurements performed in the same phantom.

The phantom allows the film to be set up in a 3-D orientation to check the field with combined beam entry. The film can be set at different layers for taking the image cut for different depth level and face to different gantry angles, collimator angle and couch angles. Most of corrections suggested in this study require additional software procedures to be developed.

Chapter 14 Electron Beam Energy Checks

14.1 Introduction

Both AAPM and ACESPM recommend that the routine energy checks for both photon and electron should be performed monthly. High-energy beams emitted from a linear accelerator are generated by high voltage power controlled microwave system. There are so many issues which could affect the energy level change. The energy level change due to acceleration, microwave frequency, and the high voltage power levels. Beam energy change could happen at any time especially for a busy machine in a radiation oncology department with a heavy patient workload.

The energy checks should be carried out by using ionization percentage depth dose scans in a water phantom. The X-ray energy is determined by depth of maximum dose distribution (d_{max}), 50% dose distribution depth (d_{50}) and the ratio of dose rate proportion between the depth 20cm and 10cm (D_{20}/D_{10} ratio). The electron beam energy is evaluated by using mean surface energy distribution (Eo), maximum dose distribution depth (d_{max}), effective range (R_p) and photon contamination tail level (D_x). Because of the complexity of the water scanning technique and the scientific resource needed, the water scan is very hard to perform monthly in most radiation oncology departments. For the photon beam, the energy consistency can be checked by comparing the dose ionisation measurement readings from two different buildup depths in solid phantom, plus the central axis maximum dose output measurement. The photon beam energy can be monitored effectively. However, the same method cannot be performed for the electron beam. That is because the percentage depth dose curve of the electron beam has a very big slope, meaning that the percentage depth dose level is sharply reduced from 80% to 10% in a very shallow short distance, especially for electron energies below 12MeV. This issue results in a practical problem for the measurement setup. If the effective point changes by even 1mm, the electron beam energy can be

affected up to 5~10%. So, the electron beam energy routine check is always a challenging question to the physicist.

In 1993, Islam used a multiple ion-chamber device component lined up under a Perspex wedge shape phantom, to take a measurement under an open electron field. The readings obtained from each individual ion-chamber corresponded to different build up thickness from different parts of the wedge phantom. By plotting the signal percentage ratio after a re-normalization process, an equivalent electron beam percentage depth dose is simulated. This method has revitalized the topic of electron routine energy checks. However, there are a few practical difficulties of using this method. Firstly the construction of the multiple ion-chamber devices would be very costly. Secondly, the calibration for multiple chamber detectors would still increase the workload of the physicist. And a further problem is that the ion-chamber cannot be small enough so that the distance gap between the signals has to be a minimum of 1.5cm. This problem makes the resulting curve poorly sampled and the D_x tail part of the curve is unable to be measured.

The consideration of using film was begun in early 1993, in the physics group of radiation oncology department, St. Vincent's hospital, Sydney. A Perspex wedge phantom was designed and used to sandwich a Kodak XV-II verification film under a large sized open electron beam field. By giving a pre-determined exposure dose to the film, the film darkness change in the wedge phantom build up area was steady and smooth. The optical density value from different points of exposed film was analyzed using a film densitometer. The corresponding thickness of the wedge material was converted into the equivalent build up depth. A curve plotted for the ratio of optical density value changes along the wedge direction represented an equivalent electron percentage depth dose curve. The major concern of using film dosimetry to take the place of an energy check was its reproducibility and reliability. Since the film densitometer utilizes a single detector analog signal, to align a film on

the densitometer is still difficult to achieve consistently accurate each time. The measurement can therefore be very time consuming.

In this study, the film dosimetry for the electron energy check was performed using a desktop scanner. A specially designed software function was developed to read the bitmap image and correct the problems related to film processing, light uniformity and background corrections. The outcome is an electron energy check which is simpler, time saving and reliable.

14.2 Method and material

To satisfy the requirement of a quick, simple and highly reproducible set up procedure a perspex wedge was chosen as the phantom with therapy verification film (Kodak X-Omat XV-II). The wedge was orientated in the cross plane of the electron beam with the heel downwards on an inclined film sandwiched by both top and base part of wedge blocks, the surface of the wedge block was perpendicular to the vertical beam. In the Gun-Target direction the wedge was centered to the beam defined by a 25cm x 25cm applicator and at 100cm SSD to the surface of the phantom. The effective measurement region was determined within the 80% of the field size width. Laterally, the centering point was such that the central ray traversed a perspex thickness about 3.0cm. The film exposure dose was 60cGy for all electron energies. A radio opaque marker was embedded on both sides of the wedge block at the central set up line projected to the film side block. This acts as a fiducial marker, visible on the processed film. Figure 1 shows the setup arrangement. The film was developed in automatic processor with a unexposed background film. The film was scanned by a document desktop scanner with transparency light source adapter. The scan signal to optical density response was calibrated by scanning the standard step wedge film, the linearity was adjusted by changing the setting of blackness and contrast setting in the scanner supporting software. The image was saved as a bitmap image. Software was developed to perform the following processes:

Equivalent depth distance calculation – calculates the corresponding thickness of the perspex (Figure 14.1) to the reading point. Each point is calculated individually by trigonometry the beam source direction taking into account the phantom wedge angle and the angle of beam direction off to the central axis (Figure 14.2).

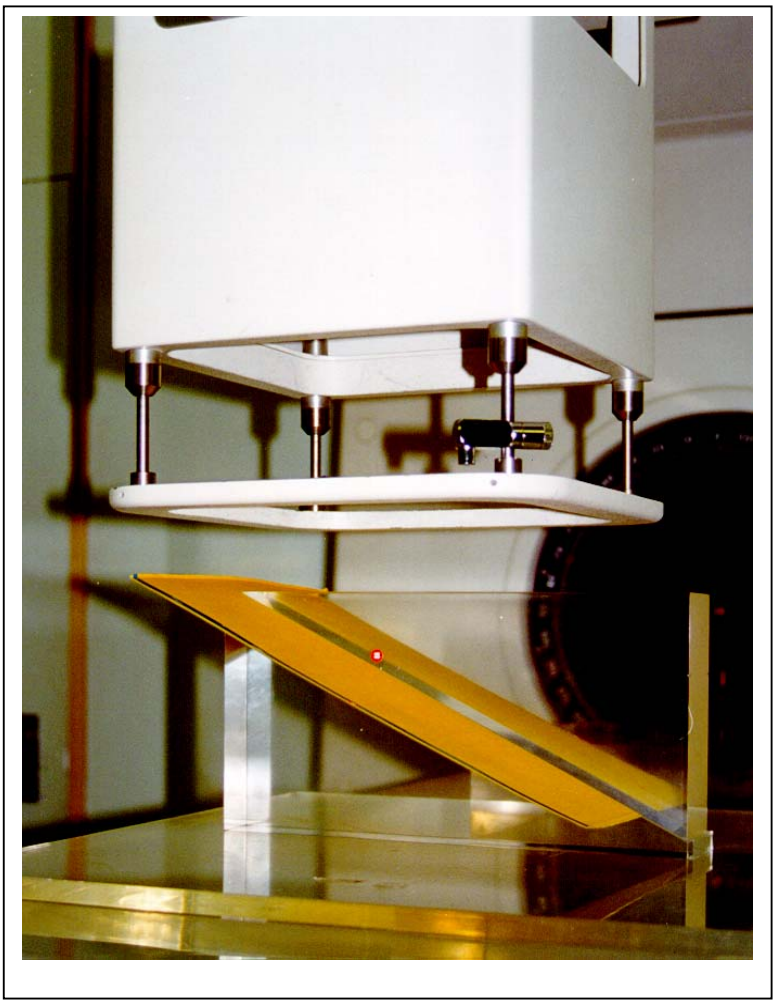

Figure 14.1 Film set up in solid wedge phantom used for Linear Accelerator electron energy check

Material density – corrects for density and alternation using inverse square law.

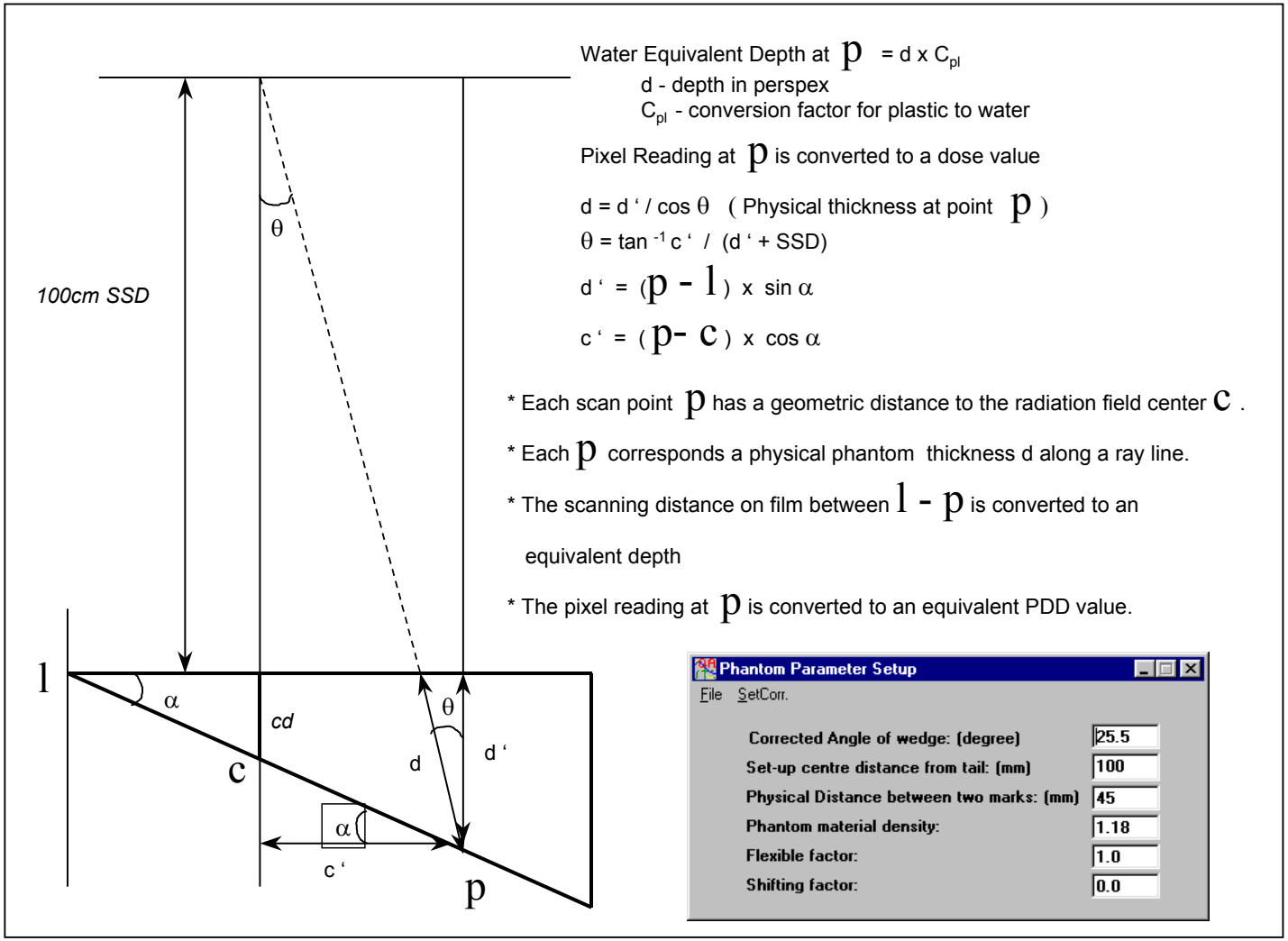

Figure 14.2. Equivalent distance calculation using triangle function in wedged phantom software function development

Off Axis Ratio – OAR table was set for the field size profiles in different build up depth. The readings were corrected by using the calculated depth distance to the OAR table (Figure 14.3).

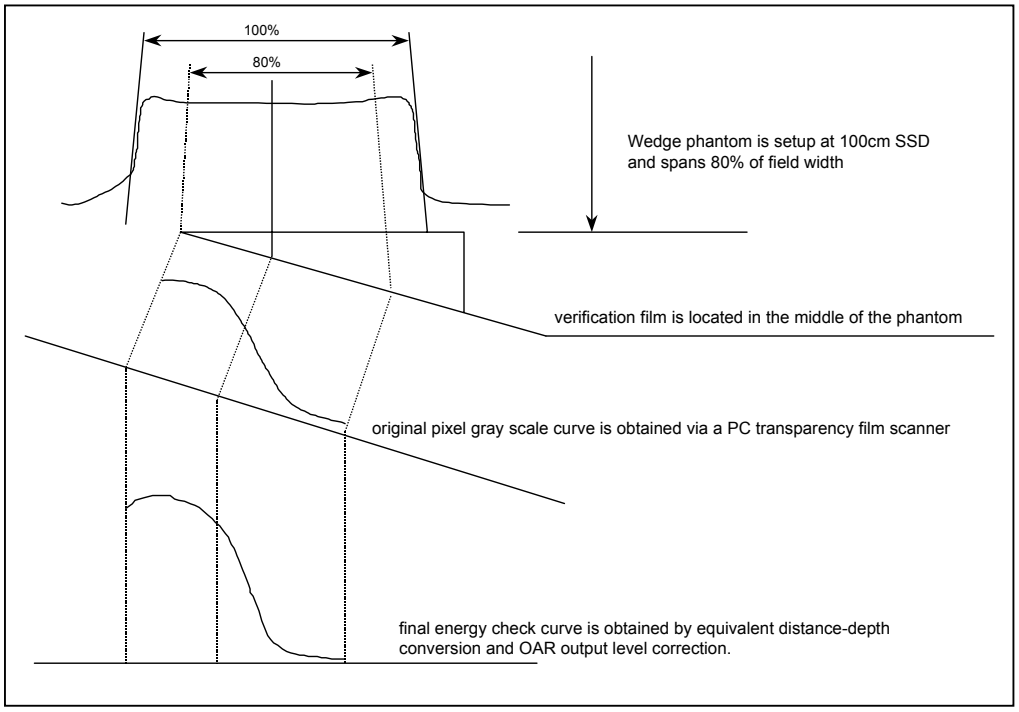

Figure 14.3. a demonstration of converting original film analysis signal in to equivalent depth corresponding depth dose data

Greyscale value irradiation dose response and background value subtraction – the GSV-Dose response curve was measured using films and each GSV subsequently converted by reading to be converted by interpolation into equivalent dose, the film background value is analyzed and subtracted off from the analysis readings (Figure 14.4).

Percentage curve processing – renormalizes the signal into a percentage and plots the percentage value versus equivalent depth (Figure 14.5).

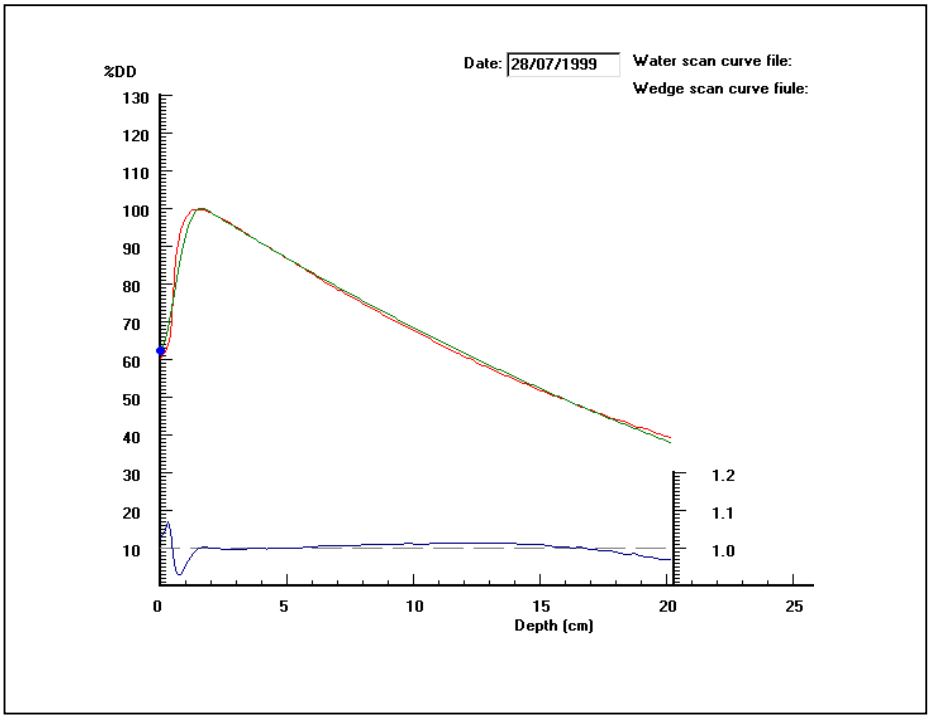

Figure 14.4 Film scan background value subtracted against the water scan value shows the perturbation from the build-up region is obvious.

Energy analysis processing – E_o, R_{max}, R_{50}, R_p, D_x are calculated and marked on the curve (Figure 14.5).

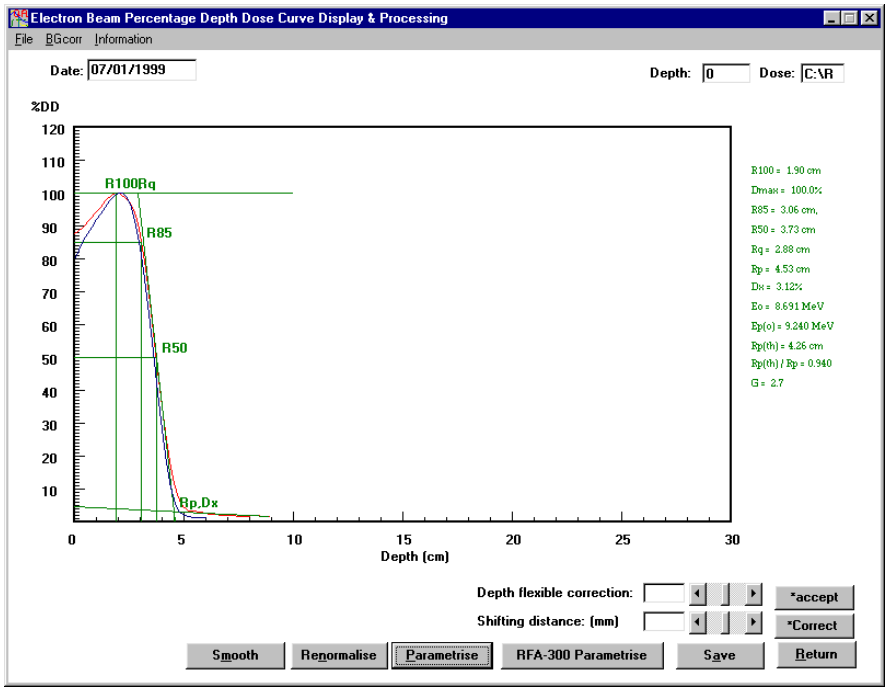

Figure 14.5 Energy check analysis performance software function interface. The water scan result can be loaded for comparison

Output report processing – Prints the curve and analysis results to the default printer. An annual analysis result trend function is included to display the variation of energy over a year (Figure 14.6).

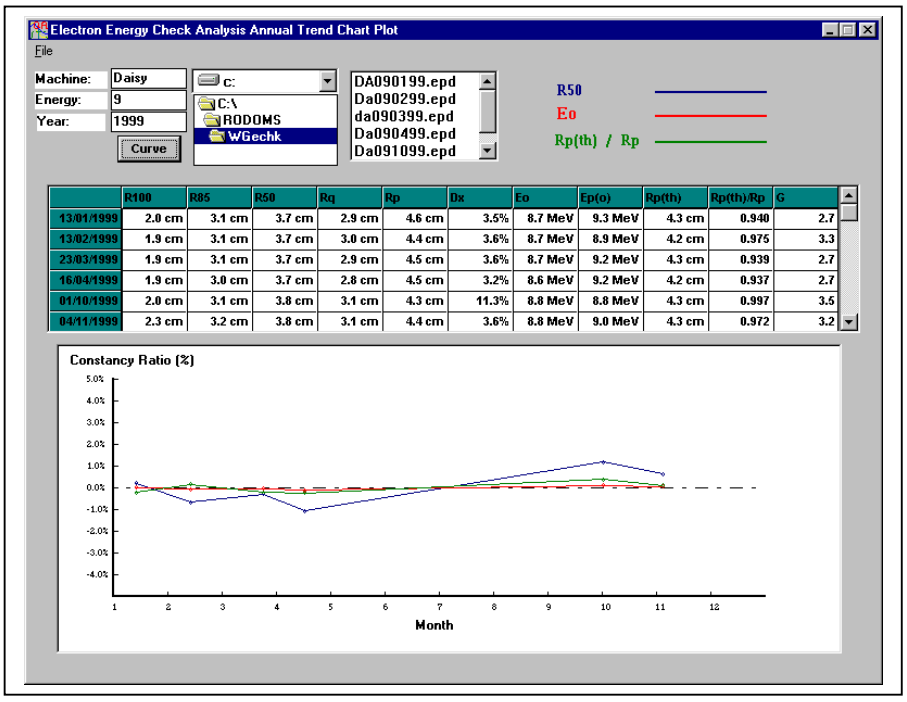

Figure 14.6 Film dosimetry Electron energy check routine work QA function in RODOMS. Electron energy check monthly trend chart.

14.3 Results

A comparison of a set of results of all the electron beam energies provided by the accelerator is presented in table 14.1. The differences between the base line water values and the perspex check values are quite small and so it can be noted that the perspex wedge phantom method simulates satisfactorily the water phantom reference situation. Of interest too is that in a series of daily measurements for a week with the wedge, the maximum difference resulted from misalignment of the phantom to the beam and of the processed film to the scanner. Table 14.2 shows the effect of a phantom shift of ±5.0mm off beam axis the wedge direction for the extreme energies of 5 and 14MeV. The maximum change in the calculated value of Eo and Ep,o is approximately 0.1MeV per mm of shift. Table 14.2 shows the effect of a shift of ±5.0mm

either way of the film's central position marks. The maximum change in the calculated value of Eo and Ep,o is just less than 0.1MeV per mm of shift.

Each energy result shows a discrepancy at the build up region. The film response dose is obviously higher than the water reference curves. And a 1-3% of higher background level even if the background film is used to subtract the film base fog value off. This value change also shows the energy dependence that makes slight differences between 5MeV and 14MeV different energy levels.

	Electron beam "Console" Energy (MeV)											
	5MeV		7MeV		9MeV		10MeV		12MeV		14MeV	
	Water	Film	water	Film	water	Film	water	Film	water	film	water	Film
R50	1.78	1.78	2.61	2.64	3.46	3.55	3.94	4.03	4.66	4.78	5.17	5.30
Rp	2.3	2.25	3.24	3.26	4.25	4.37	4.79	4.89	5.69	5.82	6.31	6.42
Eo	4.15	4.15	6.08	6.15	8.06	8.27	9.18	9.39	10.86	11.14	12.05	12.35
Ep,o	4.79	4.69	6.66	6.70	8.68	8.92	9.76	9.96	11.57	11.83	12.81	13.03

Table 14.1 Comparison of base line water value with perspex check values

Electron Beam "Console" energy (MeV)				
Calculated	5MeV		14MeV	
Change (MeV)	Shift direction		Shift direction	
In	To heel	To toe	To toe	To heel
Eo	+0.42	-0.56	+0.30	-0.54
Ep,o	+0.36	-0.50	+0.33	-0.46

Table14.2. Effect of phantom shift (5mm) off beam axis in wedge direction

14.4 Discussion

The error range given by Table 14.1 and Table 14.2 could result from variations in operation technique caused by processing, setting up, and scanning. The reliability film dosimetry could be improved by rigorous control of the technique by the operator.

The processing effects seem to not affect the final result significantly if the film response curve is calibrated by a control film strip. The background value can be deducted correctly by developing the background film at same time with the testing film. The film to OD - Dose response energy dependence produces a film OD on the film in both build-up region and the tail part of percentage depth dose curve (Figure 14.4). That is because of the higher component of lower energy scattered radiation. Low energy scattered radiation may not pass though an ionization chamber wall but will cause an over response in film darkness (OD) reading.

The need for a quick method for routine energy checking of electron beams has been previously addressed by several authors using ionization methods. In one case using a perspex wedge with a multiple ion chambers, and in the other a two step solid water block with two detectors positioned symmetrically about the beam axis. A group of workers at the Institute Gustave Roussy (IGR) in France in 1993 (*Iliev, Chavaudra, Bounik, and Nguyen, 1993*) reported the use of a perspex wedge with automatically processed film. The method presented here is both an adaptation and extension of their method. In this work the wedge is inverted. The film plane is inclined and a common centering point and constant SSD is used for all energies, so that lateral wedge displacement and vertical treatment couch adjustments are not required for each beam. Also the IGR method can visually yield a qualitative result in a manner similar to that using the Ardran and Crookes kVp test cassette in diagnostic radiology where subjective assessment of optical densities are made. In this study, the RODOMS software also corrects the uncertainties resulting film processing variations, and calculates the equivalent dose distribution properly to obtain a equivalent depth dose curve. In addition to the availability of the film record of the energy check, the software provides documentation as in figure 2 for inclusion in the quality control logbooks.

14.5 Conclusion

The approach described here for routinely checking electron beam energy is very economical of accelerator setting up and “beam-on” time. The use of a desktop computer scanner offers a very low-cost method for inclusion in quality control procedures. Precision and reproducibility of wedge positioning in the beam and placement of the processed film on the scanner can be achieved easily and routinely to within +/-1mm and so the required energy resolution for the method is satisfied.

Chapter 15 Multiple Beam Field Junction Dose Distribution Checks

(Presented at the ICRO 2001 conference, Melbourne Feb 2001)

Abstract
Film optical density vs energy dependence correction for multi-beam combined fields' exposed on one film is investigated for treatment planning QA check purposes. An exposure proportion correction table was made by calculating different exposure at the same optical density levels for different energies. Instead of correcting the film analysis curve, each entry beam exposure dose is corrected by a relative correction factor before the exposure. The corrected exposure is also compared with both ionisation measurements at reference points and TLD chip matrix readings. After the exposure proportion correction, a film can be read without applying further corrections to give realistic dose distribution. The isodose curve provides a directly visualised dose distribution and physically addresses the hot and cold spots at each field junction. The plotted results are used as a to comparison on to the treatment planning calculation as a QA document. The film dosimetry provides a simple, quick visualisation tool to apply to multi-beam combined treatment plan QA checks. The mixed energy responses on a single film can be corrected by applying the uniformity correction factor to the dose delivery before the film exposure. This correction improves the reliability and accuracy of film used in QA checks.

15.1 Introduction

Multiple combined beam radiotherapy fields are often used in treatment planning. A check of hot and cold spots at multiple beams, field junction regions is required to confirm that the dose values are within the tolerances compared with planning calculation result (Figure 15.1). Common techniques include ionisation and TLD measurement. While absolute dosimetry using ionisation chambers provides the best accuracy for point dose measurement in either solid or a water phantom, TLD chips can be located in a solid phantom to obtain the absolute dose reading for many points at same time. However, both ionisation and TLD's essentially measure point doses. To use either of these techniques to perform more detailed dose distribution checks would be difficult to set up and time consuming. Water scanning techniques provide relative percentage dose measurements, but are laborious and are most useful for single exposure beams.

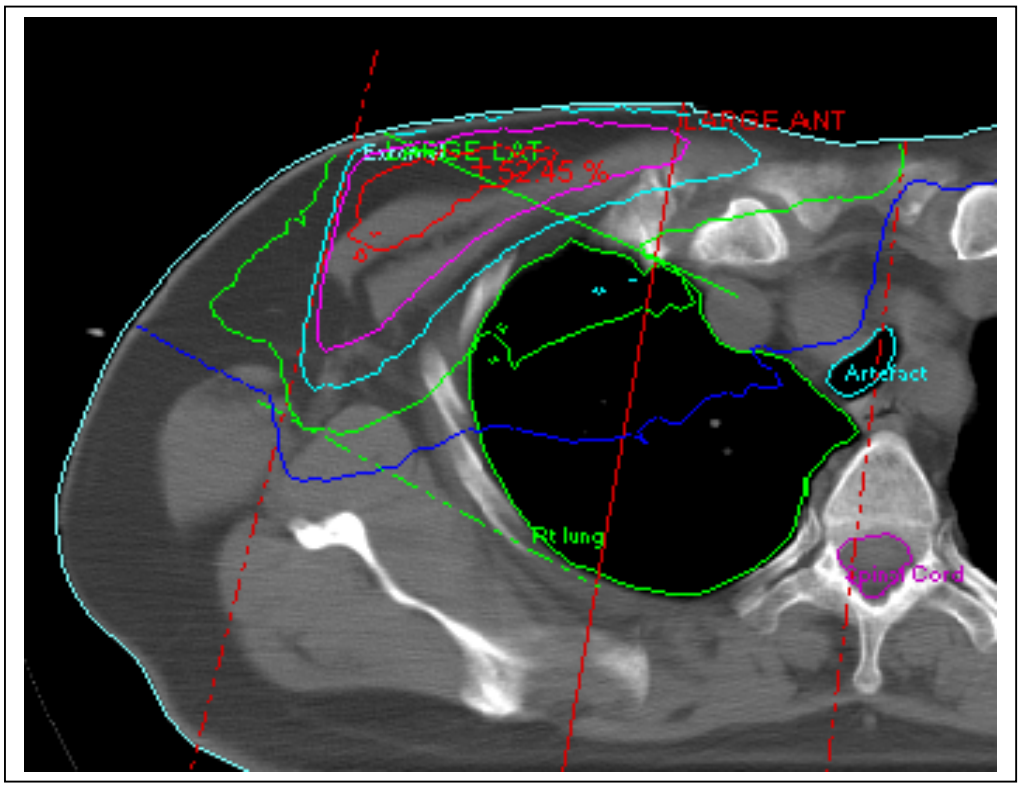

Figure 15.1. A multiple beam field combined with photon and electron beam planned on Theraplan two-D planning based on CT a chest image.

Film dosimetry has been used in radiotherapy dose distribution checks since 1960s and film has been established as a practical tool for the relative measurement of doses. The blackening of radiographic film can be analysed by film densitometry techniques to the transparency converted to optical density then converted into corresponding equivalent exposure dose. However, current film dosimetry results often are affected by many unwanted factors. The reliability of converting optical density value to equivalent dose is affected by many unstable issues such as film quality, densitometry signal quality, set-up and film development conditions. In the past ten years, film densitometry equipment has developed significantly to improve film scanning technique. Digital imaging technique has overtaken the analogue methods, the 1.0mm~2.0mm densitometry resolution has been replaced by a resolution small as 0.1mm~0.3mm. The signal to noise level has been reduced significantly by the signal depth increase from 8bit to 12, 14 or 16 bits on the greyscale value. The bit format increase has also increased the dynamic range of the optical density signal to provide a wider range for the linearity adjustment and signal quality improvement. This has significantly improved

film dosimetry reliability and reproducibility. If we make the proper signal corrections, film analysis results can be more reliable and make the film dosimetry useful for complex radiotherapy field dose distribution checks.

Many writers have reported signal correction methodologies show which that properly corrected film measurements can achieve good results. Compared with the TLD and semi-conductor dosimetry techniques, film dosimetry is easier to perform, uses less time. It does not simply provide the point dose, but images dose distribution over the whole film provide an easily visualized dose distribution which can simplifier clinical planning QA tasks.

Nowadays film calibration techniques are commonly used for a single field or beam exposed on a single film. A combined exposure with different beam type and energies on one film would unable to be calibrated using an OD-Dose response curve. This because the dose measured from an exposed film is obtained by converting the optical density signal to calibrated dose via an OD-Dose calibration curve. The film response varies with radiation type and energy. Each beam type or beam energy has it's own optical density to dose response curve. In field made up of multiple beams produced by exposing electron and photon beams with different dose and field sizes on a single film. The different responses are mixed together on that film. After the film has been developed, none of response curves can be used to perform the dose conversion. If the problem of combining dependence factors mixed on one film cannot be corrected, film dosimetry does not seem to be a suitable technique for use with combined beam field junction measurements. On another hand, if we could find a means to overcome the energy dependent problem affecting calibration, film dosimetry could be more easily used to provide easily visualised results.

This study is focused on the effect of beam type on film density and the application of energy dependence corrections applied before exposure with the aim to reduce the influence of energy dependence on film QA. We can adjust the optical density response by changing the given dose to make the

film analysis result agree with to the planning dose weight factors. The exposure rate for each field is corrected by each energy response factor.

15.2 Experimental

15.2.1 Material and Method

A Varian Clinac-2100C linear accelerator was used to investigate the calibration curves of effect beam types for 6MV photon, 9MeV, 12MeV and 16MeV electrons. The multi-field junction setting used 8cmx8cm field size for all beam types at 100cm SSD. The two fields were combined field junction edge to edge at the phantom surface. The treatment plan was performed by Theraplan version 3.1, modelled for solid water slab phantom (Figure 15.2). The exposure determined for the combined field was 60cGy for each beam in order to match the film to the linear part of the response curve region.

Figure 15.2. In-homogeneity solid water phantom used for chest wall point dose measurement using for TLD chips set up.

The planning result was compared with special a TLD chain profile check. The X-Omat XV-2 verification film was used for the film dosimetry equivalent dose distribution checks.

Both TLD and film tests were set up in solid water slabs (Figure 15.3, 15.4). The film was sandwiched between the slabs, parallel to the beam direction, with the film remaining about 3cm outside the phantom (Figure 15.6) on the incoming beam side. Two pinholes were marked to define the surface. The minimum phantom scattering build up for each side of the film is more than 5cm. The gantry was rotated to 85-degree direction to the film with 5^{o} beam entry angle. This setup was designed to reduce the influence of the edge effect, the packing material and air gap between the film and solid phantom (Figure 15.6).

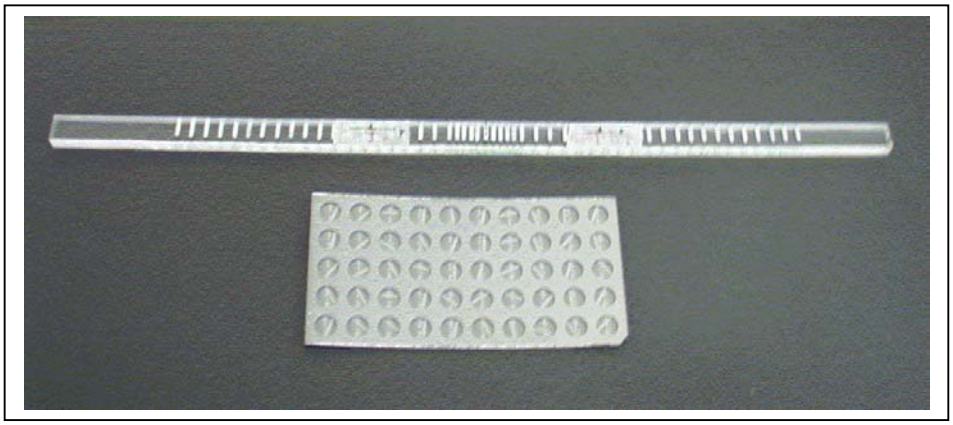

Figure 15. 3. TLD rods loaded into the stick bar shape holder for the profile curve measurement in different build up depth in solid slab phantom.

Figure 15. 4. RW3 solid water slab phantom hold the TLD stick bar set under the beam for the irradiation.

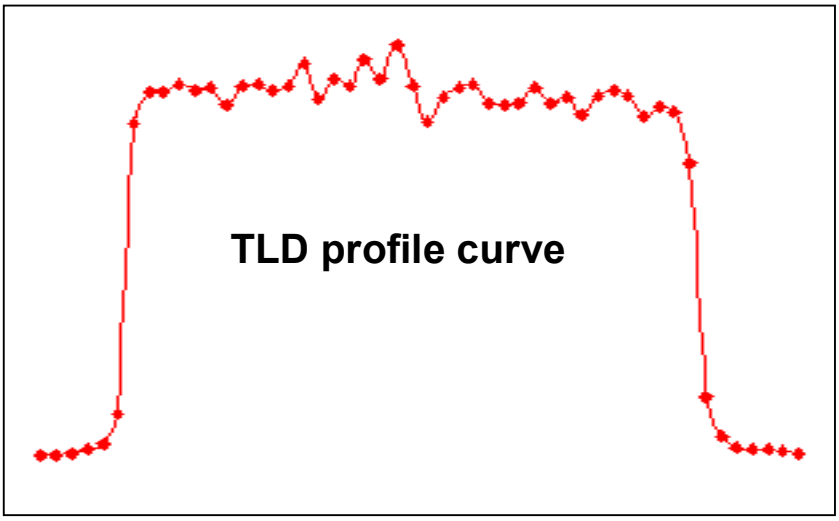

Figure 15. 5. an example profile curve generated by TLD rod readings, total processing time for on curve is around about 10hours.

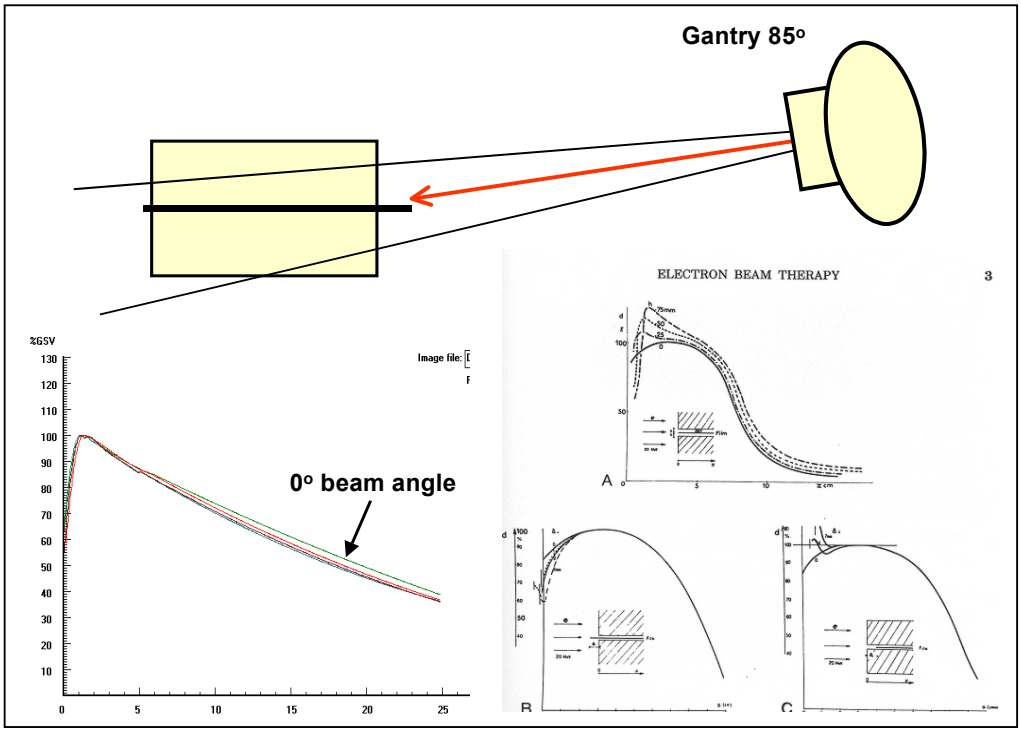

Figure 15. 6. Film set up in solid water slabs with a gantry angle 5^{o} in order to reduce the solid phantom build up effects.

The film was developed using AFGA X-ray film processor. All the measurement films and calibration filmstrips were developed using the same processor and at the same time. The film was scanned using Umax Astra-4000U desktop photo scanner with transparency scanning light source box, 14bit signal depth and 100ppi resolution (Figure 15.7). The

relationship between pixel greyscale value (GSV) to optical density was calibrated by scanning a standard step-wedge film (Figure 15.8). The scanned image was saved as Gif bit map image file for the pixel signal analysis. The image was analyzed by using the film dosimetry software package specially developed for this study, and the results compared with the planning and TLD measurements.

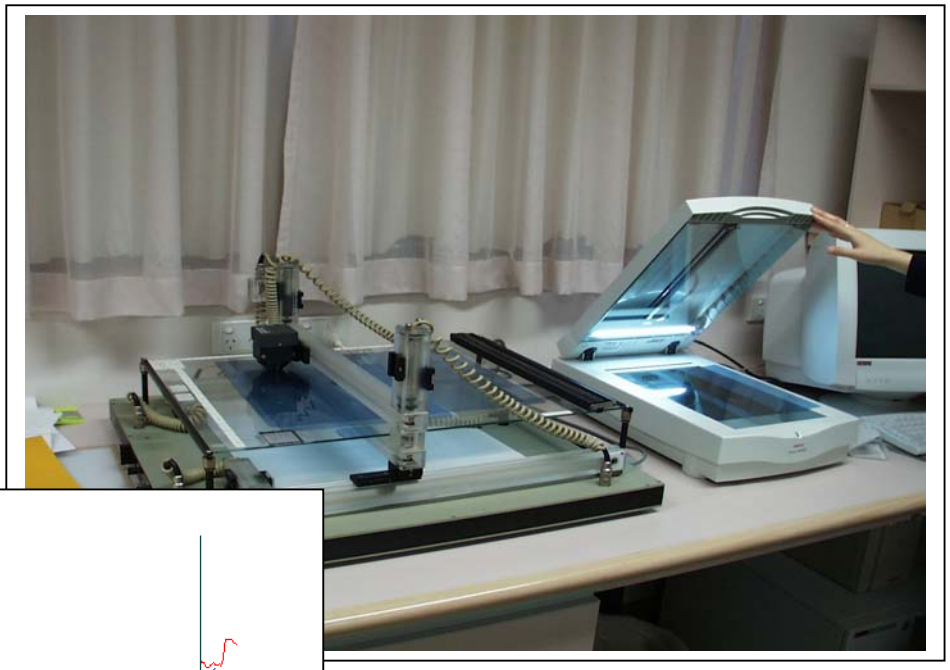

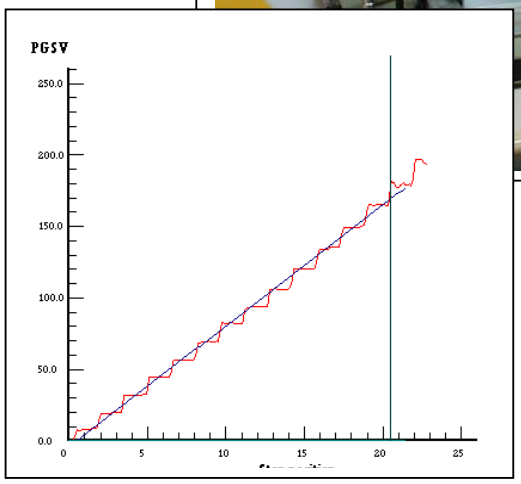

Figure 15. 7. Umax Astra-4000U desk top scanner with a transparency light adaptor. Left is the Wellhofer film densitometer.

Figure 15. 8. Film densitometry equipment signal linearity calibration.

Obtain the optical density dose response curve

1. The optical density dose response curve for each beam was obtained by exposing 10cm x 10cm field size film strips set up in the solid phantom and processed with steps of increasing exposure simultaneously under identical condition. The greyscale values read from the central axis of filmstrip and at d_{max} buildup depth. The readings were fitted by a three degree polynomial curve and used to

create the smoothed dose response curve and its coefficients. For each test film, every pixel signal is read and converted into the equivalent exposure dose by using the OD-Dose response curve. (Figure 15.9, 15.10, 15.11, 15.12)

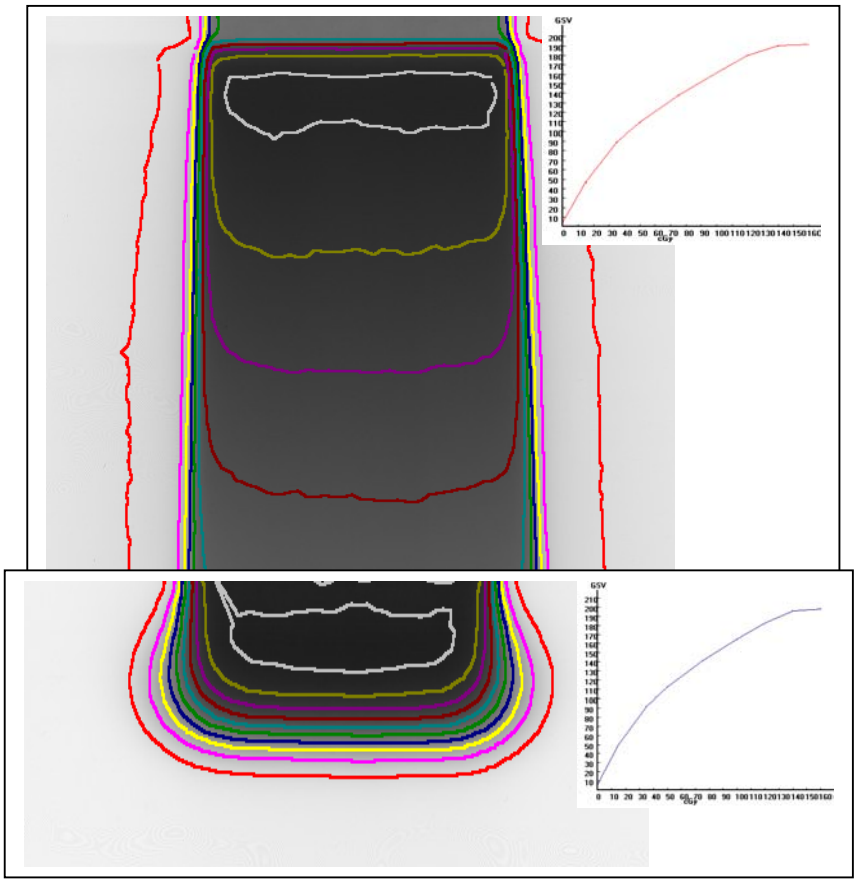

Figure 15. 9. Single type and energy beam equivalent dose calibrated by its own OD-Dose density response curve for both Photon (top) and Electron (midlle)

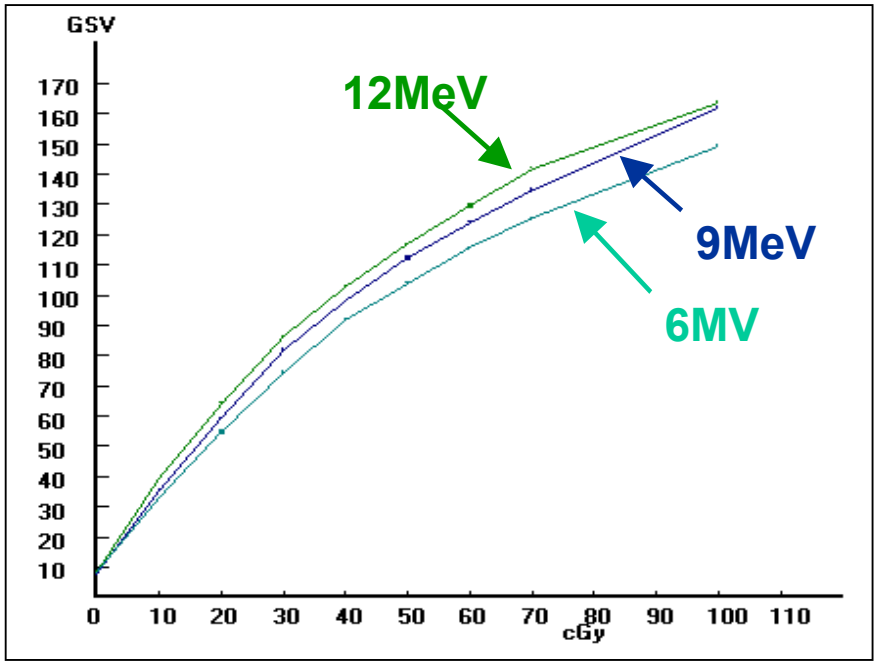

Figure 15. 10. OD-Dose response curve difference compared between different beam type and energy to show the dependence

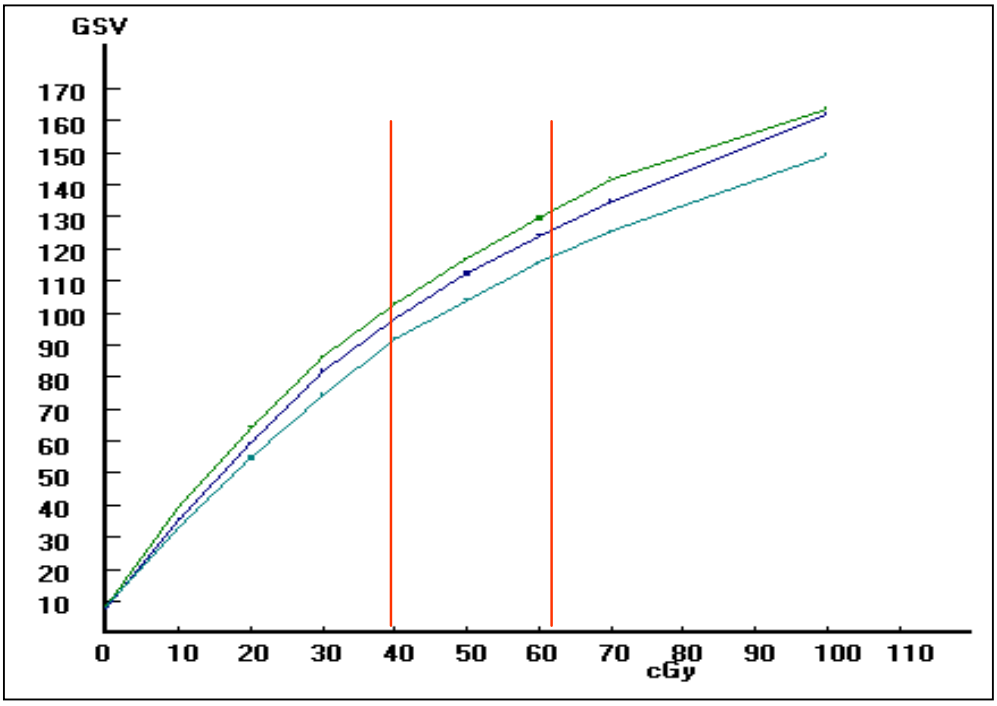

Figure 15. 11. Determine the best exposure dose region for the film and considering for all beam types involved in the combined field.

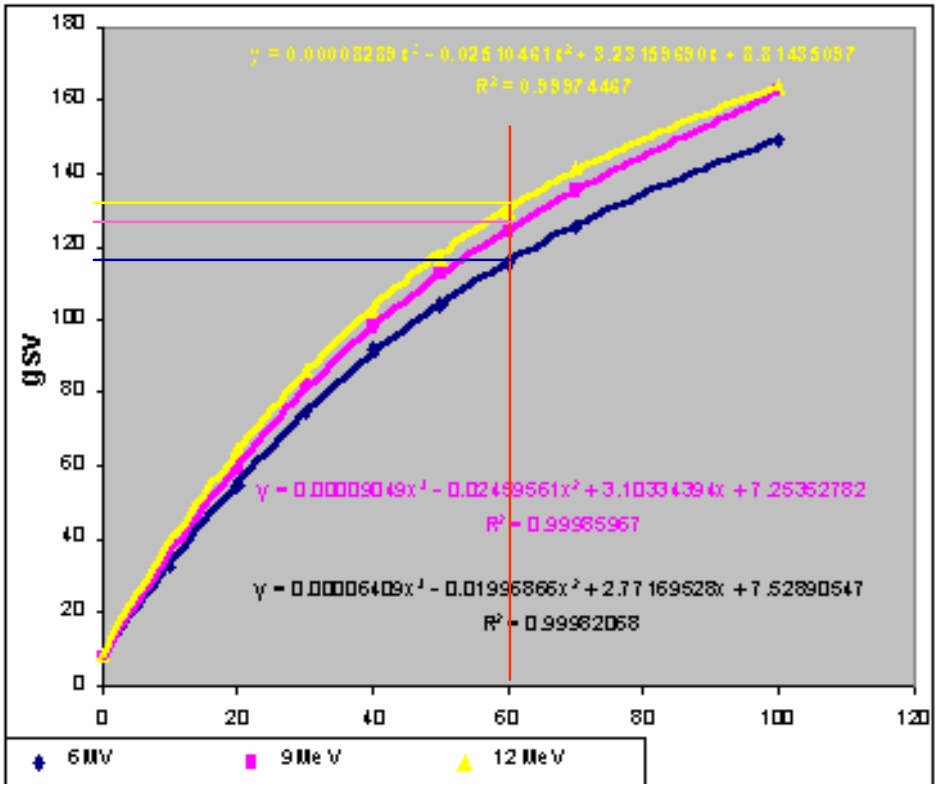

Figure 15. 12. Compare the differences against the reference curve and calculate the correction factors.

Testing film exposure and absolute dose correction

2. The best exposure dose for the XV-2 verification film was determined by the following procedures and using the OD-Dose the dose response curve. This determination has to be considered for all beam energies involved in the experimental combined field.
3. The exposure Monitor Unit was calculated using the protocol of Khan ([48]Khan, F.M., The Physics of Radiation Therapy, 2nd ed., Williams and Wilkins, Baltimore, 1994) plus an energy dependence factor (F_{exp})

$$MU = \frac{D_p}{k \cdot TPR \cdot S_c \cdot S_p \cdot \left(\frac{SCD}{SPD}\right)^2 \cdot F_T \cdot F_w \cdot OAR_d} \times F_{\exp}$$

Where

MU – monitor unit of exposure

D_p – prescription dose of the beam

K – dose per MU calibration of the accelerator

TPR – tissue-phantom ratio

S_c – collimator scatter factor

S_p – phantom scatter factor

SCD – source to calibration point distance

SPD – source to reference point distance

F_T – transmission factor for any beam attenuator between the collimator and the patient surface

F_w – wedge factor

OAR_d – off-axis ratio for irregular field

F_{exp} – Film exposure correction factor for different energies

4. F_{exp} was calculated for each beam energy using a three degree polynomial curve fitting to the GSV-Dose response. One of the beams is chosen as the reference beam:

$$F_{\exp} = \frac{a_{ref} + b_{ref} \times D_p + c_{ref} \times D_p^2 + d_{ref} \times D_p^3}{a_{\exp} + b_{\exp} \times D_p + c_{\exp} \times D_p^2 + d_{\exp} \times D_p^3}$$

Where C_{ref} represents the coefficient for the reference beam response, and C_{exp} is for the coefficients of second beam in combined field.

Theraplan treatment planning system calculation

The solid water equivalent slab phantom was modelled in the planning system. The junction field was designed according to the test film set up with same entry prescription doses. The junction field planning calculation was performed for 6MV + 9MeV, 6MV + 9MeV, and 6MV + 16MeV photon and electron combined beam plans.

TLD point dose profile comparison measurement

The TLD rod was set up in a solid phantom with the same build-up depth as the film test. 45 rods were parallel lined up in specially designed perspex TLD rod line holder. The TLD rods were separated by 3mm and 1.5mm distance at the centre of the field junction in order to catch more junction dose points. (Figure 15.5) Exposed rods were read by Harshaw TLD reader and each rod individually calibrated with sensitivity factor, reading linearity response curve, and control component readings. The measurements were taken separately for each individual beam with the same setting. The readings were then combined to the a absorbed dose profile. Since this method used a single rod for each measurement point, the profile curve data contains high noise, in order to reduce the noise level for this single reading TLD curve, each measurement was repeated twice.

15.2.3 Results

TLD measurement profile

Figure 15.16 shows the overlaying of profile curves for a multiple beam junction of combined 6MV X-ray and 12MeV Electron. A dose planning profile was confirmed by ionisation point dose measurements. The TLD reading was then linked to the absolute dose profile and shows a higher noise level with an uncertainty range of 3~5%. The profile shape and the dose value match dose planning calculation profile and well show that the TLD result would be accurate enough to be used for the comparison check with the film analysis.

Solid slab phantom lateral scatter reduction for the film dosimetry

Figure 15.6 compares the film dosimetry equivalent depth dose curve taken with same beam, same energy and field size, but with different beam entry

angles from 0 ~ 7°. The curves are overlaid for different beam entry angles. The curve with the zero entry angle (the beam direction parallel to the film setting) contains higher scatter than other curves with different entry angles. As the beam entry angle is increased, the lateral scatter gets reduced, and the film analysis result improves in comparison with water measurement results.

Film OD-DOSE response calibration and energy dependence correction

The OD-Dose response curve for different beam type and energies shows that the discrepancy in dose is up to 10%. Figure 15.10 compares the film response to 6MV X-ray, 9MeV and 12MeV Electrons. The electron beam has higher response compared with a photon beam. It is clear that the film shows an over response to electron beams compared to photon beams of the same dose of irradiation. This higher response could be caused by scattered contamination at shallow depth of electron beam fields. Each energy and type of beam has its own dose response curve. However, the response curve shape remains essentially unchanged. In Figure 15.13, the beam and energy dependence of film response are shown for different given doses. The result shows that density changes in response to different exposure for 6MV photon, 9MeV and 12MeV electrons. The maximum discrepancy is less then 1.0%.

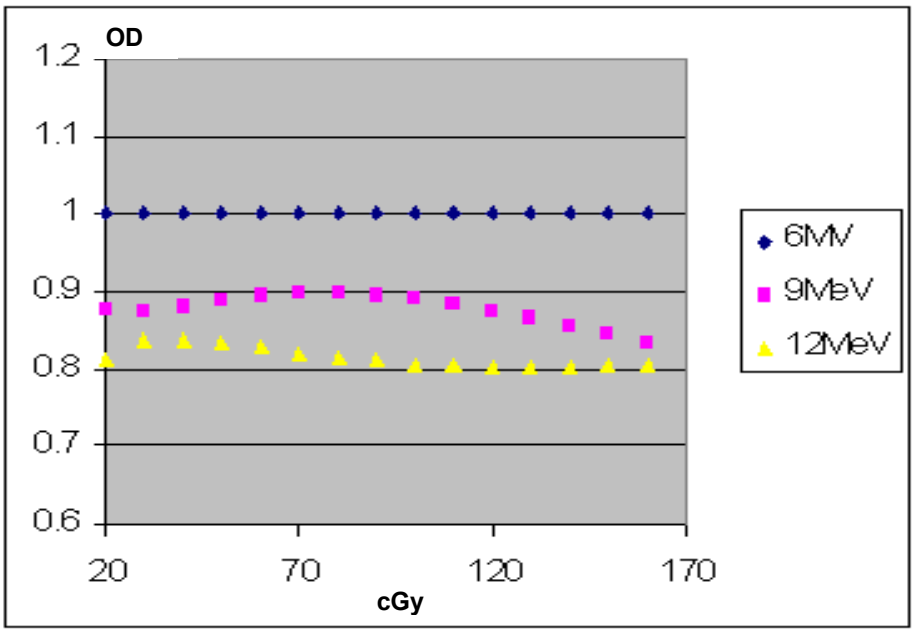

Figure 15. 13. Evaluate the uncertainty range by calculating the factors for difference dose region.

15.3 Exposure rate correction

Figure 15.14 shows an example of an exposure correction applied before the film is exposed for the combined beam field compared with the profile curve of the same field without exposure correction. The beam type and energy dependency over response showed significant improvement after the correction was applied.

Pre-exposure corrected film dosimetry result compared with planning calculation and TLD measurements

In Figures 15.17, 15.18, and 15.19, multiple beam combined field profiles are compared for different combination of 6MV + 9MeV, 6MV + 12MeV and 6MV + 16MeV photon and electrons. Each comparison field is overlaid with the curves of planning calculation (TPS), TLD rod measurement and film dosimetry results with and without pre-exposure correction. All the profile curves were investigated with same field setting and exposure, and all measurements converted into the equivalent absolute dose. The TLD measurement result is used to confirm the correctness of planning calculation. The discrepancy between TLD and the planning result in this case is within 1.0%. The disagreement between the film dosimetry curve before the exposure correction and after the exposure correction is up to 10%. The film dosimetry profile curves also give higher junction dose peak values compared with both planning and TLD results.

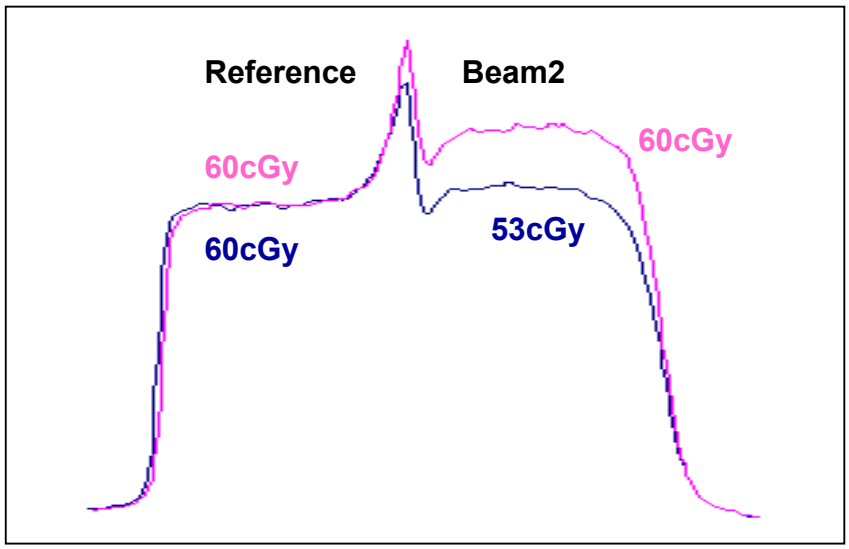

Figure 15. 14. Comparison of film dosimetry beam profile curves. Without exposure correction, beam 2 shows an over response the dose compare with reference beam. With the exposure correction, both show the significant improvement.

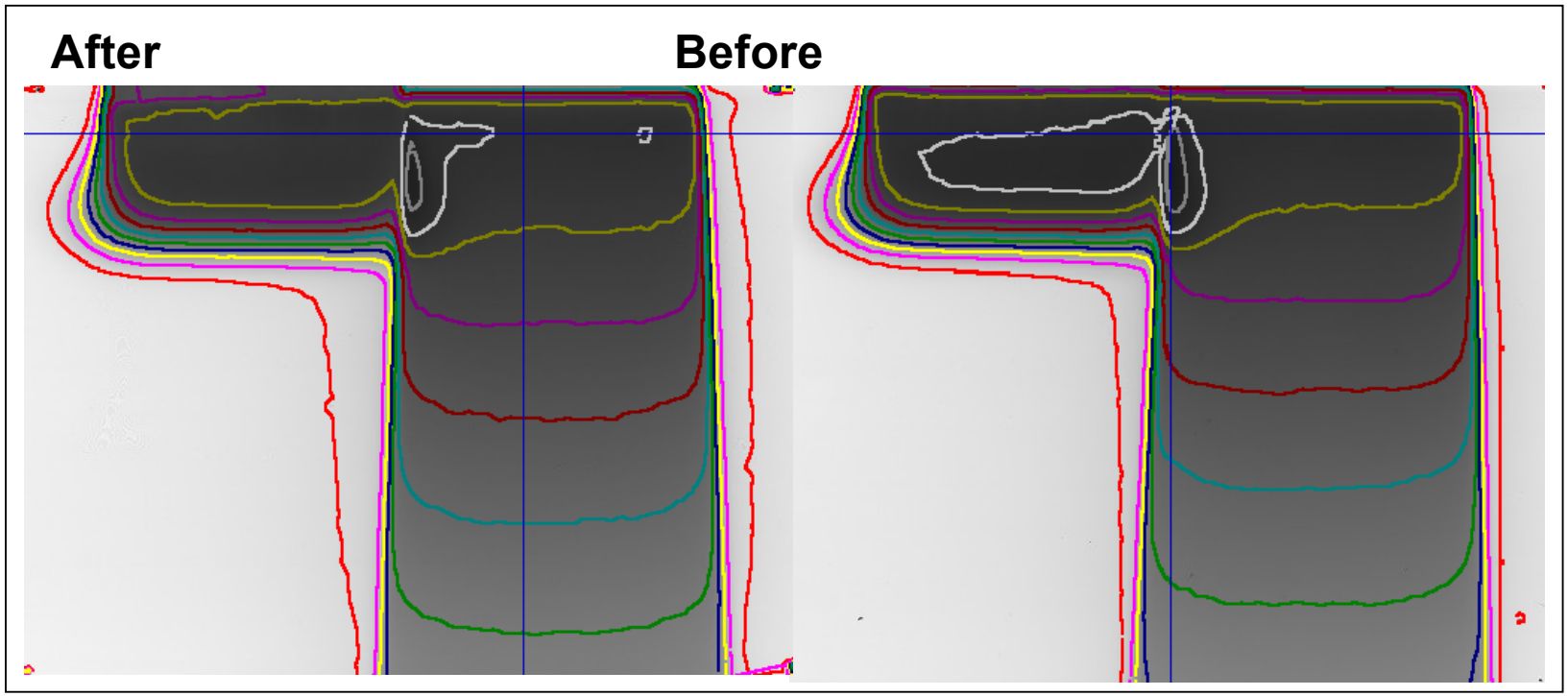

Figure 15. 15. Compare the differences against the reference isodose plotted by film densitometry program. Before the exposure dose correction, election region shows a hot high distribution area. After the exposure correction, both beam dose distribution get balanced.

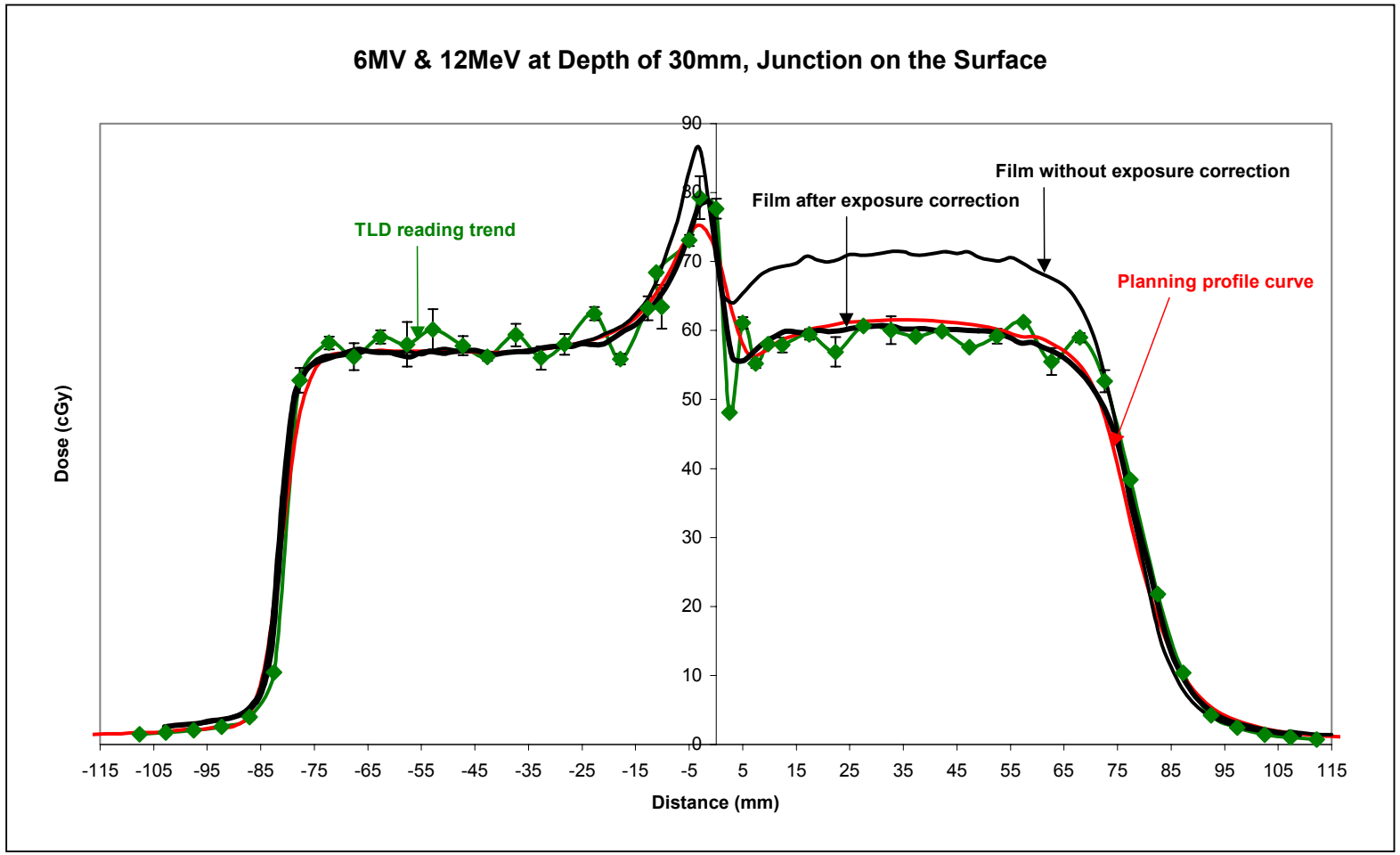

Figure 15. 16. Profile curves overlapping for the comparison. Profile investigated from Theraplan planning calculation (red), TLD reading chart (green) and film dosimetry profile curves before and after the exposure correction (black).

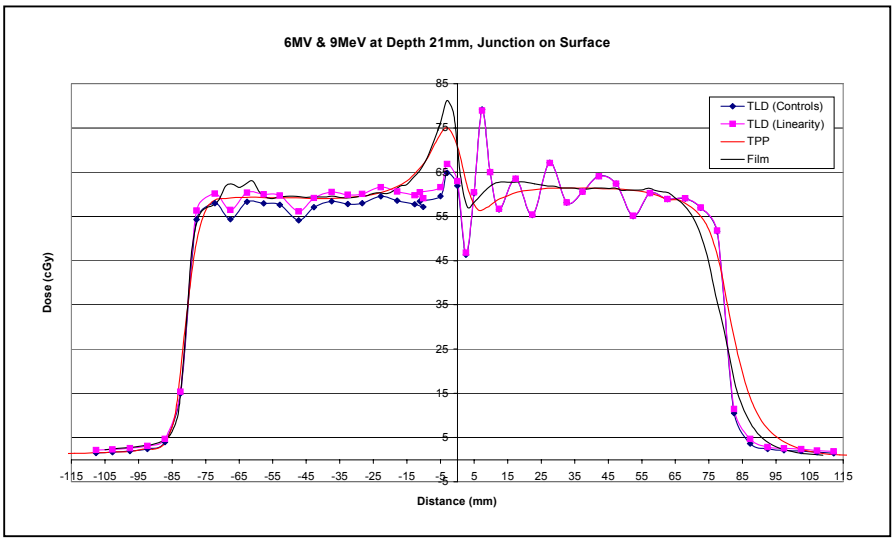

Figure 15. 17. Comparison for 6MV Photon + 9MeV Electron beams

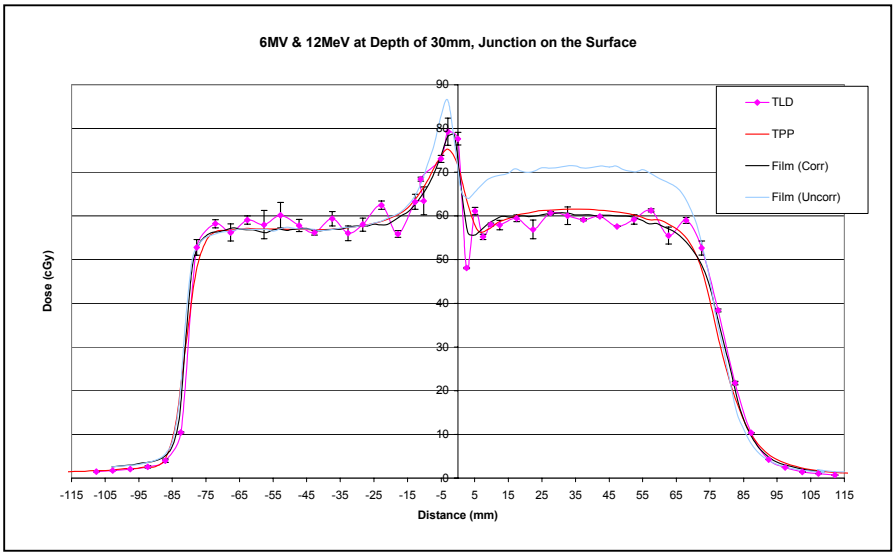

Figure 15. 18. Comparison for 6MV Photon + 12MeV Electron beams

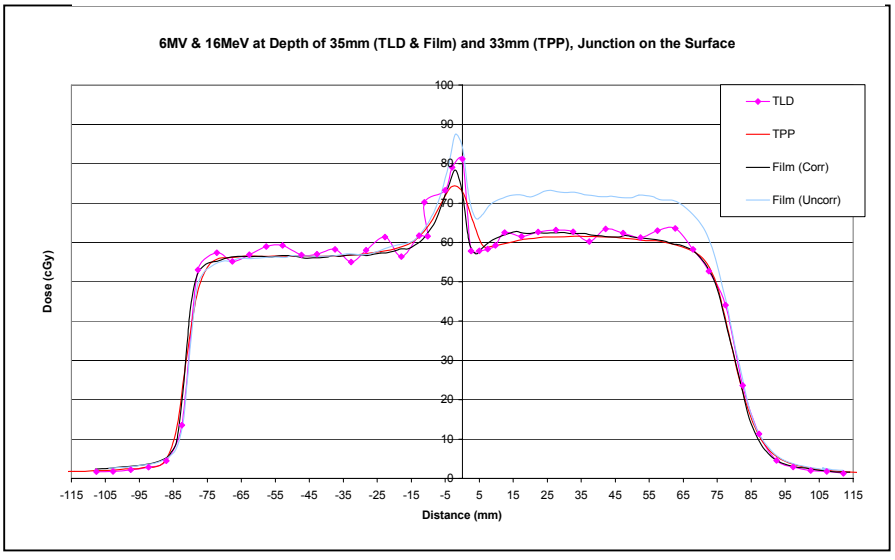

Figure 15. 19. Comparison for 6MV Photon + 16MeV Electron beams

15.4 Discussion

Although the TLD profile curve made from measurements gives higher noise level, the result shows the TLD technique provides good reliability and reproducibility for the point dose check. However, the TLD check is very time consuming in chip loading, dose correction and annealing. So while the TLD can be used as a very good method for the planning calculation check in point dose, but if It be used for the detail dose distribution checks either profile or isodose, in a routine QA purpose it would be very difficult to perform. In this study, the TLD technique is used to confirm the correctness of film calibration and to provide extra evidence to support the film dosimetry analysis results.

For film sandwiched in the solid phantom for a depth dose distribution check, direct beam entry affects the film dosimetry result by increasing the lateral scatter and producing incorrect build up effects. The result shows this perturbation caused by the film setup can be overcome by using a slight change of beam entry angle. If the beam entry is changed by using a 5 degree gantry angle, the depth distance changes for 100cm SSD could only be 1mm. For this small amount of distance change in film dosimetry is negligible.

By comparing the film profile analysis result, the difference shows that without any exposure correction, film dosimetry cannot be used for the multiple beam combined field dosimetry check. Different film density responses are observed with different beam type and energies superimposed one film. After the film is processed, it is not able to use any single energy OD-DOSE response curve to convert the equivalent dose from the density value for all the beams in the field. However, the OD-DOSE response curve which depends on the film quality, the film characteristics, beam type and energy. The changes mainly affect the signal range but not the curve shape in significance. Each curve can be simply adjusted by a response correction factor which is created by comparing the response curves for all the beams.

The comparisons show that the pre-exposure response correction improves the film dosimetry result significantly compared with both planning calculation and TLD measurement. If the film dosimetry can be possibly used for the multiple combined beam planning quality assurance checks, the advantage of the film dosimetry allows the physical visualisation of for any layer's dose distribution, significance in higher resolution, and more sensitive to the junction hot and cold spots dose checks. Also the film dosimetry is easy to set up, flexible, and provides a means to visualise dose distribution information over the fields.

Nowadays radiotherapy technology has developed to use increasingly complicated multiple beam-combined fields, dynamical treatment field and 3-D planning. Most dosimetry techniques have difficulty or unable to handle the physical measurement necessary to perform the quality assurance check of the planning calculation. From this study result we can see that by using good film analysis equipment, the signal noise can be reduced. By managing the film exposure and development using reliable processing identical conditions and time, the variations can be reduced to a very low level. By using well developed software programs, and calibrating the dose response signal carefully, accurate equivalent dose conversion and good visualised dose distribution information can be obtained.

If a single film is exposed by more than one beam type or energy, current film calibration technique cannot be used to convert the density reading to the equivalent dose correctly. Without exposure beam type and energy dependence correction, the film analysis result obviously be used to represent the real dose distribution. However, if we can give appropriate exposure dose correction before the film is taken, we can see that the improvement is significant. All the correction sequences are not difficult to perform clinically, one only needs to be careful to mention that the exposure correction should only be performed for the film check, not for any other calibration exposure or the treatment. For each planning check, we can take the optical density to dose response check for each involved beam individually. The curves can be compared to calculate an appropriate exposure dose correction factor. The

film can then be exposed using the corrected dose. By using an exposure correction method, the beam response dependence can possibly be overcome. The film analysis can use the reference OD-DOSE response curve to perform the equivalent dose conversion over the film image. By correcting the dose delivered from each beam we obtain a film that can be read without applying further corrections to give a realistic dose distribution.

15.5 Conclusions

Multiple beam type and energy combined fields are often clinically used. The physical dose distribution check is difficult to perform using ordinary dosimetry techniques. Ionisation or TLD techniques can be used for accurate point dose checking but are complex of set up and time consuming. Scanning techniques can only be performed for single beam scans. Film dosimetry is a simple and quick visualisation tool to verify treatment plans. However, different optical density responses for different beam type and energy make film dosimetry difficult to be used without correction for the multiple beam fields. This study has suggested it is possible to correct the equivalent dose for the exposure to make the optical density to dose conversion become possibly achievable. To conclude points: 1. choose one of the calibrated OD-DOSE response curves from the combined beams; 2. determine it as the reference in the combined beam group; and 3. correct the exposure rate for all other beams involved in the field; all these would make the optical densities responded on a single film get adjusted to maintain the optical density represent the planned dose in proportion, the film analysis then become possibly be performed and optical density value can be converted into the equivalent dose properly. With the simple setting up and visualisation resulting from film dosimetry, film dosimetry could become possible to be used clinically by physicists for the routine QA tool for the multiple beam combined field planning checks.

Chapter 16 High Dose Rate Brachytherapy Quality Assurance - Computerized Film Dosimetry Techniques used in HDR Brachytherapy Unit QA Checks

(Presentation for EPSM2001 conference)
(Wang Y, Cross P, Zealey W, Computerised film dosimetry applied for HDR brachytherapy unit, EPSM-2001, Australian & New Zealand wide college conference, 2001)

Abstract
A HDR brachytherapy unit quality assurance check method has been studied and developed by using film dosimetry techniques in order to assess accuracy and precision of source positioning and dwell times. Usually HDR source delivery accuracy is checked by visualisation of an autoradiograph of programmed dwell positions in a parallel linear array. In this case the developed films were analysed by computer methods. In addition, an investigation was made of curved path source delivery in an autoradiographic device with multiple, variable radial catheter channels. A computer analysis of a single film can demonstrate accuracy of source position, dwell time and time controlling linearity. This study has shown that a time change of 0.1s can result in an 8% change in dose for a given dwell position. Computerised film dosimetry techniques for HDR source delivery can provide a greater degree of accuracy and precision for position and time determination compared to direct visualisation alone. The limitations of the HDR unit for source delivery to implants of curved geometry can also be determined and consequently guide the clinician in implant design.

16.1 Introduction

The main part of routine quality assurance task performed for HDR-Brachytherapy unit includes checks for source activity, air-Kerma strength, effective-dose distribution length, source positioning accuracy and dwell-time control accuracy. The source activity and air-Kerma strength can be effectively measured by ionization measurement technique using the well-type ionization chamber since the publication of AAPM report 1994. The source delivery position and dwell-time accuracy is commonly checked by taking the verification film set into specially designed QA film setup phantom. The accuracy correctness of the source delivery position is checked by direct visualization. Since the isotope source used for the HDR unit (Ir-192), is characterized by very high local dose intensity and a 74 days half-life, a dose up to 20Gy/fraction can be delivered in

only 10~15 minutes. A 0.1 second dwell-time could produce up to 20~30cGy dose in the tissue surrounding the source at 1mm distance. The agreement between the planning calculation and physical source position and dwell-time must be checked as it is a very important part of QA tasks.

Although, the position and exposure accuracy could be affected by uncertainties in the equipment timing control system, clinical issues could also be of significance. Examples of equipment problems include those occurring in mechanical linkages and motor drive timing, and problems resulting from repeated cleaning and sterilizing the source transfer tubes and applicators. The damage caused by any of above could reduce the accuracy of positioning and speed of motion, and produce a varying dose in different channels.

Performing a routine QA film check on the position accuracy, using visual methods allows the physicist to recognize the position variations greater than 1.5mm. The change in film intensity produced by dwell-time change must be higher than 0.1 to 0.3 optical density (around 5~10cGy equivalent dose range) to be recognized by the human eye. So the visualization method result is limited except for gross deviations.

Wong et al in 2001 has reported an effective transit dose measurement algorithm via using well-type ionization chamber. By using this method, the dwell-time accuracy can be more accurately determined. However, the check must be performed one channel at a time, and checking all 18 transfer-tubes is time consuming.

For this study, it is intended to develop a film analysis technique to perform a quick, simple, and efficient routine check of source delivery position accuracy, dwell time accuracy, as well as dwell time control linearity. A software package is developed to perform the image pixel signal processing, equivalent dose data calibration, and exposure point peak value analysis for all 18 channels.

16.2 Experimental

Method and material

The experiment focused on using Kodak X-Omat XV-2 verification film set in an 18 channel film-check phantom. All the channels are connected to the HDR unit via the source transfer tubes. The source delivery position and dwell time to each channel are programmed via the console TCS (Treatment Control System) according to the QA analysis performance protocol.

The calibration film was made for a sequence of dwell times using every third channel. The dwell times for calibration are chosen to cover the dynamic range of the film in 0.1second intervals. A separate count of exposure was taken with a median exposure value to allow scatter correction. The density reading from the control film was compared with the density reading of that exposure on the density to radiation dose response calibration film. The response curve was corrected by the ratio of differences between the response curve and control reading. (Fig 16.1)

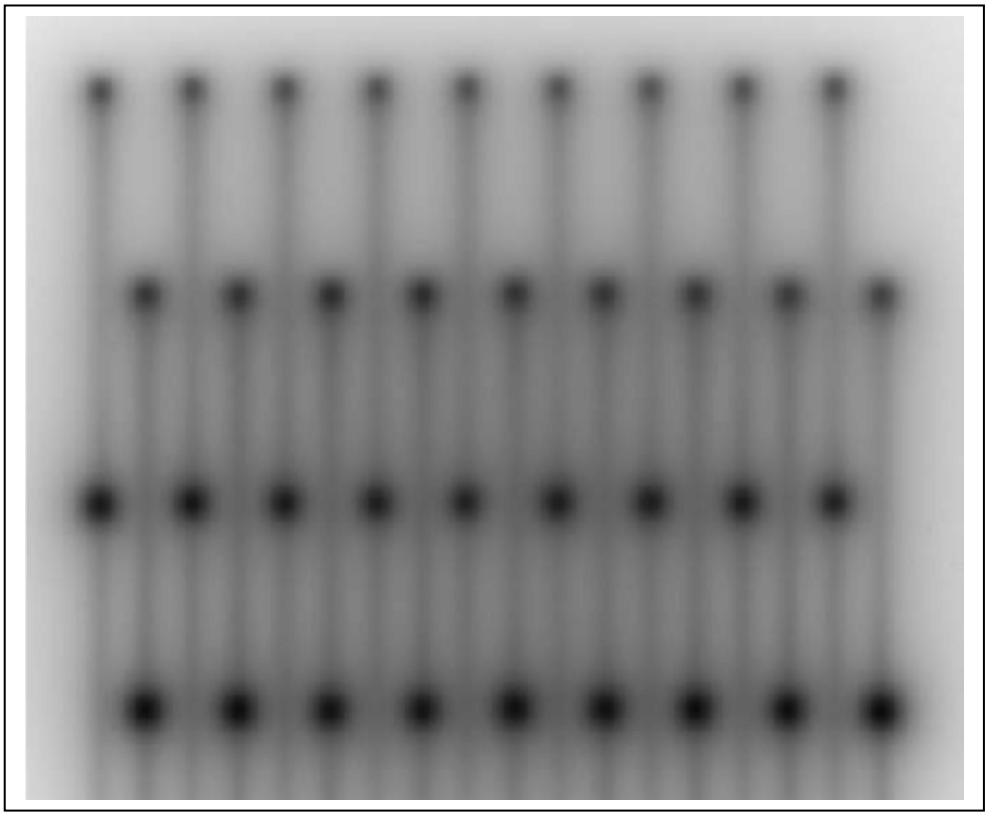

Figure 16.1 Position check performed using a flat phantom, and the dwell time to each position line used different.

The test film was exposed for all channels with two dwell positions on each channel giving a 5cm distance between each dwell position. Even channels are offset by 2.5cm from odd channels (Figure 16.4.)

The dependence of source motion and dwell time on the transfer tubes' bending radius (curvature) was tested by setting up film in a specially designed Lucite phantom with different tube radii of curvature. The radii curvature designed for the phantom range from 3.0cm to 10.0cm in increments of 2.0cm. A straight transfer tube used as a reference (Figure 16.2) the same channel and application tube was used for all the measurements. Each exposure used same dwell time with a different radius of curvature and the exposures were made one after another. The same experiment has performed on two different units in St. Vincent's Hospital Sydney and Austin & Repatriation Cancer Centre in Victoria using two similar phantoms with slightly different bending angles. (Figure 16.2)

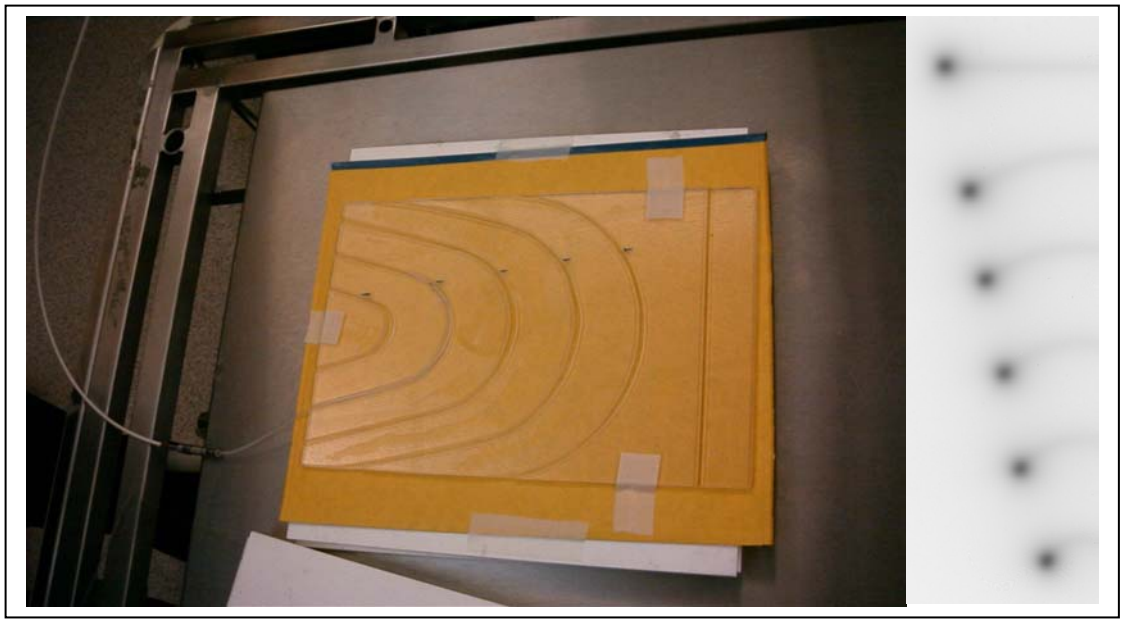

Figure 16.2 Flat phantom designed with different bending angle, to test the dwell time affected by different transfer tube bending radius.

All films were developed using automatic x-ray film processors. A background film was also processed by using same processor at same time. The films scanned using Umax 2000 computer desktop scanner with transparency adapter. The images were saved as bitmap files.

Software procedures were developed using MS Visual Basic 6.0 version. The functions perform the pixel greyscale value analysis, equivalent dose conversion, and calculation of the corrected response curve. The second part of program includes the analysis of the source positioning accuracy, delivered dose reliability and dwell time linearity.

In the film signal calibration, the peak pixel greyscale value for each point is analyzed. The exposed dose is calculated according to the source air Kermaq strength, corresponding to a dwell time setting, decay correction and film buildup distance. A plot of dose and uncorrected greyscale value, a polynomial curve was used to fit the calibration data. The reading from background film is used as the zero exposure value and the reading from control film is used to correct for scatter between the exposure points. (Fig 16.3)

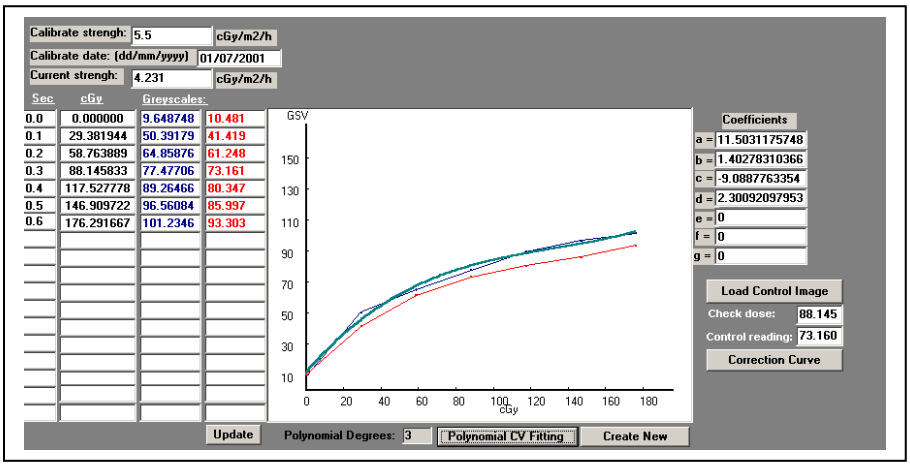

Figure 16.3 The reading from background film is used as the zero exposure value and the reading from control film is used to correct for scatter between the exposure points

The analysis of position and dwell time process is performed by digitizing the film. The program then performs an equivalent dose value conversion by using the corrected signal to irradiation dose curve. Isodose contours are superimposed over the image. The peak value of each dwell position is located and record the X, Y position and Dose recorded.

16.3 Results

The following effects were noted:

Dwell time accuracy affected by radius of curvature of the transfer tube.

The result for bending angle dependence test is shown in Figure 16.4. As the radius of the curvature decreases, the grayscale value reading decreases. For a change in radius of 2cm, the pixel intensity reading can be affected by 2~5%. This result is similar for both St. Vincent's Hospital Sydney and Austin & Repatriation Hospital Melbourne.

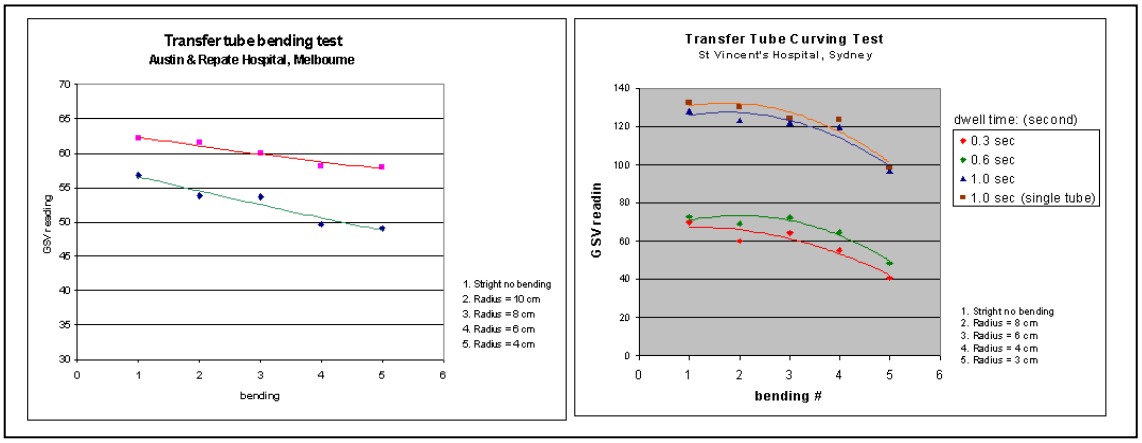

Figure 16.4 The radius of the curvature decreases, the greyscale value reading decreases. For a change in radius of 2cm, the pixel intensity reading can be affected by 2~5%.

1. Position accuracy.

The X and Y pixel position for the peak value analyzed for a source delivery position marked on the image to display the source delivery position, according to the program setting, each traveling direction Y value is compared and the maximum discrepancy is displayed. As dots for all the source positions on the screen are linked out a line-chart. The ideal dwell

position is also marked as background cross-line on each dwell position. The maximum of base line position is printed as maximum source delivery position error and compared with the tolerance value. (Figure 16.5)

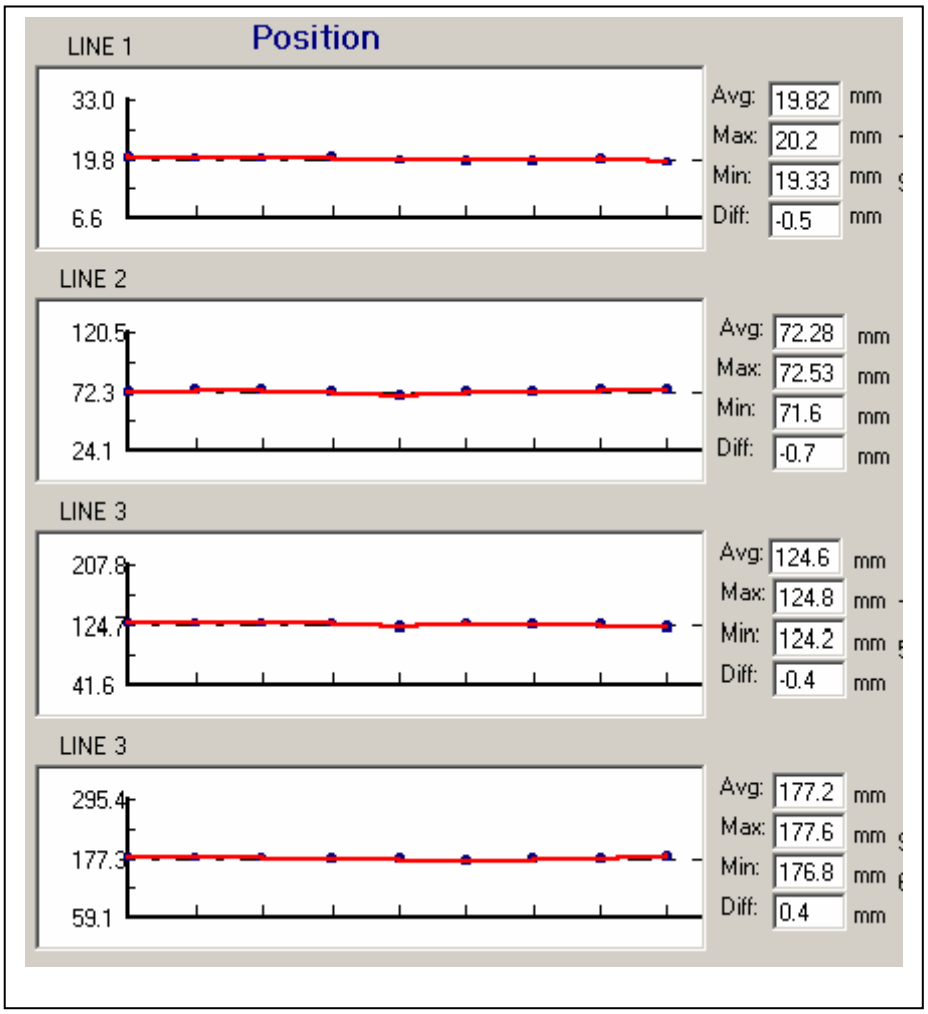

Figure 16.5. Source delivery position accuracy check result

2. **Dwell time accuracy.**

Dwell time accuracy is analyzed by comparing the peak value of each source delivered point with the baseline value, which is the polynomial curve fitting line of the average range value for all channels. (Figure 16.6) Since there is scatter inteperece between the channels, the base line mostly is a curve not a straight line. That is because the channel on each side might receive scatters from only one direction, up to 10% reading value affected by the scatter

especially for the higher exposure line. The scatter made from the neighbour channel source transit could also affect the readings. The maximum discrepancy of each individual range value compared with baseline is displayed and also compared with the tolerance.

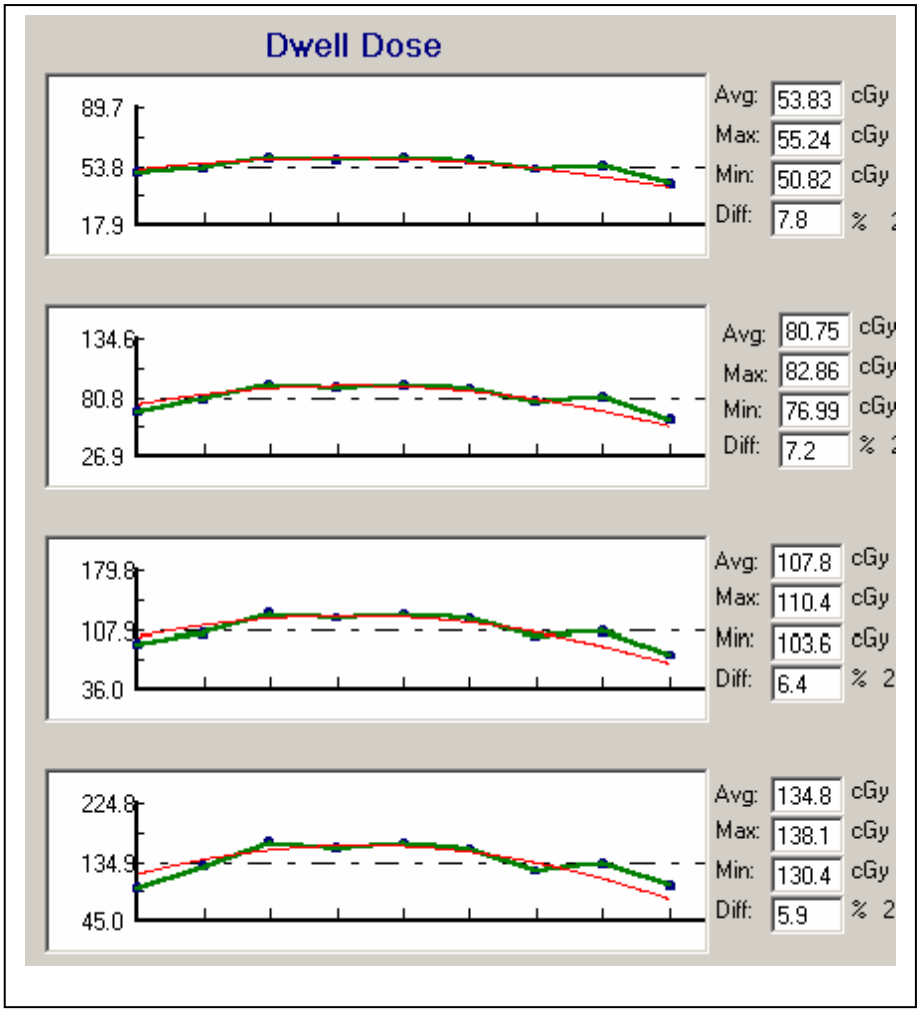

Figure 16.6. Source delivery dwell time accuracy check result

3. **Dose range linearity.**

   The average peak value of the percentage dose for each horizontal exposure line is displayed as a line chart and compared a linear fit made to the data. Scatter rises to high into the primary reading in high exposure line, the linearity of dose converted shows a higher figure up to 5% discrepancy to the linear coefficient line. (Figure 16.7)

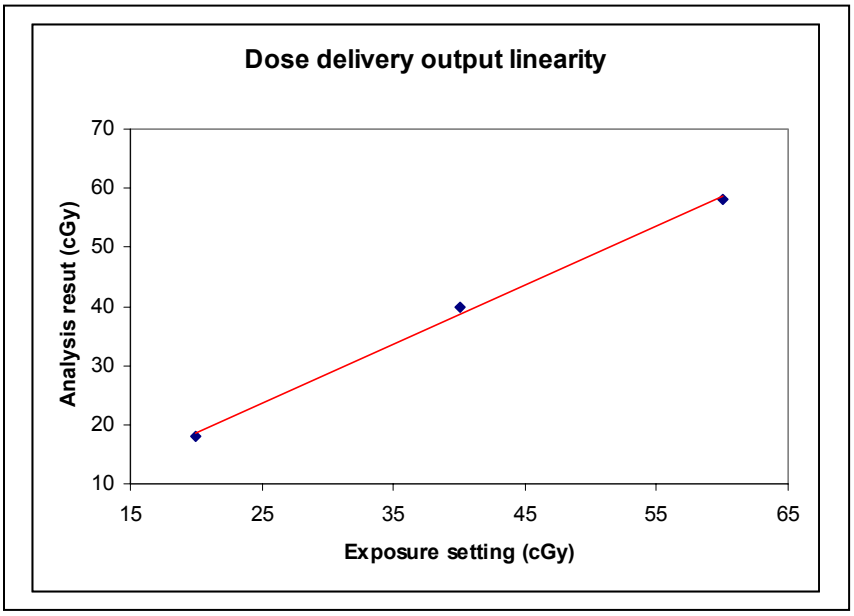

Figure 16.7. Source delivery dose range linearity checked by three different dwell times

16.4 Discussion

The reliability of using film dosimetry is always a common concern. That because the uncertainty issues included film quality, processing artifacts, and other technical operation inconsistency make the results could be up to 5% in accuracy. The result of this study shows many uncertainties of film dosimetry could be able to get overcome if we calibrate the film more carefully. And by using film analysis technique, the transfer tube quality over all channels can easily be checked at same time.

The PSGV-Dose response curve processing helped to determine the correct exposure dose level for the used film. It also provides signal to equivalent dose conversion data. Although the response curve is very sensitively influenced by different film processing periods and conditions, the shape of curve will probably not be changed significantly. However, if the exposure of response curve made on a single film, the reading for the point could be influenced by the lateral scatter created by the neighbour exposure points. This influence affecting the curve

shape change should be taken account and should be effectively corrected if the curve exposure does not use separate film-strips.

The importance of source delivery positioning accuracy check is suggested by this study. That is because the experimental result shows that the positioning accuracy could be affected by the HDR unit mechanical movement system accuracy and the transform tube quality. After each source change and service, the possibility arises that the positioning accuracy change needs to be checked by the isodose peak value comparison, as the human eye's visual perception of the film would not be able to determine a position change of less than 1.5mm.

From the result, we can see the delivery dose set by the dwell time is more varied then we expected. That is because the high-dose rate characteristic of the source makes the dwell time become sensitive. We must be notified of the dwell time accuracy within 0.1s, because any of the tube bending, dirty transmission path inside the tube can make a lot difference in the physical dwell time change.

16.5 Conclusion

The film dosimetry program function developed for the HDR quality assurance check by this study project provides a very simple and effective way to perform the HDR unit QA checks regularly, after each source change and mechanical service. By running a pre-set TCS source delivery program and taking only one film, the source delivery positioning accuracy, dwell time accuracy and dose output control linearity can be checked by film dosimetry analysis. The film dosimetry accuracy is of a significantly high level of accuracy because the control film is used for the dose response curve calibration, and full background film is also used to remove the background fog value pixel by pixel. The analysis results can be printed in text and graphical report.

Chapter 17 Summary and Conclusion

This research program commenced in 1998 to investigate digital imaging techniques instead of analog signal densitometry for use in a quality assurance (QA) program for radiotherapy treatment units. The study focused on using computer desktop scanners to create bitmap images of radiographic films. The dosimetry calibration for an irradiated film image is converted into grayscale values and correlated with corresponding radiation doses.

Based on a paper submitted in the early stage of the program, and published in the Journal of the Australasian College of Physical Scientists and Engineers in Medicine in 1998, the calibration procedure is separated into three parts consisting of

- Calibration of optical densities using a calibration film
- Correction for film development and processing effects
- Conversion of QA film image densities to radiation doses

Software has been developed for calibration, film development/processing and film dosimetry signal calibration. The program is coded using Microsoft Visual Basic version 6.0, with object oriented development structure and graphical user interface (GUI).

The digital data obtained from a commercial computer desktop scanner with transparency adaptor was analyzed to study the effect of the pixel resolution, signal format depth, dynamic range, contrast and brightness setting, light source intensity distribution over the scanning area, and CCD detector warm up effects on the accuracy of the calibration.

The film development and processing have been examined for processor dependence, chemical, temperature, artifacts and latent image effects. The film

dosimetry signal was corrected with both scanning signal and processing signal factors before conversion into an equivalent dose value.

The clinical dosimetry tests for this project included multiple combined beam film dosimetry, dynamic radiation field dose distribution analysis, brachytherapy unit dose delivery quality assurance checks and three-dimensional planning dose distribution checks.

The results of this work are reported in this thesis and in recent conference presentations. Detailed discussions include:

- A review of existing QA procedures.
- A study and literature review for film densitometry technologies
- The tasks required to solve film dosimetry problems
- The design of suitable phantoms used for different film dosimetry purpose for this study. These include wedge shaped phantoms for electron and photon energy checks, water phantoms designed for depth dose comparison test with ionization chamber techniques and cylindrical and ball shape phantoms designed for 2D and 3D radiation field film dosimetry.
- Film analysis software tools. The functions include bitmap image display, signal correction and data interpolation, curve drawing and curve fitting, physical scan distance conversion and coordinate determination, isodose tracking and plotting, three-dimensional chart displaying, and data management to store, retrieve and output the analysis results.
- Clinical applications

A number of interesting effects associated with the effect of low energy scattered radiation on film background have been studied. These were previously thought to be associated with the Cerenkov effect. However, the experiments in this study have shown that the scatter occurs in both forward and backward directions, and passes though both opaque paper and transparent plastic

material. These characteristics suggest that the background is due to low energy scattered radiation generated from the film grain emulsion layer. It can be simply corrected by comparing the background film with and without field irradiation.

Film based procedures have also been developed for dynamic fields, multiple combined beam fields and three-dimensional field dose distribution checks commonly verified by ionization or thermo-luminescent (TLD) methods. Film has the advantage of quickly showing the dose distribution in a simple setup, but hitherto has lacked the accuracy of conventional dosimetric techniques. This study has developed improvements in the accuracy of film dosimetry by correcting individual image pixel values for optical density (OD) - dose response, and film envelope material effects.

The film method can also be applied to high dose rate brachytherapy QA. Experiments focused on the determination of the accuracy of the dwell position and time control. Since very high dose activity sources are used in brachytherapy, mechanical errors or source transfer tube integrity can affect the dwell time by up to 0.05 ~ 0.1 seconds, resulting in up to 30cGy deviations from the prescribed dose. These changes are commonly be ignored.

With the completion of this study, a film dosimetry calibration package became available for routine use in both external beam and brachytherapy irradiation dose distribution checks.

The software functions developed in this study have demonstrated that film dosimetry is an easy, fast and economical technique. It can overcome the traditional uncertainties and unreliability to make film dosimetry perform more accurate QA and three-dimensional radiotherapy planning dose distribution checks.

As a completed package, the software was developed with all the functions needed to send texts and graphic results to a printer to make a well formatted

analysis report. Both the result values and image data can be stored and reloaded for review and modification purposes

The software becomes a practical tool an easy to use operation on a PC with a variety of desktop scanners with light source adaptors. Using this package, more accurate, and time saving film dosimetry techniques become clinically available now for verification of the newly introduced three-dimensional conformal radiotherapy treatment techniques.

The clinical testing performed for this project included light vs radiation field coincidence check, dose distribution isodose curve and profile curve processes, combined radiation field involved with different beam type and energies, dynamic wedge fields, and the fields for the intensity modulated radiotherapy (IMRT). The experimental result has compared with TLD and ionization measurement. Although some of the result over 3% be still higher than the tolerance of AAPM documented in TG-53 (American Association of Physicists in Medicine, Quality Assurance for Clinical Radiotherapy Treatment Planning, Report of AAPM Radiation Therapy Committee Task Group 53, Med. Phys. vol. 25, issue 10, October 1998), however, the accuracy for the film dosimetry has got improved by this study on reducing the common film dosimetry uncertainty level.

Conclusion

The aims of this project were to develop a simple technique for film dosimetry, and intended to reduce the densitometry equipment costs. By using common computer desktop photographic scanner to evaluate the possibility and reliability, a software package has developed to handle the signal calibration, correction and clinical dosimetry analysis. Using the software developed by this study, the radiation field quality assurance and treatment planning dose verification can be performed by digital image technique with simple, low cost and reliably using computer desktop document scanners.

Film quality can be evaluated by the OD-DOSE calibration function and the evaluation results can provide suggestion to the radiation oncology physicists to determine weather the film is suitable be used for the film dosimetry.

A scanner can be tested, evaluated and calibrated for the film dosimetry with the calibration of signal to radiation dose response include calibrate the optical density dynamic range by setting the brightness, control the signal noise level by changing the bitmap data format and set the signal response linearity by adjusting the contrast settings.

The software function helps user to analyze the beam type dependence, field size dependence, beam to film entry angle dependence and provide the factors to reduce the film dosimetry uncertainty level by performing the reading correction. By performing these corrections, general/average film dosimetry uncertainty level has reduced from 5-10% commonly to 2 – 4%.

This study addressed the technique to improve the accuracy of film dosimetry using digital image processing technique. The experimental result shows that the signal obtained from densitometry equipment must get corrected and calibrated before the readings can be used to represent the clinical dose. Bad scan signal alignment, unstable scanner brightness/contrast setting causes faulty film dosimetry results.

References

AAPM, A protocol for the determination of absorbed dose from high-energy photon and electron beams. Task Group No. 21, Med. Phys. 106), 741-771, 1983

AAPM, Comprehensive QA for radiation oncology: report of the Radiation Therapy Task Group 40, Med. Phys. 21:581-618, 1994

AAPM, protocol for clinical reference dosimetry of high-energy photon and electron beams, Task Group No. 51, Med. Phys. 26, 1847-1870, 1999

ACPSEM, An recommendation in quality assurance of radiotherapy equipment, APESM, August, 1997

Auxier, J. A, Dosimetry A. Physical Dose Estimates for A-bomb Survivors - Studies at Oak Ridge, U.S.A, Health Physics. 38(6):1199-1210, June 1980

Arthur G. Hans, Susan M, Jaskulski, The Basics of Film Processing in Medical Imaging, Medical Physics Publishing, 1997

Da Capo Press, The Pencil of Nature, New York 1969

Dempsey, J.F., Low, D.A., Kirov, A.S. and Williamson, J.F., *Quantitative optical densitometry with scanning-laser film digitizers*, Med. Phys., 26: 1721 - 1731, 1999.

Dodd R. J., Precise Stellar Positions Osing GALAXY – Machine Measures of a Schmorl Plate, Astronomy Journal, v77. No 4. pp 306-311, 1972

Joyce Loebl, Microdensitometer, Journal Scientific Instrument, v33, pp127, 1956

Irwin. M, Nutowuntic Plate Measuring Machine, Wrvw.ast.cam.ac.uk/~mike/apmcat, 2003

Dutreix, J. and Dutreix, A., Film Dosimetry of High-Energy Electrons, Annals New York Academy of Sciences 161 Article 1, 1969.

Dutreix J et. al., Exposure Dose Measurements, Phys. Med. Biol. 7 243-244, 1962

Farrow G and Preston D, Simple continuous chart and integrating device for a Joyce-Loebl microdensitometer, Sci. Instrum. 37 347-349, 1960

Ferdnand Hurter and Vero Driffield, "Photochemical Investigations and a New Method of Determination of the Sensitiveness of Photographic Plates", The Journal of the Society of Chemical Industry, May 31, 1890

Granke. R. C, K. A. Wright, W. W. Evans, J. E. Nelson & J. G. Trump, The Film method of tissue dose studies, Amer. J. Roentgen 72: 302 1954

Hambly N. C., Miller L., MacGillivray H. T., Herd J. T. & Cormack W. A.,Monthly Notices of the Royal Astronomical Society, Volume 298 Issue 3 Page 897, August, 1998

Hanbly N.C.; Miller L, MacGillvray. H. T, Gerd J. T, adcoimack W.A, Precision Astronometry with Supor COSMOS, Mon. Notices. Roy. Astra So., 1998

Harmant G. Pierre, Marillier Paul, Some Thought on The World's First Photograph, The Photographic Journal (London: RPS), Vol. 107 (4), 130–40, April 1967

Hedgecoe, John, Complete Guide to Black & White Photography, Sterling Publishing 1996

Heggie et.al., Applied Imaging Technolgy, St. Vincent's Hospital , Melbourne, 2001

Helmut G, Gernsheim A, THE HISTORY OF PHOTOGRAPHY: From the Earliest use of the Camera Obscura in the Eleventh Century up to 1914. First Edition, Oxford Univ. Press, London, 1955

Herschel, W, "Experiments on the refrangibility of the invisible rays of the sun.", Phil Trans. 284, 1800

Holthausen and Hamann, Film Badge Dosimetry in Atmospheric Nuclear Tests, Commission on Engineering and Technical Systems, National Research Council, 1932

Hurter F, and Driffield V, Naturalistic photography and the death of naturalistic photography, Op. cit., BookII, P.105, 1890

IAEA, Absorbed dose determination in external beam radiotherapy, technical report series no. 398, Vienna: international atomic energy agency, 2000

IAEA, Absorbed Dose Determination in Photon and Electron Beams, An International Code of Practice, Technical Report Series [TRS] No. 277, Vienna: International Atomic Energy Agency, 1987

IAEA, The use of plane-parallel ionization chambers in high-energy electron and photon beams, an International Code of Practice for dosimetry IAEA Technical Report Series No. 381, Vienna: International Atomic Energy Agency, 1997

ICRU report No. 35, International Commission on Radiation Units and Measurements, 1984

ICRU report No. 50, Prescribing, Recording, and Reporting Photon Beam Therapy, 1993

ICRU report No. 24, Determination of Absorbed Dose in a Patient Irradiated by Beams of X or Gamma Rays in Radiotherapy Procedures, 1976

IEC Document 976, Medical electron accelerators – functional performance characteristics, International Electronic Committee, 1989

Iliev, Z.P., Chavaudra, J., Bounik, H., and Nguyen, J., Verification rapide de l'energie des faisceaux d'electrons apres intervention technique ou revisions de routine. 23rd Congress of the French Society of Hospital Physics, Poitiers. 3-5 June, 1993

Islam, M.K., Rashid, H., Gaballa, H., Ting, T., and Rosenow, U.F., A simple method of producing depth ionisation data for electron energy constancy check, Med. Phys., 20(1): 187-191, 1993

Jelly, J.V., Cerenkov Radiation and its Applications, Pergamon Press, New York, 1958

Khan, F.M., The Physics of Radiation Therapy, 2nd ed., Williams and Wilkins, Baltimore, 1994

Larry J. Schoaf, The Photographic Art of William Fax Talbot, Princeton University Press, 2000

Macbeth Dersitanelar, www.buckeris.con/mocbeth/history.htm

Metcalfe Peter, Kron Tomas, Hoban Peter, The Physics of Radiotherapy X-rays from Linear Accelerators,Medical Physics publishing 1997

Michael J. Sullivan, Make Your Scanner a Great Design & Production Tool, North Light Books & An Imprint of F.W Publications Inc., 1998

Minet P, Garsou J, Chevalier P, Radiol J B, Research on a plan of treatment of the sinus with fast electrons. Photographic dosimetry, 48(5):572-85, 1965
PDS Derhimelmer www.toastioit /asticnclry/nc_cfc/measuring.html

Pratt N.M., New Problems in Astrometry, pp 299-300, Ad Tucker Pub Reidel, 1974

Robert G. Gann, Desktop Scanners Image quality evaluation, Hewlett-Packard professional books, 1999

Roentgen Wilhelm Conrad , The radiograph of Mrs. Roentgen's hand. Physicist Franz Exner in Vienna, 1896

Sir William Abney, "Investigation of the powers of the prismatic colours to heat and illuminate objects", Phil. Trans. 255, 1800

Suchowerska, N., Davison, A., Drew, J. and Metcalfe, P., The Validity of Using Radiographic Film for Radiotherapy Dosimetry, Australas. Phys. Eng. Sci. Med., 20:20-26, 1997

Suchowerska, N. P Hoban, A Davison and P Metcalfe, Perturbation of radiotherapy beam by radiographic film: measurements and Monte Carlo simulations, 1755-1765, Phys. Med. Biol. 44, 1999

Trevert Edward, Construction of x-ray equipment and conducting experiments, Bubier Publishing, Lynn, MA, 1896

Wang Y, Cross P, An evaluation of a document scanner for film dosimetry application. APESM, Vol 22 No. 1, 1999

Wang Y, Zealey, Cross P, Field segmentation film dosimetry check – Error and discrepancy study, WC2003, (World Congress of Medical Physics) August 2003

Wang Y, Zealey W, Cross P, An investigation of unexpected background value correction in film dosimetry, Conference Australian EPSM-2000 (Engineering Physics and Science in Medicine), Newcastle, NSW, Australia, Nov 2000

Wang.Y, Zealey.W, Cross.P, An investigation into the source of low energy scattered radiation of significance in film dosimetry, APESM, vol. 25, September 2002

Wang Y, Cross P, Zealey W, Computerised film dosimetry applied for HDR brachytherapy unit, EPSM-2001, Australian & New Zealand wide college conference, 2001

Wong P Y Tony, Fernando Wasantha, Johnston N Peter and Bubb F Ian, Transit dose of an Ir-192 high dose rate brachytherapy stepping source, Physics in Medicine and Biology 46(2001) 323-331, 2001

Glossary

AAPM: American Association of Physicists in Medicine

API: windows application interface screen display technique used by Microsoft window series softwares.

Artifacts: artificial marks created by careless carrying film, set up phantom quality or film development procedures on the film image that makes unwanted darkness reaction to the image analysis signal value.

Background value correction: film base fog value and film analysis signal reading from an unexposed film which is developed by same film processing procedure is to be subtracted from film analysis reading signal.

Ball-shape phantom: Special developed ball shape phantom used for 3D planning quality assurance test.

BEQS: Blocked Equivalent Square the equivalent area or square size calculated for irregular field shape

Bit depth: the length of pixel value signal data variable which is formatted in bit sizes in computing design technology.

Bitmap image: computer windows displayed digital image formed by the pixel value in matrix format distribution.

Bpp: Bits per pixel

Build-depth dependence: film optical density response to the irradiation dose differently might cause different OP-Dose converting value change when the film set up in solid phantom with different build up depth.

CCD: film digitiser designed with the technique of Change Coupled Device.

Cerenkov effect: a blue spectrum light discovered by Cerenkov, this blue light might happen on film base to purturbate the film background value.

CIS: Contact image scanner.

Combined field: multiple beam types or energies are used to involve form one irradiation field.

Cylindrical plastic phantom: cylindrical chape solid plastic block set at the collimator and gantry rotation centre for the isocentric dosimetry measurement.

DSNU: Dark signal non-uniformity

Densitometry technique: film darkness density value is measured by analysing the optical density value collected from a transparency detecting sensor.

Density ranges: optical density value used to plot the OD-Dose response curve, and determined as Y coordinate value.

Desktop scanner: a device that captures an image of an object and converts it into a digital light-intensity map for computer processing.

Digital film analysis technique: use digital image technique to process image digital grayscale value for darkness scale and convert to optical density signal.

dpi: (DPI) Dot per inch.

Double scan films: film scan is performed twice with same setup on the desktop scanner with film swapped from irradiated film to an unexposed background film to be used for the whole film background area correction value subtraction process.

Dwell time: a brachytherapy radiation source is programmed to delivery to a position with a certain seconds of time to establish the prescription dose distribution for that point.

Dynamic field: an irradiation field is formed by a dynamical moved radiation source such as Arc, virtual wedge and IMRT treatment techniques.

Dynamic range: the range of scanning signal levels effectively responding the film image darkness range. The dynamical range depends on the design of a scanner signal format bit depth.

EDR film: a model of radiograph film developed by Kodak for lower dose response but higher linearity compare with Kodak XV film, used for 3D treatment planning film dosimetry.

EDW: stand for Enhancement Dynamic Wedge, a virtual wedge beam designed to more the collimator jaw dynamically across the radiation field to form a wedge shape dose distribution in the field.

Energy dependence: By given the same exposure dose, different beam types or energies create different optical density value of darkness responded to the irradiation doses.

Equivalent depth: the film set up using solid phantom, the material density is corrected to the water equivalent and the real build up depth also need to be corrected by the inverse square law factor.

Film calibration: film image optical density signal to be corrected by different non-uniformity factors such as energy dependence, build up dependence, film processing temperature and chemical factors etc.

Film dosimetry: equivalent irradiation dose is measured by the optical density value analysis technique via irradiated film image darkness.

Film densitometer: a device components with a point light source and a light intensity detecting sensor to measure the film darkness transparency value for optical density data processing.

Film dosimetry: expose a radiographic film and analysis the darkness changes by the ruling of optical density and converting the dark intensity into a calibrated equivalent radiation dose value.

Film scanning: film darkness value read by film densitometer mm by mm along a determined straight line or read by a computer scanner on image pixel by pixel to provide a group of optical density value for different point of film image.

Full background image subtraction: when a film scanned by desktop scanner, the signal background value correction can be not only subtracted using single background value but use a double scanned background image to subtract the corresponding background value pixel by pixel.

GIF: bitmap image contain a maximum of 256 colours with an 8-bit palette though, and losslessly compress 40% of image size compare with BMP format image file.

Greyscale value (GSV): the bitmap image pixel value in Windows software is formatted into different darkness response value levels. Common greyscale level format for most of PC is 0 to 255.

GSV-Dose relationship: greyscale value to irradiation dose signal response relationship plotted as a trend curve chart.

GUI: Graphic User Interface

HDR brachytherapy: High Dose Rate brachytherapy

IAEA: International Atomic and Energy Association.

ICRU: International Committee of Radiation Unit

ICRP: International Committee of Radiation Protection

Image processing: an object scanned by a scanner to create a bitmap photo image.

IMRT: Intensity Modulation Radiotherapy Technique.

Isodose curve plotting: after all image pixel are converted into the equivalent irradiation dose, and the dose then renormalise to different percentage value, the program performs a tracking pixel by pixel and link the same percentage level point as percentage level curves.

Isodose shape graph printing: the isodose is not plotted as curve, but painted as shade colours for different percentage level area.

JPEG: a bitmap image format to cut pixel data by 50% with almost no perceived loss of quality. With great strength and compression turns the image into its greatest limitation.

Latent image: the film emulsion silver halide grains are rendered to record the exposure in an unstable condition before the film is developed.

Light source intensity distribution: the intensity of a scanner's light source reflected from different area of scanning bed.

Lpi: Line per inch.

Linear-polynomial smoothing: a special curve fitting technique designed for this project is that with a very small stepped curve, the program using loop the pick each small part of curve to perform a small degree curve fitting process to remove the signal noise.

Modulation Transfer Function (MTF): a graphic representation of the resolution capability of an imaging system or component.

MU: Monitor Unit calibrated to corresponding to a certain radiation dose for controlling irradiation delivery dose used on the radiotherapy device.

Noise analysis: to evaluate a scanner film scan signal quality and signal-to-noise level by scan a standard optical density step wedge film.

OAR/OCR: Off Central Axis Ratio

OD-Dose response: each film darkness grascale value corresponded to a exposed dose value, used for film analysis signal calibration

Optical resolution: the measurement of optical frequency response of a scanner to tells how well the system transmits high-frequency information. It is calculated by the MTF function.

PDD: Percentage Depth Dose

Photo flat-bed scanner: the desktop scanner designed to scan the photo image with the fix photo object position but performs the scanning by the light source movements.

Pixel Value: the signal distributed in matrix in digital image technique to form a digital image.

PMT: Photomulliolier tube

Phantom: Make by human tissue density equivalent material to different shapes to use as medium to build up human tissue equivalent volume for the dosimetry measurement include water phantom, inhomogeneity random phantom, and solid slabs etc.

PRNU: Photo-response non-uniformity

ppi: (PPI) Pixel per inch

QA: Quality assurance.

Renormalise: to normalise the dose value into the percentage value according to a determined reference value.

RODOMS: Radiation Oncology Dosimetry Management System, a quality assurance software package developed by the physicists in St. Vincent's Hospital, Sydney.

Scanner calibration: set up the signal to optical density response linearity for the scanner by scanning a standard optical density step wedge film, and the adjustment of brightness and contrast setting.

Silver halide: the silver containing chemical components of film emulsion grain.

Slab phantom: solid water equivalent material machined into different thickness with very smoothed contacting surface to use for the dosimetry measurement build up.

Steotatic treatment technique: a small sized field used to focus on a three-D target value to rotate gantry from three-D direction to treat the target value dynamically.

Step wedge film: a film strip is made with different standard optical density darkness area to be used for the densitometry equipment calibration.

Three-D chart graph: a group of profile or depth dose curves created by a film image analysis scan plotted together with X, Y, and D values and the display position is calculated by trigonal function.

TIFF: a flexible structure bitmap image file format with 8-byte header.

TLD: thermoluminescence dosimetry.

TAR: Tissue-Air Ratio

Tonal resolution: *see optical resolution*

TPR: Tissue Phantom Ratio

TPS: Treatment Planning System

Transparency adaptor: additional light source box added to a desktop document scanner for the transparency film scanning.

Verification film: A slower dose response characteristic film designed for higher energy and higher dose rate radiative source field check.

Warm-up factor: the scanner signal stabilised issue concerned by testing the signal response stability period after a scanner switched on.

Wedge phantom: a solid phantom is machined into a wedge shape to be used for the quick routine photon and the electron beam energy film dosimetry checks.

Appendix 1 The Characteristics of the four films which were involved in this study

Manufacturer and model	size	Thickness of emulsion	Grain shape	Average grain size	Energy response (linear region)	OD response to dose range	Source reference
Kodak XR diagnostic	8" x 12"	0.01mm	Tabular	2μm diameter 0.13μm thickness	≤ 400kV	≤ 25cGy	Kodak Oncology Image Guide, Kodak Oncology System
CEA TVS	$20x20cm^2$	10-20μm 2-5mg / cm^3	Cubic	0.1-0.3μm	50kV – 20MV	≤ 90cGy	Recommendation of AAPM Radiation Committee Task Report (TG-55)
Kodak XV-2 verification	8" x 12"	0.01mm	Tabular	2μm diameter 0.13μm thickness	50kV – 50MV	≤ 60cGy	Kodak RP/V X-Omat Therapy Verification Film Datasheet
Kodak EDR-2 radiotherapy	8" x 12"	0.01mm	Tabular	Not published	50kV – 50MV	≤ 700cGy	Radiographic Film Dosimetry, AAPM Radiation Committee Task Group Report (TG-69)

Appendix 2 Details of the processors used in the study including recommended developer temperature, development time. Some of these parameters can vary as the setting is dependent on film type and developer.

Manufacturer	Temperature of developer	Chemical pH for developer	Chemical pH for fixer	Development time	Fixing time	Washing time
AGFA X-ray	30^oC – 34^oC	10.05 – 10.35	4.3 -4.4	45 s	45 s	20 s – 30 s
Konica SRX	35^oC	10.5	4.4	35 s	35 s	25 s
Kodak X-ray	26.5^oC	10.05 – 10.35	4.3 – 4.4	1 min	1 min	2 – 5 min

Appendix 3 Details of the scanners used in the study including the spatial resolution, noise and contrast

Manufacturer and type	Nominal spatial and contrast resolution	Actual spatial and contrast resolution	Noise level	Best contrast gradient
HP 4c	8bit, A4 size, 4800 x 5000 ppi maximum resolution contrast adjustable 0-255 grayscale	Maximum effective scan size 200 x 240cm^2 Actual contrast adjustable 0 – 225	High beyond 1.5OD	50 – 90 grayscale / 1.5OD
PTW x-ray	12bit, 12” x 14” maximum size, 3200 x 4800 ppi fixed contrast setting	✓	Medium	5-100 grayscale / 3.0 OD
Umax Power 2100XL	14bit, A4 size, 4800 x 5000 ppi maximum resolution contrast adjustable 0-255 grayscale	Maximum effective scan size 200 x 240cm^2 Actual contrast adjustable 0 - 225	High beyond 3.0OD	5 – 255 grayscale / 2.8 OD
Vidar digital-16	16bit, 12” x 14” scan size, Fixed 256 grayscale	✓	Low	5 – 255 grayscale / 3.38 OD

Appendix 4

Discussion on alternative methods of area dosimetry

Several techniques, other than radiographic film, lend themselves to area dosimetry. These have undergone development recently and are not as advanced as the radiographic film techniques discussed in this thesis.
However for completeness we discuss the techniques in this appendix and indicate whether the strict protocols developed for the use of radiographic film in quality assurance can be extended to include these.

EPID dosimetry

Electronic Portal Imaging Device (EPID) was first implemented on a Siemens Mevatron Linear Accelerator in 1984 (Siemens Linear Accelerator Catalog 1984). The original EPID was intended to replace the port film for patient positional confirmation. The EPID was not successful in its early form because the image quality was not adequate for clinical usage. In 1997 Varian developed EPID for their 2100 and 6/100 linacs using flat panel amorphous silicon EPIDs. In 2003, Varian introduced a liquid ionization chamber on their 6/100 Linac.
EPIDs are commonly used for treatment position checks and provide the fundamental clinical QA tool for 3D-CRT (3-dimensional Conformal Radiation Therapy) and IMRT (Intensity Modulated Radiation Therapy). The EPID provides confirmation of the anatomy relative to the radiated field. It may also provide a comparison between the MLC field segments positional accuracy with 3D-CRT or IMRT planning.

Compared to film dosimetry, EPID is simple to setup and use. It provides an immediate image on radiation and fusion overlay. In DRR (Digital Reconstructed Radiograph) image require processing to provide qualitative images and further computer scanning for quantitative use.
EPID can be used for checking a treatment setup and may be performed before each treatment without need process film.
Compared to film dosimetry, EPID allows clinical QA to be performed daily as a matter of routine.

Some research studies discuss the use of EPID for absolute dose measurement and relative dose distribution analysis (K Pasmat 1998, C Beltran, P Vial, M Williams 2005). However Amorphous Silicon EPIDs may need to be calibrated frequently. A number of possible problems are evident insuch use:

- The EPID has a finite lifetime and the response throughout this lifetime.
- Proper calibration will require several exposures.
- The EPID structure is designed for ease of use and portability. The EPID normally does not contain water equivalent material for the beam buildup. The relative readings obtained directly from the EPID do not therefore properly represent the results obtained from water equivalent phantoms.

In summary the EPID is be good tool for the treatment setup positional checks and for IMRT planning verification. However the current design EPID is not yet suitable for the absolute dose measurement or dose distribution verification.

Flat Panel Detectors

Flat panel detectors are designed for X-ray port image or cone-beam CT on the Varian Clinac and Elekta linear accelerators. They have been introduced recently for portal imaging, position checks and IGRT (Image Guided Radiation Therapy) patient position verification. The Flat Panel responds directly to X-rays. Compared with the MV (Mega Voltage) beam EPID, the flat Panel gives better image quality. Flat panel detectors are also used to provide image digital data to build cone beam CT images for IGRT planning image overlay registration process. However, since the flat panel is not collecting signal from the treatment beam its use is confined to treatment position checks, and it cannot be used for dosimetry measurements.

TLD

TLD (Thermo-luminescence Dosimetry) is an absolute dose measurement technique implemented in 1968 (J R Cameron, 1968). TLD is widely used for radiotherapy point dose checks for 2D, 3D, 3D-CRT and IMRT.

TLD chips and rods can be simply located on a patient's skin and in a phantom to obtain accurate secondary dosimetry. In recent years TLD arrays or TLD sheet have become available for use in the verification of treatment plans. Compared with film dosimetry TLD are more easily calibrated and individually having with very good energy response, wider dynamic range and signal linearity. The beam to surface entry angles and depth dependence compare with film dosimetry are very low.

However, if TLD considered to use for the dose distribution check for 3D treatment technique,

Current TLD techniques have the following disadvantages

- A Complex readout process - TLDs need about one hour after the chips have been irradiated before they can be read. The readout takes half an hour and a further two hours are required to anneal the chips before reuse.
- Low spatial resolution - The size of the TLD and their packing density constrains the spatial resolution to a resolution of no better than $0.5cm^2$.

The TLD is commonly used for the point dose checks for patient skin dose or in 3D phantom for dose planning verification. TLD are not recommended for t for isodose distribution measurement.

Diode arrays and ionization chamber arrays

Sun Nuclear has had a commercial diode array many years. The diode array is commonly used for routine field flatness and symmetry constancy checks. In 1999, R Brown and Y Wang used a diode system for the beam energy constancy checks. In 2002, Sun Nuclear introduced MapCHECK, a 2-D diode array. MapCHECK can be used for a rapid field dose distribution measurements and is simple to setup. It has a high dynamic range but responds to the low exposures required for 3D-CRT and IMRT planning dose distribution checks. MapCHECK is used in many centres for IMRT quality assurance. Some disadvantages in using diode array include:

1. The detector array requires frequent calibration to maintain the accurate dosimetry.

2. The minimum gap between detector cells is 0.5cm, resulting in inaccuracies in field checks in the penumbral region and the junction dose checks.
3. The array panel is suitable for the Linac stability checks. It is designed without the uniform buildup and backscatter materials and therefore does not directly represent the relative dose as measured in water equivalent phantom.

Based on the above, the diode array is more commonly used for the routine field QA more than 3D planning check as the quantitative dosimetry is not reliable.

The Ionization Array is designed for the dynamic field data commissioning. Each detector in ionization array is very stable for absolute dose calibration. The ionization array is recommended for use with a 3D water phantom (Varian EDW, Siemens Virtual Wedge). It is not used for the clinical routine QA because:

1. It is expensive and easily damaged.
2. It is very complicated to setup in a water tank . the setup time averages two hours precluding use during patient treatment.
3. The resolution is low compared to a diode array because of the physical size of the ionization chamber. The minimum distance between the detectors has to be at least 1.0cm for ionization measurements.

For these reasons, the ionization chamber array is commonly used as commissioning tool and is not commonly used for routine quality assurance.

References

Pasma K L, Kroonwijk M, de Boer J C J, Visser A G, Heijmen B J M, Accurate Portal Dose Measurement with A Fluoroscopic Electronic Portal Imaging Device (EPID) for open and Wedged beams and Dynamic Multileaf Collimation, Phys. Med. Biol. 43, pp 2047-2060, 1998

Evans P M, Donovant E M, Partridge M etc, Radiological Thickness Measurement using a Liquid Ionization Chamber Electronic Portal Imaging Device, Phys. Med. Biol. 44, N89-N97, 1999

Chang J, Mageras G, Clifton Ling and Lutz W, An Iterative EPID Calibration Procedure for Dosimetric Verification that Consider the EPID Scattering Factor, Med. Phys. 28 (11), November 2001

Beltran C, Herman M, Replacement of Film and Ionization Chamber Measurement by Electronic Portal Dosimetry for IMRT QA, Med. Phys., Vol 32, pp 1987-1987, June 2005

Prabaker R, Ganesh T, Joshi R, Julka P, Rath G, Pant G, A Study On the Reproducibility of Tangential Breast Fields Using Online Electronic Portal Images, Med. Phys., Vol 32, pp 1990, June 2005

Varian, Flat-Panels use X-ray, Varian Medical System 2004 Annual Report, 2004

Elekta, Imaging and Treatment Combined in Image Guided Radiation Therapy, Elekta Synergy™ S Information Bulletin, 2005

Cameron J R, Suntharalinggam N, Kenney G N, Thermoluminescent Dosimetry, Madison: University of Wisconsin Press, 1968

Ogden K, Lavallee R, Huda W, Roskopf M, Scalzetti E, Calibration of TLD Chips to Maximize Accuracy in Radiographic Phantom Dosimetry, Med. Phys., Vol 32, pp 1907,June 2005

Ahmad M, Chen Z, Song H, Cund M, Deng J, Nath R, Application of a Gantry-mounted Diode Array System for QA Dosimetry of High-Energy Photon Beams, Med. Phys., Vol 32, pp 1991, June 2005

Wagner T, Langen K, Poole D, Meeks S, Willoughby T, Ruchala K, Evaluation of a Commercial Diode Array (Tomodose) for Tomotherapy Beam Profile Measurements, Med. Phys., Vol 32, pp 1994, June 2005

Su M, Li J, Tong S, Grant D, Farhangi E, Tapen E, Chu K, Small Electron Field Cutout Factors Measured Using a 2D Ion Chamber Array Compared to Radiographic Film, Med. Phys. Vol 32, pp 2007, June 2005

Szeglin S, Das L, Chopra K, Schuele E, Barker R, Two-Dimensional (2D) Ion Chamber Array for Radiation Dose Verification Including IMRT, Med. Phys. Vol 32, pp 2009, June 2005

Brown R, Wang Y, Tran T, Photon and Electron beam Routine Energy Check using Diode Array, EPSM-1999 conference notes, Newcastle, November 1999

Williams M, Commissioning a RTPS for IMRT, Sydney IMRT CPD Overview Training Course Notes, Sydney, Australia, October 2005

Vial P, Fundamental Aspects of RTPS commissioning, Sydney IMRT CPD Overview Training Course Notes, Sydney, Australia, October 2005